SOPAC

South Pacific Applied Geoscience Commission

TECHNICAL BULLETIN 10

MANIHIKI PLATEAU, MACHIAS AND CAPRICORN SEAMOUNTS, NIUE, AND TOFUA TROUGH: RESULTS OF TUI CRUISES

Edited by

M.A. Meylan and G.P. Glasby

MANIHIKI PLATEAU, MACHIAS AND CAPRICORN SEAMOUNTS, NIUE, AND TOFUA TROUGH: RESULTS OF TUI CRUISES

Front Cover Illustration: *Merging of manganiferous (bottom) and ferruginous (top) zones on the inner surface of a ferromanganese crust. This particular sample was dredged at Station Q880. See pages* ***fff-ff9****, this volume. Photo by Dave Cullen.*

SOPAC

South Pacific Applied Geoscience Commission

TECHNICAL BULLETIN 10

MANIHIKI PLATEAU, MACHIAS AND CAPRICORN SEAMOUNTS, NIUE, AND TOFUA TROUGH: RESULTS OF TUI CRUISES

Edited by

M.A. Meylan and G.P. Glasby

Published by the

SOPAC Secretariat

Suva, Fiji

1996

All communication to do with this and other publications of SOPAC should be addressed to:

The Director SOP AC
Secretariat Private Mail
Bag, GPO Suva, FIJI
Fax # (679) 370040
E-mail:
sunita@sopac.org.fj

This publication should be referred to as
SOPAC Technical Bulletin 10

Cataloguing-in-publication data;

Manihiki Plateau, Machias and Capricorn Seamounts, Niue, and Tofua Trough: Results of *Tui* Cruises/ edited by M.A. Meylan and G.P. Glasby. Suva, Fiji: SOP AC Secretariat, 1996.

p. cm. - (Technical Bulletin/South Pacific Applied Geoscience Commission; no. 10)
Includes bibliographic references.
ISSN 0378-6447
ISBN 982-207-005-5

I. Meylan, M.A. II. Glasby, G.P. III. Series

PREFACE

One evening in early May of 1986, we met on the afterdeck of HMNZS *Tui* to discuss plans for a volume of cruise results. Despite repeated mechanical problems and less-than-optimum dredging capabilities of the vessel, we were nearing the end of a reasonably successful research cruise. Numerous samples had been collected from the northern Cook Islands area, Niue, and seamounts adjacent to the Tonga Trench, and the geophysical data appeared to be first rate. So we talked optimistically of having a volume ready in less than two years. By the Fifteenth Session of CCOP/SOPAC in Rarotonga during September 1986, a substantial preliminary report had been assembled, with contributions from scientists who had participated in the *Tui* cruise (Glasby et al., 1986). By this time, samples collected during a second *Tui* cruise (July 1986) had been described, and arrangments were made with colleagues from around the world to perform research on specific aspects of the *Tui* material. By 1989, only a little later than hoped for, most of the papers included herein were ready for external peer review, and had already been edited by us.

The original publication plans were to prepare the *Tui* volume for inclusion in the AAPG Circum-Pacific Earth Science Series, with GPG as lead editor. Communication with the editors of the series indicated that this would indeed be the appropriate vehicle for publication. However, by the time that the *Tui* volume papers were ready for external review, the editors of the series were unable to make a commitment regarding additional volumes, and the *Tui* volume was relegated to the status of a ship without a port. Nevertheless, publication of findings related to the metal contents of manganese nodules and crusts was accomplished (Meylan et al., 1990), and some of the geophysical data had been presented at scientific meetings (Hill et al., 1989a, b, 1990).

Alternative publication plans were formulated. However, in August of 1992, GPG left the New Zealand Oceanographic Institute. By default, MAM assumed responsibility for completion of a *Tui* volume, and applied for a sabbatical leave to accomplish this task. Meanwhile, research involving *Tui* data and samples continued (Hill and Baudry, 1992; Kuzendorf and Glasby, 1992; Walter et al., 1995).

The contents of the present volume primarily reflect the original efforts of the contributing scientists, modified slightly in format, with only minimal updating to incorporate more recent literature. Despite the limitations of this unavoidable lag time for appearance, and time constraints for volume preparation, this work will be a valuable resource for marine geologists, geophysicists and biologists investigating the Southwest Pacific.

Both of us have experienced the excitement and glamour of research cruises in the SW Pacific (three of which have been undertaken together). We hope that finalizing this volume can serve as partial repayment for the opportunities that we have had.

M.A. Meylan
G.P. Glasby
Co-Chief Scientists

September 1996

REFERENCES CITED

Glasby, G.P., M.A. Meylan, B.C. McKelvey, P.J. Hill, A.T. Utanga, S.P. Helu, K.H. Rose, W. deL. Main, and E.S. Arron, 1986, Geological and geophysical studies of the Manihiki Plateau and adjacent seamounts and islands in the S.W. Pacific: HMNZS *Tui* cruise, 1986: Limited circulation preliminary report prepared for CCOP/SOPAC, unpaginated.

Hill, P.J., and N. Baudry, 1992, Southwest Pacific seamounts revealed by satellite altimetry, *in* B.H. Keating and B.R. Bolton, eds; Geology and offshore mineral resources of the Central Pacific Basin: Circum-Pacific Council for Energy and Mineral Resources, Earth Science Series, v.14, p.69-76.

Hill, P.J., W.T. Coulbourn, G.P. Glasby, M.A. Meylan, and shipboard scientists of HMNZS *'Tui'* (1986) and RV *'Moana Wave'* (1987) cruises, 1989a, Manihiki Plateau - results of recent Sea Marc II, geophysical and seafloor sampling investigations: Joint CCOP/SOPAC-IOC Fourth International Workshop on Geology, Geophysics and Mineral Resources of the South Pacific, Program and Abstracts Volume, p.58 (extended abstract/poster).

Hill, P.J., W.T. Coulbourn, G.P. Glasby, M.A. Meylan, and shipboard scientists of HMSNZ *'Tui'* (1986) and RV *'Moana Wave'* (1987) cruises, 1989b, Subduction of Capricorn and Machias guyots - structural and sedimentological processes: Joint CCOP/SOPAC- IOC Fourth International Workshop on Geology, Geophysics and Mineral Resources of the South Pacific, Program and Abstracts Volume, p.63-67 (extended abstract/poster).

Hill, P.J., W.T. Coulbourn, G.P. Glasby, and M.A. Meylan, 1990, Manihiki Plateau - results of recent resource-oriented shipboard investigations and discovery of a major ?mud volcano complex: Pacific Rim Congress 90, Proceedings, v.III, p.163-171.

Kunzendorf, H., and G.P. Glasby, 1994, Minor and rare elements in manganese crusts and nodules and sediments from the Manihiki Plateau and adjacent areas: Results of HMNZS *Tui* cruises: Marine Georesources and Geotechnology, v.12, p.271-281.

Meylan, M.A., G.P. Glasby, P.J. Hill, B.C. McKelvey, P. Walter, and P. Stoffers, 1990, Manganese crusts and nodules from the Manihiki Plateau and adjacent areas: Results of HMNZS *Tui* cruises: Marine Mining, v.9, p.43-72.

Walter, P., G.P. Glasby, W.L. Plüger, H. Kunzendorf, and M.A. Meylan, 1995, Mineralogy and composition of manganese crusts and nodules and sediments from the Manihiki Plateau and adjacent areas: Results of HMNZS *Tui* cruises: Marine Georesources and Geotechnology, v.13, p.321-337.

CONTRIBUTORS

A.G. Beu
Institute of Geological and Nuclear Science Ltd
PO Box 30368
Lower Hutt
NEW ZEALAND

D.J. Cullen
74 West Street
Greytown
Wairarapa
NEW ZEALAND

B.K. Dugolinsky
Department of Earth Sciences
State University of New York
Oneonta
New York 13820
UNITED STATES OF AMERICA

G.P. Glasby
Department of Earth Sciences
University of Sheffield
Sheffield S3 7HP
ENGLAND

K.R. Grange
W.deL. Main
D.G. McKnight
National Institute of Water and Atmosphere Research Ltd
PO Box 14901
Kilbirnie, Wellington
NEW ZEALAND

R.W. Grigg
Department of Oceanography
SOEST
University of Hawaii
Honolulu
Hawaii 96822
UNITED STATES OF AMERICA

B.W. Hayward
Auckland Institute and Museum
Private Bag
Auckland
NEW ZEALAND

S. Helu
General Manager
Tonga Water Board
PO Box 92
Nuku'alofa
TONGA

P.J. Hill
Marine Geoscience and Petroleum Geology Program
Australian Geological Survey Organisation
GPO Box 378
Canberra City ACT 2601
AUSTRALIA

B.C. McKelvey
Department of Geology and Geophysics
University of New England
Armidale
New South Wales 2351
AUSTRALIA

W.J. McCabe
R.G. Ditchburn
Institute of Geological and Nuclear Sciences Ltd
PO Box 31312
Lower Hutt
NEW ZEALAND

M.A. Meylan
Department of Geology
University of Southern Mississippi
Hattiesburg
MS 39406–5044
UNITED STATES OF AMERICA

J. Ostwald
41 Florida Avenue
New Lambton
New Castle
New South Wales 2305
AUSTRALIA

J.E.N. Veron
Australian Institute of Marine Science
PMB No. 8
Townsville M.C.
Queensland
AUSTRALIA

TABLE OF CONTENTS

Part 1: INTRODUCTION

Part 2: GEOPHYSICAL SURVEYS

Part 3: CRUSTS, NODULES, ROCKS, SEDIMENTS

Part 4: BIOLOGY AND BOTTOM PHOTOGRAPHY

Part 1

INTRODUCTION

Glasby, G.P., M.A. Meylan, P J. Hill, and B.C. McKelvey, 1996. Introduction, *in*. Meylan, M.A., and G.P. Glasby (eds) Manihiki Plateau, Machias and Capricorn Seamounts, Niue, and Tofua Trough: Results of Tui Cruises. SOPAC Technical Bulletin 10: 1-16.

INTRODUCTION

G.P. Glasby

Department of Earth Sciences, University of Sheffield, Sheffield S3 7HP, England

M.A. Meylan

University of Southern Mississippi, USM Box 5044, Hattiesburg, USA .

P.J. Hill

Australian Geological Survey Organisation, GPO Box 378, Canberra, Australia

B.C. McKelvey

University of New England, Atrnidale, New South Wales, Ausltalia

ABSTRACT

A 30 day cruise of HMNZS *Tui* from Rarotonga to Nuku'alofa was undertaken in 1986 as part of the Tripartite Programme organized by the Governments of New Zealand, Australia and the United States in co-operation with CCOP/SOPAC. The cruise involved detailed geophysical surveys of the Manihiki Plateau, Machias Seamount, Capricorn Seamount, Niue and the Tofua Trough. In addition, an attempt was made to locate cobalt-rich manganese crusts on the flanks of Manihiki and Rakahanga on the eastern side of the Manihiki Plateau; Pukapuka, Tema Reef and Nassau on the western side of Manihiki Plateau; and Machias Seamount, Capricorn Seamount and Niue by means of rock dredging. A subsequent 9 day cruise of HMNZS *Tui* from Rarotonga to Rarotonga in 1986 resulted in 16 successful dredge hauls in the southern Cook 'Islands.

OBJECTIVES

The 1986 cruise of HMNZS *Tui* to the Manihiki Plateau and adjacent areas of the SW Pacific was part of the Tripartite Programme undertaken by the Governments of New Zealand, Australia and the United States of America in co-operation with the Committee for the Co-ordination of Joint Prospecting for Mineral Resources in the South Pacific Offshore Areas (CCOP/SOPAC) to carry out a joint program of marine geoscientific research and mineral resources studies in the South Pacific region. The nature, objectives and requirements of the Tripartite Programme are outlined in the 'Agreement' signed by the three Governments (Anonymous, 1984). The objectives of the *Tui* cruise listed there are as follows:

1. Determine the areal distribution, abundance and metal content of Co-rich manganese crusts on seamounts and margins of the Manihiki Plateau and seamounts east of Tonga, including Capricorn Seamount;
2. To complete manganese nodule sampling in the Penrhyn Basin;
3. To sample sediments in the Lau Basin near Ata Island overlying the magma chamber detected by RV *S.P. Lee* during the 1982 cruises;
4. To establish the areal extent of erosion on the eastern margin of the Manihiki Plateau associated with the Western Boundary Current and sample exposed areas of bedrock for mineralization known to be associated there with volcanic basement;

5. Investigative areas of interest include: geomorphology, seafloor structure, geochemistry, geochronology, sedimentology, igneous petrology, physical oceanography.

In consultation, the two co-chief scientists modified these to the following specific objectives:

1. Study the distribution of Co-rich manganese crusts on the Manihiki Plateau and its relationship to the environments of deposition. This will involve:

   (a) a W-E transect across the plateau at 12°45'S including seismic profiles along the transect and dredging, coring and camera stations on the return E-W transect. This will include sampling deep-sea, flank and high plateau areas on both sides of the plateau in order to establish if there is any asymmetry in the distribution of crusts and sediments across the plateau. Particular attention will be paid to locating and sampling manganese crusts.

   (b) transects to Manihiki and Rakahanga and thence to Nassau, which will also involve dredging, coring and camera stations, in order to sample the flanks of atolls on the plateau and any seapeaks along the traverses for manganese crusts; areas selected include Suwarrow, Manihiki, Rakahanga, Nassau, Tema Reef and Pukapuka;

2. Study the distribution of Co-rich manganese crusts on seamounts. These include Machias Seamount, Capricorn Seamount and other unnamed seamounts. This work will involve mainly dredging;

3. Seismic profile and dredge around Niue to establish the geological structure of Niue and locate manganese crusts there;

4. Piston core between Tofua and Niue to determine volcanic ash stratigraphy in the cores in order to establish if the soils of Niue are derived from volcanism on Tofua.

The *Tui* served as a vessel of opportunity later in 1986 as a result of its participation in a military training exercise (Exercise Joint Venture), permitting collection of dredge samples in the southern Cook Islands. Note that in this volume, "the cruise" refers to the earlier 1986 *Tui* cruise, but results of the second cruise have been incorporated where appropriate.

SCIENTIFIC PARTY

The specific objectives of the cruise were accomplished to varying degrees during the run from Rarotonga to Nuku'alofa on Tongatapu (Figure 1). The scientific party for the leg was as follows:

Dr G.P. Glasby (Co-chief scientist), New Zealand Oceanographic Institute, DSIR, New Zealand

Dr M.A. Meylan (Co-chief scientist), University of Southern Mississippi, USA

Dr B.C. McKelvey, University of New England, Armidale, Australia

P.J. Hill, Bureau of Mineral Resources, Canberra, Australia

A.T. Utanga, Department of Internal Affairs, Cook Islands

S.P. Helu, Ministry of Lands, Survey and Natural Resources, Tonga

K.H. Rose, Geophysics Division, DSIR, New Zealand

W. deL. Main, New Zealand Oceanographic Institute, DSIR, New Zealand

E.S. Arron, New Zealand Oceanographic Institute, DSIR, New Zealand

VESSEL AND EQUIPMENT

The research vessel used in this cruise, HMNZS *Tui*, operates for the New Zealand Defence Scientific Establishment, principally in acoustic research rather than for deep-sea geological sampling as in this cruise. It was built in 1963 and commissioned into the RNZN in 1970. It has dimensions of 63.4 m x 11.3 m x 5.8 m and a displacement of 1050 tonnes. It has a diesel-electric drive and cruises at 12 kts. During this cruise, it carried 6 officers and 36 ratings in addition to the scientific staff.

The following equipment was used during the cruise:

Satellite Navigation – Initially Magnavox MX 702A-3 receiver interfaced with Arma Brown gyro compass Mark 26 Mod 2 and AMETEK Sonar doppler 2-axis speed log (MRQ-4015A). After Pago Pago, Magnavox MX 4102 receiver.

Echo Sounder – Raytheon Line Scan Recorder (LSR-1811-S), PTR 105-8 transceiver (12 kHz), CESP-III replica correlator; two sets of depths were recorded (in meters): (i) uncorrected, a 1500 m/sec. sound velocity in meters, (ii) corrected, by application of revised Matthews Tables. The corrected data are used throughout this volume.

Seismic reflection – Single Bolt Associates PAR air-gun model 1900 C (120/134 cu. in. chamber) operating at 1600-2000 p.s.i.; CompAir Reavell VHP15 Mark 1 reciprocating compressor, 4 stage; Air-gun firing control unit (crystal-controlled trigger delay); Seismic Engineering 2 trace marine seismic array (100 m active section, 40 MD1-SS hydrophone elements in symmetric tapered configuration); Seismic Engineering Accustreamer control panel A-2 (unity gain amplifier and depth transducer display); SIE MU-100 amplifier bank; Krohn-Hite Filter units (models 3550 and 3700); EPC graphic recorders 4600 and 4603; Racal Store 4 magnetic tape recorder, 6.25 mm tape, 4 track EM recording; Seismic profiling was carried out at nominal 7 kts., shot rate 11 or 13 secs.; EPC records - 4 second sweep, 40-300 Hz bandpass, analogue magnetic tape recording - unfiltered.

Magnetics – Geometrics G801/803 marine-airborne proton magnetometer; Hewlett-Packard 7130A strip-chart recorder; Magnetometer cycling rate 15 sec.

Gravity – La Coste and Romberg Air-Sea S-80 gravity meter system (gyro stabilized platform); Texas Instruments Servo-riter II strip chart recorder; Houston Technical Laboratories Worden gravity meter, Geodetic model (ship-shore base station gravity ties).

Digital data acquisition system – Data recorded are time and corresponding magnetic and gravity values; Monitor Labs System 9400 data conversion control system, verifer and printer; Digi-Data 1427 (1300 Series) magnetic tape recorder, 0.5 inch tape, 9-track.

Digital data logging (magnetics and gravity) – Data recorded at 20 second intervals.

Rock Dredge – 0.9 m x 0.4 m x 1.15 m

Pipe Dredge – 0.25 m x 0.9 m

Piston corer – 6 m x 0.07 m

Short corer – 0.7 m x 0.07 m

Bottom camera – Bottom photographs were taken using a Benthos remote Edgerton camera in which the position of the camera above the sea floor was determined using a 12 kHz pinger. The camera and flash were triggered by means of a trigger weight.

The rock dredge and piston corer were deployed using 14 mm wire; the pipe dredge, short corer and camera using 9 mm wire. Because of the lack of robustness of the rock dredge and wire, a conservative attitude had to be adopted to rock dredging. Part of each pipe dredge sediment sample was sieved through a cheese cloth in order to obtain a coarse fraction. From Stn U315, plastic corer tubes were fitted to the rock dredge to collect sediment samples. All sampling operations were carried out from a stern 'A' frame. At Stn U316b, the SATNAV system ceased to work and positions were fixed by radar and visual sights, astronomically, and by dead reckoning to Pago Pago. A second SATNAV was made available by CCOP/SOPAC in Pago Pago and this was employed for the remainder of the cruise. Because of the loss of three rock dredges on the Manihiki Plateau, sheet steel was purchased in Pago Pago and two additional rock dredges were manufactured on the ship.

MANIHIKI PLATEAU

The Manihiki Plateau is a 500,000-km^2 nearly flat-topped feature in the northern Cook Island group. Its depth is typically 2400-3000 m above a surrounding oceanic depth of 5500 m. Three distinct provinces are recognized on the plateau, the High, the North, and the Western plateaus. The Manihiki is surrounded by the Penrhyn Basin to the east and the Samoan Basin to the southwest. Danger, Nassau, Suwarrow, Manihiki and Rakahanga islands rise from the western and eastern parts of the plateau. The geology of these islands has been described by Wood and Hay (1970).

In spite of the large area of the plateau, it has been relatively little studied. The initial work of Heezen et al. (1966) and Winterer et al. (1974) outlined the principal structural features of the plateau. Winterer (1976), Hussong et al. (1979), Carlson et al. (1980), Watts et al. (1980), Henderson and Gordon (1981), Schlanger et al. (1981), Nur and Ben-Avraham (1982), Mahoney (1984), and Maxwell (1985) have extended this work and commented on the origin of the plateau. The top of the plateau is covered by approximately 1 km of stratified carbonate ooze and basal volcaniclastics. The plateau is thought to have formed 110-105 Ma as a result of voluminous volcanic eruptions, although the ages of the islands protruding above the plateau are unknown. Geologically, the plateau is considered complex. Lonsdale (1981) has plotted the pathways of Pacific bottom water and shown that the northward migration of Antarctic Bottom Water is more pronounced in the Samoan Basin to the southwest of the plateau than in the Penrhyn Basin to the east. This suggests a possible asymmetry in erosion in deep-sea areas surrounding the plateau.

In 1973, the R/V *Glomar Challenger* drilled a 943 m hole (site 317) into a basinal area of the High Plateau at a depth of about 2600 m (Jenkyns, 1976). In 1984, R/V *Sonne* mapped an area of 1800 km^2 on the northeastern flank of the plateau in an attempt to locate copper-impregnated sediments similar to those reported for DSDP hole 317 (Beiersdorf and Erzinger, 1989). A 1987 cruise of R/V *Moana Wave* discovered a field of volcano-like cones surrounding a seamount at the NE edge of the Manihiki Plateau, about 50 km SW of Rakahanga (Hill et al., 1990; Coulbourn and Hill, 1991). This unusual set of features was investigated further during R/V *Sonne* cruise SO 67-1 (Beiersdorf, 1990).

Manganese nodules from the eastern flanks of the plateau were first reported by Heezen et al. (1966), who also noted evidence of bottom current activity in bottom photographs taken there. The distribution of nodules and crusts in a polygon on the eastern flanks of the plateau in a depth range 2000-5250 m was studied by Bezrukov (1971, 1973), who found their distribution more complex than reported by Heezen et al. Two NW-SE transects across the plateau were carried out by the Geological Survey of Japan in 1980 (Mizuno and Nakao, 1982; Usui, 1983). The plateau itself was found to be largely barren of nodules, the high rate of sedimentation probably preventing nodule growth. R/V *Sonne* also recovered manganese nodules, associated with a strongly eroded plateau edge on the northeastern flank of the plateau (Beiersdorf and Erzinger, 1989). The occurrence of thick manganese encrustations (ca. 40 mm) has been reported on Albert Henry Seamount north of Pukapuka (Cullen and Burnett, 1986; Cullen, this volume). Chemical analyses of nodules from the plateau were reported by Horn et al. (1973), who gave an average Co content of two plateau nodules as 0.51% compared to 0.31% for adjacent deep-sea nodules. Usui and Mochizuki (1982) reported a mean Co content of six plateau nodules of 0.22%. A summary of data on nodules from the plateau is given by Exon (1981). Based on various criteria, Cronan (1984) suggested that various elevated areas on the Manihiki Plateau (Pukapuka Island, Danger Island, Tema Reef, Nassau Island, Rakahanga Island, Manihiki Island, Suwarrow Island) might be prospective for Co-rich manganese crusts.

The object of the present survey was to sample the plateau in order to define more closely the distribution of sediments and manganese nodules and crusts there. Particular attention was paid to areas such as the eastern flanks of this plateau where nodules have previously been recovered and elevated areas where Co-rich manganese crusts might be present. Some limited sampling of deep-sea areas on either side of the plateau was also carried out for comparative purposes. A geophysical profile was conducted across the plateau to study the structure of the plateau and to give some additional control in sampling manganese deposits. Results of this work have been published by Hill et al. (1989a, 1990).

COBALT-RICH MANGANESE CRUSTS

The occurrence of elevated Co contents in manganese crusts from shallow-water seamount environments was first noted by Menard (1964) and Mero (1965). It was not until the Midpac '81 cruise of R/V *Sonne* to the Line Islands and Mid-Pacific Mountains, however, that the potential of Co-rich crusts as a possible economic resource became recognized (Halbach et al., 1982; Halbach and Manheim, 1984; Manheim, 1986). In the *Sonne* survey, it was found that the Co content of manganese nodules and crusts increased from less than 0.4% at water depths of more than 4000 m to 1.2% in the top 5 mm-thick layer of seamount crusts and the crusts display a mean thickness of more than 20 mm in upper slope areas (equivalent to about 16 kg of dry crustal material per square meter of crustal surface). This survey suggested that these crusts might be a possible economic source of metals such as Co and Pt.

This work stimulated much interest and a substantial literature now exists on these deposits (cf. Glasby, 1986). For instance, the U.S. Geological Survey conducted a cruise of R/V *S.P. Lee* to the Necker Ridge, Horizon Guyot and S.P. Lee Guyot in 1983 to study the distribution of these deposits (Hein et al., 1985, 1987) and the U.S. Minerals Management Service commissioned an overview of the potential of these Co rich crusts (Clark et al., 1985). In the SW Pacific, Aplin and Cronan (1985) studied crusts from the Line Islands Archipelago between 15°S and 17°N and Cronan (1984) suggested a number of criteria for locating Co-rich crusts as well as a number of possible areas worthy of investigation in the SW Pacific. For Co-rich crusts to occur in the CCOP/SOPAC area, Cronan (1984) suggested that the following criteria should be met:

(a) Depth between 300-2000 m;

(b) Latitude not more than about 15°S;

(c) Exposed non-sedimented slopes.

It is also perhaps worth listing the following factors considered by Clark et al. (1985) to be important in the formation of Co-rich crusts:

1. Crusts occur on seamount and guyot areas which are older than 25 m.yr.;
2. The maximum thickness and metal content of crusts occur within the 800-2400 m depth zone;
3. Maximum crust coverage and occurrences occur within 5-15° of the equator;
4. Two generations of crust occur, the older between 16-9 Ma and a younger from 8 Ma to the present;
5. Areas of greatest economic potential occur where both crust generations are present.

In the SW Pacific, virtually nothing was known of the distribution of Co-rich manganese crusts with the exception of Aplin and Cronan's (1985) work on the Line Islands. It was therefore thought most desirable to carry out a preliminary survey of some possible areas to see if such deposits do occur in the SW Pacific. In selecting areas for survey, particular attention was paid to areas selected by Cronan (1984) as having the most potential. These included the slopes of various islands on the Manihiki Plateau as well as Machias Seamount off Samoa.

In this regard, it should be noted that the Manihiki Plateau itself lies beneath the depth that Co-rich crusts are thought to occur and previous dredge hauls had failed to reveal the occurrence of manganese crusts on the Capricorn and Machias Seamounts. Further, the slopes of the various islands on the Manihiki Plateau which Cronan (1984) had considered prospective for Co-rich crusts had, in fact, never been sampled, the age of these islands is unknown and the geology of the islands has been studied only at the reconnaissance level (Wood and Hay, 1970). The suggested occurrence of such crusts there was therefore speculative. For this reason, it was felt that a more general survey of the Manihiki Plateau and various seamounts (including geophysical and sedimentological aspects) was necessary in order to place the results of this survey in a proper perspective.

NARRATIVE

The *Tui* left Wellington, New Zealand, on March 18, 1986, and arrived Rarotonga, Cook Islands, on April 1. It departed Rarotonga on April 5 and arrived Nuku'alofa, Tonga, on May 5. A short refuelling stop was made in Pago Pago, American Samoa, on April 24. The *Tui* departed Nuku'alofa on May 9 and arrived in Auckland, New Zealand, on May 15, 1986.

During the course of the cruise, the *Tui* was subject to numerous breakdowns in gear which required substantial onboard repair work and necessitated some modifications to the cruise plan. Problems occurred even before commencement of the Rarotonga-Nuku'alofa leg. Because of a fault to the automatic steering, the *Tui* was diverted to Auckland during the voyage from Wellington-Rarotonga for repairs which lasted five days. For this reason, the planned sampling program between Wellington and Rarotonga was cancelled, although gravity, magnetic and bathymetric profiles were obtained along the transect.

The ship's track and station positions are shown on Figure 1, and a listing of the waypoints used in setting the ship's track is given in Appendix A of this chapter. A summary of station data is given in Appendix B.

The cruise commenced with a profiling transect from Rarotonga to Suwarrow employing gravity, magnetics and bathymetry. Seismic profiling commenced at 14° 29.1'S, 162° 12.3'W. During this transect, the ship's track crossed certain gravity anomalies recorded by SEASAT in order to establish whether these anomalies correspond to the occurrence of seamounts. A rock dredge was lost at the first attempt to dredge a seamount along this transect. This induced a certain amount of caution in the earlier part of the sampling program. For this reason, sampling around

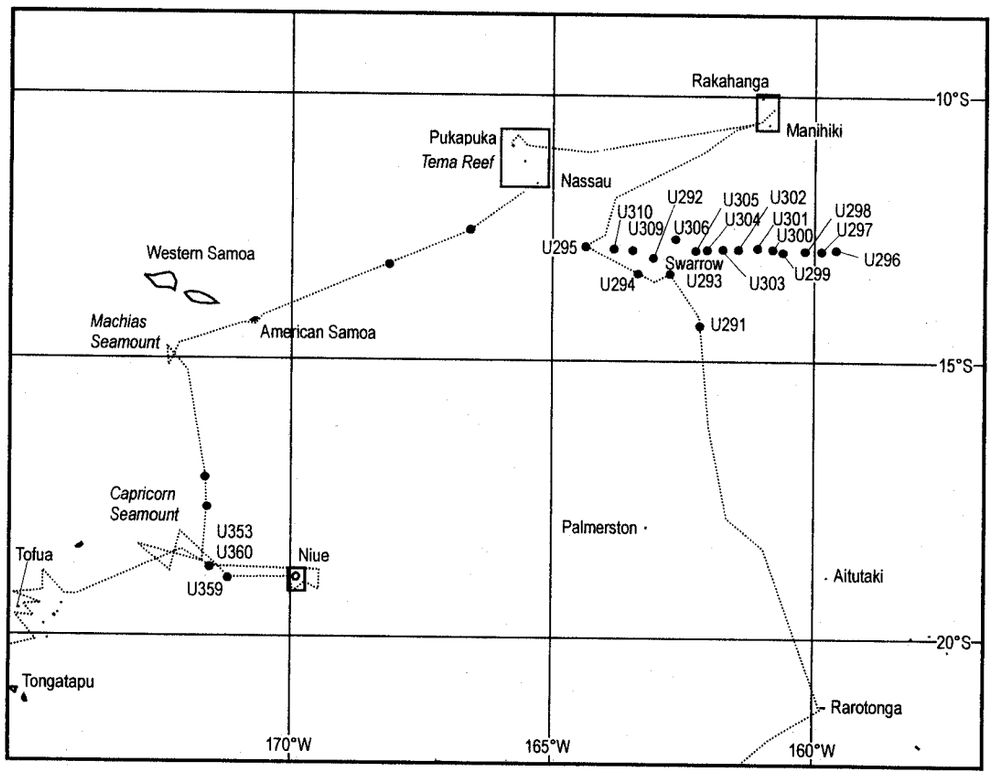

Figure 1. Map of ship track and station locations.

Suwarrow was restricted to pipe dredging away from the steepest parts of the slope of the island.

A W-E transect was then carried out across the Manihiki Plateau at 12° 45'S, employing seismic reflection profiling, gravity, magnetics and bathymetry. On the return transect at this latitude, sampling of the main features of the plateau as well as deep-water features to each side of the plateau was undertaken using a variety of sampling gear. On the return track, a minor detour of about 8 n.m. to the north of the original line was made between 12° 27.0'S, 162° 57.0'W and 12° 38.0'S, 163° 19.0'W to obtain additional bathymetric data. A bathymetric profile of the transect showing station locations and station data is shown in Figure 2.

A SW-NE transect employing seismics, gravity, magnetics and bathymetry was then carried out from Stn U310 to Rakahanga and Manihiki (Figure 3). The transect passed over the position of DSDP hole 317 in order that the seismic stratigraphy could be correlated with drill hole data. An unusual piercement structure was recorded in the thick sedimentary sequence which was originally attributed to the occurrence of mud volcanoes (Hill et al., 1990; Coulbourn and Hill, 1991), but subsequently shown to be ocean island basalts (Beiersdorf et al., 1995).

A sampling program was then undertaken around Rakahanga and Manihiki in an attempt to locate manganese crusts around the slopes of those islands. For this reason, rock dredges were deployed at various depths around the islands. It was noted that a shoulder on the volcanic slope of Manihiki immediately south of the island shown on the NZOI Manihiki and Rakahanga chart and based on two spot soundings is an artifact. A pipe dredge and bottom camera station was also taken in the deep water east of Manihiki to examine the occurrence of manganese nodules at the base of the slope of the plateau (Figure 4).

A profiling transect was then undertaken to Pukapuka. This profile included only magnetics and bathymetry and began and concluded with a radar fix on an adjacent island. Gravity data acquisition was suspended while the SATNAV was out of operation because of the high positional accuracy required for reduction of such data.

A sampling program was then carried out around Pukapuka, Tema Reef and Nassau, again in an attempt to locate manganese crusts (Figure 5). Rock dredges were therefore deployed at various depths around the islands. Stn U324, taken approximately 0.15 n.m. from the reef on the western end of Pukupuka (Danger Island), proved particularly exciting. Deep stations were also taken to the east and west of Nassau to examine the occurrence of manganese nodules there. The ship was then underway to Pago Pago.

On leaving Nassau, a slight deviation in the ship's route was made in order to investigate a geoid anomaly observed in SEASAT/GEOS-3 satellite altimeter data. As suspected, the anomaly represented a previously unmapped

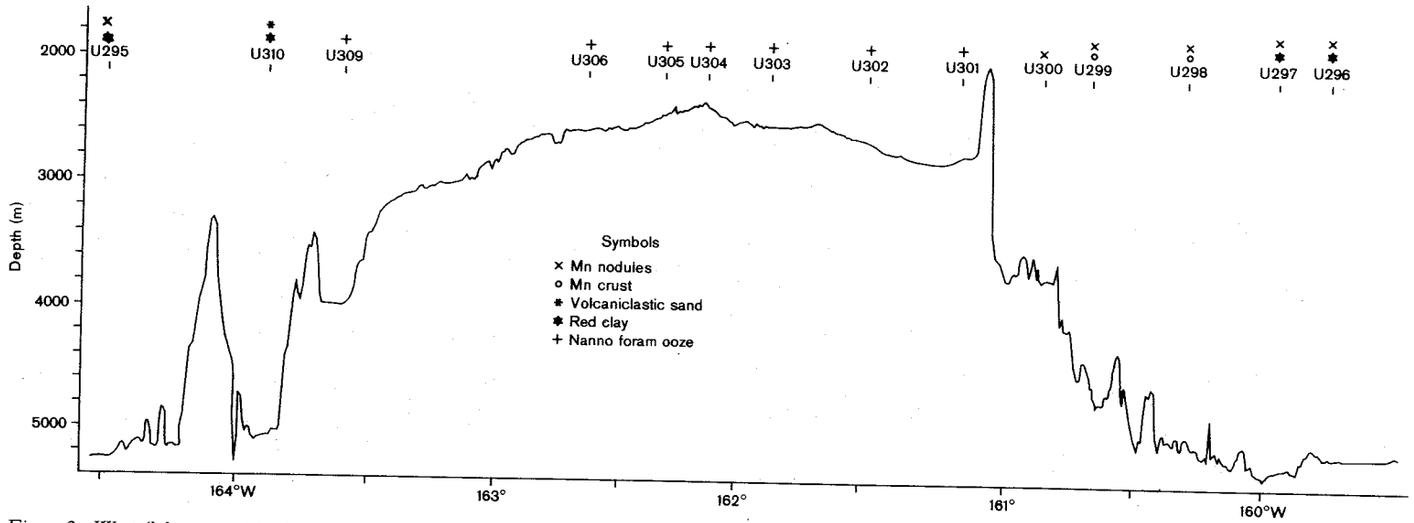

Figure 2. West (left) to east (right) transect across the Manihiki Plateau at 12°45′ S. Lat. showing bathymetry (VE 54×), station locations, and type of sample.

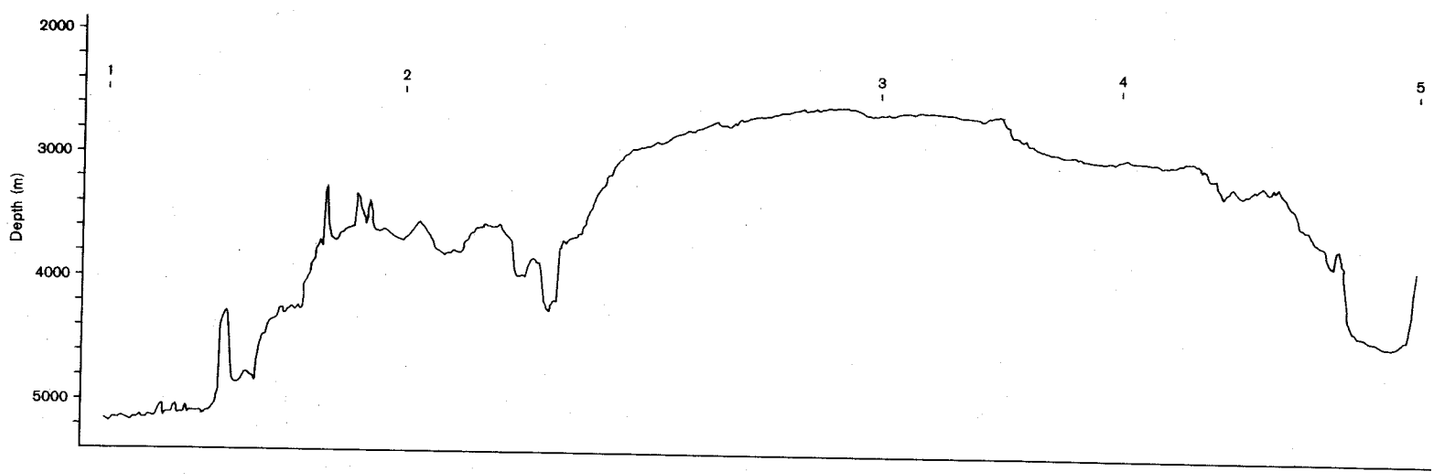

Figure 3. SW (left) to NE (right) transect of the Manihiki Plateau; numbers above the bathymetric profile represent way points. Their positions are as follows:

1. 12°47.8′ S 163°54.1′ W
2. 11°50.0′ S 164°54.0′ W
3. 11°00.1′ S 162°15.8′ W (DSDP site 317)
4. 10°30.0′ S 161°36.0′ W
5. 10°00.0′ S 160°37.0′ W

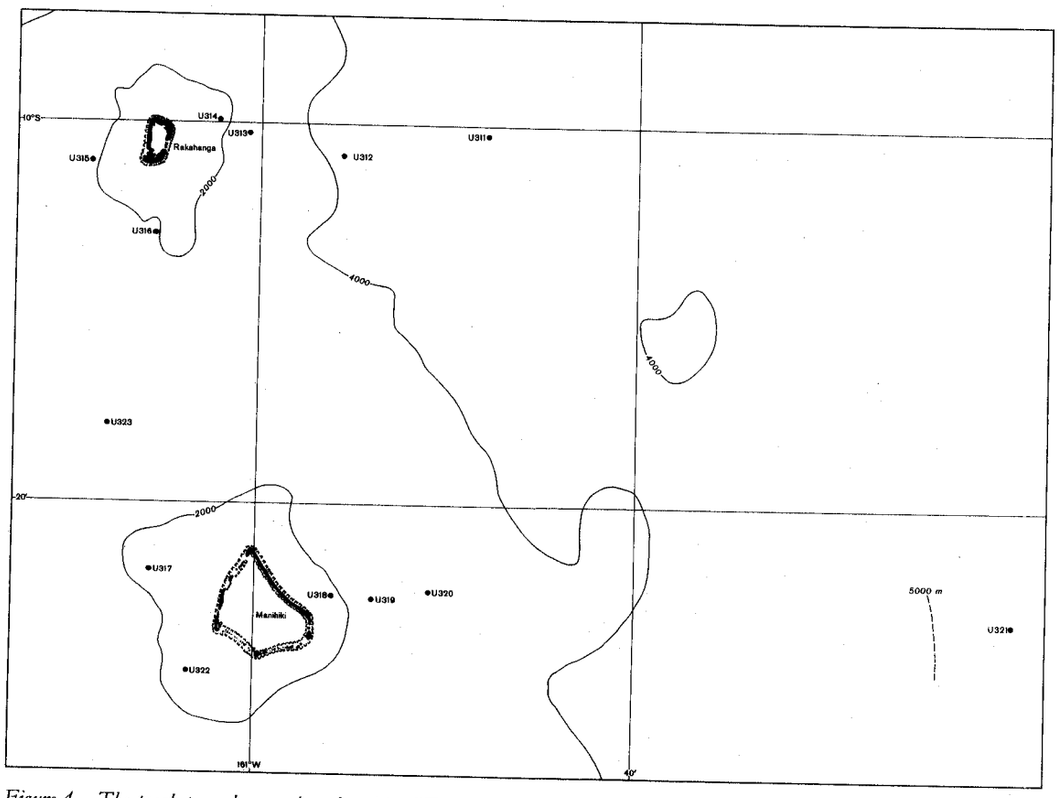

Figure 4. The track passed over a broad positive SEASAT gravity anomaly, which was found to coincide with a basement high. A 600 m-high fault scarp (at 16° 55'S 171° 31'W) formed the ?WNW-trending northern edge of this basement block.

seamount. This seamount, designated as T1, is located in the Samoan Basin at 12° 25.2'S, 166° 27.9'W, and is 2825 m high (Hill and Baudry, 1992). At Pago Pago, the CCOP/ SOPAC SATNAV was installed.

From Pago Pago, the ship proceeded to Machias Seamount recording gravity, magnetics and bathymetry. At Machias Seamount, seven rock dredges were attempted (six successful) to study the distribution of rock type with water depth. Samples were obtained between 670-4077 m. The shallowest depth recorded for the seamount was 616 m at 14° 57.9'S, 172° 13.6'W. A bathymetric profile across the seamount is shown in Figure 6. Results of this work have been published by Hill (1989), Coulbourn et al. (1980), Hill et al. (1989b), and Hill and Tiffin (1993).

From Machias Seamount to Capricorn Seamount, gravity, magnetics and bathymetry were recorded. The track passed over a SEASAT gravity anomaly, which was found to coincide with a basement high. A 600 m-high fault scarp at 16° 55'S, 171° 39'W forms the ?WNW-trending northern edge of this block. At Capricorn Seamount, E-W and S-N geophysical transects (seismic reflection, gravity, magnetic and bathymetry) were undertaken across the seamount (Figures 7, 8). Seven rock dredges (six successful) were then attempted at a range of depths (942-4689 m) on the seamount.

From Capricorn Seamount to Niue, gravity, magnetics and bathymetry were recorded. One piston core (U353) was attempted. Although unsuccessful, the short (trigger) corer contained two manganese nodules in the core catcher which suggested a high abundance of manganese nodules.

Around Niue, a detailed seismic, gravity, magnetic and bathymetry profile was undertaken. Five rock dredges were then undertaken (four successful) in the depth range 346-2456 m (Figure 9). The shallowest samples taken on the SW side of the island were an attempt to deduce the lithology of the volcanic edifice of Niue. An error in the position of Niue in the NZOI Niue Chart was noted, the charted position 1.6 n.m. north of its actual position.

It was then intended to take a series of piston cores on a transect from Niue to Tofua and one such core (U359) was obtained. At Stn U360, however, successive attempts with a pipe dredge (U360c) and a gravity corer (U360d) resulted in the loss of the sampling equipment together with a substantial amount of wire. This effectively ended the ship's deep-sea sampling capability. The ship then headed towards Tofua via Capricorn Seamount. A minimum depth for Capricorn Seamount was recorded on this run (447 m at 18° 37.8'S, 172° 06.4'W). This compares to 395 m recorded by Brodie (1965) for the "smaller flat-topped knoll" on the top of the seamount. A detailed seismic,

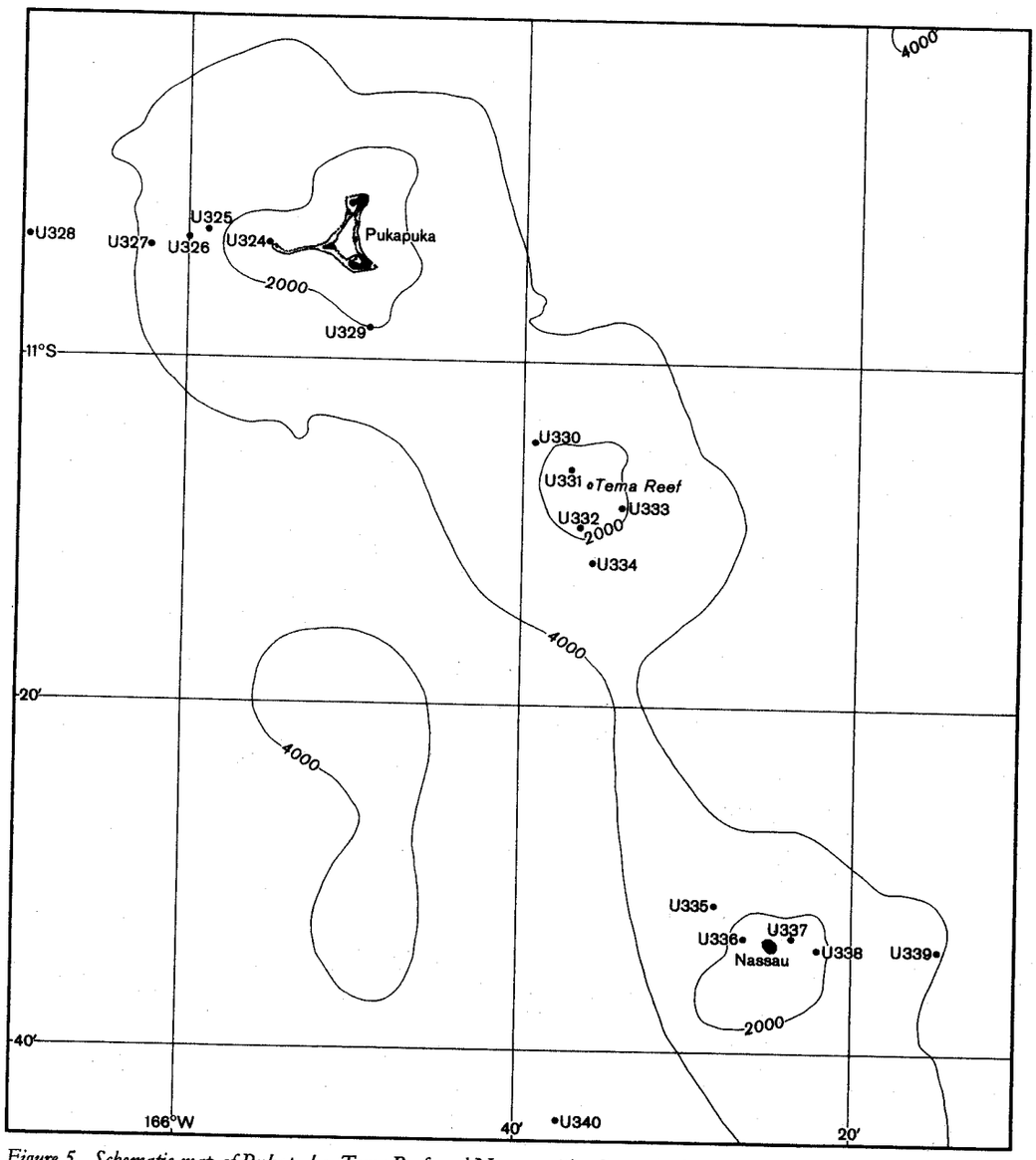

Figure 5. Schematic map of Pukapuka, Tema Reef, and Nassau with adjacent bathymetry and station locations.

Table 1. Summary of station success.

Gear	No. of Stns	Successful	Unsuccessful[1]
Bottom camera	6	5	1
Piston, gravity corers	5	2	3
Short corer	1	1	0
Pipe dredge	19	18	1
Rock dredge[2]	76	61	15
TOTAL	**107**	**87**	**20**

[1] no sample/photo return or gear lost; lost 3 rock dredges, 1 pipe dredge, 1 gravity corer (3.3 m), 1 wide-mouthed block, 6750 m of 14 mm wire and 5300 m of 9 mm wire

[2] during sampling in the southern Cook Islands, only the rock dredge was used; 16 of 19 dredging attempts were successful

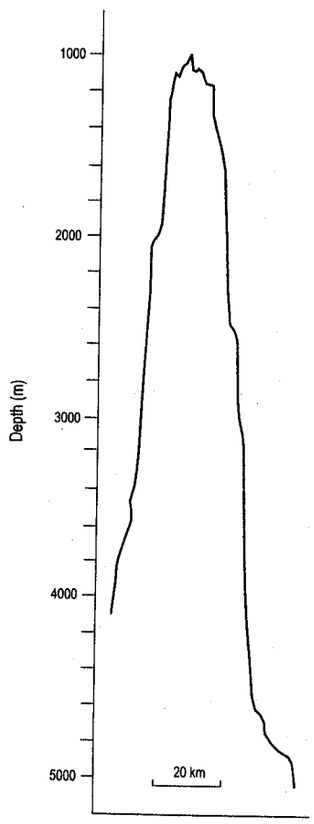

Figure 6. NW-SE bathymetric profile across Machias Seamount from 14°51.5' S, 172°21.0' W to 15°10.6' S, 172°00.2' W. Gradient of right-hand slope is 0.12 (7°).

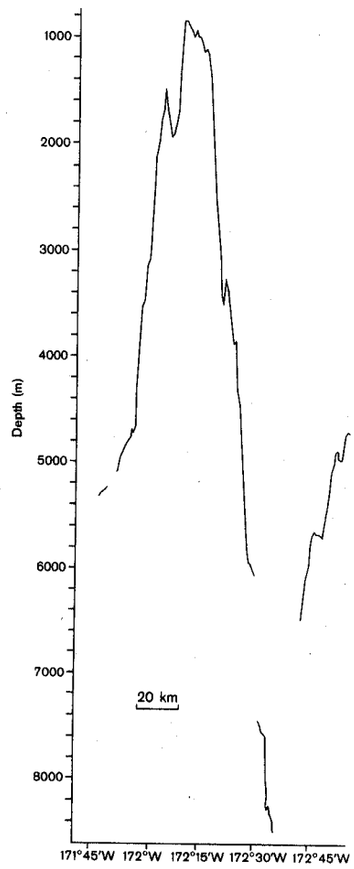

Figure 7. E-W bathymetric profile across Capricorn Seamount and Tonga Trench from 18°44.1' S, 171°48.4' W to 18°27.0' S, 172°54.4' W. Gradient of right-hand slope is 0.17 (10°).

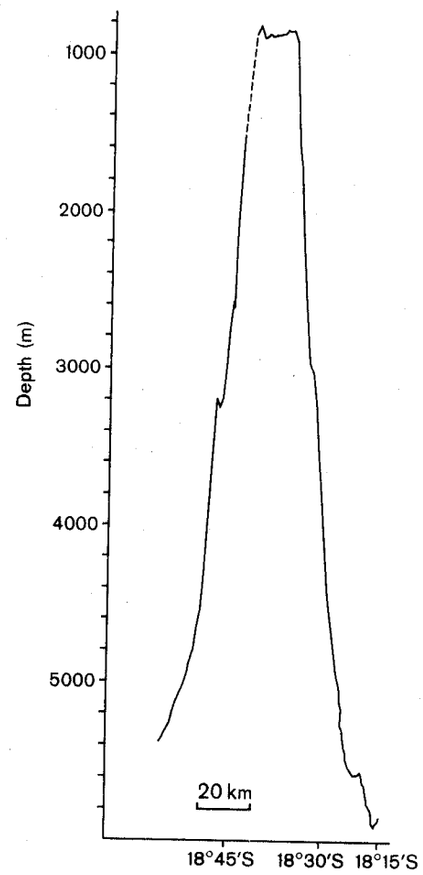

Figure 8. S-N bathymetric profile across Capricorn Seamount from 18°56.1' S, 172°17.9' W to 18°12.0' S, 172°06.5' W. Gradient of right-hand slope is 0.14 (8°).

gravity, magnetic and bathymetric profile was then run across the Tofua Trough, in part to deduce the volcanic ash thickness and stratigraphy in the Trough.

SUMMARY OF SAMPLES AND DATA COLLECTED

Overall, an 81% success rate was obtained for the sampling gear during the cruises, the pipe dredge (which samples mainly sediment and manganese nodules) and the bottom camera being particularly successful (Table 1). For the rock dredge, a higher success rate was obtained later in the cruise around Machias Seamount, Capricorn Seamount and Niue (89%) than earlier in the cruise around the islands of the Manihiki Plateau (74%). This presumably reflects on improvement in technique during the cruise.

The success rates determined for rock dredging are misleading, however, in as much as many of the hauls contained only a few pebbles. The difficulty of sampling in steep volcanic terrain is a major factor in reducing the success rate of rock dredging. Many of the better hauls contained coral rubble but samples of volcanic rock were much more difficult to recover. In part, this is a result of the relative lightness of the NZOI rock dredges and the fact that a 14 mm wire was used. Even attempts to dredge talus at the base of slopes rather than the steeper rock faces met with limited success. It is therefore felt that more robust dredging gear than used here is required if truly satisfactory results are to be obtained in this type of terrain. Nonetheless, in spite of the inevitable sampling bias that the limited dredging success rate entails and the limited sampling time available for the surveys around these islands and seamounts, it is considered unlikely that we failed to locate any major deposit of thick manganese crusts.

Bathymetric, gravity (4100 km), and magnetic data (5200 km) were collected in transit between station clusters, except for the southern Cook Islands, where only bathymetric profiling was conducted. Additionally, 2200

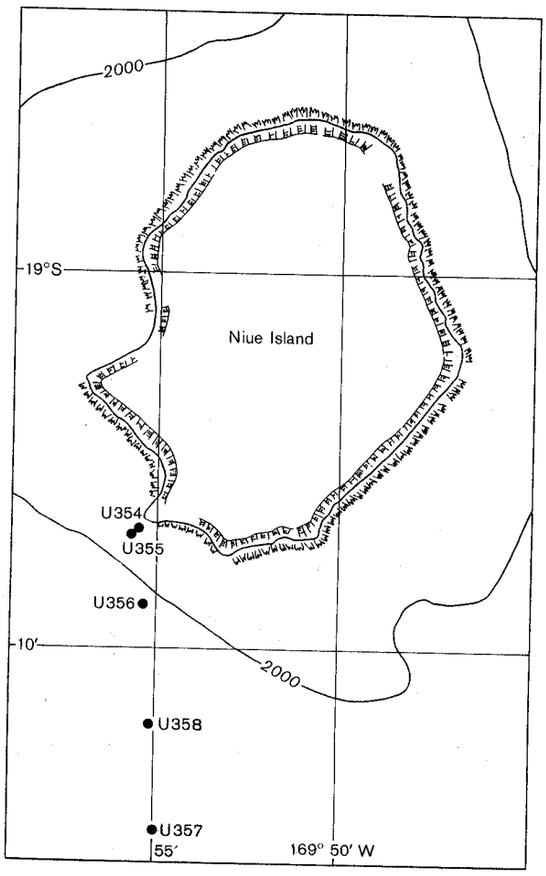

Figure 9. Schematic map of Niue and adjacent bathymetry with station locations.

km of good quality single-channel seismic reflection profile records were obtained using an air-gun. These include a S-N traverse approaching Suwarrow, a W-E traverse across the Manihiki Plateau along 12°45' S.Lat., a SW-NE traverse from the Samoan Basin to Rakahanga over DSDP site 317 (to allow correlation of reflectors with drill-hole stratigraphy), N-S and E-W crossings of Capricorn Seamount, short runs around Niue, a zig-zag pattern southward along the Tofua Trough, and a crossing of a fracture zone near the Tonga-Kermadec Trench between Tonga and New Zealand, the latter obtained during the post-cruise return voyage from Nuku'alofa to Auckland.

SOUTHERN COOK ISLANDS

The southern Cook Islands are part of a linear island chain, the Cook - Austral chain, extending 2000 km in a NW-SE direction. The geology of several of these islands has been mapped (Wood and Hay, 1970) and magnetic surveys carried out (Lumb and Carrington, 1971). K-Ar dating of volcanic rocks has been used to determine the geological history of the chain (Dalrymple et al., 1975; Turner and Jarrard, 1982; Duncan and Clague, 1985). The height of the Cook - Austral swell has been discussed by Crough (1978, 1984). McNutt and Menard (1978) have reported on the uplift of several of these islands and these ideas have been discussed by Jarrard and Turner (1979). Four uncharted seamounts have been postulated along the chain based on satellite altimeter data (Lambeck and Coleman, 1982).

Nonetheless, surprisingly little information exists on the offshore areas of these islands. Summerhayes (1967) discussed the offshore geology based principally on bathymetric data collected during the 1965 Eclipse expedition. Bäcker et al. (1976) reported some thin manganese encrustations from the base of the Rarotonga volcano. More recently, Lewis et al. (1980) studied the reef terrace of Rarotonga. However, there appears to have been no systematic attempt to dredge around these islands.

During 1986, HMNZS *Tui* visited the southern Cook Islands as part of Exercise Joint Venture. The opportunity was taken to dredge the flanks of these islands at various depths. The objectives of this cruise were as follows:

1. To establish if there are any manganese crusts or any manganese staining on rocks on the flanks of the islands;
2. To examine the extent of slumping of reef material down the slope of the islands;
3. To examine the nature of the volcanic rocks that make up the islands.

During the period 21-30 July, HMNZS *Tui* occupied 19 stations, of which 16 were successful. The stations were around Mauke Island (4), Monowai Seamount (1), Mitiaro (4), and Rarotonga (10). Because of rough weather, a dredge was lost on Monowai Seamount and fewer stations were occupied than had been anticipated. Amongst other things, this meant that no samples were collected from the flanks of seamounts in the region. Station data are included in Appendix B.

ACKNOWLEDGEMENTS

We are particularly indebted to the Captain of HMNZS *Tui*, Lt. Commander M.D. Lloyd, and the officers and crew of the *Tui* for the very considerable assistance given to the scientific program which enabled the program to be maintained in spite of the considerable difficulties encountered.

For the HMNZS *Tui* Exercise Joint Venture, we thank the Captain of HMNZS *Tui*, Lt. Commander R.D. Cass, and the officers and crew of *Tui* who carried out this program. Mr Tom Wichman of the Scientific Research Division of the Prime Minister's Department (Cook Islands) acted as Chief Scientist and Mr Aturangi Hosking of the Survey Department (Cook Islands) as Assistant Scientist.

REFERENCES CITED

Anonymous, 1984, Agreement between the governments of New Zealand, Australia and the United States of America in co-operation with the Committee for the Co-ordination of Joint Prospecting for Mineral Resources in South Pacific Offshore Areas relating to the conduct of a joint programme of marine geoscientific research and mineral resource studies of the South Pacific region Second Phase: New Zealand Treaty Series 1984, No. 21, 44 p.

Aplin, A.C., and D.S. Cronan, 1985, Manganese oxide deposits from the central Pacific Ocean, I. Encrustations from the Line Islands Archipelago: Geochimica et Cosmochimica Acta, v.49, p.427-436.

Bäcker, H., G.P. Glasby, and M.A. Meylan, 1976, Manganese nodules from the Southwestern Pacific Basin: NZOI Oceanographic Field Report, No. 6, 88 p.

Beiersdorf, H., ed., 1990, Geoscientific investigations at the Manihiki-Plateau: Final Report, R/V *Sonne* Research Cruise SO 67-1, BGR/SOPAC.

Beiersdorf, H., and Erzinger, J., 1989, Observations on the bathymetry and geology of the northeastern Manihiki Plateau, southwestern Pacific Ocean: South Pacific Marine Geology Notes, v.3(4), p.33-46.

Beiersdorf, H., W. Bach, R. Duncan, J. Erzinger, and W. Weiss, 1995, New evidence for the production of EM-type ocean island basalts and large volumes of volcaniclastites during the early history of the Manihiki Plateau: Marine Geology, v.122, p.181-205.

Bezrukov, P.L., 1971, The main scientific results of the 48th voyage of the R/V Vityaz in the Pacific Ocean (May to September, 1970): Oceanology, v.11, p.457-463.

Berzrukov, P.L., 1973, On the sedimentation in the northern part of the South Pacific, *in* R. Fraser, comp., Oceanography of the South Pacific 1972: Wellington, New Zealand National Commission for UNESCO, p.217-219.

Carlson, R.L., N.L. Christensen, and R.P. Moore, 1980, Anomalous crustal structures in ocean basins: Continental fragments and oceanic plateaus: Earth and Planetary Science Letters, v.51, p.171-180.

Clark, A.K., P. Humphrey, C.J. Johnson, and D.K. Pak, 1985, Resource assessment: Cobalt-rich manganese crust potential: U.S. Department of the Interior, Minerals Management Service, OCS Study MMS 85-0006, 35 p. + 6 plates.

Coulbourn, W.T., and P.J. Hill, 1991, A field of volcanoes on the Manihiki Plateau: Mud or lava?: Marine Geology, v.98, p.367-388.

Coulbourn, W.T., P.J. Hill, and D.D. Bergersen, 1989, Machias Seamount: Sediment remobilization, tectonic dismemberment and subduction of a guyot: Geo-Marine Letters, v.9, p.119-125.

Cronan, D.S., 1984, Criteria for the recognition of areas of potentially economic manganese nodules and encrustations in the CCOP/SOPAC region of the central and southwestern tropical Pacific: South Pacific Marine Geology Notes, v.3(1), p.1-17.

Crough, S.T., 1978, Thermal origin of mid-plate hot-spot swells: Geophysical Journal of the Royal Astronomical Society, v.55, p.45-469.

Crough, S.T., 1984, Seamounts as recorders of hot-spot epeirogeny: Geological Society of America Bulletin, v.95, p.3-8.

Cullen, D.J., and W.C. Burnett, 1986, Phosphorite associations on seamounts in the tropical southwest Pacific Ocean: Marine Geology, v.71, p.215-236.

Dalrymple, G.B., R.D. Jarrard, and D.A. Clague, 1975, K-Ar ages for some volcanic rocks from the Cook and Austral islands: Geological Society of America Bulletin, v.86, p.1463-1467.

Duncan, R.A., and D.A. Clague, 1985, Pacific plate motion recorded by linear volcanic chains, *in* A.E.M. Nairn, F.G. Stehli, and S. Uyeda, eds., The ocean basins and margins, vol. 7A, New York, Plenum Press, p.89-121.

Exon, N.F., 1981, Manganese nodules in the Cook Islands region, southwest Pacific: South Pacific Marine Geology Notes, v.2(4), p.47-65.

Glasby, G.P., 1986, Marine minerals in the Pacific: Oceanography and Marine Biology Annual Review, v.24, p.11-64.

Halbach, P., and F.T. Manheim, 1984, Potential of cobalt and other metals in ferromanganese crusts on seamounts of the Central Pacific Basin: Marine Mining, v.4, p.319-336.

Halbach, P., F.T. Manheim, and P. Otten, 1982, Co-rich ferromanganese deposits in the marginal seamount regions of the Central Pacific Basin - results of the Midpac '81 Expedition: Erzmetall, v.35, p.447-453.

Heezen, B.C., B. Glass, and H.W. Menard, 1966, The Manihiki Plateau: Deep-Sea Research, v.13, p.445-458.

Hein, J.R., F.T. Manheim, W.C. Schwab, and A.S. Davis, 1985, Ferromanganese crusts from Necker Ridge, Horizon Guyot and S.P. Lee Guyot: Geological considerations: Marine Geology, v.69, p.25-54.

Hein, J.R., L.A. Morgenson, D.A. Clague, and R.A. Koski, 1987, Cobalt-rich ferromanganese crusts from the Exclusive Economic Zone of the United States and nodules from the oceanic Pacific, *in* D.W. Scholl, A. Grantz, and J.G., Vedder, eds., Geology and resource potential of the continental margin of western North America and adjacent ocean basins - Beaufort Sea to Baja California: Circum-Pacific Council for Energy and Mineral Resources, Earth Science Series, v.6, p.753-771.

Henderson, L.J., and R.G. Gordon, 1981, Oceanic plateaus and the motion of the Pacific plate with respect to the hotspots [abstract]: EOS Transactions of the American Geophysical Union, v.62, p.1028.

Hill, P.J., 1989, Subduction at the northern Tonga Trench – recent SeaMARC II, GLORIA and geophysical results: BMR Research Symposium 'Geoscience Mapping towards the 21st Century', 7p. (extended abstract).

Hill, P.J., and D.L. Tiffin, 1993, Geology, sediment patterns, and widespread deformation on the sea floor off Western Samoa revealed by wide-swath imagery: Geo-Marine Letters, v.13, p.116-125.

Hill, P.J., and N. Baudry, 1992, Southwest Pacific seamounts revealed by satellite altimetry, *in* B.H. Keating and B.R Bolton, eds; Geology and offshore mineral resources of the Central Pacific Basin: Circum-Pacific Council for Energy and Mineral Resources, Earth Science Series, v.14, p.69-76.

Hill, P.J., W.T. Coulbourn, G.P. Glasby, M.A. Meylan, and Shipboard Scientists, 1989a, Manihiki Plateau: Results of recent SeaMARC II, geophysical and seafloor sampling investigations: Programme and Abstracts Volume for the JointCCOP/SOPAC–IOC Fourth International Workshop on Geology, Geophysics and Mineral Resources of the South Pacific, Canberra, CCOP/SOPAC Miscellaneous Report 79, p.58-62.

Hill, P.J., W.T. Coulbourn, G.P. Glasby, M.A. Meylan, and Shipboard Scientists, 1989b, Subduction of Capricorn and Machias guyots: Structural and sedimentological processes: Programme and Abstracts Volume for the Joint CCOP/SOPAC–IOC Fourth International Workshop on Geology, Geophysics and Mineral Resources of the South Pacific, Canberra, CCOP/SOPAC Miscellaneous Report 79, p.63-67.

Hill, P.J., W.T. Coulbourn, G.P. Glasby, and M.A. Meylan, 1990, Manihiki Plateau - results of recent resource-oriented shipboard investigations and discovery of a major ?mud volcano complex: Pacific Rim Congress 90, Proceedings, Vol. III, p.163-171 + p.C9.

Horn, D.R., B.M. Horn, and M.N. Delach, 1972, Ocean manganese nodules: Metal values and mining sites: U.S. International Decade of Ocean Exploration, Technical Report No. 4, 57 p.

Hussong, D.M., L.K Wipperman, and L.W. Kroenke, 1979, The crustal structure of the Ontong Java and Manihiki oceanic plateaus: Journal of Geophysical Research, v.84B, p.6003-6010.

Jarrard, R.D., and D.L. Turner, 1979, Comments on 'lithospheric flexure and uplifted atolls' by M. McNutt and H.W. Menard: Journal of Geophysical Research, v.84, p.5691-5694.

Jenkyns, H.C., 1976, Sediments and sedimentary history of the Manihiki Plateau, South Pacific Ocean, *in* Initial Reports of the Deep-Sea Drilling Project, v.33: Washington, D.C., U.S. Government Printing Office, p.873-890.

Lambeck, K., and R. Coleman, 1982, Verification of bathymetric charts from satellite altimeter data in the region of the Cook Islands: New Zealand Journal of Science, v.25, p.183-194.

Lewis, K.B., A.T. Utanga, P.J. Hill, and S.G. Kingan, 1980, The origin of channel-fill sands and gravels on an algal-dominated reef terrace, Rarotonga, Cook Islands: South Pacific Marine Geological Notes, v.2(1), p.1-23.

Lonsdale, P., 1981, Drifts and ponds of reworked pelagic sediment in part of the southwest Pacific: Marine Geology, v.43, p.153-193.

Lumb, J.T., and L. Carrington, 1971, Magnetic surveys in the south-west Pacific and rock sampling for magnetic studies in the Cook Islands: Bulletin of the Royal Society of New Zealand, v.8, p.81-89.

McNutt, M., and H.W. Menard, 1978, Lithospheric flexure and uplifted atolls: Journal of Geophysical Research, v.83, p.1206-1212.

Mahoney, J.J., 1984, A Nd and Sr isotopic study of Pacific Ocean plateaus: Initial results [abstract]: EOS Transactions of the American Geophysical Union, v.65, p.297.

Manheim, F.T., 1986, Marine cobalt resources: Science, v.232, p.600-608.

Maxwell, J.C., 1985, What is the lithosphere?: Physics Today, v.30(9), p.32-40.

Menard, H.W., 1964, Marine geology of the Pacific: New York, McGraw-Hill, 271 p.

Mero, J.L., 1965, The mineral resources of the sea: Amsterdam, Elsevier, 312 p.

Mizuno, A., and S. Nakao, eds., 1982, Regional data on manganese nodules, geophysics, and manganese nodules: The Wake-Tahiti transect in the Central Pacific, January-March 1980 (GH80-1 Cruise): Geological Survey of Japan, Cruise Report No. 18, 399 p.

Nur, A., and Z. Ben-Avraham, 1982, Oceanic plateaus, the fragmentation of continents, and mountain building: Journal of Geophysical Research, v.87B, p.3644-3661.

Schlanger, S.O., H.C. Jenkyns, and I. Premoli-Silva, 1981, Volcanism and vertical tectonics in the Pacific Basin related to global Cretaceous transgressions: Earth and Planetary Science Letters, v.52, p.435-449.

Summerhayes, C.P., 1967, Bathymetry and topographic lineation in the Cook Islands: New Zealand Journal of Geology and Geophysics, v.10, p.1382-1399.

Turner, D.L., and R.D. Jarrard, 1982, K-Ar dating of the Cook-Austral island chain: A test of the hot-spot hypothesis: Journal of Volcanology and Geothermal Research, v.12, p.187-220.

Usui, A., 1983, Regional variation of manganese nodule facies on the Wake-Tahiti transect: Morphological, chemical and mineralogical study: Marine Geology, v.54, p.27-51.

Usui, A., and T. Mochizuki, 1982, Regional variation of manganese nodule chemistry from Wake to Tahiti, GH80-1 cruise: Geological Survey of Japan, Cruise Report No. 18, p.338-354.

Watts, A.B., J.H. Bodine, and N.M. Ribe, 1980, Observations of flexure and the geological evolution of the Pacific Ocean Basin: Nature, v.283, p.532-537.

Winterer, E.L., 1976, Anomalies in the tectonic evolution of the Pacific: American Geophysical Union, Geophysical Monograph, v.19, p.269-278.

Winterer, E.L., P.F. Lonsdale, J.L. Matthews, and B.R. Rosendahl, 1974, Structure and acoustic stratigraphy of the Manihiki Plateau: Deep-Sea Research, v.21, p.793-814.

Wood, B.L., and R.F. Hay, 1970, Geology of the Cook Islands: New Zealand Geological Survey Bulletin, n.s., 82, 103 p.

APPENDIX A
WAY POINTS USED IN SETTING SHIP'S TRACK

Rarotonga - Suwarrow

18° 23.0'S	160° 57.0'W
17° 52.0'S	161° 38.0'W
16° 18.0'S	162° 00.0'W
14° 07.0'S	162° 15.0'W
13° 15.0'S	162° 47.0'W
13° 15.0'S	163° 00.0'W
13° 00.0'S	163° 09.0'W

Transect of Manihiki Plateau at 12° 45'S (W-E)

12° 45.0'S	164° 30.0'W
12° 45.0'S	159° 45.0'W

Stn U310 - Rakahanga / Manihiki

12° 48.8'S	163° 54.1'W
12° 30.0'S	164° 05.0'W
11° 50.0'S	163° 54.0'W
11° 00.1'S	162° 15.8'W (DSDP hole 317)
10° 30.0'S	161° 36.0'W
10° 00.0'S	160° 37.0'W

Rakahanga / Manihiki-Pukapuka

10° 15.7'S	161° 07.7'W (U323)
11° 00.0'S	164° 30.0'W
10° 55.3'S	165° 34.3'W
10° 42.1'S	165° 45.4'W
10° 55.9'S	165° 52.8'W

Pukapuka - Pago Pago

12° 30.0'S	166° 40.0'W
13° 10.0'S	168° 11.0'W

Pago Pago - Machias Seamount

14° 46.0'S	172° 05.0'W
15° 13.0'S	172° 22.5'W

Machias Seamount - Capricorn Seamount

14° 51.0'S	172° 20.7'W
15° 13.0'S	172° 00.0'W
17° 15.0'S	171° 36.0'W
17° 46.0'S	171° 36.0'W

Capricorn Seamount

18° 47.5'S	171° 42.0'W
18° 39.0'S	172° 12.0'W
18° 28.0'S	172° 54.0'W
18° 58.0'S	172° 17.5'W
18° 39.0'S	172° 12.0'W
18° 16.5'S	172° 06.0'W

Niue (Positions taken from N.Z. Oceanographic Insitute Chart of Niue)

18° 54.2'S	169° 55.6'W
18° 54.2'S	169° 26.0'W
19° 16.0'S	169° 26.0'W
19° 06.0'S	169° 48.7'W
19° 17.0'S	169° 56.7'W
19° 06.7'S	169° 55.7'W
19° 07.8'S	169° 59.4'W
19° 03.1'S	169° 57.5'W
19° 02.1'S	170° 01.7'W

Niue - Nuku'alofa

18° 37.0'S	172° 00.0'W
18° 39.0'S	172° 12.0'W
19° 26.0'S	174° 00.0'W
19° 26.0'S	174° 12.3'W
19° 03.0'S	174° 43.2'W
19° 25.5'S	174° 36.0'W
19° 25.0'S	175° 10.3'W
19° 42.5'S	174° 35.6'W
19° 42.5'S	175° 02.0'W
19° 54.2'S	174° 49.8'W
19° 50.0'S	175° 22.0'W
20° 08.5'S	174° 57.0'W
20° 11.5'S	175° 22.0'W

APPENDIX B
STATION SUMMARY

Stn	Lat. S	Long. W	Depth (m)[1]	Bottom Topography	Gear	Results[2]
U291	14°17.1'-14°17.1'	162°10.1'-162°10.5'	1377-1407	Slope of seamount south of Manihiki Plateau	Rock dredge	Lost
U292	12°55.8'-12°56.0'	163°08.8'-163°08.9'	3036-3026	North of Suwarrow on Manihiki Plateau	Rock dredge	L, R
U293	13°14.3'	162°48.2'	2921-2916	Eastern slope of Suwarrow on Manihiki Plateau	Pipe dredge	S
U294	13°15.1'-13°15.1'	163°28.3'-163°28.4'	3829	Southern slope of Manihiki Plateau, west of Suwarrow	Pipe dredge	S, V
U295	12°45.2'-12°45.1'	164°30.7'-164°30.7'	5283	Deep basin adjacent to abyssal hills, west of Manihiki Plateau in Samoan Basin	Pipe dredge	N, S
U296a	12°44.7'-12°44.8'	159°44.4'-159°44.9'	5130	Small sediment pond within abyssal hills, Penrhyn Basin	Pipe dredge	B, N, S
U296b	12°44.4'	159°45.0'	5119	Small sediment pond within abyssal hills, Penrhyn Basin	Bottom camera	28 exposures
U297a	12°44.2'	159°55.3'	5227	Sediment-covered horst ca. 10 km across, elevated about 50-100 m above adjacent abyssal hills, Penrhyn Basin	Short corer	0.5 m sediment core
U297b	12°43.9'-12°44.3'	159°56.5'-159°56.6'	5330-5320	Sediment-covered horst ca. 10 km across, elevated about 50-100 m above adjacent abyssal hills, Penrhyn Basin	Bottom camera	10 exposures
U298	12°45.5'-12°45.3'	160°15.9'-160°16.5'	4996	Lower slope of eastern margin of Manihiki Plateau	Pipe dredge	C, N, S, V
U299a	12°47.7'-12°47.8'	160°41.2'-160°41.3'	4637	Lower slope of eastern margin of Manihiki Plateau	Rock dredge	N
U299b	12°45.1'-12°45.2'	160°42.8'-160°42.9'	4469-4464	Lower slope of eastern margin of Manihiki Plateau	Rock dredge	C
U300	12°45.8'-12°45.8'	160°51.3'-160°51.4	3747-3758	Narrow undulating terrace on eastern slope of Manihiki Plateau	Rock dredge	B, N
U301	12°42.1'-12°41.9'	161°09.8'-161°09.7'	2720	Eastern side of crest of Manihiki Plateau	Pipe dredge	B, S
U302	12°43.9'-12°43.9'	161°30.6'-161°30.7'	2630	Eastern side of crest of Manihiki Plateau	Pipe dredge	S
U303	12°44.8'-12°44.8'	161°49.9'-161°50.2'	2530	Eastern side of crest of Manihiki Plateau	Pipe dredge	S
U304a	12°45.2'-12°45.0'	162°05.3'-162°05.4'	2366	Eastern side of crest of Manihiki Plateau	Pipe dredge	S
U304b	12°43.2'-12°42.3'	162°03.4'-162°03.4'	2435	Eastern side of crest of Manihiki Plateau	Bottom camera	29 exposures
U305	12°49.6'-12°48.5'	162°16.1'-162°16.9'	2395-2385	Eastern side of 50 m-high pinnacle on crest of Manihiki Plateau	Pipe dredge	S
U306a	12°37.1'	162°41.1'	2460	Crest of Manihiki Plateau	Piston corer	2.18 m sediment core (but short corer empty)
U306b	12°37.1'	162°42.8'	2465	Crest of Manihiki Plateau	Bottom camera	0 exposures
U307	12°47.2'	163°31.4'	3586	Upper slope of western margin of Manihiki Plateau	Pipe dredge	B, L, S
U308a	12°46.9'-12°46.9'	163°33.3'-163°32.7'	3763-3707	Lower slope of western margin of Manihiki Plateau	Rock dredge	L
U308b	12°47.2'-12°47.3'	163°33.7'-163°33.5'	3991	Lower slope of western margin of Manihiki Plateau	Rock dredge	C, V
U309	12°46.3'-12°46.3'	163°36.4'-163°36.5'	4001	Flat sediment pond in trough just west of western margin of Manihiki Plateau	Pipe dredge	S
U310	12°48.9'-12°48.9'	163°54.2'-163°54.0'	5150	Small deep basin west of peak flanking western side of Manihiki Plateau	Pipe dredge	S
U311	10°00.6'-10°00.5'	160°47.9'-160°47.8'	4412	Gentle slope, deep basin east of Rakahanga	Pipe dredge	S
U312	10°01.8'-10°01.6'	160°55.6'-160°55.8'	4001-3971	Eastern slope of Rakahanga volcanic edifice, near base	Rock dredge	S
U313	10°00.5'-10°00.6'	161°00.6'-161°00.9'	2891-2640	Eastern slope of Rakahanga volcanic edifice	Rock dredge	Empty
U314	9°59.8-'9°59.9'	161°02.0'-161°02.2'	1843-1620	Eastern slope of Rakahanga volcanic edifice	Rock dredge	C
U315	10°02.0'-10°01.9'	161°09.0'-161°08.7'	1863-1535	SW slope of Rakahanga volcanic edifice	Rock dredge	C
U316a	10°05.8'-10°05.9'	161°05.6'-161°05.6'	2361-2387	SE slope of Rakahanga volcanic edifice	Rock dredge	Empty
U316b	10°05.8'-10°05.7'	161°05.4'-161°06.1'	2600	SE slope of Rakahanga volcanic edifice	Rock dredge	B, C, L(?), R, S, V, garnet xl
U317	10°23.7'-10°24.2'	161°05.6'-161°05.4'	2161-2111	Western slope of Manihiki Island volcanic edifice	Rock dredge	B, R, S, V, breccia, chert

Stn	Lat. S	Long. W	Depth (m)[1]	Bottom Topography	Gear	Results[2]
U318	10°24.8'-10°24.9'	160°56.0'-160°56.1'	1684-1555	Eastern slope of Manihiki Island volcanic edifice	Rock dredge	L, S
U319	10°24.8'-10°25.2'	160°53.6'-160°51.0'	2906-2911	Eastern slope of Manihiki Island volcanic edifice, just above base	Rock dredge	C, R
U320	10°24.3'-10°25.2'	160°50.5'-160°51.0'	3813-3788	Eastern slope of Manihiki Island volcanic edifice, near base	Rock dredge	S
U321a	10°23.5'-10°23.5'	160°20.9'-160°21.1'	5114-5047	Rolling abyssal hills east of Manihiki Island	Pipe dredge	B, N, S, V
U321b	10°23.1'-10°23.0'	160°21.7'-160°21.9'	5258	Rolling abyssal hills east of Manihiki Island	Bottom camera	25 exposures
U322a	10°29.2'-10°28.5'	161°03.0'-161°03.1'	1818-1570	SW slope of Manihiki Island volcanic edifice	Rock dredge	Empty
U322b	10°28.9'-10°28.3'	161°03.4'-161°03.1'	1754-1560	SW slope of Manihiki Island volcanic edifice	Rock dredge	B, C, L, S
U323	10°15.7'-10°15.8'	161°07.8'-161°07.5'	3066-2971	Northern slope of Manihiki Island volcanic edifice	Rock dredge	B, R, S, V
U324	10°53.0'-10°52.7'	165°55.2'-165°55.4'	417-446	Steep slope just west of Pukapuka westernmost reef	Rock dredge	B, L, R, S
U325	10°52.4'-10°52.6'	165°58.6'-165°57.9'	1585-1446	Western slope of Pukapuka volcanic edifice	Rock dredge	B, N, R
U326	10°52.8'-10°52.5'	166°00.0'-165°59.8'	2161-2121	Western slope of Pukapuka volcanic edifice	Rock dredge	B, C, S, V
U327	10°53.2'-10°53.3'	166°02.4'-166°01.6'	3394-3217	Western slope of Pukapuka volcanic edifice	Rock dredge	B, N, S, V
U328	10°52.9'-10°52.6'	166°09.4'-166°08.6'	4837-4796	Abyssal hills on slope near base of western side of Pukapuka volcanic edifice	Pipe dredge	L, N, R, S, V
U329	10°58.1'-10°57.9'	165°49.2'-165°48.9'	2825-2450	Eastern slope of Pukapuka volcanic edifice	Rock dredge	R
U330	11°04.6'-11°04.7'	165°39.2'-165°39.0'	2036-1833	NW slope of Tema Reef volcanic edifice	Rock dredge	Empty
U331	11°06.0'-11°06.2'	165°37.0'-165°36.6'	1407-1100	NW slope of Tema Reef volcanic edifice	Rock dredge	B, R
U332	11°09.4'-11°08.6'	165°36.6'-165°36.3'	1377-1199	SE slope of Tema Reef volcanic edifice	Rock dredge	B, C, L(?), R, S, V
U333a	11°08.2'-11°07.8'	165°33.8'-165°34.0'	1622-1656	SE slope of Tema Reef volcanic edifice	Rock dredge	Lost
U333b	11°08.3'-11°08.2'	165°34.0'-165°34.4'	1913-1575	SE slope of Tema Reef volcanic edifice	Rock dredge	B, C, R, S
U334	11°11.6'-11°11.5'	165°35.8'-165°35.6'	2916-2851	Southern slope of Tema Reef volcanic edifice	Rock dredge	R
U335a	11°31.2'-11°31.7'	165°28.4'-165°28.0'	2545-2161	Northern slope of Nassau volcanic edifice	Rock dredge	R, V
U335b	11°31.1'-11°31.5'	165°28.3'-165°28.0'	2500-2251	Northern slope of Nassau volcanic edifice	Rock dredge	Empty
U336a	11°32.9'-11°32.7'	165°27.8'-165°26.8'	1431-1397	Northern slope of Nassau volcanic edifice	Rock dredge	Empty
U336b	11°33.3'-11°33.3'	165°26.7'-165°26.3'	1297-981	Northern slope of Nassau volcanic edifice	Rock dredge	C, S
U337	11°32.2'-11°33.4'	165°23.5'-165°23.8'	1001-884	Eastern slope of Nassau volcanic edifice	Rock dredge	B, R, S, chert nodule
U338a	11°33.6'-11°33.7'	165°21.3'-165°22.0'	1962-1744	Eastern slope of Nassau volcanic edifice	Rock dredge	Empty
U338b	11°34.0'-11°33.8'	165°21.9'-165°22.2'	1610-1694	Eastern slope of Nassau volcanic edifice	Rock dredge	Lost
U339	11°33.8'-11°34.2'	165°15.0'-165°14.9'	4204-4219	Abyssal plain at eastern base of Nassau volcanic edifice	Pipe dredge	B, N, S, V
U340	11°43.8'-11°44.4'	165°37.9'-165°36.9'	5268-5253	Abyssal plain west of Nassau volcanic edifice	Pipe dredge	B, N, S, V
U341a	15°04.2'	172°16.2'	2306-2316	SE slope of Machias Seamount	Rock dredge	Empty
U341b	15°04.2'	172°16.7'	2495-2500	SE slope of Machias Seamount	Rock dredge	B, L, R, V
U342	15°00.9'-15°00.5'	172°08.3'-172°12.2'	1350	Southern slope of Machias Seamount	Rock dredge	B, L(?), R
U343	14°56.2'-14°56.6'	172°15.1'-172°15.2'	730-715	NW side of Machias Seamount near crest	Rock dredge	B, L, R, S, V
U344	14°56.9'-14°57.3	172°14.2'-172°13.8'	675-670	Crest of Machias Seamount	Rock dredge	B, R, S, V
U345	14°56.1'-14°56.8	172°15.3'-172°14.6'	1972-2166	NW slope of Machias Seamount	Rock dredge	B, L, R, V
U346	14°51.1'-14°51.6	172°20.6'-172°20.1'	4077	NW slope of Machias Seamount, near base	Rock dredge	L, R, V, breccia
U347	18°24.3'-18°24.7'	172°13.8'-172°13.6'	3905-3864	NW slope of Capricorn Seamount	Rock dredge	S
U348	18°27.7'-18°26.5'	172°13.1'-172°12.5'	2825-2640	NW slope of Capricorn Seamount	Rock dredge	V
U349	18°31.5'-18°32.4'	172°11.5'-172°11.1'	1873-1853	NW slope of Capricorn Seamount	Rock dredge	V
U350	18°34.1'-18°34.5'	172°09.8'-172°08.8'	1021-922	Northern side of Capricorn Seamount crest	Rock dredge	R
U351a	18°39.1'-18°40.2'	172°12.2'-172°11.4'	996-976	Crest of Capricorn Seamount	Rock dredge	B, S, V

Stn	Lat. S	Long. W	Depth (m)[1]	Bottom Topography	Gear	Results[2]
U351b	18°39.7'-18°39.5'	172°10.8'-172°10.5'	942-932	Crest of Capricorn Seamount	Rock dredge	S, V
U352	18°54.4'-18°53.4'	172°11.2'-172°11.3'	4684-4689	SE slope of Capricorn Seamount	Rock dredge	L, R, S, V
U353	18°53.6'	177°28.7'	5495	Flat area between seamounts and rolling abyssal hills, Capricorn-Niue	Piston corer	Empty (but N, S in short corer)
U354	19°08.6'-19°08.6'	169°55.3'-169°55.0'	346-467	Steep slope off rocky SW point of Niue	Rock dredge	R
U355	19°08.7'-19°08.7'	169°55.6'-169°54.6'	586-487	SW slope of Niue volcanic edifice	Rock dredge	Empty
U356	19°10.2'-19°10.0'	169°55.0'-169°54.7'	1873-1100	SW slope of Niue volcanic edifice	Rock dredge	B, R
U357	19°16.8'-19°16.9'	169°55.2'-169°55.6'	3612-3596	Break in steep slope on south side of Niue volcanic edifice	Rock dredge	C, R, S, V
U358	19°13.5'-19°13.0'	169°54.8'-169°54.8'	2520-2450	SW slope of Niue volcanic edifice	Rock dredge	C, R
U359	19°05.3'	171°06.9'	5299	Flat trough between Niue and Capricorn Seamount	Piston corer	5.02 m sediment core (but short corer empty)
U360a	18°53.2'-18°52.3'	171°27.8'-171°29.6'	5495	Abyssal plain, Niue-Tofua transect	Bottom camera	20 exposures
U360b	18°51.2'	171°33.3'	5443	Abyssal plain, Niue-Tofua transect	Piston corer	Empty (as was short corer)
U360c	18°49.7'-18°49.5'	171°36.9'-171°37.2'	5495	Abyssal plain, Niue-Tofua transect	Pipe dredge	Lost, along with 4300 m of 9 mm wire
U360d	18°49.3'	171°38.7'	5485	Abyssal plain, Niue-Tofua transect	Gravity corer (3.3 m)	Lost, along with 5000 m of 14 mm wire
U361	20°13.0'	157°18.7'	1426-1516	SE slope of Mauke	Rock dredge	C
U362	20°15.9'	157°19.7'	685-626	SE slope of Mauke	Rock dredge	R, S
U363	20°16.2'	157°20.8'	2640-2780	SE slope of Mauke	Rock dredge	C, S, V
U364	20°15.3'	157°20.7'	1903-2062	SE slope of Mauke	Rock dredge	Empty
U365	20°10.5'	158°36.3'	750-890	Slope of Monowai Seamount	Rock dredge	Lost
U366	19°54.8'	157°40.0'	1101-1179	SE slope of Mitiaro	Rock dredge	B, R
U367	19°55.2'	157°39.3'	1744-1635	SE slope of Mitiaro	Rock dredge	C
U368	19°56.5'	157°37.6'	2161-2341	SE slope of Mitiaro	Rock dredge	Empty
U369	19°54.6'	157°38.3	2141-2441	SE slope of Mitiaro	Rock dredge	C, L
U370	21°10.5'	159°46.5'	1021-1080	NE slope of Rarotonga	Rock dredge	R, V
U371	21°09.4'	159°47.3'	1486-1516	NE slope of Rarotonga	Rock dredge	R, S, V
U372	21°07.8'	159°47.4'	2042-2092	NE slope of Rarotonga	Rock dredge	R, S
U373	21°06.5'	159°47.2'	2450-2490	NE slope of Rarotonga	Rock dredge	S
U374	21°08.2'	159°46.5'	1972-2012	NE slope of Rarotonga	Rock dredge	S
U375	21°18.2'	159°44.3'	1272	SE slope of Rarotonga	Rock dredge	B, C, R, S, V
U376	21°19.5'	159°42.7'	1992-1968	SE slope of Rarotonga	Rock dredge	L(?), R, S, V
U377	21°20.3'	159°41.6'	2450-2296	SE slope of Rarotonga	Rock dredge	B, R, S, V, phosphorite(?)
U378	21°21.8'	159°39.7'	3031-2961	SE slope of Rarotonga	Rock dredge	R, S
U379	21°18.4'	159°44.9'	715-824	SE slope of Rarotonga	Rock dredge	V

[1] Corrected with Matthew's Tables

[2] Abbreviations for sample types:

- B = biological material, including various shells, teeth, and other hard parts, but excluding corals and microfossils
- C = manganese crusts
- L = limestone, mostly foraminiferal
- N = manganese nodules
- R = coral, mostly reefal, but including deep-water and precious varieties
- S = sediment
- V = volcanic rock, mostly basalt, pumice, tuff

Part 2

GEOPHYSICAL SURVEYS

Hill, P.J., and G.P. Glasby, 1996. Capricorn Seamount - geology and geophysics of a subducting guyot, *in:* Meylan, M.A., and G.P. Glasby (eds) Manihiki Plateau, Machias and Capricorn Seamounts, Niue, and Tofua Trough: Results of *TIli* Cruises. SOPAC Technical Bulletin 10: 17-29.

CAPRICORN SEAMOUNT-GEOLOGY AND GEOPHYSICS OF A SUBDUCTING GUYOT

P.J. Hill

Australian Geological Survey Organisation, GPO Box 378, Canberra *ACT* 2601, Australia

G.P. Glasby

Department ofEanb Sciences, University of Sheffield, Sheffield S3 7HP, England

ABSTRACT

Capricorn Seamount is a 5000 m-tall circular guyot with a basal diameter of about 100 km. It is located on the eastern wall of the Tonga Trench, at the edge of the Pacific plate. New bathymetric, seismic reflection, gravity, and magnetic data acquired during the *Tui* cruise, in conjunction with dredge samples, permit us to refine interpretations of the structure and origin of the seamount.

The summit area is flat-topped at two levels, about 450 m and 900 m below sealevel, and both surfaces dip gently towards the trench. Seismic reflection profiles indicate that the summit area is underlain by a well-stratified, gently undulatory-folded sedimentary section about 500 m thick, probably reefal (lagoonal?) limestone. Platform margin reefs are not evident, and may have been down-faulted:
Dredging on the lower summit surface recovered pteropod sand, pumice, and a limestone boulder. Dredge samples from the flanks include a variety of volcanic rocks, mostly basaltic.

The lower western slope of Capricorn Seamount is already at the trench axis. Plate flexure accompanying subduction beneath the Indo-Australian plate has produced a system of closely spaced normal faults which affect both volcanic basement and the sedimentary section. These strike N-S, essentially parallel to the trench; fault throws are mostly 20-1 00 m beneath the flat summit, and increase northward and southward on the upper flanks. Up to several hundred meters of sediment occur in small sediment ponds on the western slope of the seamount, dipping gently away from the trench, which may reflect fault-block back-tilting.

A relatively featureless residual gravity field supports the assumption that Capricorn has a uniform density and regional isostatic compensation of the seamount load on the lithosphere. A mean density of 2.56 t/m^3 has been calculated, consistent with a seamount composed largely of dense basalt, both flows and intrusions. Depth to magnetic basement beneath the summit coincides with the seismically determined base of the sedimentary capping. The magnetic field itself is rather complex. Possible WNW-ESE - trending anomalies east of Capricorn may represent part of a previously unrecognized LMA pattern in the area. Modelling confirmed the inhomogeneous magnetic nature of the volcanic edifice or underlying crust (or both). It may be that Capricorn Seamount possesses a normally magnetized core, mantled by reversely magnetized volcanics.

INTRODUCTION

Capricorn Seamount (Figure 1) was first surveyed by RV *Horizon* in 1953 during the Scripps Institution of Oceanography Capricorn Expedition and named after the expedition (Raitt et al., 1955). The seamount was shown to rise more than 8500 m above the base of the Tonga Trench and 5000 m above the level of the sea-floor to the east. It was seen to be approximately flat-topped with the surface sloping gently (45' - 1°) to the west. A minimum depth of 395 m was recorded. Three dredge hauls were attempted but all were unsuccessful. Menard (1964) subsequently referred to this feature as Capricorn Guyot. This feature was called Capricorn Tablemount by the Circum-Pacific Map Project (CPCEMR, 1978), but Capricorn Seamount on the GEBCO chart (Anonymous, 1982).

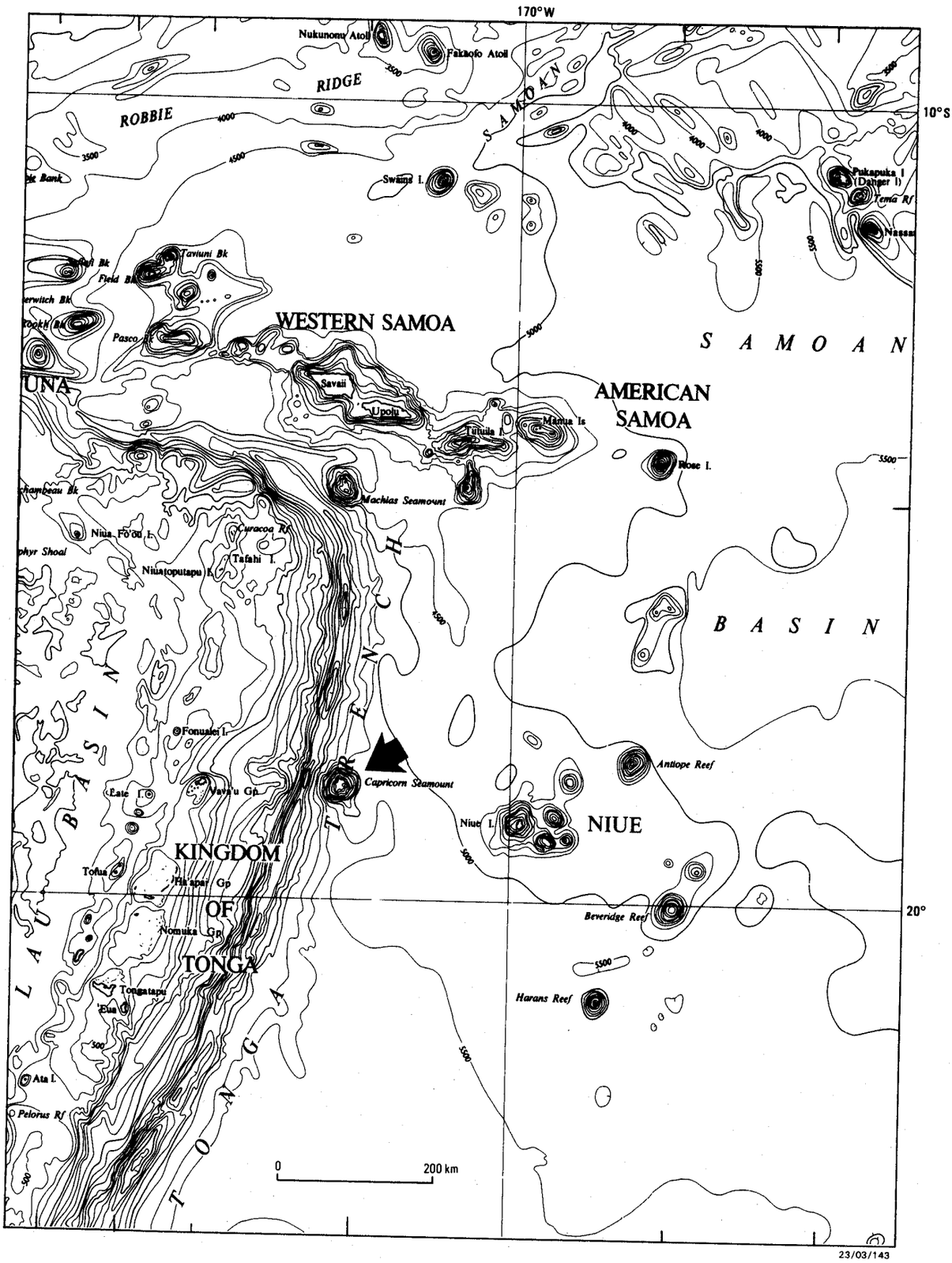

Figure 1. Location map and regional tectonic setting. Bathymetric base map (500 m contours) after Kroenke et al. (1983).

In 1958, RNZFA *Tui* carried out further sounding and dredged a sea-floor sample from a depth of 843-880 m (Kustanowich, 1962; Brodie, 1965). A schematic bathymetric map was drawn by Brodie, 1965. The main flat-topped area of the seamount was shown to be in the depth range of 800-1000 m and have a diameter of about 18 km. The minimum depth (395 m) was seen to correspond to a flat-topped knoll on the eastern margin of the summit area. Brodie (1965) recognized the 450 m and 900 m surfaces of the seamount as being wave cut and supported this conclusion with the observation of smooth limestone pebbles in the dredge haul. Manganese oxides completely covered the limestone pebbles. Brodie also attempted to interpret the geological history of the seamount.

In 1980, Cullen and Burnett (1986) dredged at two stations on Capricorn Seamount in a search for phosphorite nodules but recovered only pumice.

The 1986 HMNZS *Tui* geophysical coverage is depicted on the track map of Figure 2. All lines shown were surveyed for gravity, magnetics and 12 kHz PDR bathymetry. In addition, single-channel seismic profiling was completed along the E-W line over the summit area of Capricorn Seamount and across the Tonga Trench (X -X'), and also along the S-N line over the summit area (Y-Y').

The sea-floor sampling program at Capricorn Seamount was aimed at recovering representative seamount material, including FeMn-oxide crusts. Seven dredge hauls were made at various locations on the seamount (Figure 1) and each produced sample return. Results of this work have been published by Hill (1989) and Hill et al. (1989).

TECTONIC SETTING AND SEISMICITY

The sea-floor morphology (Figure 1) and seismicity (Figure 3) of the area in the vicinity of Capricorn define the major tectonic elements and reflect their tectonic interaction. The Pacific plate is subducting beneath the Tonga Ridge in an approximately E-W direction at a rate of 9+ cm/year (CPCEMRC, 1984). This convergence is the product of back-arc spreading in the Lau Basin and large-scale relative motion of the Australian and Pacific plates.

Capricorn Seamount is situated right on the edge of the subducting Pacific plate, precariously poised on the outer wall of the Tonga Trench (Figures 1 and 4). With the lower western flank already at the trench axis, subduction of the seamount is underway, though still at an early stage.

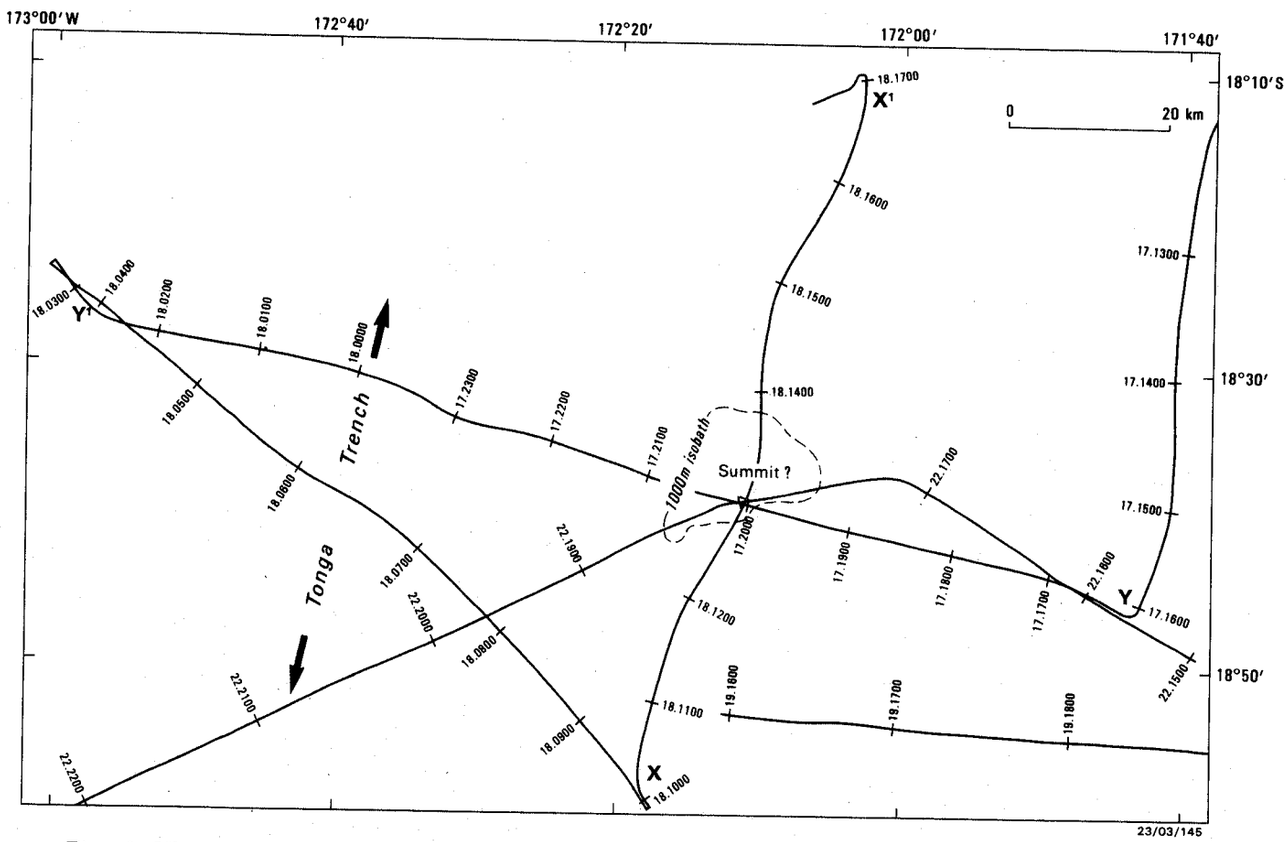

Figure 2. HMNZS Tui *geophysical survey lines across and in the vicinity of Capricorn Seamount. Hourly positions are annotated with survey number (GI), Julian day and GMT (dd.hhmm).*

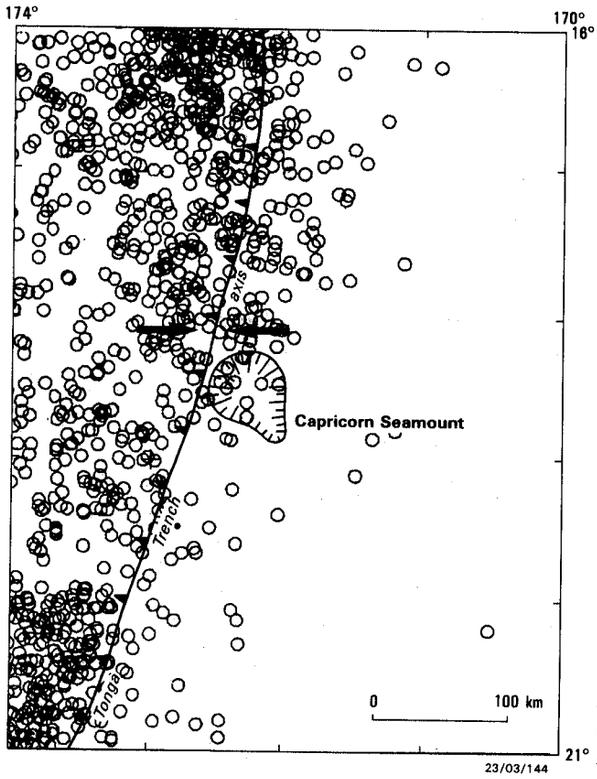

At the present convergence rate, the summit of Capricorn Seamount is expected to reach the trench axis within about 500,000 years.

The seismicity map (Figure 3) shows the very high earthquake activity west of the Tonga Trench axis associated with underthrusting of the Pacific plate beneath the Tonga Ridge (Isacks et al., 1969). Earthquakes are shallow (0-70 km) along the trench, but deepen to the west in conformity with a Wadati-Benioff zone that dips to the west at about 45° for foci in the shallow-intermediate depth range (Hamburger and Isacks, 1987). Though less intense than to the west, seismic activity east of the trench axis is still moderately high within about 150 km of the axis (Figure 3). Capricorn Seamount is located within this zone. Earthquakes to the east of the trench axis are all shallow (less than 70 km deep) and result from internal deformation of the Pacific plate. Focal mechanism studies (Johnson and Molnar, 1972; Chen and Forsyth, 1978) indicate two types of focal-

Figure 3. Seismicity of the Capricorn Seamount area. Epicenter locations (open circles) have been plotted from data provided by the National Geophysical Data Center, Boulder, Colorado. The arrows indicate the direction of Australian/Pacific plate convergence (CPCEMR, 1984).

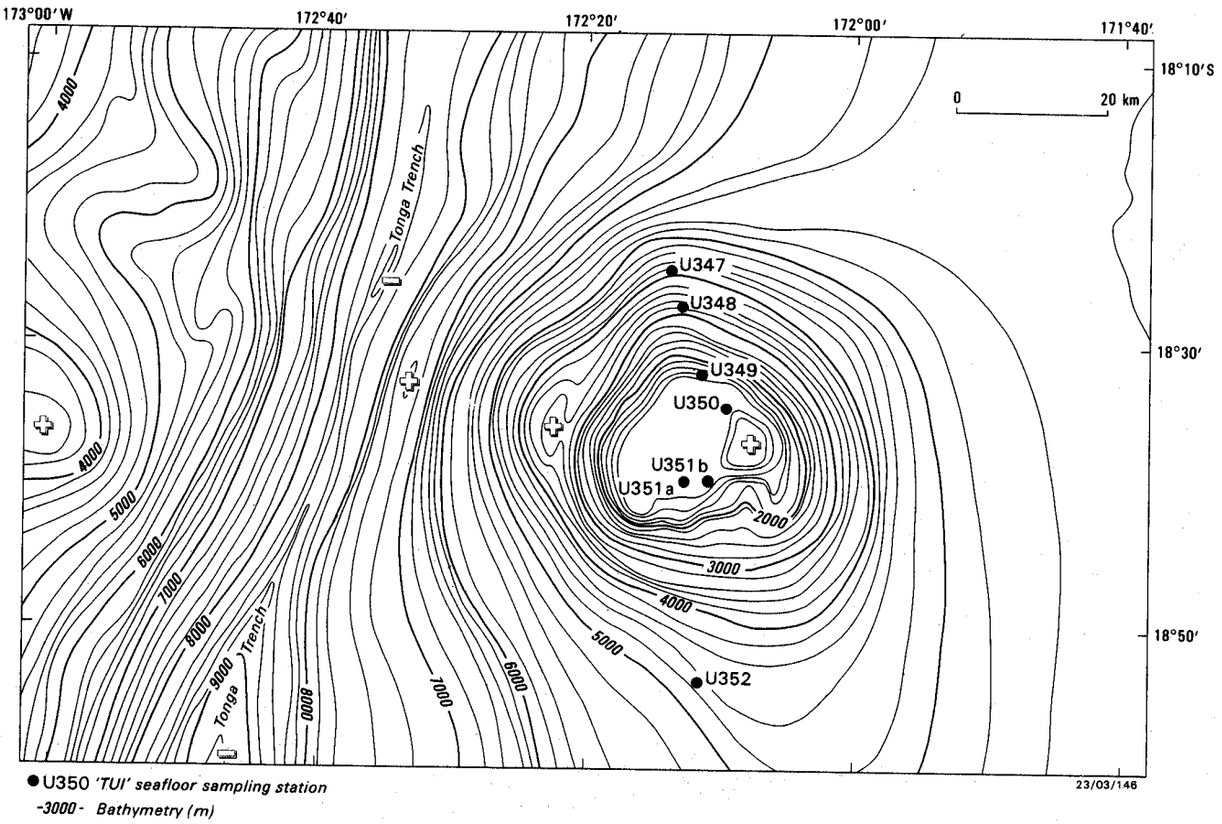

Figure 4. Bathymetry of the Capricorn Seamount/Tonga Trench area at 200 m contour interval. Tui *dredge sites are shown by solid circles annotated with station number.*

mechanism solution, (i) normal faulting on fault planes striking approximately N-S, and (ii) thrust faulting, also on northerly striking planes, but dipping steeply to the west. Bending of the Pacific plate as it enters the trench and longitudinal compressive stress within the plate are believed responsible for these styles of structural deformation.

Bathymetric rises and gravity highs on the seaward side of deep-sea trenches have been modelled as upward flexure of the oceanic lithosphere behaving as a thin elastic sheet overlying a fluid substratum (Hanks, 1971; Watts and Talwani, 1974). An outer rise and gravity high are present east of the trench in the Capricorn Seamount area (see Chase et al., 1982, and Haxby, 1987), but are not clearly defined because of local variations in both bathymetry and gravity field, particularly to the north of the seamount. From a bathymetric profile south of Capricorn, Dubois et al. (1975) estimated the amplitude of the bathymetric bulge as 240 m. This suggests that Capricorn was uplifted by a similar amount on its approach to the trench.

BATHYMETRY COMPILATION

A new bathymetric map of the Capricorn Seamount area, including the adjacent Tonga Trench, has been produced (Figure 4). The map is based on the 1986 *Tui* data recorded along tracks shown in Figure 2. The compilation includes extra detail of the Capricorn Seamount summit area provided by soundings from the 1953 R/V *Horizon* survey (Raitt et al., 1955), together with infill of remaining bathymetry data gaps utilizing the 200 m contours shown on the map of Chase et al. (1982).

GRAVITY AND MAGNETIC CONTOUR MAPS

Contour maps of free-air anomaly (Figure 5) and magnetic anomaly (Figure 8) for Capricorn Seamount and the adjacent Tonga Trench were prepared solely from the 1986 *Tui* data. This was because very few other research cruises had recorded magnetic and gravity data over the area, and the limited data that were available appeared to be of poor quality or to have navigational inconsistencies.

The free-air anomalies are based on the old Potsdam datum of 9812740 $\mu m/sec^2$ and were calculated from the 1930 International Gravity Formula. The magnetic anomalies are based on the IGRF80 global reference field (Peddie, 1982).

MORPHOLOGY AND SEISMIC EVIDENCE

As the bathymetric contours (Figure 4) and seismic sections (Figure 7) indicate, Capricorn Seamount is a large guyot of 100 km basal diameter located on the seaward wall of the Tonga Trench. The center of the seamount is only 45 km from the trench axis. The trench is about 9 km deep in

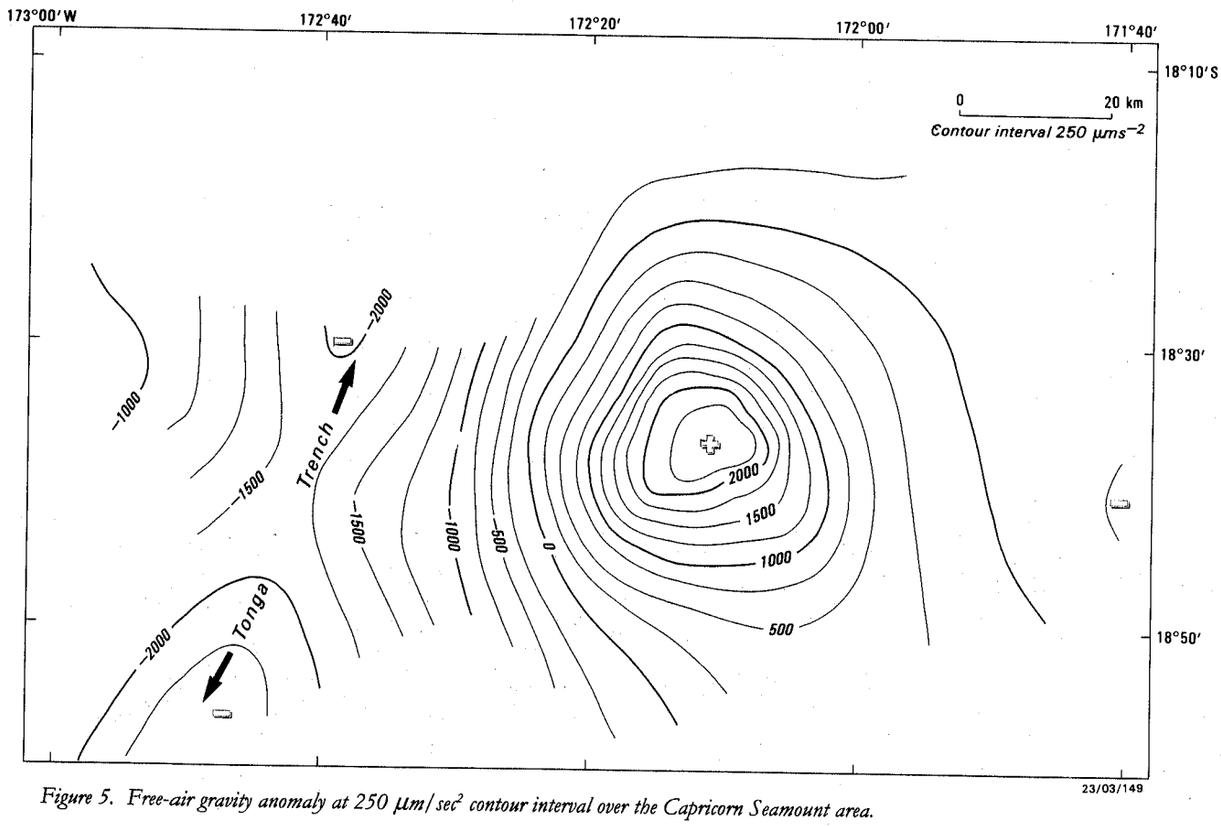

Figure 5. Free-air gravity anomaly at 250 $\mu m/sec^2$ contour interval over the Capricorn Seamount area.

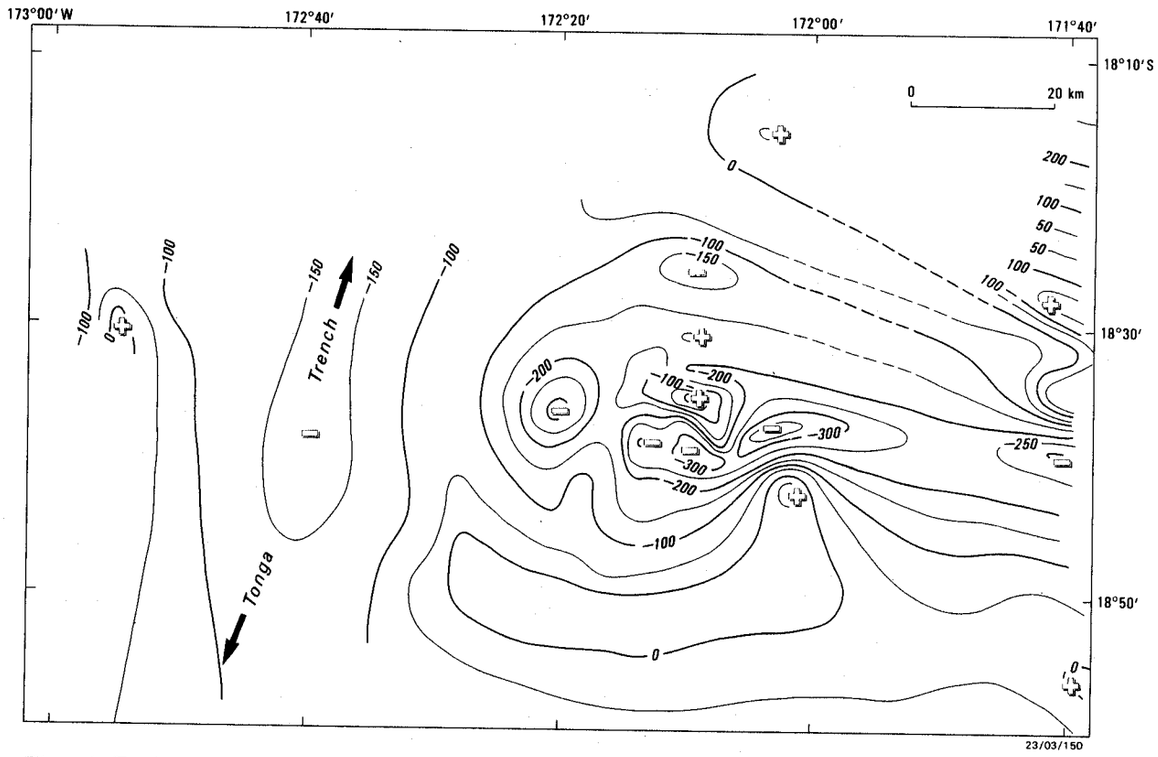

Figure 6. Total magnetic intensity anomaly at 50 nT interval over the Capricorn Seamount area. The magnetic anomaly field is based on the IGRF80 reference field.

the region, with local shallowing of the trench bottom by several hundred meters immediately west of the seamount. This shallowing is probably due to the combined effect of (i) the lower seamount flank starting to subduct, and (ii) a build-up of talus derived from the disintegrating slopes of the seamount.

The lower trench is V-shaped in cross-section adjacent to Capricorn Seamount, with both eastern and western slopes inclined at about 9.5°. To the north and south of the seamount the western slope remains much the same, while the eastern slope decreases markedly to about 4.5°. The upper flanks of the seamount are relatively steep with gradients generally in the range 15°-35°. The slopes become more gentle towards the base of the seamount, particularly on the western and southern sides where the lower slopes have gradients on the order of only 3°-4°. At least several local topographic highs with 100-300 m relief exist on the trench-facing flank of Capricorn (Figures 4 and 7).

The summit area of the seamount is flat-topped at two levels. Both surfaces dip gently towards the trench. The larger surface lies at a depth of about 800-1000 m and is inclined at approximately 1.7° towards the trench (Figure 8). The smaller (22 km^2), but higher, surface lies on the eastern side of the summit area at about 450 m depth (Brodie, 1965). The shallowest depth recorded by the *Tui* for Capricorn Seamount (440 m) was over a point on the southern margin of this elevated area.

As seen in the seismic enlargements and corresponding line drawings (Figure 8), the summit area is underlain by a sedimentary section 0.5 sec thick. Assuming a sediment velocity of 2.0 km/sec, this thickness translates to 500 m of sediment. On the basis of the sampling data (see the following section), it appears that the sediments comprise reefal limestones, while seismic basement corresponds to basaltic rocks of the volcanic substructure.

A system of closely-spaced, steeply-dipping faults affects both volcanic basement and the sedimentary section. The faults strike predominantly in a N-S direction, parallel to the trench axis. Beneath the planar summit area, fault throws are typically 20-100 m but beyond this area (on the upper flanks of the seamount) the magnitude of throw appears to increase to several hundred meters or more. The faults are interpreted as normal faults produced by brittle fracture of the upper crust in response to tensional stress created by flexure of the Pacific plate as it enters the trench. Such fault systems have been recorded seaward of other trenches in the Pacific (Stauder, 1968; Hanks, 1971, Jones et al., 1979; Fryer and Smoot, 1985).

Seabeam and seismic mapping of an area over the southern Tonga Trench by the 1986 SEAPSO V expedition (Herzer, 1986) revealed classic horst and graben structures trending N-S which are attributed to bending of the Pacific plate at the trench. At the northern end of the Tonga Trench, SeaMARC II images of Machias Seamount indicate

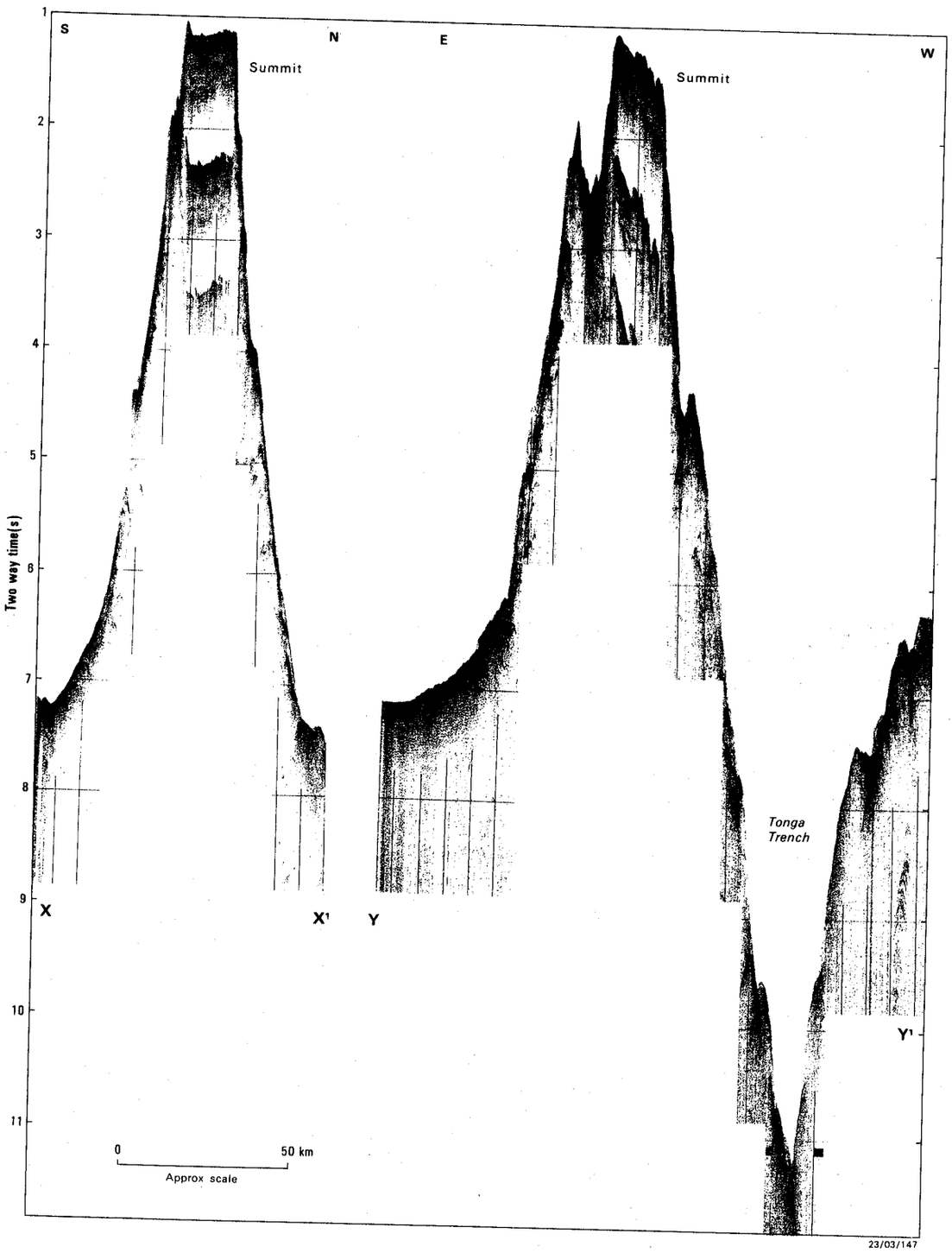

Figure 7. E-W and S-N seismic profiles across Capricorn Seamount. Profile locations X-X' and Y-Y' are given in Figure 2.

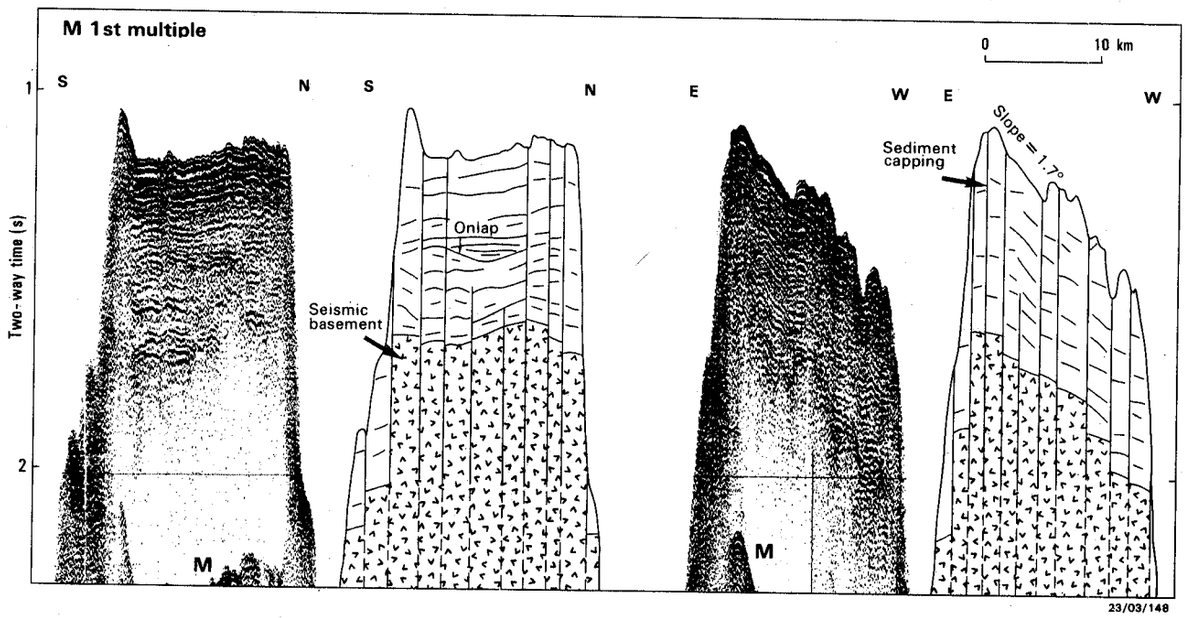

Figure 8. Seismic detail of the Capricorn summit region. Parts of the seismic profiles of Figure 7 are reproduced in enlarged form together with line drawing interpretations.

considerable tectonic dismemberment by normal faulting as the guyot descends the outer trench wall (Coulbourn et al., 1989).

The 1.7° westward tilt of the summit area is reflected in the dip of the bedding within the sedimentary capping and also by the basement surface. This tilt is believed to be due to movement of the seamount down the inclined outer wall of the trench. The parallelism of basement, bedding and seamount summit suggests typical atoll evolution followed by 'drowning', involving subaerial planation of an oceanic volcano, subsidence and upward growth of coral reef forming a limestone platform, and finally rapid subsidence below the photic zone preventing further coral development.

The bedding within the sedimentary capping is best seen in the S-N seismic section which has not suffered major disruption by faulting. The capping is well stratified, with beds sub-parallel and mainly gently undulating. Many of the reflectors can be followed almost completely across the width of the summit area. The presence of onlap halfway down the sedimentary section (Figure 8) suggests a lateral facies change or unconformity at the base of this sequence; the latter possibility may signify a period of emergence. The general continuity of reflectors indicates that much of the section may comprise lagoonal sediments. Fringing reef buildups may have largely been faulted off the sides of the summit area. Strong hummocky reflectors near the base of the section may represent early reef development.

Sediment thickness at the base of the seamount to the east, north and south appears to be about 0.3-0.5 sec. Bedding character ranges from hummocky to chaotic, no distinct reflector sequences being present. The sediments are probably fan and slump deposits derived from mass wasting and tectonic erosion of the seamount flanks. Basement is not clearly defined but appears to be irregular and faulted.

The seismic data over the inner (insular) trench wall show no clear evidence of a substantial sediment thickness, possibly because of the masking effect of the steep and rugged sea-floor topography. Small sediment ponds in local depressions on the insular slope can be seen, however. These contain up to several hundred meters of sediment which appear to dip gently (0.5°-1°) away from the trench axis, suggesting possible tilting back of the 'accretionary' prism to accommodate subduction of the lower western flank of Capricorn. Such back-tilting of the inner trench wall has been observed at the southern end of the Tonga Trench where seamounts of the Louisville Ridge are being subducted (Herzer, 1986).

DREDGING RESULTS

Seven sites were dredged on Capricorn Seamount (Figure 4). Three stations (U347-U349) were sited on the NNW flank, another three (U350, U351a and U351b) were positioned on the summit area, while the last (U352) was sited on the lower southern slope of the seamount. Sediment, reef rock and volcanic rock were all found in the dredges (Table 1).

Our dredging data are supplemented by that of the 1958 RNZFA *Tui* expedition, during which a single dredge haul recovered seafloor material from a depth of 843-880 m at the SW corner of the gently sloping summit area (Kustanowich, 1962; Brodie, 1965). The samples recovered included flat limestone pebbles coated with Mn-oxide, pumice, foraminiferal sand and dead solitary corals. The

Table 1. Capricorn Seamount dredge samples.

Station	Depth (m)	Sample Description
U347	3905-3864	Nanno-bearing abyssal clay
U348	2825-2640	Amygdaloidal basalt/welded tuff (?)
U349	1873-1853	Basalt breccia
U350	1021-922	Coralline limestone block, fragments with slight Mn-staining
U351a	996-976	Calcareous sand with pteropod shells and pumice
U351b	942-932	Calcareous sand with pteropod shells and pumice
U352	4684-4689	Coralline limestone rubble; basaltic gravel; calcareous abyssal clay

limestone contained remains of molluscs, brachiopods and large foraminifera, but no corals. The brachiopods and foraminifera date the primary fragments in the limestone as Miocene. The matrix may be of Pliocene-Holocene age.

In summary, the dredging results indicate that Capricorn Seamount is a volcanic edifice of basaltic composition, capped by a Miocene limestone platform. Unconsolidated sediments of foraminiferal sand, shell and coral fragments, and pumice mantle the relatively flat-lying limestone platform. The lower slopes of the seamount are covered by abyssal clays and sediment fans containing limestone and volcanic erosional products transported from higher levels on the seamount by debris flows.

The shallowest recovery of basalt was from station U349 (1837-1853 m). This implies a maximum thickness of about 1000 m for the limestone platform, which is consistent with the seismically determined thickness of approximately 500 m. The brecciated nature of the basalt from U349 may be a product of the extensive normal faulting seen in the seismic sections.

GRAVITY FIELD AND MODELLING RESULTS

Free-air anomaly and sea-floor topography in the area of Capricorn Seamount and adjacent Tonga Trench correlate very well, as can be seen by comparing Figure 4 (bathymetry) and Figure 5 (gravity contours). A gravity high of +2460 $\mu m/sec^2$ is centered over the summit of Capricorn Seamount. The field decreases rapidly over the flanks of the seamount, particularly so on the trench side, and attains a minimum of about -2250$\mu m/sec^2$ in a broad gravity trough directly above, and aligned with, the trench axis. Over the relatively flat sea-floor to the east of Capricorn (5500 m water depth), the free-air anomaly is correspondingly smooth and averages about -100 $\mu m/sec^2$.

Three-dimensional gravity modelling of the seamount was undertaken to assess mean density and to reveal any anomalous mass distributions within the edifice. Utilized for the modelling was the method of Plouff (1976), which enables calculation of gravity fields for geologic bodies of complex shape by approximating them by a set of polygonal prisms. The method includes provision for inversion of observed gravity data to yield least-squares estimates of density. Uniform density and regional isostatic compensation of the seamount load were assumed for modelling Capricorn.

The seamount topography was approximated by a stack of 9 polygonal slabs (A-I, see Figure 9). The outline (in plan) of each polygonal prism closely matches the bathymetric contour (Figure 4) corresponding to the depth of the upper surface of the prism. The composite body has a depth extent of 0.6-7.0 km. For the gravity inversion, the observed input data consisted of 143 gravity values interpolated from the gravity contours (Figure 5) over a 4 km x 4 km grid within the rectangular area shown in Figure 9. The area selected was centered on the seamount summit and limited in its E-W extent to minimize undesirable biasing effects on the calculations due to the relatively steep gravity gradient over the outer trench wall.

The modelling produced a value of 2.56 ± 0.02 t/m^3 for the best-fit density (assuming sea-water density of 1.03 t/m^3), with correlation coefficient 0.99 and gravity datum of -860 $\mu m/sec^2$.

The residual field (Figure 10) is fairly flat, particularly over the summit region, and this serves to confirm the general validity of the gravity model. The minor decrease in residual gravity toward the eastern margin of Figure 10 is due to uncorrected effect of the non-linear gravity gradient over the trench wall. The -200$\mu m/sec^2$ residual gravity low just to the east of the summit area, and the +300 $\mu m/sec^2$ high just NW of the summit area, may represent genuine mass deficiency and mass excess, respectively. Insufficient data control may be partly responsible for the +300 $\mu m/sec^2$ high, since the high is located between survey lines.

The calculated mean density of 2.56 t/m^3 is consistent with a seamount composed largely of basaltic rocks, including dense flows and intrusions.

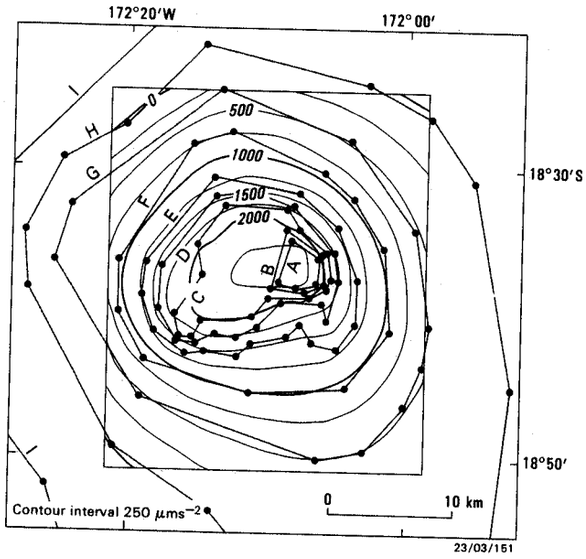

Figure 9. Gravity anomaly (at 250 μm/sec² contour interval) for seamount density of 2.56 t/m³. The seafloor topography is represented by polygonal bodies (A-I) with depth extents (km) as follows: A=0.6-0.8, B=0.8-1.0, C=1.0-1.4, D=1.4-2.0, E=2.0-3.0, F=3.0-4.0, G=4.0-5.0, H=5.0-6.0, I=6.0-7.0. The polygonal outlines are shown as dashed lines and the vertices as dots. A regional gravity correction of -860 μm/sec² has been added.

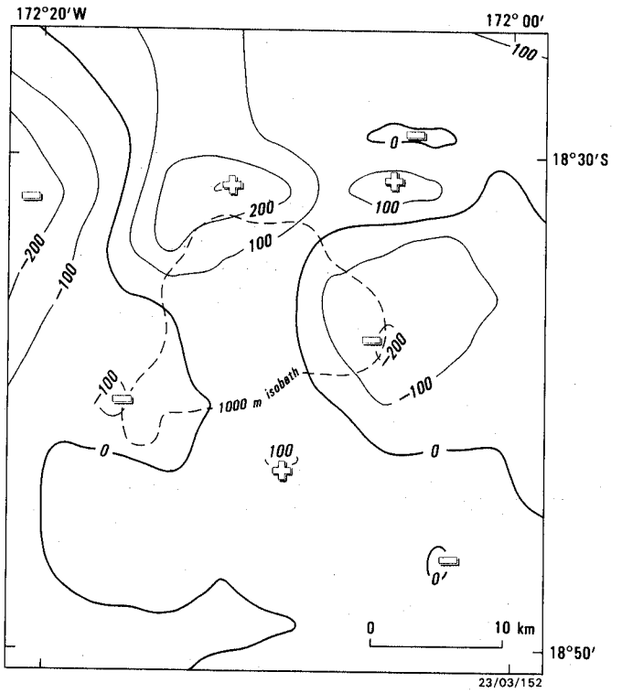

Figure 10. Residual gravity at 100 μm/sec² contour interval over Capricorn Seamount.

MAGNETIC FIELD AND INTERPRETATION

The magnetic field over Capricorn Seamount (Figure 6) is complex. The IGRF80 anomaly range is approximately -350 to +50 nT. Over the trench axis to the west, the field is seen as a broad linear low with a value of -150 nT trending parallel to the trench. North and south of Capricorn, the field is relatively flat with long wavelength variations only on the order of about 50 nT. East of Capricorn the field is moderately anomalous.

The anomalous field east of Capricorn is of medium-long wavelength with local peak to peak variations of up to 400 nT. The seafloor in this area lies at a depth of about 5.5 km and is fairly flat. The anomalies are therefore not due to seafloor topography. However, judging from some relatively short-wavelength anomalies in the field, magnetic inhomogeneity must be present at fairly shallow depth in the oceanic crust. The magnetic sources have no significant expression in the free-air gravity profile. The anomalies may represent oceanic magnetic lineations produced by geomagnetic field reversals, lineations that have not been recognized previously. Such a notion is supported by findings of the SEAPSO V expedition (Herzer, 1986), which reported similar unexplained E-W-trending magnetic anomalies on the edge of the Pacific plate about 700 km south of Capricorn on supposed Cretaceous magnetic quiet zone crust (CPCEMR, 1984). The possibility that the anomalies recorded may be due to ionospheric effects has been considered but discounted, since the anomalies are of too high amplitude to be diurnal variations, and too smooth to be the result of magnetic storm activity.

Capricorn Seamount may be constructed on oceanic crust similar to that to the east. If this is the case, some of the complexity of the field over Capricorn may be explained by magnetic heterogeneity of the underlying crust. An attempt was made to model the seamount as a uniformly magnetized volcanic edifice topped by a non-magnetic platform of variable thickness. The three-dimensional magnetic modelling method of Plouff (1976) was used with similar polygonal prism representation of the volcanic pedestal as in the gravity case, but with the omission of some of the upper polygonal slabs to simulate a non-magnetic capping. No reasonably close or realistic fits to the observed data were achieved, confirming the inhomogeneous magnetic nature of the volcanic edifice or underlying crust, or both.

Despite the complexity, there does appear to be a rough symmetry to the field about a N-S line through the center of the seamount. The pair of dipolar anomalies over the eastern flank (-350/+50 nT) and western flank (-300/-80 nT) cannot readily be reconciled with a seamount magnetization that is radially symmetric. The anomalies may be due to isolated magnetic bodies beneath the flanks or could be part of an E-W-trending magnetic lineation pattern originating from the underlying oceanic crust. Although the seamount is of composite magnetization, the general N-S alignment of bipolar anomalies suggests that

the magnetization is predominantly meridional and either normal or reversed. The meridional magnetization implies little or no rotation of the seamount since construction.

The local magnetic high over the northern part of the summit area and the magnetic low over the southern part of this area signify that the seamount may possess a normally magnetized core, the upper part of which has a diameter of about 10 km. The magnetic low over the lower northern flank of the seamount and the high over the lower southern flank suggest that the core is mantled by reversely magnetized volcanics.

As a means of estimating magnetic source depths and to obtain some idea of the geometry of the causative bodies, the automatic interpretation technique of Werner deconvolution (Jain, 1976; Hsu and Tilbury, 1977) was applied to the long E-W and S-N magnetic profiles across the summit of Capricorn. The sections of profile processed are indicated in Figure 2 as X-X' and Y-Y' and correspond to the seismic lines (Figure 7). The results of the analysis are depicted in Figure 11 (E-W line) and Figure 12 (S-N line) for both thin sheet (dike) model and interface (contact, fault) model. Corresponding magnetic and bathymetric profiles are also shown on the plots. The symbols represent

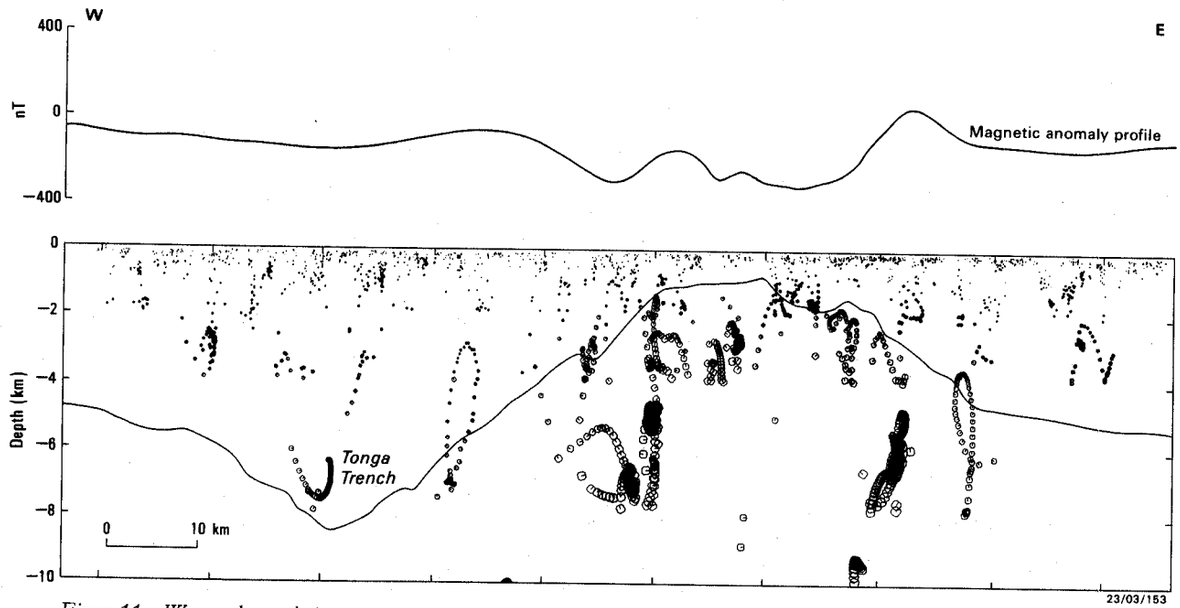

Figure 11a. Werner deconvolution magnetic source estimates (thin-sheet model) for the E-W magnetic profile across Capricorn Seamount and Tonga Trench (profile location is given by Y-Y' in Figure 2). The magnetic profile and bathymetry along the line are also shown.

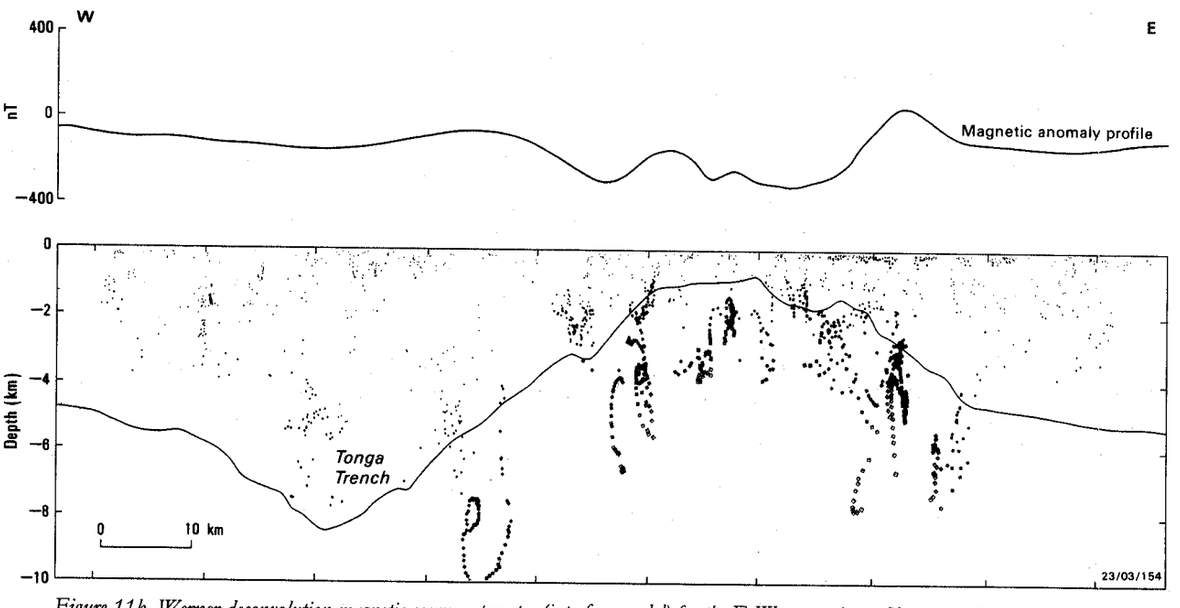

Figure 11b. Werner deconvolution magnetic source estimates (interface model) for the E-W magnetic profile across Capricorn Seamount and Tonga Trench (profile location is given by Y-Y' in Figure 2). The magnetic profile and bathymetry along the line are also shown.

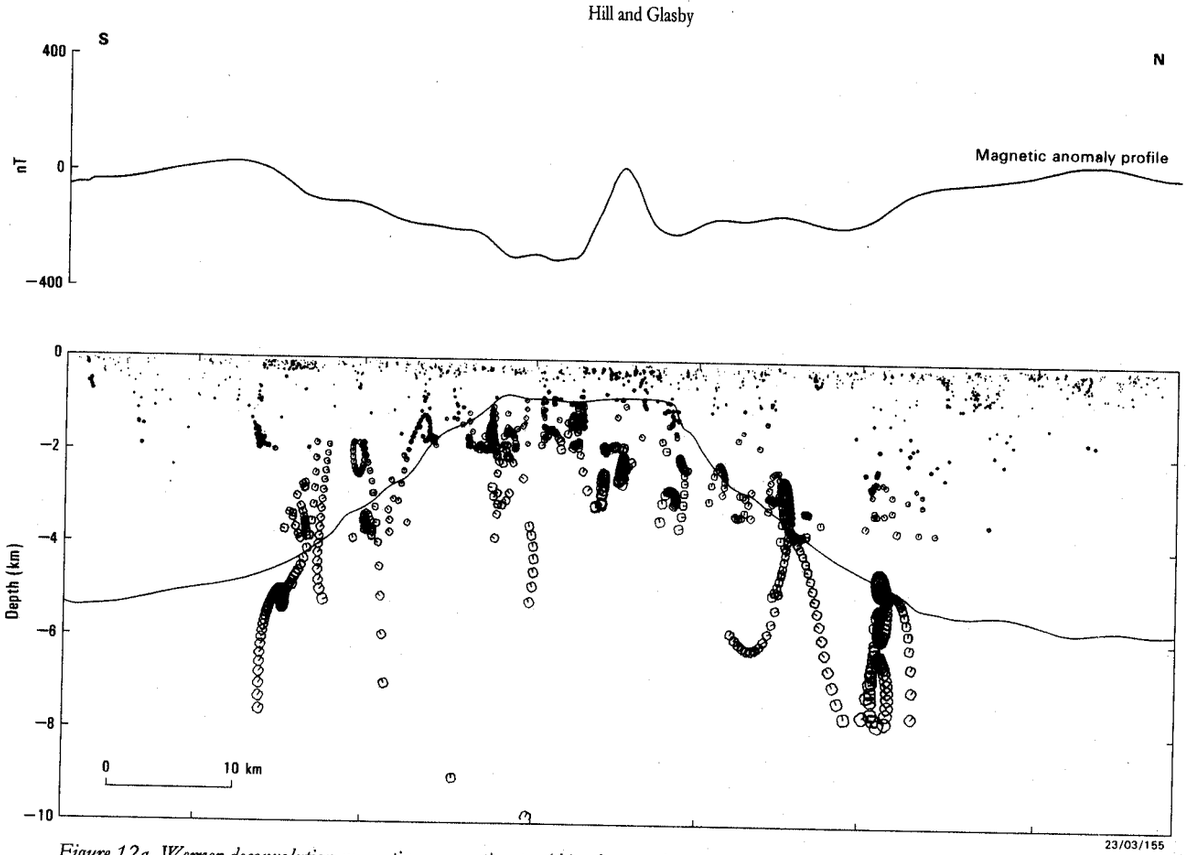

Figure 12a. Werner deconvolution magnetic source estimates (thin-sheet model) for the S-N magnetic profile across Capricorn Seamount (profile location is given by X-X' in Figure 2). The magnetic profile and bathymetry along the line are also shown.

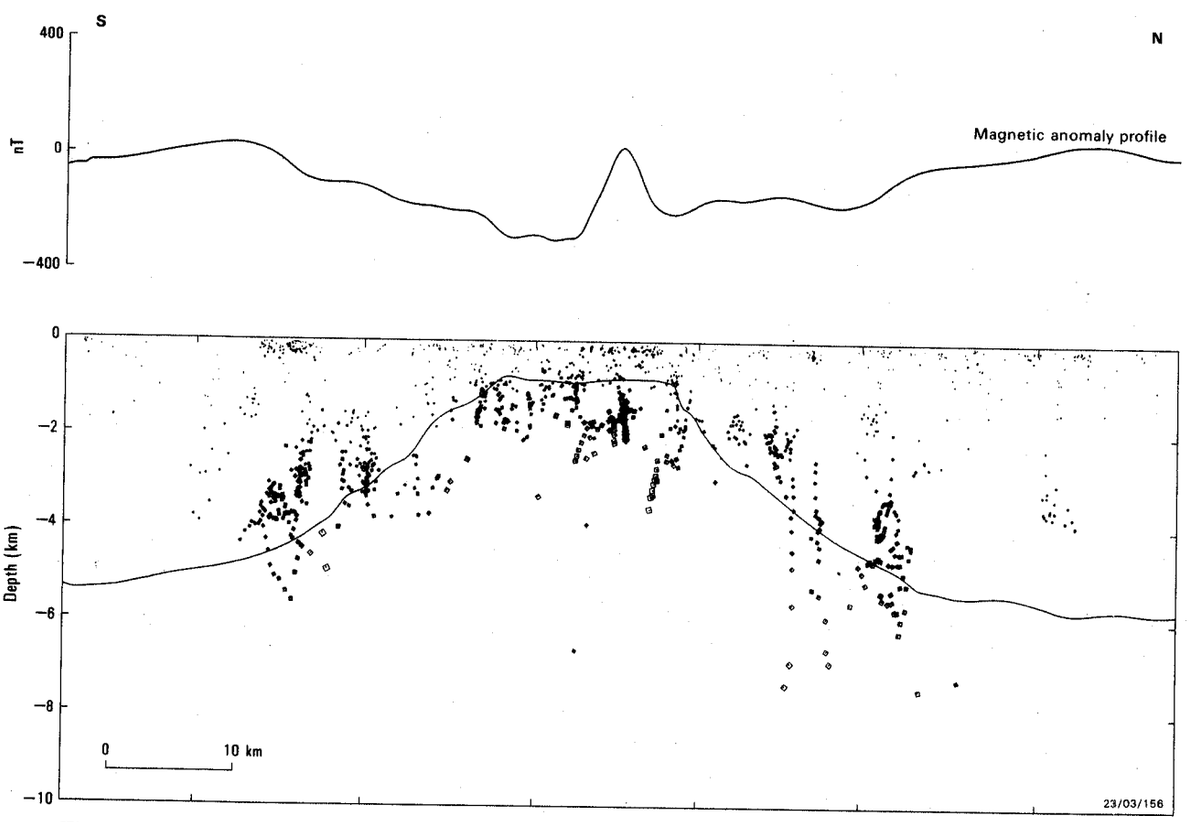

Figure 12b. Werner deconvolution magnetic source estimates (interface model) for the S-N magnetic profile across Capricorn Seamount (profile location is given by X-X' in Figure 2). The magnetic profile and bathymetry along the line are also shown.

the tops of estimated magnetic sources and are proportional in size to the magnetization intensity. A clustering of depth estimates is generally indicative of a good solution; isolated estimates are not highly significant. The sprinkling of low intensity estimates plotted in the upper part of the water column is due to normal levels of non-geologic recording noise, plus 'mathematical' noise introduced in the computer processing.

The magnetic depth estimates broadly correlate with the surface and interior of Capricorn Seamount. No major magnetic sources are interpreted at or below seafloor in the area of the Tonga Trench axis and lower insular trench wall. This is not surprising because the magnetic profile over this area is smooth and relatively flat. Of particular interest is depth to magnetic basement beneath the summit area of the seamount. The tops of the more pronounced clusters of estimates lie at an average depth of about 1.3-1.4 km below sea-level. This coincides with the seismically determined base of the sedimentary capping. Other magnetic source clusters lie at greater depth beneath the summit area, but the shapes of the causative magnetic bodies are not readily deducible from the plots. Such magnetic sources are symptomatic of the general magnetic inhomogeneity of the whole seamount.

REFERENCES CITED

Anonymous, 1982, General bathymetric chart of the oceans: GEBCO.

Brodie, J.W., 1965, Capricorn Seamount, south-west Pacific Ocean: Transactions of the Royal Society of New Zealand, Geology, v.3, p.151-158.

Chase, T.E., B.A. Seekins, S.C. Vath, and M.A. Cloud, 1982, Topography of the Tonga region: USGS-CCOP/SOPAC South Pacific Project Chart (12-27°S, 180-170°W), Department of the Interior, United States Geological Survey.

Chen, T., and D.W. Forsyth, 1978, A detailed study of two earthquakes seaward of the Tonga Trench: Implications for the mechanical behaviour of the oceanic lithosphere: Journal of Geophysical Research, v.83, p.4995-5003.

Coulbourn, W.T., P.J. Hill, and D.D. Bergersen, 1989, Machias Seamount, Western Samoa: Sediment remobilization, tectonic dismemberment and subduction of a guyot: Geo-Marine Letters, v.9, p. 119-125.

CPCEMR (Circum-Pacific Council for Energy and Mineral Resources), 1978, Geographic map of the Circum-Pacific region, Southwest Quadrant: AAPG, scale 1:10,000,000.

CPCEMR (Circum-Pacific Council for Energy and Mineral Resources), 1984, Plate tectonic map of the circum-Pacific region, Pacific Basin sheet: AAPG, scale 1: 17,000,000.

Cullen, D.J., and W.C. Burnett, 1986, Phosphorite associations on seamounts in the tropical southwest Pacific Ocean: Marine Geology, v.71, p.215-236.

Dubois, J., J. Launay, and J. Recy, 1975, Some new evidence on lithospheric bulges close to the island arcs: Tectonophysics, v.26, p.189-196.

Fryer, P., and N.C. Smoot, 1985, Processes of seamount subduction in the Mariana and Izu-Bonin trenches: Marine Geology, v.64, p.77-90.

Hamburger, M.W., and B.L. Isacks, 1987, Deep earthquakes in the southwest Pacific: A tectonic interpretation: Journal of Geophysical Research, v.92, p.13841-13854.

Hanks, T.C., 1971, The Kurile-Hokkaido Rise system: Large shallow earthquakes and single models of deformation: Geophysical Journal of the Royal Astronomical Society, v.23, p.173-189.

Haxby, W.F., 1987, Gravity field of the world's oceans. A portrayal of gridded geophysical data derived from SEASAT radar altimeter measurements of the shape of the ocean surface: National Geophysical Data Center, NOAA, Boulder, Colorado.

Herzer, R.H., 1986, Report on Seabeam research cruise, SEAPSO Leg V, N/O *Jean Charcot*, Louisville Ridge/Tonga-Kermadec region: CCOP/SOPAC, Suva, Cruise Report 120.

Hill, P.J., 1989, Subduction at the northern Tonga Trench – recent SeaMARC II, GLORIA and geophysical results: BMR Research Symposium 'Geoscience Mapping towards the 21st Century', 7 p. (extended abstract).

Hill, P.J., W.T. Coulbourn, G.P. Glasby, M.A. Meylan, and Shipboard Scientists, 1989, Subduction of Capricorn and Machias guyots: Structural and sedimentological processes: Programme and Abstracts Volume for the Joint CCOP/SOPAC–IOC Fourth International Workshop on Geology, Geophysics and Mineral Resources of the South Pacific, Canberra, CCOP/SOPAC Miscellaneous Report 79, p.63-67.

Hsu, H.D., and L.A. Tilbury, 1977, A magnetic interpretation program based on Werner deconvolution: Bureau of Mineral Resources, Australia, Record 1977/50.

Isacks, B., L. Sykes, and J. Oliver, 1969, Focal mechanisms of deep and shallow earthquakes in the Tonga-Kermadec region and the tectonics of island arcs: Geological Society of America Bulletin, v.80, p.1443-1470.

Jain, S., 1976, An automatic method of direct interpretation of magnetic profiles: Geophysics, v.41, p.531-541.

Johnson, T., and P. Molnar, 1972, Focal mechanisms and plate tectonics of the southwest Pacific: Journal of Geophysical Research, v.77, p.5000-5032.

Jones, G.M., T.W.C. Hilde, G.F. Sharman, and D.C. Agnew, 1979, Fault patterns in outer trench walls and their tectonic significance, *in* S. Uyeda et al., eds., Geodynamics of the western Pacific (supplement to Journal of Physics of the Earth), Advances in Earth and Planetary Sciences, v.6, Japan Scientific Societies Press, p.85-101.

Kroenke, L.W., C. Jouannic, and P. Woodward, 1983, Bathymetry of the southwest Pacific, Chart 1 of Geophysical atlas of the southwest Pacific: CCOP/SOPAC, Suva, Fiji.

Kustanowich, S., 1962, A foraminiferal fauna from Capricorn Seamount, south-west equatorial Pacific: New Zealand Journal of Geology and Geophysics, v.5, p.427-434.

Menard, H.W., 1964, Marine geology of the Pacific: New York, McGraw-Hill, 217 p.

Peddie, N.W., 1982, International Geomagnetic Reference Field: The third generation: Journal of Geomagnetism and Geoelectricity, v.34, p.309-326.

Plouff, D., 1976, Gravity and magnetic fields of polygonal prisms and application to terrain corrections: Geophysics, v.41, p.727-741.

Raitt, R.W., R.L. Fisher, and R.C. Mason, 1955, Tonga Trench: Geological Society of America, Special Paper 62, p.237-254.

Stauder, W., 1968, Tensional character of earthquake foci beneath the Aleutian trench with relation to sea-floor spreading: Journal of Geophysical Research, v.73, p.6693-7701.

Watts, A.B., and M. Talwani, 1974, Gravity anomalies seaward of deep-sea trenches and their tectonic implications: Geophysical Journal of the Royal Astronomical Society, v.36, p.57-90.

Hill, P.J. 1996: Niue and adjacent seamounts, *In:* Meylan, M.A. and G.P. Glasby (eds) Manihiki Plateau, Machias and Capricorn Seamounts, Niue, and Tofua Trough: Results of Tui Cruises. SOPAC Technical Bulletin 10: 31-44.

NIUE AND ADJACENT SEAMOUNTS

P.J. Hill

Australian Geological Survey Organisation, GPO Box 378, Canberra, Australia

ABSTRACT

Niue is an isolated raised atoll 270 km east of the Tonga Trench and about 550 km south of the Samoan chain. A fringing coral reef encircles the island at sea level. Endeavor Seamount occurs 40 km to the ENE of Niue, and Lachlan Seamount is located 30 km to the SE. Bathymetric mapping, dredge sampling, seismic reflection profiling, and gravity and magnetic mapping and modelling provide evidence for variations in the development history of these three volcanic edifices.

Niue and its companion seamounts have roughly circular outlines at ocean depths less than about 3 km, and rise from a seafloor about 4750 m deep. The southwest flank of Niue is unusually steep, possibly due to the explosive removal of part of the original volcanic edifice, the debris now occurring as a large mound or fan at the base of the slope. Endeavor Seamount has a summit with considerable relief and a minimum depth of about 1300 m, whereas Lachlan Seamount has an approximately planar summit surface at a water depth of about 1055 m and a minimum depth of about 650 m. The existence of a seamount immediately east of Lachlan has been disproved by bathymetric mapping.

No *in situ* volcanics were recovered from the flanks of Niue, Endeavor, or Lachlan, but altered tuff and vesicular basalt were dredged from the lower slope of the south side of Niue. Neither these volcanics nor coral rubble from shallower depths displayed Mn crusts any thicker than about 3 mm.

Niue and its associated volcanic edifices likely formed by the early to mid-Miocene eruption of basalt onto middle to Late Cretaceous oceanic crust that had attained high flexural rigidity; there is no evidence of an associated lithospheric depression (moat). Niue consists of a core of pillow basalts and interbedded tuff overlain (except on the southwest) by an ash/tuff sequence and capped by a carbonate platform. Gravity and magnetic surveys on the island had suggested the southwestern side of the island is underlain by a dome-shaped, flat-topped, dense volcanic core at 300-400 m below sea level, and this is supported by marine data and modelling. A core density of 2.41 t/m^3 has been calculated, along with an upper edifice density of2.16 t/ m^3. The upper part of the island platform is middle to late Miocene in age, and composed of coral - foraminiferal - algal calcarenite and reefal limestones. Pleistocene uplift of the now-raised atoll may have been the result of pre-subduction flexure of the oceanic lithosphere.

Magnetic modelling indicates that Niue is not uniformly magnetized. The core of Niue appears to be reversely magnetized whereas the ash/ tuff sequence may have a normal polarity. The core of Lachlan may have formed contemporaneously with that of Niue, as it also may be reversely magnetized. However, Endeavor appears to be of normal polarity, and may have erupted somewhat later. Neither Lachlan nor Endeavor display evidence of a sedimentary capping, but neither summit has been dredged.

INTRODUCTION

Niue is an isolated, raised coral atoll in the southwest Pacific Ocean about 270 km east of the Tonga Trench (Figure 1). The island is roughly oval-shaped with a N-S length of 22 km and E–W width of 17 km. It rises steeply from a surrounding ocean depth of about 4750 m. Major nearby submarine features include Endeavour Seamount, 40 km to the ENE, and Lachlan Seamount, 30 km SE of Niue.

Much of the former atoll morphology has been preserved (Schofield, 1959). The relatively flat-lying central part of the island is about 35 m above sea-level and represents the floor of the original Mutalau Lagoon. This area rises outwards to what was the ancient atoll rim (Mutalau Reef) and now forms the highest part of the island - a peripheral ridge 60-70 m above sea-level. From the ridge, the land surface drops abruptly down to sea-level in a series of terraces, the most prominent of which is the Alofi Terrace at 23 m. A fringing coral reef about 100 m wide encircles the island at sea-level.

Radiometric dating puts the age of emergence of the atoll (Mutalau Reef) at a maximum of 700,000 years (Fieldes et al., 1960). Fauna from the raised lagoon have been dated as Plio-Pleistocene (Schofield, 1959). Schofield (1959) correlated the reef and terrace levels with well-established Pleistocene sea-levels in Britain. Further correlation was made by Schofield and Nelson (1978), who remarked that the coastal terrace sequence on Niue was virtually identical to that on the islands of the southern Cook group 1000 km or so to the east. If correct, such observations imply that the terraces on Niue were produced solely by eustatic sea-level stillstands without any post-Mutalau Reef uplift of the island being involved. In contrast, Dubois et al. (1975) proposed that the Pleistocene emergence of Niue is due to uplift, and based their argument on the hypothesis that oceanic lithosphere behaves as an elastic plate and flexes upwards prior to subduction, forming an outer bathymetric rise seaward of deep-sea trenches (Watts and Talwani, 1974). The amplitude of the rise off the Tonga Trench is roughly 240 m, which is smaller than for a number of other trench systems for which estimates lie in the range 307-513 m (McAdoo and Martin, 1984). Calculations indicate that 64 km of movement towards the Tonga Trench produced the 70 m uplift of Niue.

The geology of Niue has been described by Schofield (1959), Schofield and Nelson (1978), Jacobson and Hill (1980a, 1980b), and Hill (1983). The soils of Niue are thin, radioactive and thought to have been derived largely from ash fall-out produced by eruption of regional volcanoes, particularly those of the Tongan arc to the west (Wright and Van Westerndorp, 1965). Whitehead et al. (1990) have shown that there is also an unusually high Hg content in the soils, associated with the radioactivity and the goethite/gibbsite content of the soils. Whitehead et al. (1992) have concluded that the anomalous radioactivity of the soils is due to adsorption of uranium from seawater onto highly weathered volcanic ash during at least one period of brief Pleistocene submergence.

Geological mapping indicates that, apart from the veneer soil, the upper part of the island platform is composed entirely of carbonate lithologies. These comprise coral - foraminiferal - algal calcarenite and reefal limestones, dolomitized to varying degree. Groundwater and mineral exploration drilling has proved carbonates exist to a depth of at least 300 m. Paleontological dating of drill-core samples from most of the carbonate sequence to a depth of 170 m below sea level yielded a middle to late Miocene age (G.C.H. Chaproniere in Jacobson and Hill, 1980b). Aharon et al. (1993) noted leached, chalky intervals in the latest Miocene section, 35-140 m below sea level, that mark the position of dissolution unconformities representing episodes of eustatic sea level fall that they correlate to the Messinian salinity crisis. Magnetic and gravity surveys conducted on Niue (Hill, 1983) suggest that the southwestern part of the island is underlain by a flat-topped, dome-shaped dense volcanic core at a depth of 300-400 m below sea-level. The core is interpreted as having a lateral density contrast of 0.20 t/m and a reverse magnetization of 3.0 A/m.

The 1986 *Tui* cruise appears to have been the first to focus on the geology and geophysics of the Niue seamounts. The single-channel seismic, magnetic, gravity and 12 kHz bathymetry coverage achieved is indicated on the track map of Figure 2. The resultant extension of magnetic and gravity coverage offshore from Niue significantly improves control on the modelling of the volcanic substructure of the island and adjacent seamounts. In addition to the geophysical survey, five sites were dredged to the south of Niue in water depths ranging from about 350 to 3600 m, with the objective of recovering volcanic rocks from the island pedestal and manganese crusts.

BATHYMETRY COMPILATION

The 1986 *Tui* survey work around Niue and nearby seamounts Lachlan and Endeavour has contributed substantially to knowledge of the bathymetric details of the area. The only previous comprehensive bathymetric compilation was made 20 years earlier (Brodie, 1966). Since then a significant amount of new data, including our own, has become available. This has allowed production of an updated bathymetric map with 500 m contour interval (Figure 3).

The new compilation is based on:

1. The 1986 *Tui* results
2. British Admiralty Chart 1174 - Niue and Suwarrow Island (Niue 1:150,000), 1982 with additional control provided by:
3. the Niue Island 1:200,000 chart (Brodie, 1966)
4. 1:1,000,000 Ocean Sounding Charts 355 and 356 compiled by the Hydrographic Office of the Royal New Zealand Navy

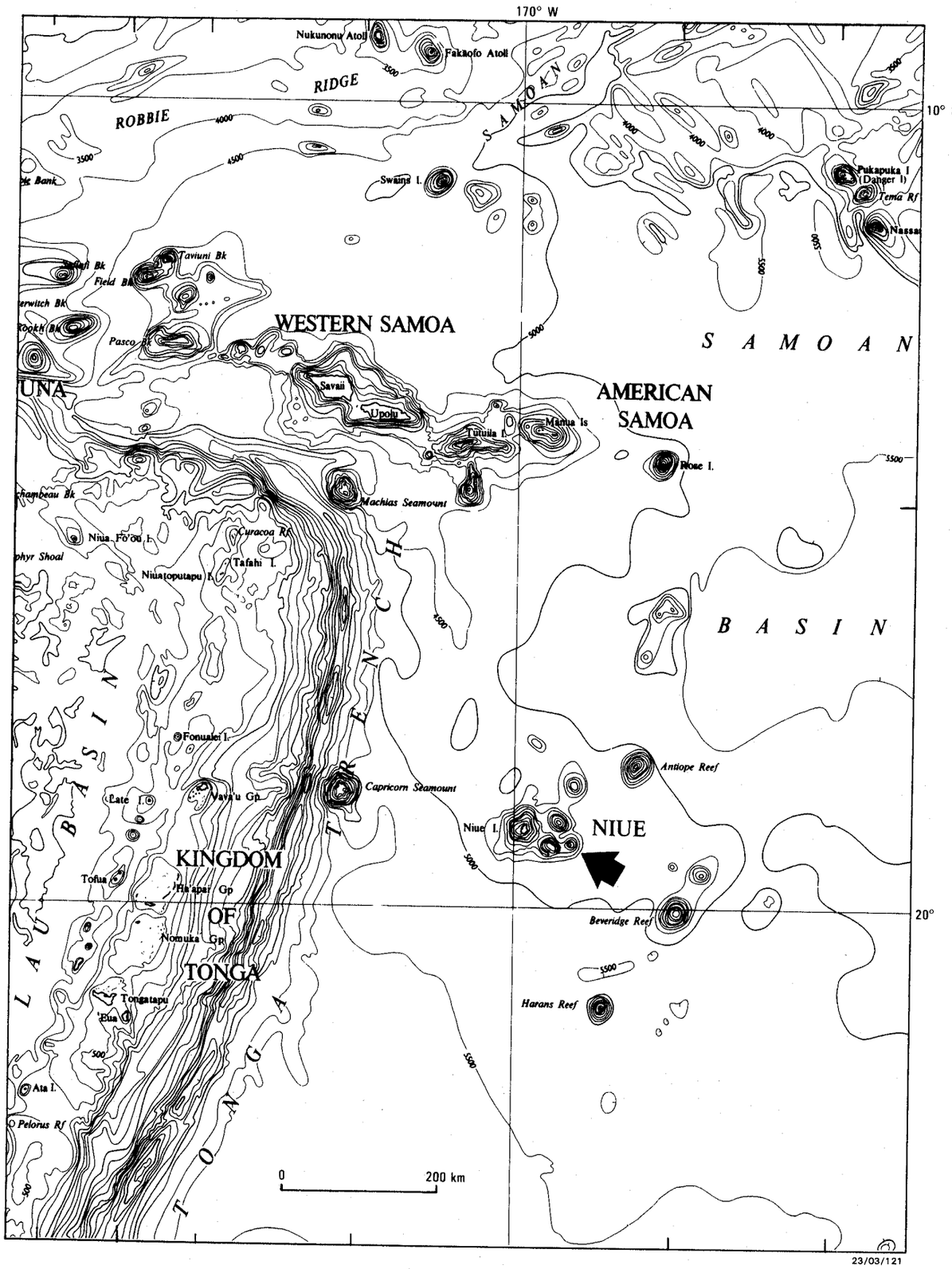

Figure 1. Location map and regional tectonic setting. Bathymetric base map (500 m contours) after Kroenke et al. (1983).

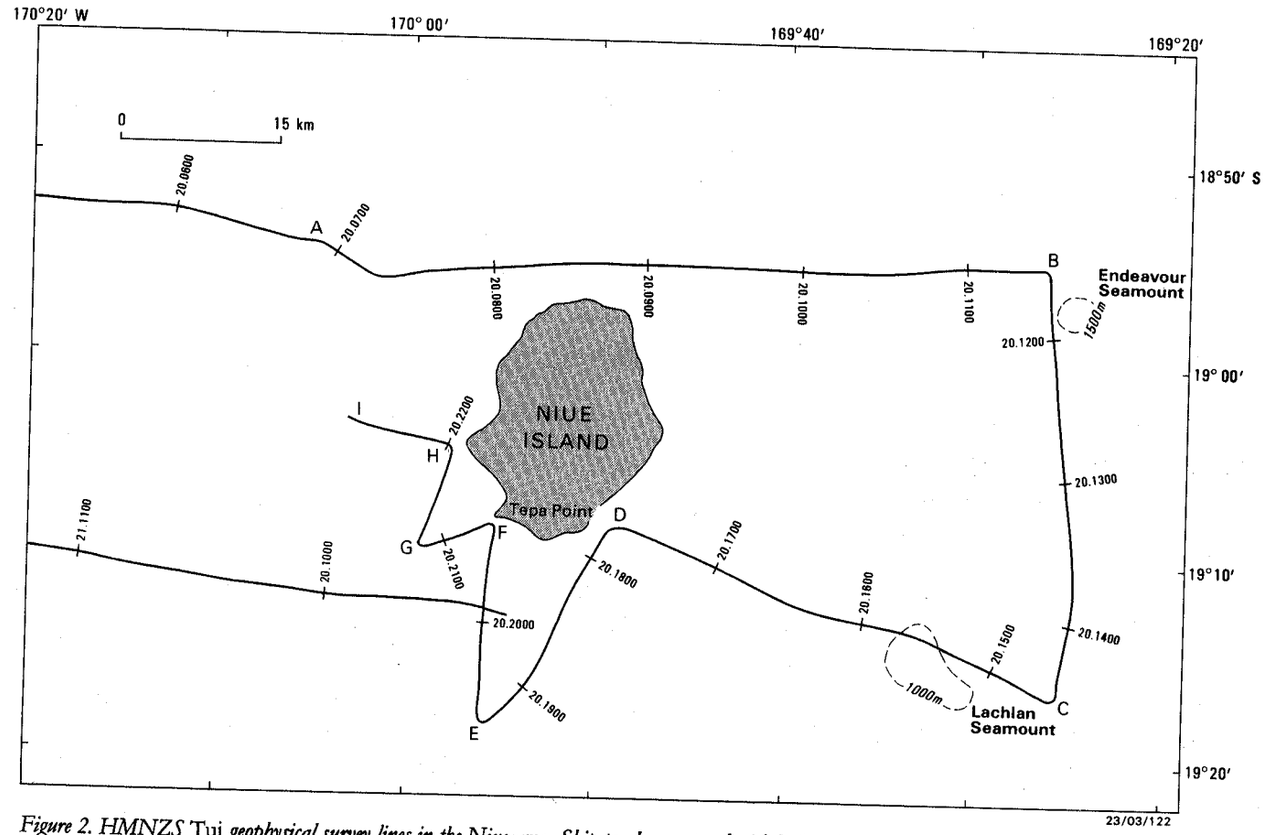

Figure 2. HMNZS Tui *geophysical survey lines in the Niue area. Ship track annotated with Julian day and GMT.*

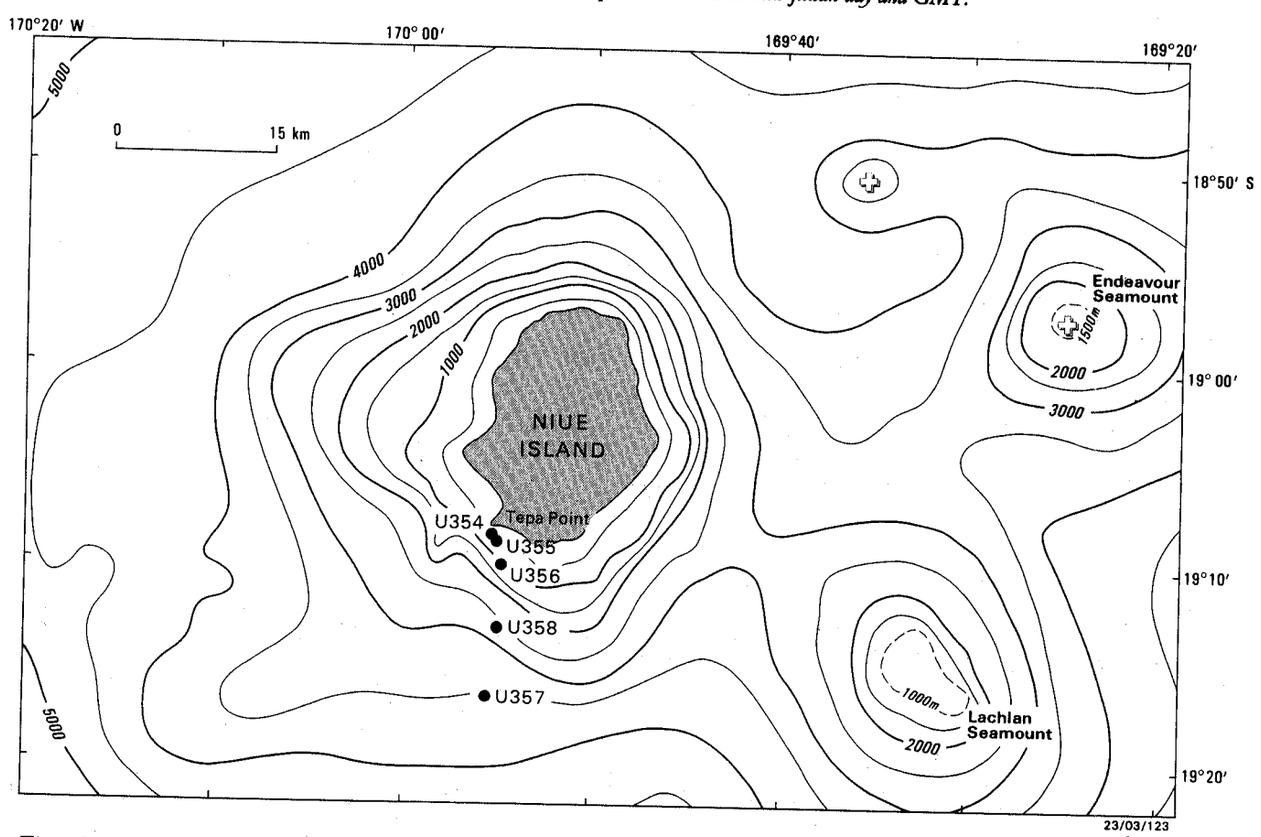

Figure 3. Bathymetry of the Niue seamounts area at 500 m contour interval. Tui *dredge sites (solid circles) are annotated with station number.*

5. digital data from research cruises available through the National Geophysical Data Center, Boulder, Colorado. Cruises with bathymetric data coverage in the map area of Figure 3 included:
   (i) *Vema* 1962 (Lamont-Doherty Geological Observatory)
   (ii) *Hakuho Maru* 1968 (University of Tokyo)
   (iii) *Melville* 1974 (Scripps Institution of Oceanography)
   (iv) *Conrad* 1974 (Lamont-Doherty Geological Observatory).
6. the 1982 USGS compilation for the Tonga region (bathymetry to west of Niue, Chase et al., 1982).

It should be mentioned that Niue is positioned about 2.5 km too far north on the Niue Island 1:200,000 chart (Brodie, 1966). This discrepancy was discovered on our first approach to Niue using satellite navigation. British Admiralty Chart 1174 appears to show Niue correctly located and was used subsequently as a guide for navigation close to the island.

Another significant charting error was detected during the bathymetry compilation, concerning the moderately large seamount shown immediately to the east of Lachlan Seamount. This feature is indicated on charts of Mammerickx et al. (1973) and Kroenke et al. (1983), as well as a number of other recent bathymetric maps. It appears to have been charted on the basis of soundings made by *Tui* in 1963. There is evidence to suggest that the soundings were mis-plotted, an error that has been perpetuated on sheets such as Ocean Sounding Chart 356. A critical sounding of 1534 m, for example, appears to be located about 14 km too far east. Re-positioned, it falls on Lachlan Seamount. It seems, therefore, that no seamount exists immediately to the east of Lachlan Seamount. This conclusion is supported by data from a nearby French hydrographic traverse made in 1976/77, indicating water depths of about 4700 m in the area.

GRAVITY AND MAGNETIC CONTOUR MAPS

Gravity and magnetic maps of the Niue seamounts area have been prepared. These depict gravity anomaly at a 250 μm/sec² contour interval (Figure 4), and magnetic anomaly at a 100 nT contour interval (Figure 5). The maps are based largely on our cruise data combined with an extensive land-based network of gravity and magnetic observations on Niue Island (Hill, 1983). Other research cruises which were sources of data include *Vema* 1962 (gravity), *Hakuho Maru* 1968 (gravity and magnetics), *Melville* 1974 (magnetics) and

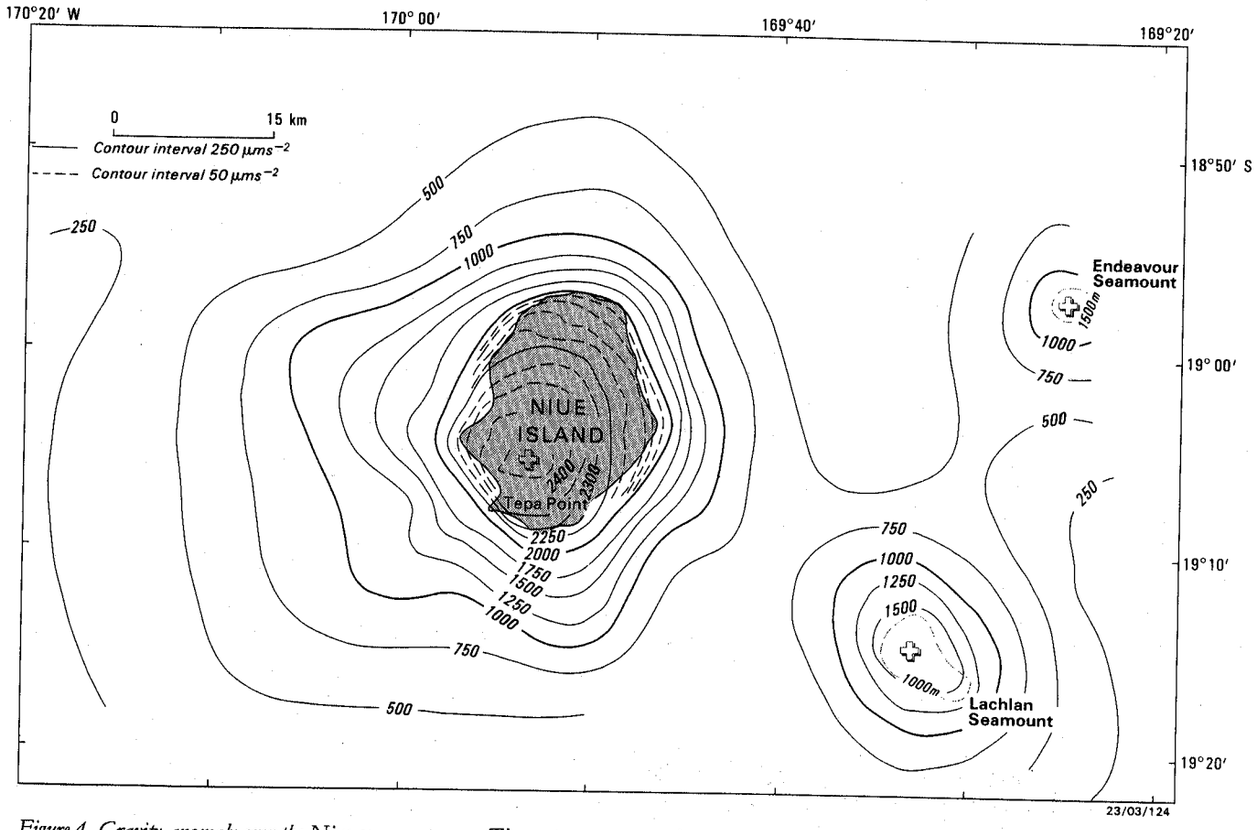

Figure 4. Gravity anomaly over the Niue seamounts area. The contours represent free-air anomaly over the ocean and Bouguer anomaly on land (Niue Island). Contours shown as solid lines are at 250 μm/sec² contour interval, while dashed contours (over Niue) are at 50 μm/sec² interval.

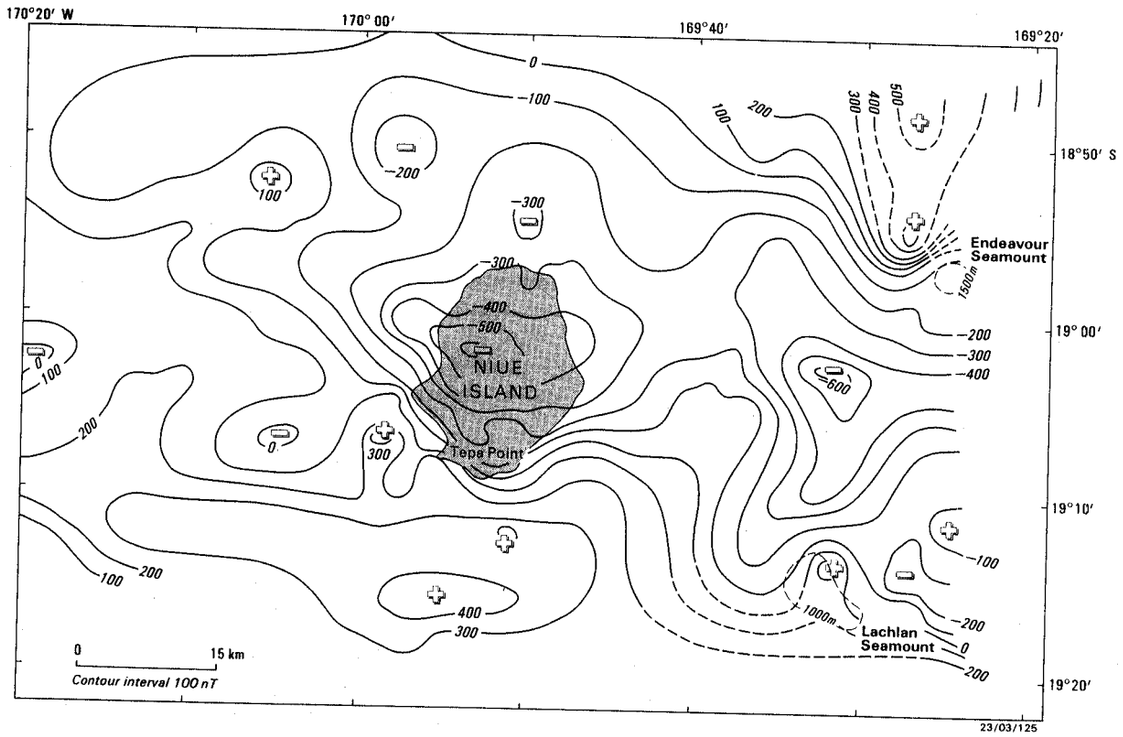

Figure 5. Total magnetic intensity anomaly at 100 nT contour interval over the Niue seamounts area. The magnetic anomaly field is based on the IGRF80 reference field.

Conrad 1974 (gravity and magnetics). The Geophysics Division of the New Zealand DSIR also supplied marine magnetic data, acquired in 1963.

The gravity data are based on the Washington, D.C. (Commerce Floor) datum of 9801187 μm/sec^2 (Woollard and Rose, 1960; Robertson, 1965), with free-air anomalies calculated using the 1930 International Gravity Formula. The gravity anomaly map has been compiled from free–air anomalies at sea and Bouguer anomalies on land (density 2.1 t/m^3 for above-sealevel topography). The magnetic anomaly values are relative to the global IGRF80 reference field (Peddie, 1982).

DREDGING RESULTS

Five dredge hauls (U354–U358) were made on the southern flank of Niue in an effort to sample volcanic core rocks and manganese crusts. The dredge locations are indicated on the bathymetric map (Figure 3) and also denoted on the seismic sections (Figure 6) to give an idea of their relative settings on the submarine slope off Tepa Point.

The paucity of volcanics and the general small quantity of material recovered in the rock dredge hauls was disappointing, especially in light of the concerted efforts made to achieve optimum recovery off Niue (Table 1). It can only be concluded that the rock dredging equipment was just too light for the job. The submarine slopes off Tepa Point are quite steep (30–35°) and believed to be surfaced by high strength material such as relatively fresh volcanic core rock (?basalt) and carbonates. The rock dredge/winch combination appears to have had inadequate ripping capability to deal with such surfaces and consequently no *in situ* volcanics were recovered off Niue.

The altered tuff and vesicular basalt recovered are of particular significance to our investigation. Nevertheless, the limited quantities of these volcanic rocks recovered makes assessment of how representative they are of the Niue edifice rather speculative.

BATHYMETRY AND SEISMIC RESULTS

The geophysical lines completed are shown in Figure 2. The ship sailed a W–E line north of Niue, turned south to pass over Endeavour Seamount, then turned west to cross Lachlan Seamount and continued on to the area south of Niue to complete a zig-zag pattern over the southern flank of the seamount before commencing dredging operations. Seismic data were not recorded on the line out of the area towards Capricorn Seamount.

Time constraints meant that only one pass over Endeavour Seamount and Lachlan Seamount was possible. These features had not been accurately charted in the past and so our lines may not have passed directly over their

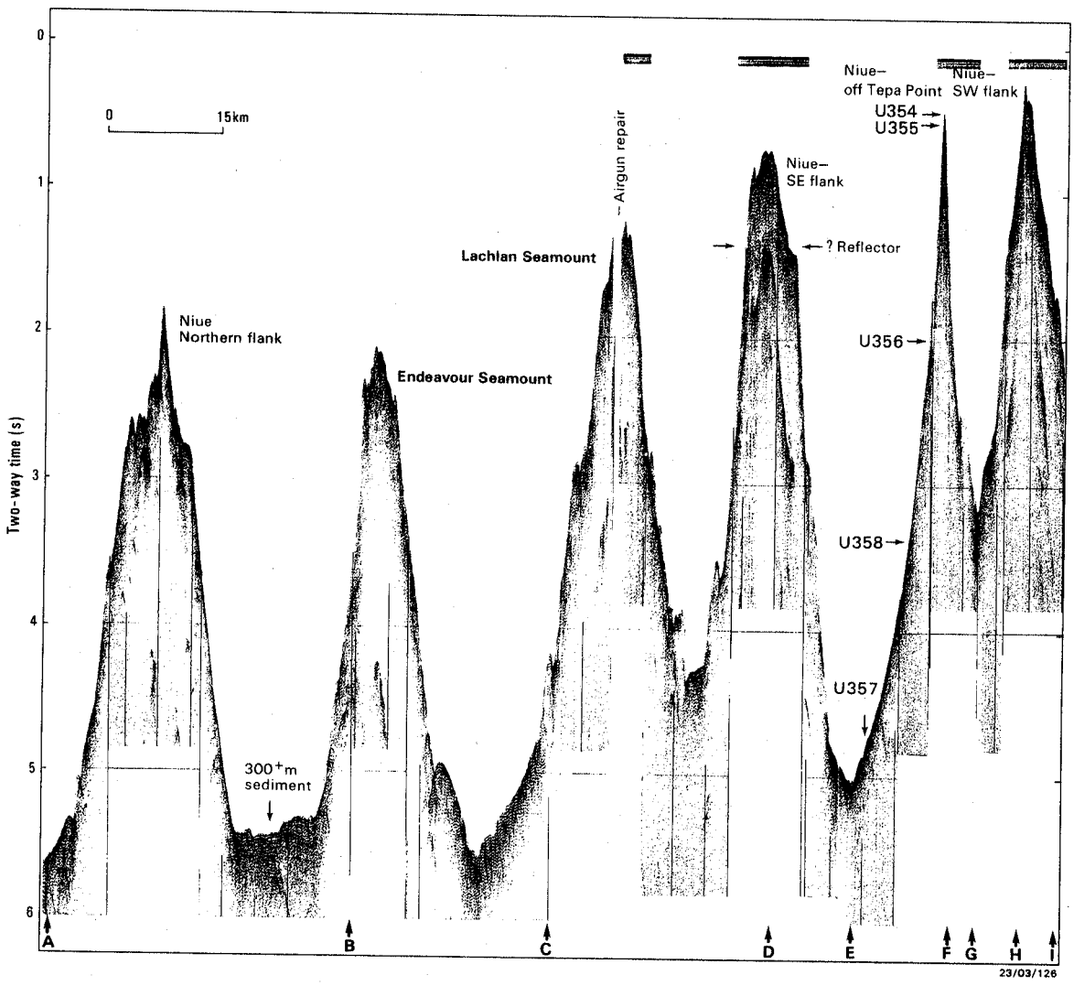

Figure 6. Seismic profiles over the Niue seamounts. The profile locations are given by A-I which denote course change positions (see Figure 2). Arrows indicate the locations of dredge sites U354-U358 on the southern flank of Niue.

Table 1. Dredge samples.

Station	Depth range (m)	Material recovered
U354	346-467	Coral (6 fragments, 16-29 mm diam.)
U355	586-487	Dredge empty
U356	1873-1100	Coral (250 fragments, 10-150 mm diam.; also many smaller pieces)
U357	3612-3596	Altered tuff, most with Mn crust 2-3 mm thick (14 lumps, 18-45 mm diam.)
		Black vesicular basalt (1 piece, 27 mm diam.)
		Coral (1 fragment, 77 mm diam., silicified?)
		Pumice (1 pebble, 25 mm diam.)
U358	2520-2450	Coralline limestone rubble with Mn crust up to 3 mm thick (3 pieces, 8-34 mm diam.)
		Coralline limestone rubble lacking Mn crust (3 fragments, 24-95 mm diam.)

highest points, though we believe they did pass over the summit areas. Shallowest depth recorded for Endeavour Seamount was 1625 m, while for Lachlan Seamount it was 920 m. Soundings plotted on Ocean Sounding Sheet 356 show slightly shallower minimum depths for these features (1308 m and 646 m, respectively). Bathymetric profiles presented by Summerhayes (1967) include crossings of Endeavour and Lachlan Seamounts. These profiles show summit topographies similar to those seen on our records, and is confirmation that we did, in fact, pass over the summit areas of the seamounts so that our images of the seamounts are not expected to be unduely distorted by the effects of side-echoes.

The seamounts rise from a surrounding ocean depth of about 4750, gently at first, then much more steeply towards their summits. Slopes are on the order of 5° at the 3500 m isobath, but then steepen upwards to an average of 15–20° before reaching the 2000 m isobath. Around Niue the steepest submarine slopes (approximately 30-35°) lie between the 2000 m isobath and the coastline.

The southwest flank of Niue is particularly steep. The isobaths show a pronounced general NW-SE trend in this area, broken only locally SW of Tepa Point by an isolated bathymetric high, and suggest the existence of a major structural zone intersecting the SW flank of Niue. In deeper water farther to the SW, the 3500 and 4000 m isobaths extend outward in a lobate pattern to outline a large mound or fan at the base of the seamount.

Though no extensive seismic coverage of the lower slopes of the seamounts was obtained, there is evidence, especially between north of Niue and Endeavour Seamount (see Figure 6), that these are underlain by several hundred meters of chaotically-bedded sediment over an irregular and faulted basement. The sediment probably consists of talus and slump deposits derived from higher on the seamount flanks. The mixture of lithologies recovered at station U357 tends to support this.

Though the middle and upper slopes of the seamounts are generally too steep for seismic mapping of internal structure, a fairly strong reflector appears to be present beneath the upper SE flank of Niue (Figure 6) at about 1.3 sec (two-way time). A significant break in submarine slope or terrace is present where this reflector crops out. The reflector may mark the boundary between an overlying ash/tuff sequence and underlying basalt flows (volcanic core). This is discussed further in the section on gravity/magnetic modelling.

Sections of the 12 kHz bathymetric records have been reproduced (Figure 7) to display details of the summit topography of Endeavour and Lachlan Seamounts. The summit area of Endeavour Seamount is of high relief, and consists of a central peak flanked by numerous steep-sided local topographic highs. The jagged appearance of the summit suggests a high degree of erosional dissection, though it is possible that the individual small peaks may represent parasitic cones. There is no evidence of a sediment capping. Lachlan Seamount also has jagged summit topography, though no central peak, and the suggestion of an approximately planar surface at about 1055 m water depth. This surface may represent a summit crater, with the 150 m–high peak on the eastern side being a parasitic cone or elevated part of the crater rim. As for Endeavour Seamount, no sedimentary section is obvious in the seismic data, though some record of the summit area was lost during repair of a leaking air-gun.

GRAVITY FIELD OVER THE NIUE SEAMOUNTS

By comparing the bathymetry and gravity contour maps (Figures 3 and 4, respectively) it is obvious that the gravity anomalies closely reflect the seafloor topography. An along-track high of 1150 $\mu m/sec^2$ was recorded over the summit area of Endeavour Seamount, while a maximum value of 1700 $\mu m/sec^2$ was recorded over Lachlan Seamount. The gravity high of 2470 $\mu m/sec^2$ on Niue is eccentrically located on the island, and lies to the southwest over an interpreted dense volcanic core (Hill, 1983). Further evidence that the center of mass of the Niue edifice lies toward the southwest of the island rather than directly beneath its center can be seen in the 500, 750 and 1000 $\mu m/sec^2$ contours which display a distinct outward bulge to the southwest.

MAGNETIC FIELD OVER THE NIUE SEAMOUNTS

Large variations in total field anomaly occur over the Niue seamount area (Figure 5). The IGRF80 magnetic anomaly has a range of about -600 to +500 nT.

An extensive and deep (-600 nT) negative anomaly is located over the north-central section of Niue. The field increases rapidly to the south, over the southern sector of Niue, and then levels out onto a +400 nT high over the ocean about 12 km south of the island. The field over Niue has been interpreted as reversely magnetized core located beneath the SW portion of the island (Hill, 1983).

In the case of Endeavour Seamount, an intense high of +500 nT is located just to the NW of the summit. This high may be related to the large high (greater than +500 nT) recorded on the *Melville* line about 15 km to the north. The field appears to be fairly flat over the summit area of the seamount and decreases to a -400 nT low 10 km to the south. Lachlan Seamount has a +100 nT high over the northern part of its summit area. The field decreases northward to a marked -600 nT low situated about halfway between Lachlan and Endeavour Seamounts.

Large data gaps still exist around Endeavour Seamount, particularly to the east, and around Lachlan Seamount, particularly to the south. Until these seamounts have their magnetic fields surveyed in more detail, attempts to make reasonably accurate estimates of their magnetization

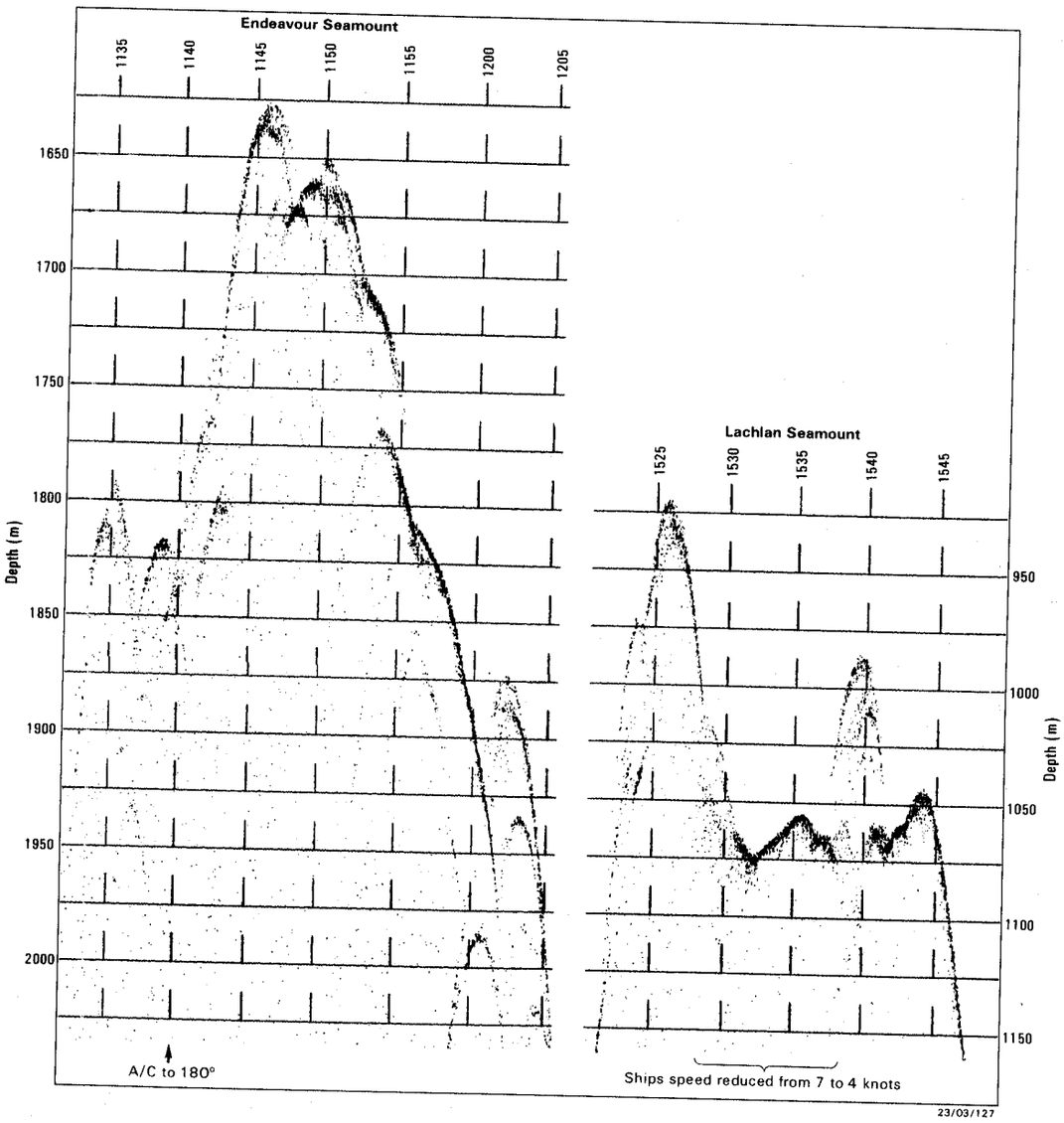

Figure 7. 12 kHz bathymetric records showing morphological detail of the Endeavour and Lachlan Seamount summit areas.

parameters would be premature. A rough qualitative assessment can be made, however. Assuming that the seamounts possess a fairly uniform, mainly thermoremanent magnetization and that no rotation has taken place, it appears that Endeavour Seamount may be of normal polarity, while Lachlan Seamount is probably reversely magnetized, as is the core of Niue.

The large magnetic high to the south of Niue and the large high recorded on the *Melville* line to the north of Endeavour Seamount cannot be attributed directly to magnetization of the seamounts, and probably originate from magnetic heterogeneities within the underlying oceanic crust. Polarity reversals in the crust acquired during accretion may be the source of the anomalies, although no well-defined magnetic lineation pattern has been identified in the region (CPCEMR, 1984; Cande, 1989) and it has been assumed that the oceanic crust in the area was formed during the long interval of normal polarity in the Cretaceous. A recent map (CPCEMR, 1991) shows an inferred magnetic anomaly M0 (118 Ma) crossing Niue in a northeasterly direction.

GRAVITY AND MAGNETIC MODELLING

The gravity and magnetic fields over Niue and adjacent offshore areas have now been mapped in sufficient detail to allow reasonably precise calculation of density and magnetization parameters, and to permit an attempt at modelling the internal structure of the edifice. Adequate gravity data are also available to enable rough calculations

of Endeavour Seamount and Lachlan Seamount densities to be made, though their magnetic fields are not known well enough to allow confident estimates of their magnetic parameters.

The gravity and magnetic fields of the Niue seamounts were analyzed for this study by the 3-dimensional modelling methods of Plouff (1975a, 1975b, 1976). The techniques permit calculation of the gravity and magnetic fields of geological bodies with complex shape by simulating them by an assemblage of polygonal prisms. Seamounts are readily modelled by approximating their submarine topography by a stack of polygonal prisms with vertical sides which follow the bathymetric contours. The measured anomaly data can be inverted to yield least-squares estimates of density and magnetization parameters, plus a planar regional gravity/magnetic field.

The submarine edifice of Niue was approximated by a set of nine polygonal slabs (A–I) as defined in Figure 8. The vertices of the polygonal bodies were selected so that the polygonal outlines closely matched respective bathymetric contours (Figure 3). The composite body represents a depth extent of 0-4.5 km below sea-level. Observed gravity anomaly values were scaled over a 4 km x 4 km grid within the boxed area centered on Niue shown in Figure 8. Least squares comparison between the 100 observed and calculated values gives a best fit density of 2.32 ± 0.02 t/m^3 for the edifice, assuming a density of 1.03 t/m^3 for sea-water. The calculated regional gravity anomaly datum was +280 μm/sec^2, and the standard deviation between observed and calculated values was 80 μm/sec^2. The theoretical gravity contours are shown in Figure 8, and as can be seen, closely match the observed data (Figure 4). An important difference is obvious on Niue Island, however, with the observed high appreciably displaced to the southwest. The gravity measurements made on the island are significantly more accurate (better than ± 5 μm/sec^2) than those from adjacent offshore areas. In addition, the gravity field flattens out over the island so that any underlying anomalous mass distributions become more apparent in the data and are not disguised by high gradients associated with steep or rugged terrain of the island slopes.

Apparent mean densities were calculated for the edifices of Endeavour Seamount and Lachlan Seamount in a fashion similar to that for Niue, except that representative observed gravity values were selected from or close to ship tracks rather than from a regular grid because of the non-uniform data coverage (Table 2). Endeavour Seamount was approximated by six polygonal bodies with depth extents 1.5–2.0, 2.0–2.5, 2.5–3.0, 3.0–3.5, 3.5–4.0 and 4.0–4.3 km. Lachlan Seamount was modelled as seven bodies with depth extents 0.75–1.0, 1.0–1.5, 1.5–2.0, 2.0–2.5, 2.5–3.0, 3.0–3.5 and 3.5–4.3 km.

For magnetic modelling tests of the Niue edifice a similar spatial grid of observed data to that used for the gravity modelling was adopted. One modification, however, was the discarding of the southernmost row of data points to prevent excessive interference on solutions by the extensive magnetic high to the south of Niue which does not appear to be directly related to magnetization of the seamount. This left a grid of 90 data points at 4 km spacing within the boxed area shown in Figure 9.

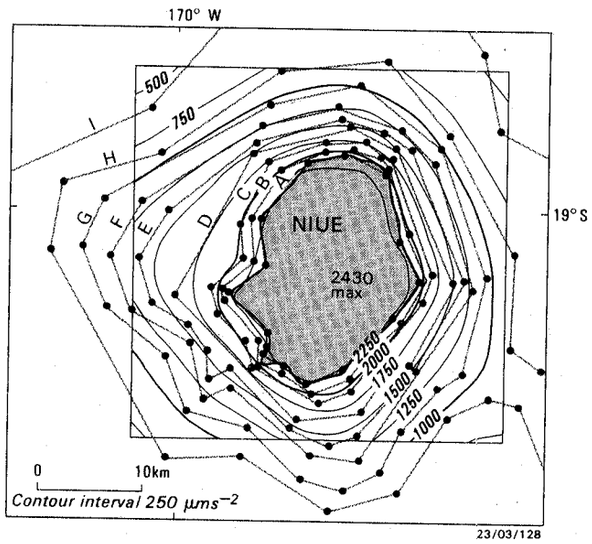

Figure 8. Gravity anomaly (at 250 μm/sec^2 contour interval) for Niue seamount density of 2.32 t/m^3. The seafloor topography is represented by polygonal bodies (A-I) with depth extents (km) as follows: A=0-0.25, B=0.25-0.5, C=0.5-1.0, D=1.0-1.5, E=1.5-2.0, F=2.0-2.5, G=2.5-3.0, H=3.0-4.0, I=4.0-4.5. The polygon vertices are shown as dots. A regional gravity correction of +280 μm/sec^2 has been added.

*Table 2. Apparent mean densities calculated from gravity values.**

Seamount	Best-fit density	Standard deviation(observed-calculated gravity)	Regional gravity datum
Endeavour	2.54 ± 0.11 t/m^3	40 μm/sec^2	220 μm/sec^2
Lachlan	2.76 ± 0.05 t/m^3	50 μm/sec^2	30 μm/sec^2

*assuming sea-water density = 1.03 t/m^3

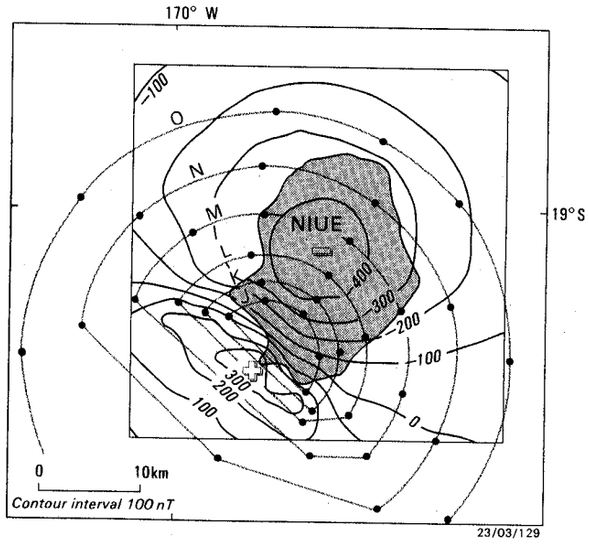

Figure 9. Magnetic anomaly (at 100 nT contour interval) for the volcanic core model. The core is represented by polygonal bodies with depth extents (km) as follows: J=0.5-0.7, K=0.7-1.0, L=1.0-2.0, M=2.0-3.0, N=3.0-4.0, P=4.0-5.0. The vertices of the polygons are shown as dots. A regional magnetic correction of -70 nT has been added.

In magnetic modelling of the Niue edifice, the first approach was to assume uniform magnetization and to try an experimental least-squares best-fit to the observed data. The same polygonal representation of the submarine topography as in the gravity modelling was used. Not unexpectedly, the best solution for this model yielded a poor fit to the data. Further attempts to find an acceptable solution were made by removing the uppermost polygon from successive models, in order to simulate an increasing thickness of non-magnetic top section to the edifice. Only marginal improvement was achieved, however. Obviously, the edifice is not uniformly magnetized, even allowing for a non-magnetic capping.

The next approach was to attempt to model the field by a magnetic core within the edifice, as suggested by the two-dimensional modelling of Hill (1983). Following some trial-and-error adjustments of core position and shape, a good fit to the observed data was achieved. The optimum model is shown in Figure 9, together with the calculated field based on best-fit intensity of total magnetization 2.93 A/m, declination 206° and inclination 35.5°. The multiple correlation coefficient for this fit is 0.89, and the standard deviation for observed-calculated data is 90 nT with a regional magnetic datum of -70 nT.

The modelled core is reversely magnetized and centered on Tepa Point on the SW side of Niue. It is dome-shaped and flat-topped at a depth of 500 m. The dome-like symmetry of the core is flawed to the SW of Niue where it appears that a large section of its flank has been removed.

In order to highlight anomalous density distributions directly beneath the island, residual gravity over Niue was calculated and a contour map produced (Figure 10). The residual gravity values were calculated by subtracting theoretical gravity for the best-fit island pedestal density of 2.32 t/m^3 from the observed gravity. The residual gravity contours show a relative high of 250 μm/sec^2 located over the SW of Niue, above the top of the magnetic core, which implies a relatively high density for the core.

A rough estimate of the density contrast of the core can be obtained by least-squares fitting of calculated anomalies produced by the core model to corresponding residual gravity values which are based on observed data. In doing this one obtains +0.25 t/m as the density contrast of the core. Individual core and upper edifice densities can then be readily determined by modelling of the combined structure with a few trial sets of density values. This yields a core density of 2.41 t/m^3 and an upper edifice density of 2.16 t/m^3.

Dense cores appear to be a common feature of Pacific atolls and volcanic islands (Robertson, 1967a, 1967b, 1970, 1987). Some seamounts have been modelled as having a core that is both dense and also highly magnetized (e.g., Woodward, 1970; Davey, 1973).

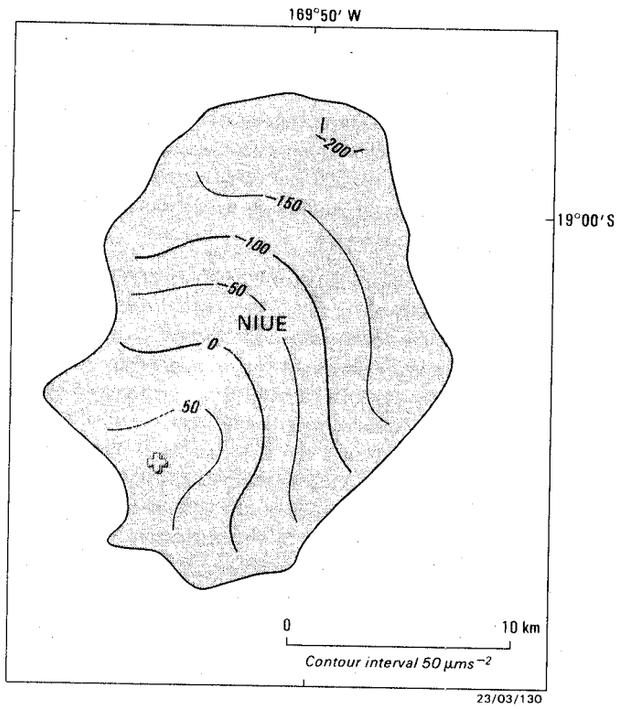

Figure 10. Residual gravity over Niue at 50 μm/sec^2 contour interval.

COMMENTS ON MODELLING RESULTS

In the preceding gravity analysis, it has been assumed that the Niue seamounts are located on an essentially planar lithosphere, implying that the seamount loads are supported by regional rather than local isostatic compensation. This assumption appears to be valid since there is no evidence of local lithospheric depression as might be expressed by bathymetric or gravitational moating around the seamounts. Neither are the calculated densities excessively low, as would be the case for local compensation. The calculated values are typical for common seafloor lithologies, and are in line with the range of 2.3-2.6 t/m^3 most frequently reported in the literature for estimates of mean seamount density. The volcanic edifices must, therefore, have been constructed well off the mid-ocean spreading axis on cold lithosphere of high flexural rigidity (Watts and Ribe, 1984).

The least-squares calculation of seamount densities involved computation of gravity base levels as a by-product of the analysis. From the gravity anomaly map (Figure 4) it appears that the mean regional gravity anomaly is about +200 μm/sec^2, which approximately corresponds to the mean of the base level calculated for Niue (+280 μm/sec^2), Endeavour Seamount (+220 μm/sec^2) and Lachlan Seamount (+30 μm/sec^2). The variations in datum are not appreciable and may well reflect factors that should genuinely contribute to the respective base level. Such factors include choice of depth extent of the polygonal model, anomalous masses in the underlying crust or a regional gravity gradient. It is possible, on the other hand, that these variations are partly the result of severe perturbations in the observed data not accounted for in the modelling assumptions, such as the presence of gross lateral density variations in seamount or crust. The possible error in calculated densities is expected to be less than 0.10 t/m^3 (for datum error of 100 μm/sec^2 or slightly more, depending on the amplitude of the seamount gravity anomaly).

Inclination (I) of the earth's magnetic geocentric dipole field at latitude λ is given by $\tan I = 2 \tan \lambda$. The magnetization vector calculated for the core of Niue is inclined at 35.5° which corresponds to a paleolatitude of 19.6°S. This compares with the present latitude of Niue of 19.1°S, and is consistent with a northerly drift of Niue on the Pacific plate since the core cooled below the Curie point. Uncertainty in the magnetization parameters, largely due to inadequate control on the core geometry, prevent confident determination of virtual geomagnetic pole and hence paleomagnetic age for Niue.

EVOLUTION OF THE NIUE SEAMOUNTS

The Niue seamounts are believed to have evolved through a progression of stages (A–D) as depicted in Figure 11, and described below.

Stage A

During the Early-Middle Miocene, pillow basalts erupted onto seafloor of mid–Late Cretaceous age (70–100 Ma old at the time). The volcanism may have been initiated at a point of crustal weakness as the Pacific plate drifted over a mantle hot-spot. This conjectured hot-spot may now be located just east of Rarotonga, having created the Capricorn–Niue–Rarotonga chain of seamounts.

Continued volcanic activity produced a core of pillow-lavas and interbedded tuffs about 4 km high, with the summit reaching close to or slightly above sea-level. This was the proto-core of Niue with a density of 2.41 t/m^3 and high thermoremanent magnetization (2.93 A/m), imparted at a time of polarity reversal in the earth's magnetic field.

Construction of the Lachlan Seamount core may have been contemporaneous with that of Niue because of common location on a NW-trending structural weakness in the crust and because they both appear to possess reversed thermoremanent magnetization. The high density of Lachlan Seamount (2.76 t/m^3) suggests that the feature was built from dense basaltic flows which probably coalesced with

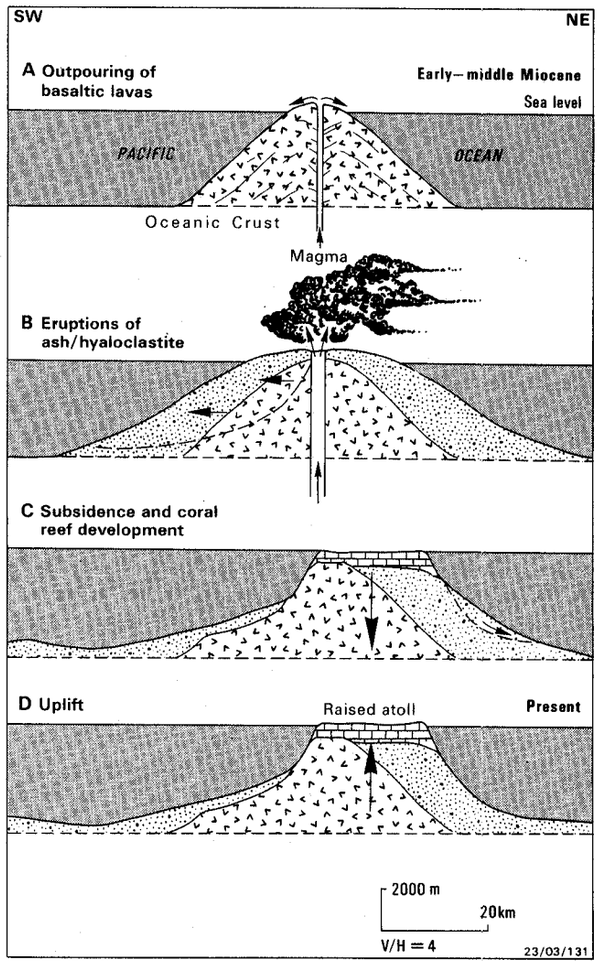

Figure 11. Conceptual evolution of Niue, stages A-D.

those of Niue to produce a low saddle between the two edifices. Significant invasion of the core by dikes and other intrusions may be a factor contributing to the high density of Lachlan Seamount.

Being located east of Niue (in the younging direction of the hot-spot trace) and, apparently possessing a normal magnetic polarization, Endeavour Seamount may have evolved somewhat after the other two seamounts. A moderate density (2.54 t/m^3) suggests that the core was built mainly of pillow basalts.

Stage B

With the summit of Niue near sea-level, a change in style of volcanism took place, with basalt flows giving way to explosive eruptions of ash and hyaloclastite. The free expansion of magmatic gases in the shallow marine or subaerial conditions without the confining hydrostatic pressures of the earlier deep-sea phase of volcanism may have contributed to the change, as might possible magmatic differentiation. Ash-falls and other pyroclastic deposits built up over the basalt core to form a cap almost 3 km thick. Consisting of loosely packed, essentially randomly oriented particles, these volcanic sediments would have low bulk magnetization and also low density (2.16 t/m^3). The altered tuff and vesicular basalt dredged at station U357 are probably part of this unit.

A massive explosive eruption and/or caldera collapse marked the termination of volcanic activity. This cataclysmic event resulted in the removal of a large section of the SW flank of the volcano. If an explosive event was responsible, the section may have either blown out, or became detached and moved downslope as a great submarine landslide, with the resultant debris possibly now forming the seafloor apron and mounded area to the SW of Niue.

Stage C

With the volcano extinct, subaerial erosion and wave action planated the upper surface to sealevel. A carbonate reef began to develop in the shallow-water tropical environment. The reef continued to grow upwards, forming an atoll as the volcanic base subsided. Evolution of atolls and subsidence mechanisms have been discussed by a number of workers (Menard, 1973; Detrick and Crough, 1978; Scott and Rotondo, 1983). Niue is considered to have developed as a typical atoll, with subsidence produced by (i) depression of the lithosphere in isostatic response to the volcanic load, and (ii) cooling and sinking of the surrounding lithosphere as the mantle hot-spot was over-ridden. The coral limestone cap attained a maximum thickness of 500-600 m.

Loading by the limestone cap combined with diagenesis, compaction and deformation of the volcanic sediments produced gravitational instability in the flanks of the edifice expressed episodically as major submarine landslides. The embayed coastal outline of Niue is believed to be due to such mass movements. Large limestone chasms oriented sub-parallel with the coastline are common along the coastal strip. Interpreted as solution channels developed along tensional gashes, they are further evidence of slump activity (Schofield, 1959). Concave 'bights' in coastal outlines, as seen on Niue, are a common feature of Pacific atolls and represent a mature stage in development of atoll morphology (Fairbridge, 1950).

Stage D

Uplift of the atoll commenced as early as 700,000 years ago (Fieldes et al., 1960), as Niue, conveyed on the Pacific plate, began to ascend the outer rise seaward of the Tonga Trench (Dubois et al., 1975). The raised atoll now stands 70 m above sea-level.

REFERENCES CITED

Aharon, P., S.L. Goldstein, C.W. Wheeler, and G. Jacobson, 1993, Sea-level events in the South Pacific linked with the Messiinian salinity crisis: Geology, v.21, p.771-775.

Brodie, J.W., 1966, Niue Island provisional bathymetry: New Zealand Oceanographic Institute Chart, Island Series, scale 1:200,000.

Cande, S.C., J.L. LaBrecque, R.L. Larson, W.C. Pittman III, X. Golovchenko, and W.F. Haxby, 1989, Magnetic lineations of the world's ocean basins: AAPG Map Series, scale 1: 26,950,000 at equator (Mercator projection).

Chase, T.E., B.A. Seekins, S.C. Vath, and M.A. Cloud, 1982, Topography of the Tonga region: USGS-CCOP/SOPAC South Pacific Project Chart (12-27°S, 180-170°W), Department of the Interior, United States Geological Survey.

CPCEMR(Circum-Pacific Council for Energy and Mineral Resources), 1984, Plate tectonic map of the circum-Pacific region, Pacific Basin sheet: AAPG, scale 1: 17,000,000.

CPCEMR(Circum-Pacific Council for Energy and Mineral Resources), 1991, Tectonic map of the circum-Pacific region, southwest quadrant: Map CP-37, U.S. Geological Survey, scale 1: 10,000,000.

Davey, F.J., 1973, Gravity and magnetic measurements over Aotea Seamount, eastern Tasman Sea: New Zealand Journal of Geology and Geophysics, v.16, p.1047-1054.

Detrick, R.S., and S.T. Crough, 1978, Island subsidence, hot spots and lithospheric thinning: Journal of Geophysical Research, v.83, p.1236-1244.

Dubois, J., J. Launay, and J. Recy, 1975, Some new evidence on lithospheric bulges close to island arcs: Tectonophysics, v.26, p.189-196.

Fairbridge, R.W., 1950, Landslide patterns on oceanic volcanoes and atolls: Geophysical Journal, v.115, p.84-88.

Fieldes, M., G. Bearling, G.G.C. Claridge, N. Wells, and N.H. Taylor, 1960, Mineralogy and radioactivity of Niue Island soils: New Zealand Journal of Science, v.3, p.658-675.

Hill, P.J., 1983, Volcanic core of Niue Island, southwest Pacific Ocean: BMR Journal of Australian Geology and Geophysics, v.8, p.323-328.

Jacobson, G., and P.J. Hill, 1980a, Groundwater resources of Niue Island: Bureau of Mineral Resources, Australia, Record 1982/40.

Jacobson, G., and P.J. Hill, 1980b, Hydrogeology of a raised coral atoll - Niue Island, South Pacific Ocean: BMR Journal of Australian Geology and Geophysics, v.5, p.271-278.

Kroenke, L.W., C. Jouannic, and P. Woodward, 1983, Bathymetry of the Southwest Pacific: CCOP/SOPAC, Fiji, Chart, scale 1:6442192.

Mammerickx, J., S.M. Smith, I.L. Taylor, and T.E. Chase, 1973, Bathymetry of the South Pacific: Chart 13, Scripps Institution of Oceanography.

McAdoo, D.C., and C.F. Martin, 1984, SEASAT observations of lithospheric flexure seaward of trenches: Journal of Geophysical Research, v.81, p.3201-3210.

Menard, H.W., 1973, Depth anomalies and the bobbing motion of drifting islands: Journal of Geophysical Research, v.78, p.5128-5137.

Peddie, N.W., 1982, International Geomagnetic Reference Field: the third generation: Journal of Geomagnetism and Geoelectricity, v.34, p.309-326.

Plouff, D., 1975a, Derivation of formulas and FORTRAN programs to compute magnetic anomalies of prisms: National Technical Information Service, U.S. Department of Commerce, Report PB-243-525, 112 p.

Plouff, D., 1975b, Derivation of formulas and FORTRAN programs to compute gravity anomalies of prisms: National Technical Information Service, U.S. Department of Commerce, Report PB-243-526, 90 p.

Plouff, D., 1976, Gravity and magnetic fields of polygonal prisms and application to terrain corrections: Geophysics, v.41, p.727-741.

Robertson, E.I., 1965, Gravity base stations in the South-west Pacific Ocean: New Zealand Journal of Geology and Geophysics, v.8, p.424-439.

Robertson, E.I., 1967a, Gravity effects of volcanic islands: New Zealand Journal of Geology and Geophysics, v.10, p.1466-1483.

Robertson, E.I., 1967b, Gravity survey in the Cook Islands: New Zealand Journal of Geology and Geophysics, v.10, p.1484-1498.

Robertson, E.I., 1970, Additional gravity surveys in the Cook Islands: New Zealand Journal of Geology and Geophysics, v.13, p.184-198.

Robertson, E.I., 1987, Gravity survey on Atafu atoll, Tokelau Islands, Southwest Pacific Ocean: New Zealand Journal of Geology and Geophysics, v.30, p.211-212.

Schofield, J.C., 1959, The geology and hydrology of Niue Island, South Pacific: New Zealand Geological Survey Bulletin 62.

Schofield, J.C., and C.S. Nelson, 1978, Dolomitisation and Quaternary climate of Niue Island, Pacific Ocean: Pacific Geology, v.13, p.37-48.

Scott, G.A.J., and G.M. Rotondo, 1983, A model for the development of types of atolls and volcanic islands on the Pacific lithospheric plate: Atoll Research Bulletin No. 260, Smithsonian Institute, Washington, D.C.

Summerhayes, C.P., 1967, Bathymetry and topographic lineation in the Cook Islands: New Zealand Journal of Geology and Geophysics, v.10, p.1382-1399.

Watts, A.B., and N.M. Ribe, 1984, On geoid heights and flexure of the lithosphere at seamounts: Journal of Geophysical Research, v.89, p.11152-11170.

Watts, A.B., and M. Talwani, 1974, Gravity anomalies seaward of deep-sea trenches and their tectonic implications: Geophysical Journal of the Royal Astronomical Society, v.36, p.57-90.

Whitehead, N.E., J. Barrie, and P. Rankin, 1990, Anomalous Hg contents in soils of Niue Island, South Pacific: Geochemical Journal, v.24, p.371-378.

Whitehead, N.E., R.G. Ditchburn, W.J. McCabe, and P. Rankin, 1992, A new model for the origin of the anomalous radioactivity in Niue Island (South Pacific) soils: Chemical Geology (Isotope Geoscience Section), v.94, p.247-260.

Woodward, D.J., 1970, Gravity and magnetic anomalies over the Derwent Hunter Guyot, Tasman Sea: New Zealand Journal of Geology and Geophysics, v.13, p.117-125.

Woollard, G.P., and J.C. Rose, 1960, Final report on gravity program: Woods Hole Oceanographic Institute, Ref. No. 60-26.

Wright, A.C.S., and F.J. Van Westerndorp, 1965, Soils and agriculture of Niue Island: New Zealand DSIR, Soil Bureau, Bulletin 17.

Hill, P J., and S. Helu, 1996: Sedimentation patterns and structure of Tofu a Trough: a forearc basin on the Tonga Ridge, *in:* Meylan, M.A., and G.P. Glasby (eds) Manihiki Plateau, Machias and Capricorn Seamounts, Niue, and Tofua Trough:
Results of *Tui* Cruises. SOP AC Technical Bulletin 10: 45-60.

SEDIMENTATION PATTERNS AND STRUCTURE OF TOFUA TROUGH: A FOREARC BASIN ON THE TONGA RIDGE

P.J. Hill

Australian Geological Survey Organisauon, GPO Box 378, Canberra, Australia

S. Helu

Tonga Water Board, P.O. Box 92, Nuku'alofa, Tonga

ABSTRACT

The Tofua Trough is a linear sediment-filled basin within the Tonga Ridge. It is about 500 km long and where best developed is 30-40 km wide, 1800 m deep, and contains about 2 km of sediments. The structure and nature of sediment ftIling of the Tofua Trough have been interpreted from 500 km of geophysical proftles, recorded over 11 survey lines criss--crossing the trough in a zig-zag pattern. These include 12 kHz bathymetry, single-channel seismic reflection (airgun), magnetics, and gravity.

The general sedimentation pattern in the trough is a thickening of units toward the center, reflecting intrabasinal sag or continual subsidence during sediment accumulation. The sediment fill is seismically well stratified, the reflections being well developed, closely spaced, and near horizontal or dipping at shallow angles. Beds lap onto the Tonga platform on the east, with the margin of the Tonga platform being stepped down by a series of 45°-60°-dipping normal faults which form a composite scarp. Steep normal faults also occur in the middle of the trough. Beds on the west are either truncated by faults or interfinger with the more chaotically bedded proximal units of the volcanic edifices. The hummocky surface of the lower flank of the Home Reef volcanic edifice may be due to recent slumping of volcaniclastics. The trough-facing flank of a large submarine volcano just north of Kao has a similar irregular surface; the relief is due to slumping and sliding of several sediment sheets, 50 m thick and up to 4 km long, down the side of the edifice. In addition to normal faults, piercements assumed to be volcanic in origin were observed on the seismic reflection profiles.

The free-air gravity field of the Tofua Trough and adjacent Tofua volcanic arc and Tonga platform displays numerous anomalous features, partly due to seafloor topography and partly to 'lateral sub-bottom density variations. The gravity low over the trough reflects the deeper water and the presence of a thick sequence of presumed relatively low density volcanogenic/hemipelagic sediment. This is strongly supported by gravity modelling. There is also a good match between observed and calculated gravity obtained for a modelled sediment thickness of 2.0 km in the trough, supporting previous seismic refraction and reflection evidence. Basement is not clearly defined in our data.

The magnetic field is also highly anomalous, the larger anomalies associated mainly with the volcanoes of the Tofua magmatic arc. There is a relatively subdued magnetic field over the limited area of the Tonga platform surveyed; even the major trough/platform boundary faults are not strongly expressed. Four submarine volcanoes crossed show strong magnetic anomalies consistent with normal magnetization, suggesting formation during the Brunhes, but a seamount just north of Kao displays an anomaly which implies some internal reverse magnetization. The observed magnetic field of the Tofua Trough correlates very poorly with theoretical seafloor spreading anomaly profiles calculated assuming a simple spreading geometry.

Tonga platform to the east (Figures 1, 2). The structure is about 500 km long, extending from Ata Island in the south to Fonualei Island in the north. It is best developed, however, north of Tongatapu between latitudes 19°00'S and 20°30'S, to the west of the Ha'apai group of coral islands on the Tonga platform. Here the trough is 30-40 km wide, 1800 m deep, and contains about 2 km of sediments.

The Tonga arc-trench system, together with the Mariana arc-trench system, has been widely recognized as the type example of a simple island arc with an active marginal basin (Karig, 1970; Packham, 1978; Hawkins et al., 1984). Tofua Trough forms an integral and distinct architectural element of the Tonga arc. For this reason, study of its structural and stratigraphic development in what is perceived as a relatively uncomplicated tectonic setting contributes to the general understanding of geotectonic processes and their interactions in modern island arc environments, and recognition and interpretation of ancient arc-trench assemblages (e.g., Dickinson, 1971; Leitch, 1984).

As yet, no significant mineral resource potential has been identified in the trough itself. The Tonga platform, adjacent to the trough, is considered prospective for petroleum and has been actively explored by oil companies (Tongilava and Kroenke, 1975; Maung et al., 1981). Hydrothermal mineral deposits associated with volcanic activity along the Tofua magmatic arc may have formed at depth within the Tofua Trough sediment pile (Cronan et al., 1984).

Geophysical systems operated on the *Tui* cruise included single-channel seismic with 120 in^3 airgun source, magnetics, gravity and 12-kHz bathymetry. Profiles of 500 km total length were recorded over a pattern of 11 survey lines (A-K) criss-crossing the trough (Figure 3).

TECTONIC AND GEOLOGICAL FRAMEWORK

The region lies at the extreme eastern boundary of the Australian plate, adjacent to the Pacific plate (Figure 2). This convergent plate boundary is marked by the 10,500 m-deep, NNE-trending Tonga Trench at which the Pacific plate is being subducted beneath the Tonga Ridge along a Wadati-Benioff zone dipping to the west at about 45° (Isacks et al., 1969; Hanus and Vanek, 1979; Hamburger and Isacks, 1987). The Tonga Ridge consists of two principal structural components, (i) the reef and coral island-studded Tonga platform, and (ii) the Pliocene(?)-Holocene, mainly andesitic, volcanic cones of the Tofua magmatic arc located along the western margin of the ridge. The platform and volcanic chain are separated by Tofua Trough. Extending to the west of the Tonga Ridge is the 2000-3000 m-deep Lau Basin, which is bounded to the west by the meridional Lau Ridge.

The Lau Basin is characterized by a relatively shallow depth (2000-3000 m compared with the 5000-6000 m-deep Pacific Basin to the east), rough acoustic basement, thin sediment cover, and high but variable heatflow. On the basis of this, and the recovery by dredging of fresh tholeiitic, mid-ocean ridge-type basalts (MORB), the Lau Basin has been interpreted as an actively spreading backarc basin separating the old forearc platform and active volcanoes of the Tonga arc from the remnant volcanic arc of the Lau Ridge (Karig, 1970; Sclater et al., 1972; Hawkins, 1974; Gill, 1976).

Various models for opening of the Lau Basin have been proposed (Sclater et al., 1972; Lawyer et al., 1976; Weissel, 1977; Falvey, 1978; Eguchi, 1984), or implied from maps of tectonic fabric presented (Cherkis, 1980; Larue et al., 1982; Malahoff et al., 1982). The models are based mainly on evidence from magnetic lineation patterns, and to a lesser extent on seismicity, earthquake focal mechanisms, seafloor morphology, sediment thickness, age and petrology of seafloor samples, and paleomagnetism. A major problem in elucidating the detailed tectonic evolution of the Lau Basin has been that the magnetic lineations which reflect crustal accretion and seafloor spreading processes have been difficult to map. This difficulty in identifying and correlating magnetic lineations suggests short spreading ridge segments and general structural complexity of the basin, and is responsible for the diversity in interpretations. Proposed spreading geometries include, (i) a Y-shaped configuration of spreading ridges and transforms involving interaction of a number of micro-plates (Weissel, 1977; Falvey, 1978), (ii) a curved spreading ridge disrupted only in a minor way by transform offsets (Cherkis, 1980), and (iii) a uniform system of NW–SE–trending transforms and NE-SW spreading axes continuous along the length of the basin (Sclater et al., 1972; Eguchi, 1984). The spreading geometry depicted in Figure 2 is based on the seismotectonic interpretation of Eguchi (1984).

Identification of the oldest magnetic anomaly in the central Lau Basin (south of Peggy Ridge and west of Tofua Trough) has varied among investigators working on different magnetic data sets. The oldest anomaly according to Weissel (1977) is 2A, according to Cherkis (1980) is 3A, and Larue et al. (1982) map it as 3. Thus from magnetic data alone, onset of seafloor spreading in the central Lau Basin is placed at 3.5–5 Ma with opening proceeding at a total rate of 50-76 mm/year. Weissel (1977) suggested, however, that a deep 80 km-wide subsidiary basin adjacent to the Lau Ridge may have been the site of initial separation of the Lau and Tonga Ridges at 5–6 Ma, but that it was abandoned by a ridge crest jump to the east (at about 3.5 Ma).

The Lau Basin is geochemically zoned (Hawkins and Melchoir, 1985), with normal type (N–MORB) basalts forming the modern basement for the central part of the basin and transitional type basalts (similar to those of the Mariana Trough) underlying the older western margin of the basin. The eastern side of the basin close to the active Tofua magmatic arc is also considered to be floored by transitional type basalts (Falloon et al., 1987), but this remains untested due to burial by products of the recent volcanism.

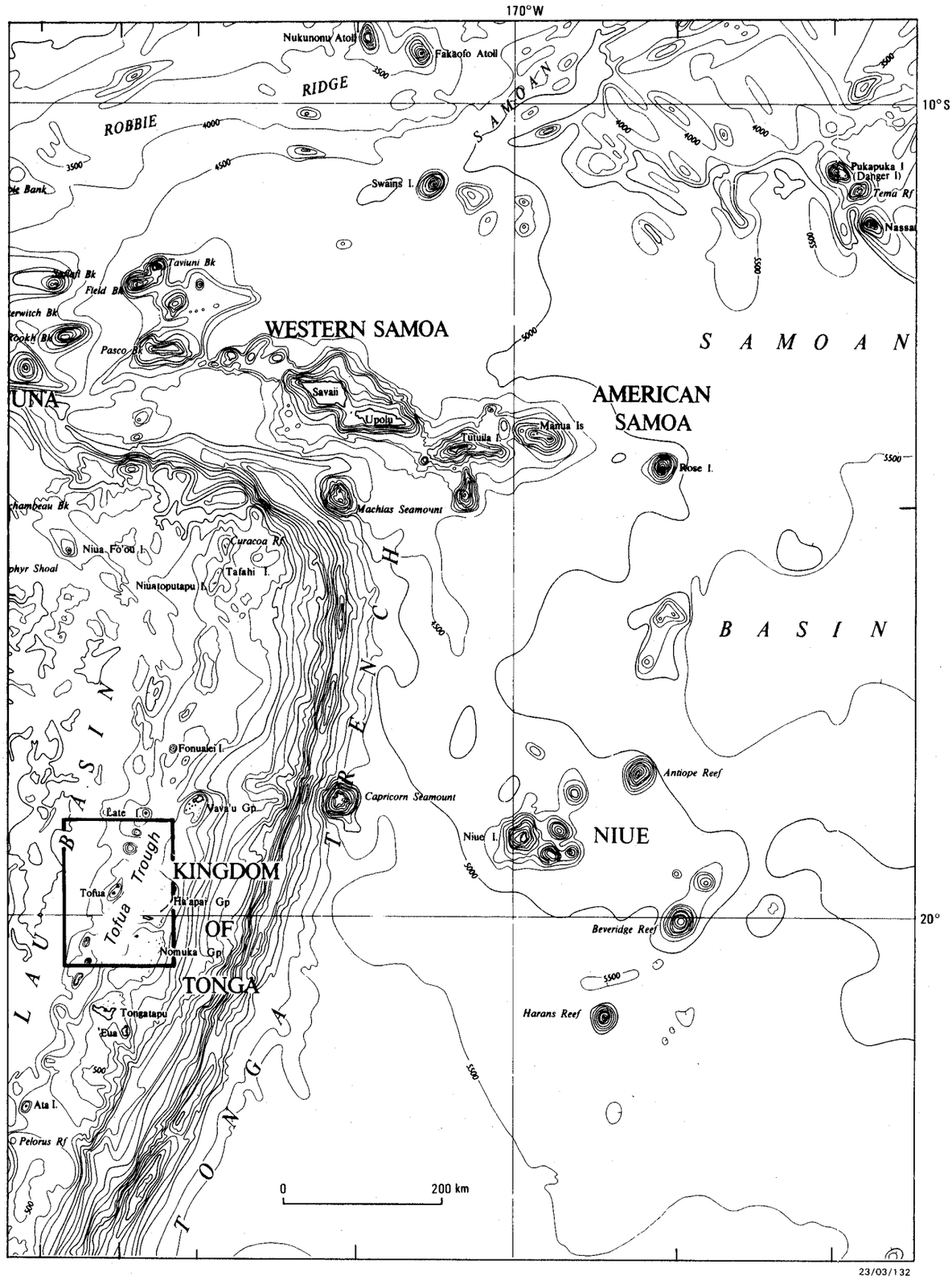

Figure 1. Location map. Bathymetry after Kroenke et al. (1983); isobaths in meters. Study area outlined by box.

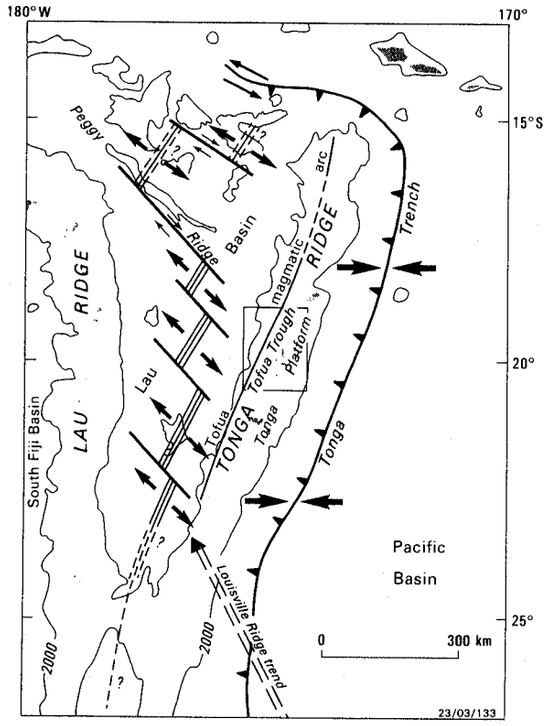

Figure 2. Regional tectonic setting and major structural elements. Lau Basin seafloor spreading geometry after Eguchi (1984) and Lewis (1985).

Forearc sediments on the Tonga Ridge are up to 5 km thick and consist of a nearly continuous sequence of Middle Eocene-Holocene volcaniclastics and carbonates overlying igneous basement of pre-Middle Eocene age (Cunningham and Ascombe, 1985). The sediment pile thins towards the eastern rim of the platform; Oligocene beds are thin or absent. Basement is represented by exposures of a basalt-rhyolite suite of island arc tholeiitic affinity on the island of 'Eua.

The geological evolution of the Tonga platform has been described in recent accounts (Maung et al., 1981; Kroenke, 1984; Scholl et al., 1985b; Exon et al., 1985; Herzer and Exon, 1985; Lewis, 1985). Tonga platform basement is believed to have originally formed part of an Eocene forearc adjacent to New Caledonia on the ancestral Inner Melanesian arc. The Oligocene geological record shows that this period was one of limestone deposition and quiescence in volcanic activity, with widespread uplift and emergence and generally thin sediment accumulation. Opening of the South Fiji Basin in the late Oligocene rafted the 'Eua arc fragment (Lau–Tonga Ridge) eastward. Arc volcanism began by early Middle Miocene with volcanic centers located on the western side of the Lau-Tonga Ridge. At this time the Tonga platform was a forearc basin resembling the present one, with volcaniclastic deposits thickly accumulating near the volcanic arc and thinning eastwards towards an outer high. Intrusive activity was common during this period.

A decrease in volcanic activity is indicated in the Late Miocene. However, evidence from wells drilled on Tongatapu suggests that volcaniclastic sedimentation continued well into the Early Pliocene before a change to limestone deposition in Late Pliocene-Holocene, though there is uncertainty as to how much of the volcaniclastic sequence may represent older, reworked material. As the Lau Basin opened in Early Pliocene time, the forearc (now the Tonga platform) was rafted away to the east, resulting in extinction of the volcanic arc left behind on the Lau Ridge. Volcanism reappeared in the Late Pliocene at the western margin of the Tonga platform with construction of the volcanic chain of the Tofua magmatic arc, along which activity continues to the present time.

During the Pliocene-Holocene, thermal uplift and subsidence associated with rifting and spreading in the Lau Basin have been complicated by tectonic adjustments to oblique subduction of the Louisville Ridge beneath the platform (Dupont and Herzer, 1985). Uplifts, both regional and local, have produced a widespread unconformity in the Early Pliocene. Two principal sets of normal faults have developed since Late Pliocene time, (i) a westerly-dipping set related mainly to Lau Basin rifting and subsidence, and (ii) a set cutting orthogonally across the NNE-trending axis of the forearc basin, probably activated in response to Louisville Ridge subduction.

SEDIMENTS AND ARC VOLCANISM

Seafloor sediment samples were recovered by coring and dredging from stations distributed over an extensive area of the Tofua Trough during 1981 and 1982 research cruises of RV *Tangaroa* (Cronan et al., 1984). Sediments were generally found to consist of greater than 75% volcanic debris, fine sand to silt size, composed of acidic glass shards, calcic plagioclase, and clinopyroxene, with minor amounts of opaques. Rapid accumulation rates of volcanic material are indicated by the low concentration of biogenic components. The seafloor sampling results are consistent with the numerous charted sediment notations for Tofua Trough on British Admiralty Chart 2421 (1984). The annotations indicate a bottom predominantly of "volcanic sand" with some areas of "cinders" and "pumice", and only a few locations marked as "coral". The volcanic sediments are undoubtedly the result of volcanic activity along the adjacent Tofua magmatic arc, both because of the proximity of the arc and the silicic nature of the sediments. Coral fragments were recovered from the middle of the trough (water depth about 1700 m) as well as along its margins. The coral was probably transported by sediment gravity flows from the shallow waters of the Tonga platform and from reefs developed along the arc, reefs that have formed either as local narrow fringing reefs around subaerial volcanoes or were constructed on shallow volcanic banks.

Some insight into the sedimentology of Tofua Trough may be obtained by briefly reviewing what is known of the geology and volcanic processes taking place along the Tofua volcanic arc, since it is the arc that is the primary source of sediment. Bryan et al. (1972) estimated that volcanic eruptions along the arc have averaged about one every four years during this century, discounting small submarine eruptions that may have passed unnoticed or unrecorded. Volcanic events other than mild solfataric activity appear to have a periodicity of 20-50 years, and most eruptions are of short duration, lasting from a few

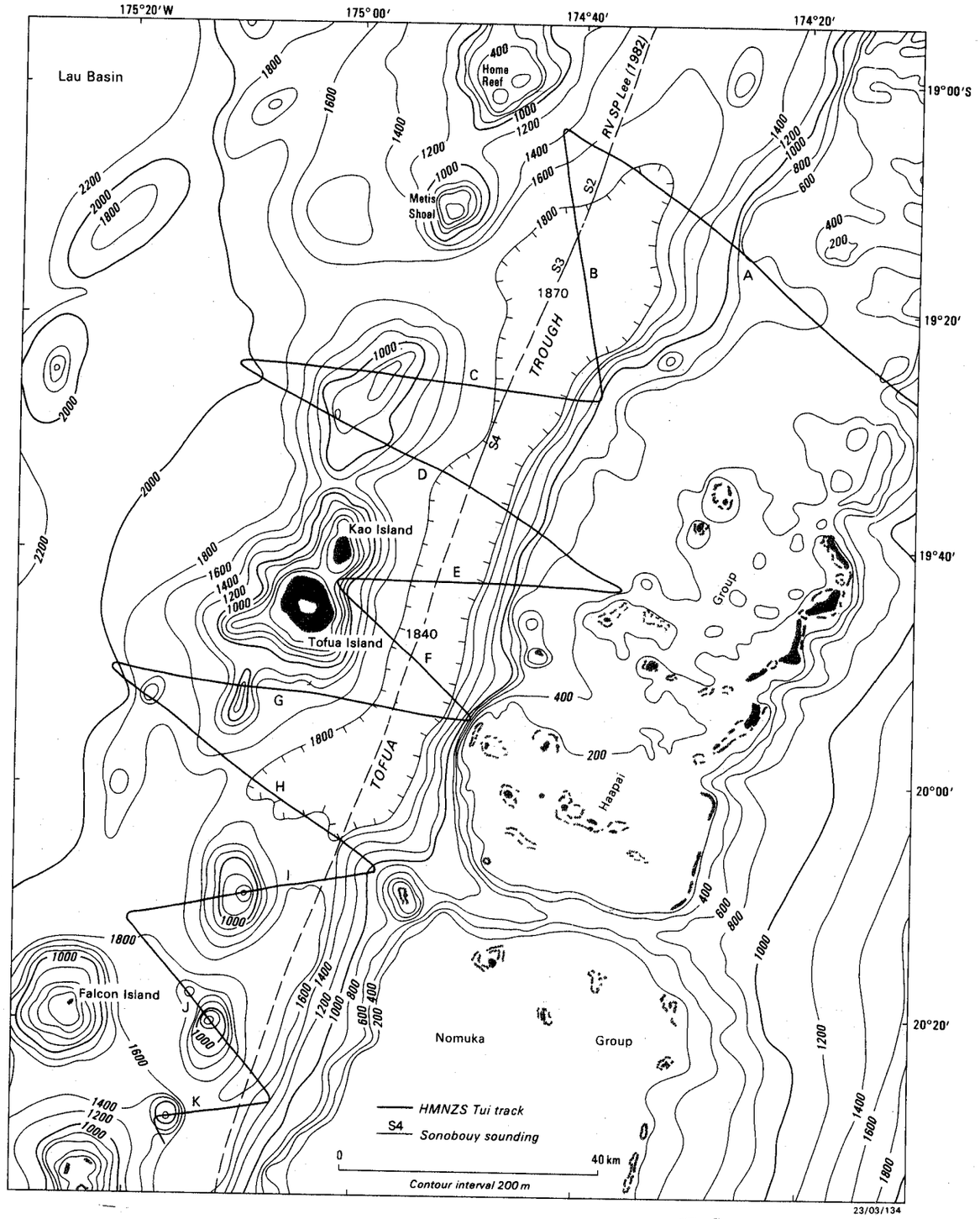

Figure 3. Tofua volcanic arc, Tofua Trough and Tonga platform geophysical survey lines and bathymetry.

months to a year. Existing records do not reveal any close relationship of periods of activity between adjacent volcanic centers. Geological and/or petrological studies of most of the volcanic islands and shoals adjacent to our area of investigation have been undertaken; those studied include (from north to south) Late Island, Home Reef, Metis Shoal, Kao, Tofua, Falcon, Hunga Tonga and Hunga Ha'apai Islands. A summary of the more important aspects of the geology and volcanic activity of the islands relevant to sedimentation in the adjoining Tofua Trough is provided below. For more detailed discussions the reader is referred to Schofield (1967), Bauer (1970), Melson et al. (1970), Baker et al. (1971), Mulder and Nieuwenhiuzen (1971); Bryan et al. (1972), Ewart et al. (1977), and Cunningham and Anscombe (1985).

Late: The island is a conical volcanic peak about 540 m high and 6 km in diameter at sea level, with a well-developed central crater at its summit. The volcano last erupted in 1854 and still shows some weak solfataric activity in the crater. A number of small cinder cones are located on the western flank of the volcano. The extensive lowland areas to the north and east of the central cone are composed of rough, blocky lava flows mantled by ash deposits. The lavas on Late are all of basaltic andesite or andesite.

Home Reef: Very little is known about this structure. British Admiralty Chart 2421 indicates that the seafloor on the flanks of the seamount is composed mainly of patches of volcanic sands and pumice; coralline sediment was recorded at several sites on the southeast flank. A reported submarine eruption in 1984 took place about 6 km southeast of the reef.

Metis Shoal: The shoal represents a submarine volcano that last erupted in 1967-68 with explosions of steam, ash, and bombs. An island at least 0.5 km long and 24 m high was produced, but was soon eroded to beneath wave base. The erupted product consisted of vesicular rhyolite glass.

Kao: Kao is the highest volcano of the Tofua chain, and consists of a steep-sided symmetrical strato-volcano rising to an elevation of about 1125 m. The remnants of a crater or coalescing craters can be seen near the summit. The slopes of Kao are mantled by ash, cinder, and flows, all apparently of recent origin since erosion has not incised deeply into the flanks of the volcano. No historic eruptions are known on Kao. The exposed lava flows are mainly augite andesite.

Tofua: Tofua is an active composite volcano 8-10 km across, with a large (4 km diameter) central collapse caldera containing a fresh-water lake and recent volcanic deposits (tuff, lapilli tuff, cinder, and some lava flows). Lofia Cone within the caldera last erupted in 1959.

Four stratigraphic units have been mapped on Tofua: (oldest) Hamatua Formation of pre-caldera age (?Late Pleistocene), Hokula Froth Lava - possibly contemporaneous with the caldera collapse; post-caldera Kolo Formation; and (youngest) Lofla Formation comprising deposits recently erupted from within the caldera. Erosional unconformities separate the Hokula Froth Lava from the underlying Hamatu Formation and overlylng Kolo Formation. The Hamatu Formation consists of lava flows of basaltic andesite, hypersthene-bearing augite andesite, andesite, and augite dacite. It is thought to have been part of an older cone, possibly resembling Kao, which was largely destroyed as the caldera was created. A 500 m-thick section of the Hamatua Formation is exposed in the walls of the caldera, where individual flow units are seen to average 20 m in thickness.

The Hokula Froth Lava comprises a number of microvesiculated flow units of andesitic composition, each unit being about 5-6 m thick. The formation is exposed in sea cliffs along the northwest coast of Tofua. The post-caldera Kolo Formation is composed of lapilli tuff-breccia, tuff, unconsolidated ash, and cinder and andesite lava flows up to 20 m thick. Aconsolidated lapilli-tuff breccia member lies unconformably on the Hamatua Formation on the southern, eastern and northern flanks of Tofua, forming a blanket more than 30 m thick over the entire area. The recently-deposited Lofia Formation is composed of lithologies similar to those of the Kolo Formation, but its distribution is limited essentially to the confines of the caldera.

Falcon Island (also called Fonua Foou): Falcon Island is the top of an active volcano that, like Metis Shoal, was successively built up above sea level and then eroded back down. It has had two major periods of activity during historic time, the first between 1877-1894 and the second between 1921-1936. Such long periods of sustained activity are unusual for volcanoes of the Tofua chain. An augite andesite was erupted in 1885 and in 1927 andesitic pyroclastic debris was ejected.

Hunga Tonga and Hunga Ha'apai: These islands appear to be the northern and western subaerial erosional remnants of a once much larger active volcanic cone. Submarine eruptions were recorded in 1912 and 1937 at a site several kilometers to the south of Hunga Tonga. The volcanics of the islands consist of alternating layers of andesitic lava flows and pyroclastics (scoria, lapilli and ash), which dip gently away from the center of the volcanic edifice. Much of the surface of the islands is covered by a reddish volcanic ash.

PREVIOUS GEOPHYSICAL INVESTIGATIONS

Early work in the area included that of the Capricorn Expedition (1952-53), during which a deep seismic refraction sounding was made along Tofua Trough near Kao Island; two similar soundings were made farther to the east in the Tonga Trench (Raitt et al., 1955). In 1972, the Mobil Oil research ship *Fred H. Moore* recorded a number of multichannel seismic lines across Tonga Ridge; an interpretation of two of the lines (72-200 and 72-202) has been published (Kroenke and Tongilava, 1975). Between

1975-1978, ORSTOM (Office de la Recherche Scientifique et Technique Outre-Mer, Noumea) surveyed Tonga Ridge with an extensive network of single-channel seismic, magnetic and gravity traverses during the AUSTRADEC IV, EVA III and EVA VII research programs. During the EVA VII program, seven seismic refraction profiles were recorded along an east-west transect across Tonga Ridge at about 11°30'S (Pontoise et al., 1980; Pontoise and Latham, 1982), just to the north of the Capricorn Expedition refraction transect.

Petroleum exploration began in Tonga in 1970 following the discovery of thermogenic crude oil seepages on Tongatapu and 'Eua. Much of the Tonga platform has been mapped with oil company seismic lines, and five exploration wells have been drilled on Tongatapu (Tongilava and Kroenke, 1975; Maung et al., 1981). The southern Tonga platform was investigated in 1982 by RV *S.P.Lee* (Scholl and Vallier, 1985) using multichannel seismic, gravity, magnetics, sonobuoy seismic refraction, and seafloor sampling methods. During this cruise, single-channel seismic and several sonobuoy refraction profiles were recorded along the axis of Tofua Trough (Figure 3) while the ship was in transit to the main study area south of Tongatapu. The MS *Natsuchima*, in 1984, completed a geophysical and geological research study of the Tonga Ridge north of Vava'u (Honza, Lewis et al., 1985). Although the area investigated lies just beyond the northern extent of the Tofua Trough, the results of the cruise are useful for comparing the geology of sections of the Tonga Ridge with and without a forearc Tofua Trough.

BATHYMETRY

The bathymetry of Tofua Trough and adjacent areas is based largely on the compilation by Chase et al. (1982), modified by the new bathymetric control provided by the HMNZS *Tui* survey (200 m contour interval; Figure 3). Additional useful sources of data were the 1:200,000 chart by Eade (1972) and British Admiralty Chart 2421 ("Tonga or Friendly Islands") printed in 1984.

The deepest part of Tofua Trough lies between 19°05' – 20°05'S and is outlined by a closed 1800 m isobath. Within this area the seafloor is fairly flat, sloping down only very gently to the middle of the trough. Maximum depths attained are 1840 m east of Tofua Island and 1870 m southeast of Metis Shoal. The Tonga platform, which bounds the trough to the east, is generally shallower than 500 m. The trough/platform boundary is formed by a WNW-facing submarine escarpment with 1200-1600 m relief and average slope of 8°-18°. Numerous submarine and subaerial edifices of the NNE-trending Tofua volcanic chain (including Home Reef, Metis Shoal, Kao, Tofua, Falcon, Hunga Tonga and Hunga Ha'apai Islands) separate Tofua Trough from the 2200+ m-deep Lau Basin to the west. The submarine slopes on the volcanic edifices are moderately steep with gradients mainly in the range 6°–15°. Because the volcanic chain is not strictly linear but consists of a band of edifices 20-30 km wide, the western margin of the trough is not clearly defined. The trough appears to become narrower towards its southern end. This is probably partly due to the volcanic chain being more diffuse in this region, with some edifices located within the trough itself.

SEISMIC, GRAVITY, AND MAGNETIC SURVEY DATA

Line drawing interpretations of the seismic reflection records for Lines A-C, D-F, G-H, and I-K are shown in Figures 4, 5, 6 and 7, respectively. Free-air gravity and magnetic anomaly profiles for these lines are presented above corresponding seismic sections. The magnetic anomaly data are relative to IGRF80 (Peddie, 1982).

SEISMIC RESULTS

The seismic sections across Tofua Trough (Figures 4–7) show the sediment fill in the trough to be highly stratified, with beds generally sub-horizontal or dipping at shallow angles. Structural disruption of the strata is evident, and varies over the trough from very minor to locally severe. The observed structures are primarily normal faults and piercements, produced by tectonism and volcanic activity. Basement is not clearly defined in our data, but a sedimentary section of at least 1.8 sec (two-way time, corresponding to a thickness of about 1800 m (assuming a velocity of 2.0 km/sec) is indicated. This is in accord with interpretations of EVA729 and AUS401 seismic profiles over the deepest part of the trough northeast of Kao/Tofua Island (Dupont, 1982), showing about 2.2 sec (two-way time) of sediment fill. Refraction data from the RV *S.P. Lee* cruise (Childs, 1985; Childs, pers. comm.) (sonobuoys S2, S3, S4; Figure 3) indicate low velocity sub-bottom layers of velocity 1.6-2.1 km/sec and a combined thickness of 2.05 km/sec, overlying a 4.1 km/sec substratum of presumed basement, thus confirming that the sediment fill in the trough is about 2.0 km thick.

The strata in the trough appear, based on seismic records, to consist of depositional units with thickness on average of 25-35 m. The thickness of these primary beds is difficult to estimate with accuracy because of resolution limits imposed by the frequency content of the seismic signal, and because some apparent stratification may be due to effects of airgun bubble-pulse oscillation as well as inter-layer reverberation. Each of the observed layers may represent a depositional cycle associated with a major eruptive episode from a volcanic center on an adjacent section of the chain. The beds lap onto the down-faulted Tonga platform which forms the eastern boundary of the trough, and generally inter-finger with the more chaotic proximal units of the volcanic constructions which are part of the volcanic arc, forming the western boundary of the trough.

The beds dip gently from the Tonga platform boundary,

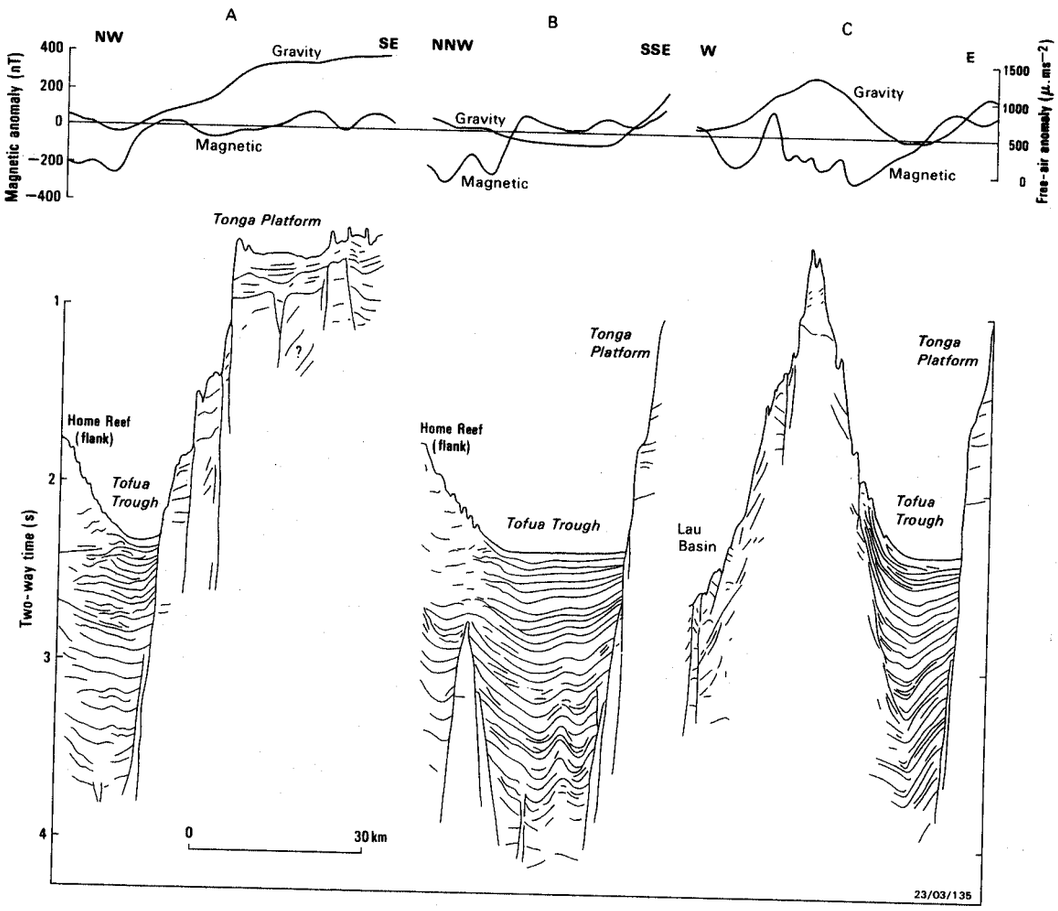

Figure 4. Seismic line drawing interpretations, free-air gravity profiles, and magnetic anomaly profiles - Lines A, B, and C.

and also generally from the volcanic arc side. On the arc side the beds are commonly truncated by normal faults. Some apparent truncation may be due to obliteration of the underlying section by thick lava flows emanating from the nearby volcanic centers. Where such truncation occurs, the deeper beds often show a continuing westward dip (e.g., Line E, Figure 5; Line K, Figure 7). Discounting local structural variations, the overall pattern seen in the trough is an intrabasinal sag, most pronounced in the deeper strata and almost imperceptible in the near-surface beds which lie close to horizontal, at least where the trough is relatively wide. This sediment sag is well developed along Line B (Figures 4 and 8) and Line C (Figure 4), and has a magnitude of about 300 m in the deeper part of the section.

The progressive down-bowing of the sediment pile appears to be an accommodation response to excess space being generated near the base of the accumulating pile. Mechanisms producing this extra volume include, (1) compaction by sediment loading, particularly of relatively porous strata such as ash beds, and (2) trough dilation through (i) subsidence of the trough floor, perhaps by continued down-faulting along the eastern boundary fault system, partly as an isostatic response to loading of the crust to the west by the arc volcanoes and their volcanogenic sediment aprons, and/or (ii) tectonic widening of the trough in an intra-island arc tensional stress field acting transverse to the arc.

The middle and eastern half (Tonga platform side) of the trough is characterized by closely-spaced sub-parallel reflectors with high continuity of up to several tens of kilometers, and sequences which show low-angle onlap at their base. Such seismic patterns are best seen in the EVA729 (Dupont, 1982; Figure V-11) and 1982 *S.P. Lee* reflection profiles which were shot along the trough axis, but are also well illustrated in the seismic profile of Line B (Figures 4 and 8). Such patterns are typical of onlapping-fill seismic facies (Sangree and Widmier, 1977) deposited in basin slope and floor environments. In the Tofua Trough they probably consist predominantly of volcaniclastic deposits transported down from the island-arc volcanoes by low-velocity turbidity currents. Carbonate debris from reef buildups and, to a minor extent, pelagic deposits, are also likely to be carried into the trough at less frequent intervals by sediment gravity flow from high on the Tonga platform as well as from parts of submarine volcanic edifices within the photic zone where coral reefs have

developed. The trough deposits are expected to contain interbeds of hemipelagic sediment and ash fallout. Although sediment grain size in an onlapping-fill seismic facies is predominantly fine (silt-fine sand in Tofua Trough, judging from the seafloor sampling results), some thin beds of coarser volcaniclastic sand borne by intermittent high-energy turbidity currents are likely to be present, particularly on the arc side of the trough.

Where structural modification has not severely disrupted the strata, some beds of the Tofua Trough can be traced beneath the lower flanks of volcanic edifices (Line C, Figure 4; Line E, Figure 5) and can be seen to thin and converge upwards. These up-slope depositional units may be proximal volcaniclastic turbidites, or alternatively may represent debris flows or pyroclastic flows that have been partly converted by surface transformation to turbidites (Fisher, 1984) and subsequently deposited more distally on the floor of the trough.

Tofua Trough reflectors can also be traced beneath the lower flank of the Home Reef submarine volcano (Lines A and B, Figures 4 and 8). This seismic transparency suggests that the flanks are composed of volcaniclastic sediments and are largely devoid of massive lava flows. The beds within the edifice and beneath it, to a level about 300 m below the floor of the adjacent Tofua Trough, appear highly deformed. The volcanic sediments are probably of relatively low strength and may have been affected by slumping at or soon after deposition, or alternatively, have been deformed at a later stage by differential loading as the volcanic pile grew upwards with continuing eruptions. The hummocky surface topography on the lower flank of the Home Reef volcano may be slumping of recently deposited volcaniclastics, the volcano still being quite active, the last eruption (submarine) having been recorded In 1984.

There is further evidence for extensive and large scale mass wasting on the submarine flanks of the volcanic edifices. The lower, trough-facing flank of the large

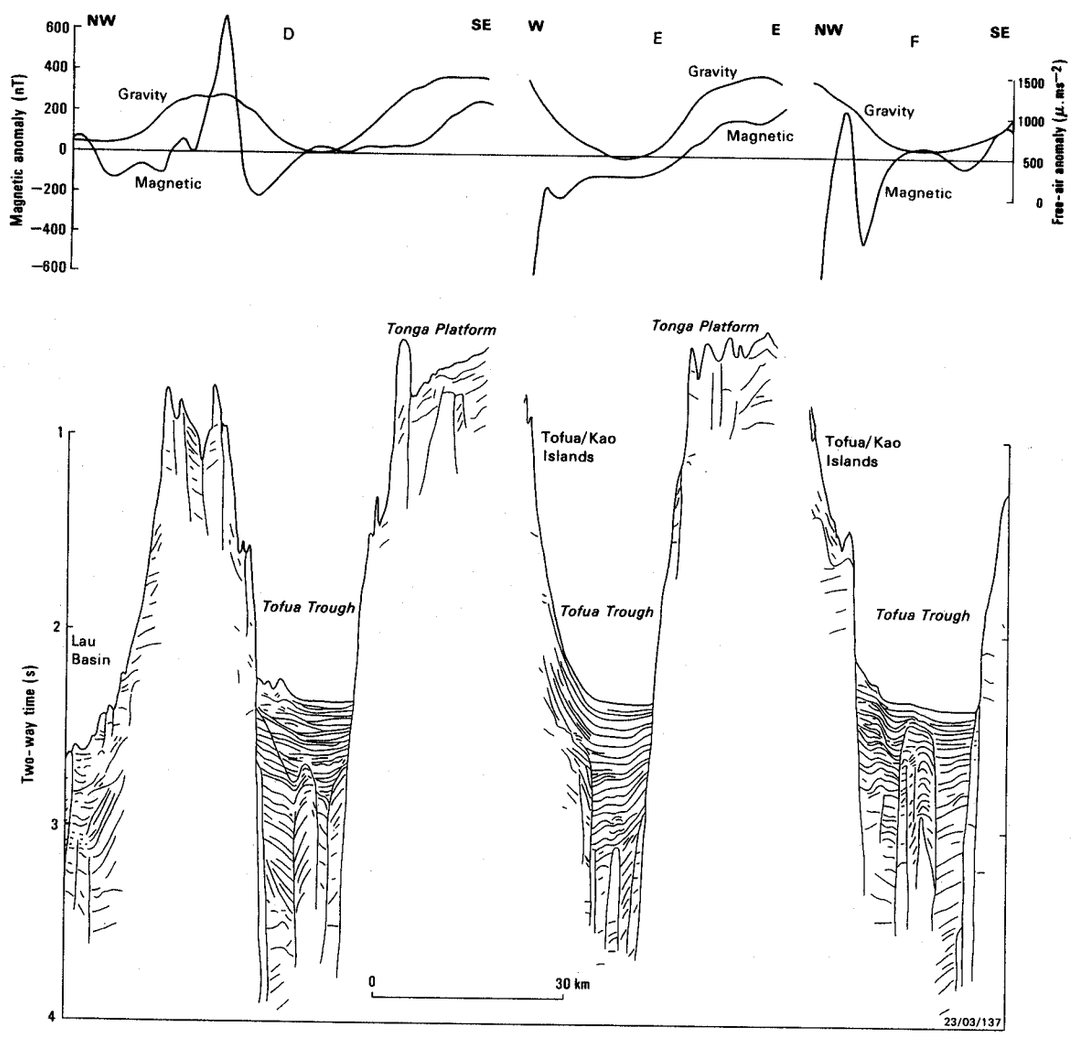

Figure 5. Seismic line drawing interpretations, free-air gravity profiles, and magnetic anomaly profiles - Lines D, E, and F.

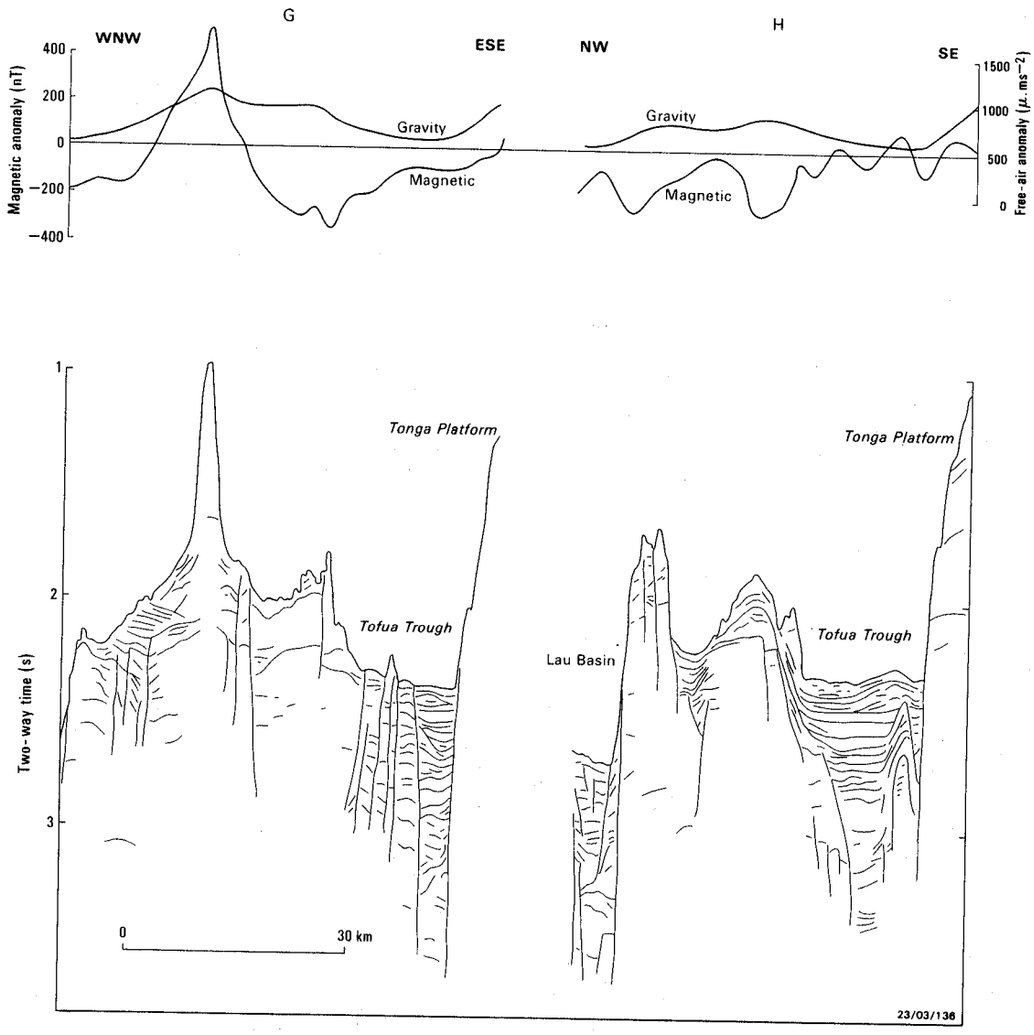

Figure 6. Seismic line drawing interpretations, free-air gravity profiles, and magnetic anomaly profiles - Lines G and H.

submarine volcano just north of Kao has irregular topography similar to that seen on the Home Reef volcano. A seismic profile (Line C, Figure 4) shows that the topographic relief is due to the slumping and sliding of several sediment sheets, 50 m thick and up to 4 km long, down the side of the edifice. Line D (Figure 5) also shows a large hummocky deposit of slumped material at the base of the slope. Slightly older, lensoid slump deposits can be seen in the section at this location. On the Lau Basin-facing lower flank of this volcano, chaotic bedding extending deep into the section suggests that slumping has been active here for some time. Other examples of chaotic seismic expression signifying probable slump deposits can be seen in the sections at the base (Lau Basin side) of submarine volcanoes crossed by Lines I and J (Figure 7).

The hummocky build-up seen on Line H (Figure 6) at the base of the Tonga platform escarpment may represent material that has slumped from high on the platform, but may also consist of lavas or pyroclastics that have been extruded out onto the trough floor from an adjacent eruptive center for which there is evidence in the section. Volcanic structures can also be seen within the Tofua Trough section on Lines B (Figures 4 and 8) and F (Figure 5).

Only limited seismic coverage of the Tonga platform was obtained during our survey; parts of Lines A, D, and E (Figure 3) extend over its western margin. Seismic detail below 0.5-1 sec sub-bottom (two-way time) has been lost because of the strong water-bottom multiple. Seismic profiles (Figures 4 and 5) show a pinnacled seafloor on the platform, probably representing reef constructions, below which lies about 100-200 m of sediment. This ?Late Pliocene-Holocene unit is underlain by an erosional unconformity that dips gently to the west, and truncates block-faulted older rocks of the Tonga platform succession (Eocene–Early Pliocene).

GRAVITY AND MAGNETIC EXPRESSION

The free-air gravity field over Tofua Trough and adjacent marginal zones is highly anomalous (Figures 4 - 7), varying in amplitude from about 500 μm/sec² to 1500 μm/sec². The variations in gravity can be attributed largely to sea-floor topography and partly to lateral density variations in the sub-bottom, while the positive gravity bias is a reflection of the major positive gravity anomaly normally present along the crest of active island arcs (Talwani, 1970).

The broad gravity low observed over Tofua Trough is due to the combined effect of deeper water in the trough and the thick sequence of young, relatively low density volcanogenic/hemipelagic sediment that has accumulated in the trough. This is confirmed by 2-dimensional gravity modelling (Figure 9) along Line D, which transects the central part of the trough almost orthogonally and also crosses the adjacent volcanic chain to the west and the Tonga platform on the eastern side of the trough. Following Misseque and Malahoff (1982), a density of 2.0 t/m³ was adopted for the arc-derived volcaniclastic sediment pile within the trough and that deposited as a sediment wedge on the Lau Basin side of the volcanic chain. Similarly, 2.4 t/m³ was taken as the density of the upper section of the Tonga platform, the basement beneath the trough and also the submarine volcano just to the north of Kao Island. A good match between observed and calculated gravity was obtained for a modelled sediment thickness of 2.0 km in the

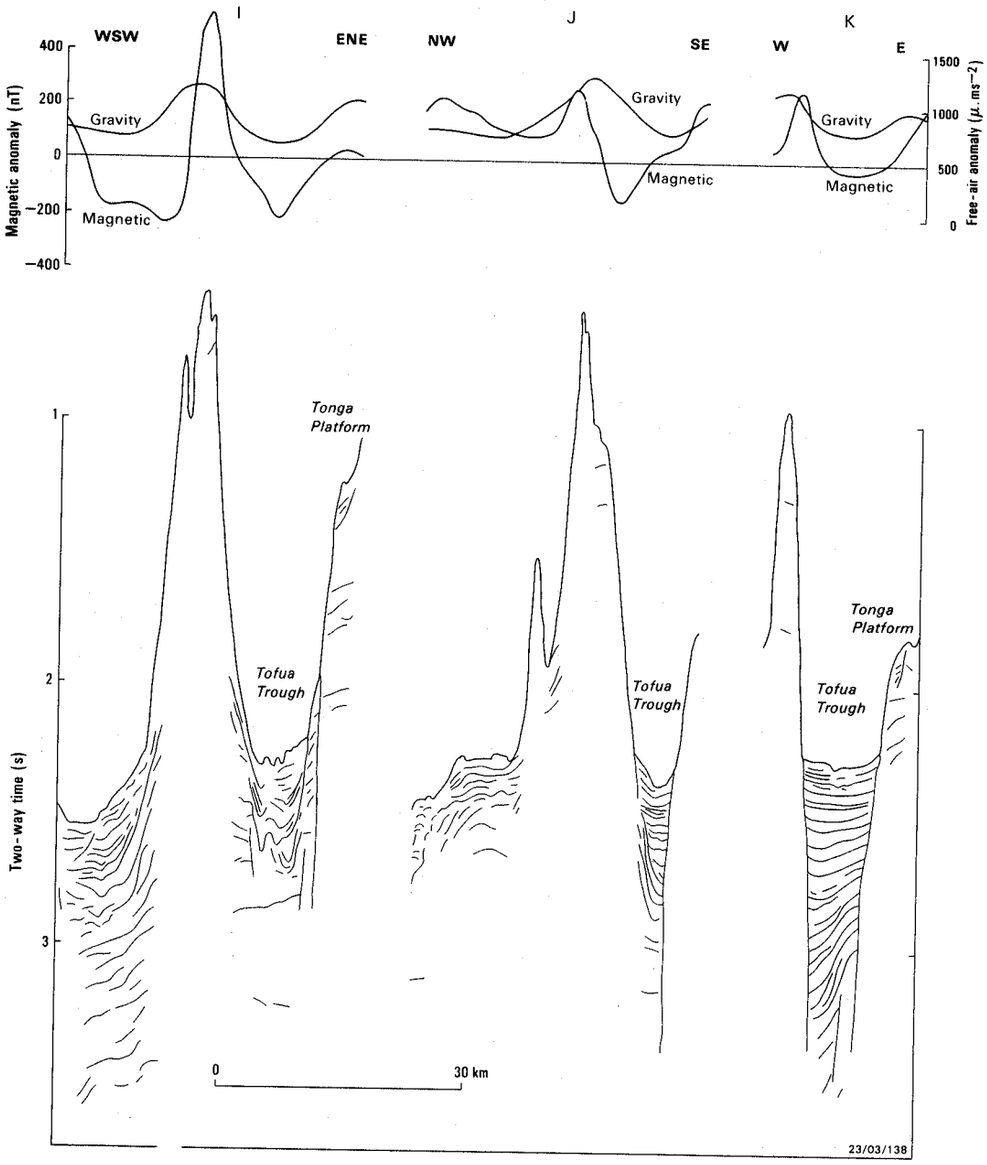

Figure 7. Seismic line drawing interpretations, free-air gravity profiles, and magnetic anomaly profiles - Lines I, J, and K.

trough, a result which supports the seismic refraction and reflection evidence.

The magnetic field is also highly anomalous over the Tofua Trough region. Magnetic variations of up to about 1200 nT were recorded, though anomaly amplitudes are more commonly on the order of several hundred nT. The larger anomalies are associated mainly with submarine and subaerial volcanoes of the Tofua volcanic chain.

The limited magnetic coverage of the Tonga platform adjacent to Tofua Trough shows a relatively subdued field with anomalies mainly significantly less than 200 nT in amplitude. The field is predominantly of moderate wavelength and there is no appreciable expression of seafloor topography in the profiles. Even the major trough/platform boundary faults are not strongly expressed in the magnetics, although there is some indication of a general increase in field strength across the boundary from west to east. Interpretation of the magnetics suggests that, (i) (?Eocene) magnetic basement is weakly magnetized, or is located at a substantial depth (possibly >1-2 km) beneath the platform in the area investigated, (ii) much of the magnetic variation is due to sources at intermediate depth within the section, probably the Miocene volcaniclastics and intrusions, and (iii) units at shallow depth (approximately 0-150 m) beneath the platform are non-magnetic or only weakly magnetic and probably consist of volcaniclastic sediments and reefal carbonates.

The volcanoes of the Tofua chain are mainly andesitic in composition and are considered to be composite structures built up by a combination of lava flows and pyroclastic deposits, with minor intrusions (mainly dikes) emplaced as feeders for the extrusives. Because of the high proportion of pyroclastic material, both induced and remanent magnetization are expected to be significant potential contributors to the overall magnetic field produced by these structures. This contrasts with the magnetization of mid-ocean basaltic volcanoes for which remanent magnetization is generally by far the most important component on account of the higher lava:clastic ratio.

The geomagnetic field in the Tofua Trough area presently has an inclination of -40° and declination 13.5°E (Fabiano et al., 1983), an orientation not appreciably different from that of a geocentric dipole field which at latitude 20°S would have an inclination of -36°. Thus a young submarine volcanic cone in the Tofua Trough area would be expected to produce a bipolar magnetic anomaly pattern, aligned N-S with the positive anomaly to the north, at sea level directly above the cone. This assumes normal polarity of the earth's

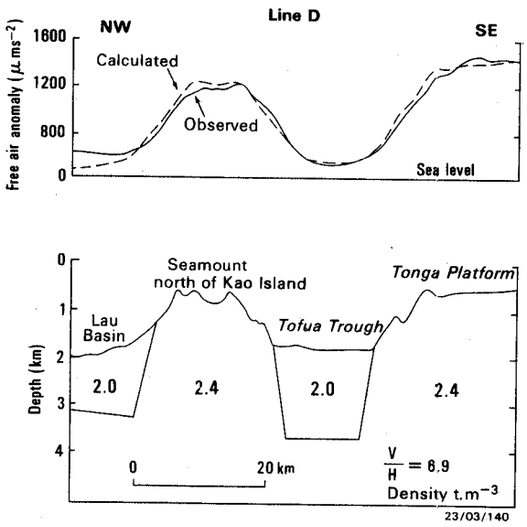

Figure 9. Tofua Trough gravity model (Line D); calculated (2-dimensional model) and observed profiles [top], with assumed density and sediment thickness schematic cross-section [bottom].

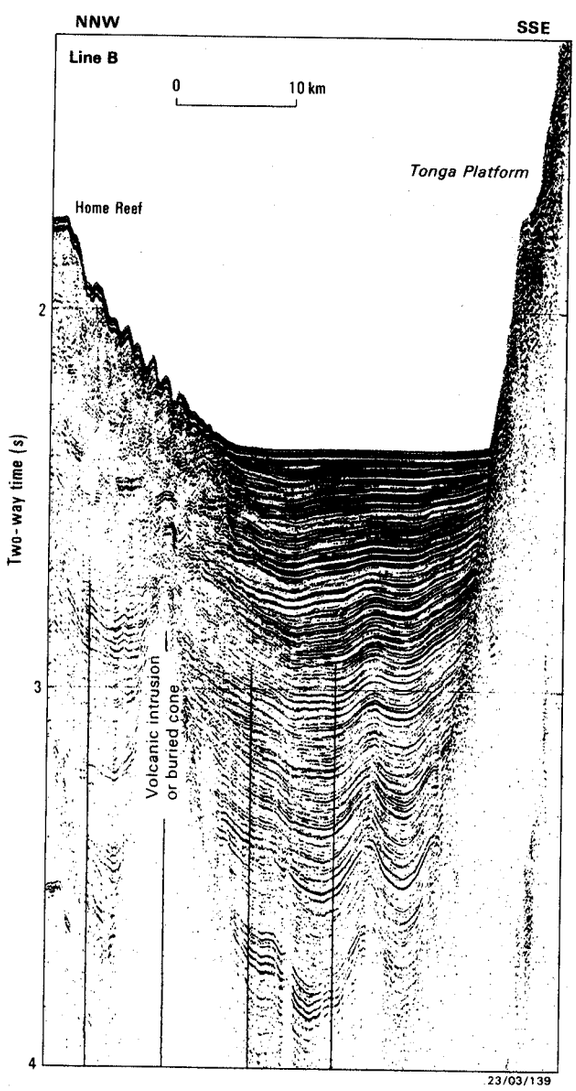

Figure 8. Seismic profile across Tofua Trough (Line B) showing thick, well-stratified sediment fill (greater than 1.8 sec two-way time) and volcanic intrusion or buried volcano within the section.

field during construction of the volcano. A different, more complex magnetic anomaly pattern is likely if the earth's field was of reverse polarity at the time, due to a mixture of opposing induced and remnant magnetization directions within the interior of the cone.

The four submarine volcanoes crossed on Lines C, I, and K (Figure 3) show strong magnetic anomalies consistent with normal magnetization, suggesting that these volcanoes formed in the past 0.7 Ma during the Brunhes normal chron rather than during an earlier period of reversed polarity. Paleomagnetic measurements made on lavas from Tofua and the island of Hunga Ha'apai (Tarling, 1965) indicate that the remanent magnetization coincides fairly closely with the direction of the present field of the earth, implying a recent age. A small discrepancy is attributed to recent secular variation. The subbottom volcanic structure within the Tofua Trough sediments at the NNW end of Line B (Figure 4) also appears to be normally magnetized, though the local field is disturbed to some extent by nearby volcanic edifices of Home Reef and Metis Shoal. The magnetic anomaly associated with the large unnamed seamount located just north of Kao Island (and crossed by Lines C and D; Figures 4, 5) is of complex shape. Based on the morphology of the seamount, the anomaly is not compatible with a 100% normal magnetization. Some internal reverse magnetization can be inferred, implying that parts of this edifice may be older than 0.7 Ma.

There is a possibility of interference between magnetic anomalies produced by andesitic volcanics of the Tofua chain and magnetic lineations resulting from Lau Basin seafloor spreading. Cherkis (1980) showed magnetic anomaly 3A coinciding with the Tofua Trough in this area, while Larue et al. (1982) plotted magnetic anomaly 3 in the same position. The observed magnetic field correlates very poorly with theoretical seafloor spreading anomaly profiles calculated assuming a fairly simple spreading geometry, the conflicting interpretations being symptomatic of this.

SHALLOW STRUCTURE

The principal geological structures mapped in the Tofua Trough area are shown in Figure 10. Normal faults and volcanic build-ups are the main structural elements. The NNE-trending system of normal faults which marks the western limit of the Tonga platform and controls the eastern extent of Tofua Trough is a prominent structural feature of regional scale. The Tonga platform/Tofua Trough boundary slopes WNW at about 20°-25° and is formed by a series of normal faults with dips of 45°-60° which step the Tonga platform block down to depths in excess of 1.8 km below the seafloor in the trough, making the combined throw greater than 3.4 km. The faults are segmented by poorly defined WNW- and NW-striking faults which cut across the Tonga platform, and were probably produced by differential uplift of the forearc as it swept over subducting ridges and seamounts of the Louisville Ridge.

The seismic sections show steeply dipping normal faults in places offsetting Tofua Trough sediments in the middle of the trough, particularly along the central part of the trough in the vicinity of the large Kao and Tofua volcanoes (Figures 5 and 6). They are common adjacent to the volcanic chain, both on the Lau Basin side as well as in Tofua Trough. Some appear to be growth faults produced as volcaniclastics were shed off the arc, while others are associated with volcanic diapirism.

Volcanic centers, whether subaerial, submarine, or subbottom, are distributed along a 40 km-wide band trending NNE (Figure 10). They extend from close to the Tofua Trough/Tonga platform boundary fault(s) to about 15 km west of the main line of subaerial volcanoes. The locations of the volcanic centers are probably controlled by NNE-striking basement faults, though there is no compelling evidence for this in our data.

CRUSTAL STRUCTURE

Sonobuoy refraction data are available which allow the Tofua Trough to be examined in the broader context of the overall crustal structure of the Tonga island arc. The data sources, to which reference has already been made, include the Capricorn Expedition (Raitt et al., 1955), the French EVA VII program (Pontoise et al., 1980; Pontoise and

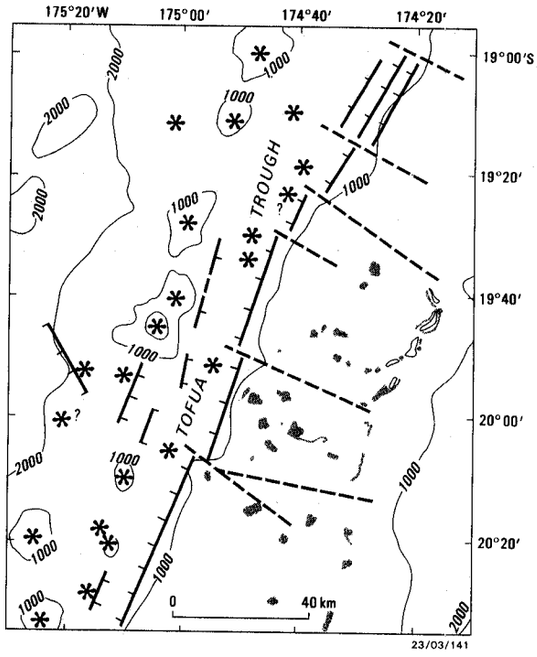

Figure 10. Map of principal structural features. The star symbols correspond to ?Pliocene - Holocene volcanic centers. Major faults are represented by heavy lines ticked on the downthrown side; inferred faults are shown as broken lines. Bathymetric contour interval 1000 m.

Latham, 1982), and the more recent Tripartite I *S.P. Lee* cruise (Childs, 1985). The sonobuoy sounding locations are distributed latitudinally across the Tonga arc just to the north of Kao/Tofua Islands. The crustal cross-section of Figure 11 is oriented normal to the arc and located roughly along an extended Line D (Figure 3). The bathymetry beyond our data from Line D has been taken from Chase et al. (1982), while the seismic velocity structure is based on the sonobuoy data projected onto the cross-section.

Revised interpretations of the *S.P. Lee* Tofua Trough sonobuoy soundings (S2, S3, S4; Figure 3) have been provided by Jon Childs (pers. comm.), yielding new interpretations of crustal structure (Table 1).

The accuracy of the S2 interpretation for the deeper layers may be affected, however, by the presence of an underlying buried volcanic cone or intrusion seen in the seismic section of Line B (Figure 8).

Table 1. Seismic velocity and thickness of crustal layers.

Sonobuoy	Layer	Velocity (km/sec)	Thickness
S2	1	1.6	1.08
	2	2.9	0.97
	3	4.1	–
S3	1	1.6	1.07
	2	2.9	–
S4	1	1.6	1.08
	2	2.4	–

The crustal velocity structure as portrayed in Figure 11 shows a marked discontinuity across the major boundary faults at the western margin of the Tonga platform. The data suggest that the volcanic chain and Tofua Trough are founded on transitional oceanic crust of the Lau Basin. This hypothesis is consistent with interpretations of Lau Basin seafloor spreading anomalies (Cherkis, 1980; Larue et al., 1982), but conflicts with the observations of Kroenke and Tongilava (1975), who traced Middle Eocene-Lower Miocene strata of the Tonga platform beneath Tofua Trough on two oil company seismic lines crossing the forearc just north and south of Tongatapu. North of Vava'u the volcanic arc is located at the crest of the Tonga Ridge, there being no structural equivalent to Tofua Trough. The arc is, however, adjoined on both sides by a thick sequence of young volcaniclastic sediments within an isostatically(?) downwarped basin (Kitekei'aho et al., 1985). This sediment pile is up to 2.0 sec (two-way time) thick, much the same thickness as deposits along the volcanic chain adjacent to Tofua Trough. On the northern Tonga Ridge, the sediments are unconformably underlain by Upper Miocene and older rocks similar to those beneath the Tonga platform. In their interpretation of *S.P. Lee* multi-channel seismic profiles across the southern Tonga platform, Herzer and Exon (1985) showed up to 1.6 sec (two-way time) of sediment in the southern extension of Tofua Trough. Their reflector horizon A, representing the latest Miocene/Early Pliocene unconformity, is mapped within the sedimentary section. The seismic basement is not identified, though Scholl et al. (1985a) interpreted it equivocally as 'late Cenozoic arc basement' in their Figure 3.

Clearly, additional deep seismic refraction and reflection investigations of Tofua Trough are required to establish more convincingly whether the young, mainly volcanogenic sediments in the trough are underlain by a down-faulted Tonga platform-type section (essentially Eocene-Miocene) or by back-arc basalts of the Lau Basin. The sediments in the trough may be floored by both types of 'basement', each underlying different parts of the trough, as the data seem to suggest.

The crustal structure shown in Figure 11 suggests that Tofua Trough developed by subsidence of the trough/volcanic arc area relative to the Tonga platform by normal faulting at the major boundary fault system, in a manner analogous to half-graben formation. The mechanisms by which this may have occurred (and probably continuing at present) include, (i) isostatic adjustment of the crust due to additional loading imposed by the build-up of arc-derived volcanic products, and (ii) thermal subsidence of the crust on cooling as the Lau Basin seafloor spreading axis moved progressively westward. Tofua Trough appears to be a subsiding rift basin, contained on its western side by the growing volcanic build-ups of the Tofua volcanic chain.

ACKNOWLEDGEMENTS

Jon Childs of the U.S. Geological Survey (Menlo Park, California) provided revised interpretations of the 1982 RV *S.P. Lee* sonobuoy refraction data.

REFERENCES CITED

Baker, P.E., P.G. Harris, and A. Reay, 1971, The geology of Tofua Island, Tonga, *in* R. Fraser, compiler, Cook Bicentenary Expedition in the south-west Pacific: Royal Society of New Zealand, Bulletin 8, p.67-79.

Bauer, G.R., 1970, The geology of Tofua Island, Tonga: Pacific Science, v.24, p.333-350.

Bryan, W.B., G.D. Stice, and A. Ewart, 1972, Geology, petrography, and geochemistry of the volcanic islands of Tonga: Journal of Geophysical Research, v.77, p.1566-1585.

Chase, T.E., B.A. Seekins, S. Vath, and M.A. Cloud, 1982, Topography of the Tonga region: USGS-CCOP/SOPAC South Pacific Project, Department of the Interior, United States Geological Survey.

Cherkis, N.Z., 1980, Aeromagnetic investigations and sea floor spreading history in the Lau Basin and northern Fiji Plateau: CCOP/SOPAC Technical Bulletin 3, p.37-45.

Childs, J.R., 1985, Acoustic properties of sediment on the southern Tonga Platform as determined from seismic sonobuoy studies, *in* D.W. Scholl and T.L. Vallier, eds., Geology and offshore

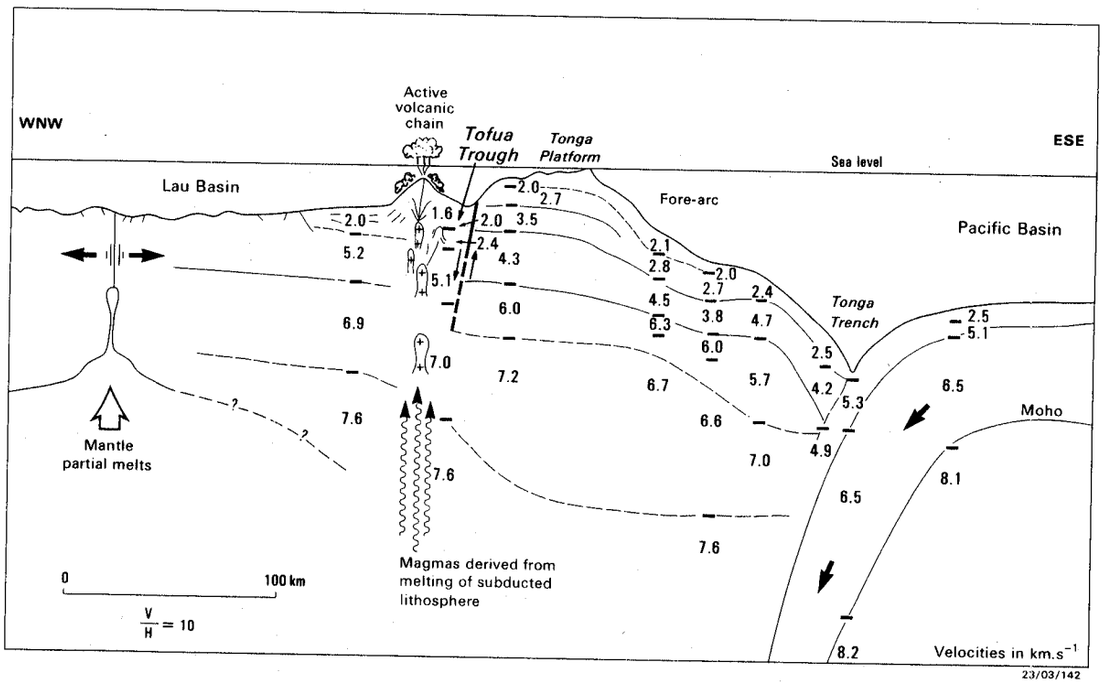

Figure 11. Crustal cross-section through the Tonga arc, based on seismic refraction and reflection data. Broad black arrows show direction of relative plate motion - (i) convergence by subduction of the Pacific plate at the Tonga Trench on the right of the figure, and (ii) opening of the Lau Basin on the left.

resources of Pacific island arcs - Tonga region: Circum-Pacific Council for Energy and Mineral Resources, Earth Science Series, v.2, p.37-48.

Cronan, D.S., S.A. Moorby, G.P. Glasby, K. Knedler, J. Thompson, and R. Hodkinson, 1984, Hydrothermal and volcaniclastic sedimentation on the Tonga-Kermadec Ridge and its adjacent marginal basins, *in* B.P. Kokelaar and M.F. Howells, eds., Marginal basin geology: Oxford, Blackwell Scientific Publications, p.137-149.

Cunningham, J.K., and K.J. Anscombe, 1985, Geology of 'Eua and other islands, Kingdom of Tonga, *in* D.W. Scholl and T.L. Vallier, Pacific island arcs - Tonga region: Circum-Pacific Council for Energy and Mineral Resources, Earth Science Series, v.2, p.221-257.

Dickinson, W.R., 1971, Clastic sedimentary sequences deposited in shelf, slope, and trough settings between magmatic arcs and associated trenches: Pacific Geology, v.3, p.15-30.

Dupont, J., 1982, Morphologie et structures superficielles de l'arc insulaire des Tonga-Kermadec, *in* Contributions a l'etude geodynamique du Sud-Ouest Pacifique: Paris, ORSTOM, no. 147, p.263-282.

Dupont, J., and R.H. Herzer, 1985, Effect of subduction of the Louisville Ridge on the structure and morphology of the Tonga Arc, *in* D.W. Scholl and T.L. Vallier, eds., Geology and offshore resources of Pacific island arcs - Tonga region: Circum-Pacific Council for Energy and Mineral Resources, Earth Science Series, v.2, p.323-332.

Eade, J.V., 1972, Ha'apai bathymetry: New Zealand Oceanographic Institute Chart, Island Series, scale 1:200,000.

Eguchi, T., 1984, Seismotectonics of the Fiji Plateau and Lau Basin: Tectonophysics, v.102, p.17-32.

Ewart, A., R.N. Brothers, and A. Mateen, 1977, An outline of the geology and geochemistry and the possible petrogenetic evolution of the volcanic rocks of the Tonga-Kermadec-New Zealand island arc: Journal of Volcanology and Geothermal Research, v.2, p.205-250.

Exon, N.F., R.H. Herzer, and J.W. Cole, 1985, Mixed volcaniclastic and pelagic sedimentary rocks from the Cenozoic southern Tonga platform and their implications for petrolem potential, *in* D.W. Scholl and T.L. Vallier, eds., Geology and offshore resources of Pacific island arcs - Tonga region: Circum-Pacific Council for Energy and Mineral Resources, Earth Science Series, v.2, p.75-107.

Fabiano, E.B., N.W. Peddie, and A.K. Zunde, 1983, The magnetic field of the earth, 1980 (magnetic declination and magnetic inclination charts): Department of the Interior, U.S. Geological Survey.

Falloon, T.J., D.H. Green, and A.J. Crawford, 1987, Dredged igneous rocks from the northern termination of the Tofua magmatic arc, Tonga and adjacent Lau Basin: Australian Journal of Earth Sciences, v.34, p.487-506.

Falvey, D.A., 1978, Analyses of palaeomagnetic data from the New Hebrides: Bulletin of the Australian Society of Exploration Geophysics, v.9(3), p.117-130.

Fisher, R.V., 1984, Submarine volcaniclastic rocks, *in* B.P. Kokelaar and M.F. Howells, eds., Marginal basin geology: Oxford, Blackwell Scientific Publications, p.5-27.

Gill, J.B., 1976, Composition and age of Lau Basin and Ridge volcanic rocks; implications for evolution of an inter-arc basin and remnant arc: Geological Society of America Bulletin, v.87, p.1384-1395.

Hanus, V., and J. Vanek, 1979, Morphology and volcanism of the Wadati-Benioff Zone in the Tonga-Kermadec system of recent subduction: New Zealand Journal of Geology and Geophysics, v.22, p.659-671.

Hawkins, J.W., 1974, Geology of the Lau Basin, a marginal sea

behind the Tonga Arc, *in* C. Burk and C. Drake, eds., Geology of continental margins: New York, Springer-Verlag, p.505-520.

Hawkins, J.W., S.H. Bloomer, C.A. Evans, and J.T. Melchior, 1984, Evolution of intra-oceanic arc trench systems: Tectonophysics, v.102, p.175-205.

Hawkins, J. W., and Melchoir, J.T., 1985, Petrology of the Mariana Trough and Lau Basin basalts: Journal of Geophysical Research, v.90, p.11431-11468.

Herzer, R.H., and N.F. Exon, 1985, Structure and basin analysis of the southern Tonga forearc, *in* D.W. Scholl and T.L. Vallier, eds., Geology and offshore resources of Pacific island arcs - Tonga region: Circum-Pacific Council for Energy and Mineral Resources, Earth Science Series, v.2, p.55-73.

Karig, D.E., 1970, Ridges and basins of the Tonga-Kermadec island arc system: Journal of Geophysical Research, v.75, p.239-254.

Kitekei'aho, T., D. Tappin, E. Honza, Y. Okuda, T. Miyazaki, T. Yokokura, K.B. Lewis, and D.L. Tiffin, 1985, Seismic profiles from northern Tonga, *in* E. Honza, K.B. Lewis, and shipboard party, A marine geological and geophysical survey of the northern Tonga Ridge and adjacent Lau Basin: Mineral Resources of Tonga, Field Report no. 1, p.31-35.

Kroenke, L.W., 1984, Cenozoic tectonic development of the Southwest Pacific: CCOP/SOPAC Technical Bulletin 6.

Kroenke, L.W., and S.L. Tongilava, 1975, A structural interpretation of two reflection profiles across the Tonga Arc: CCOP/SOPAC South Pacific Marine Geological Notes, v.1(2), 15 p.

Kroenke, L.W., C. Joannic, and P. Woodward, 1983, Bathymetry of the Southwest Pacific, Chart 1 of Geophysical Atlas of the Pacific: CCOP/SOPAC, Suva, Fiji.

Larue, B.M., B. Pontoise, A. Malahoff, A. Lapouille, and G.V. Latham, 1982, Basins marginaux actifs du Sud-Ouest Pacifique: plateau Nord-Fidjien, bassin de Lau, *in* Contributions a l'etude geodynamique du Sud-Ouest Pacifique: Paris, ORSTOM, no. 147, p.363-406.

Lawyer, L.A., J.A. Hawkins, and J.G. Sclater, 1976, Magnetic anomalies and crustal dilation in the Lau Basin: Earth and Planetary Science Letters, v.33, p.27-35.

Leitch, E.C., 1984, Marginal basins of the SW Pacific and the preservation and recognition of their ancient analogues: a review, *in* B.P. Kokelaar and M.F. Howells, eds., Marginal basin geology: Oxford, Blackwell Scientific Publications, p.97-108.

Lewis, K.B., 1985, Tectonic setting of the northern Tonga Arc and Lau Basin: background to the Natsuchima 84 cruise, *in* E. Honza, K.B. Lewis, and shipboard party, A marine geological and geophysical survey of the northern Tonga Ridge and adjacent Lau Basin: Mineral Resources of Tonga, Field Report no. 1, p.19-29.

Malahoff, A., R.H. Feden, and H.S. Fleming, 1982, Magnetic anomalies and tectonic fabric of marginal basins north of New Zealand: Journal of Geophysical Research, v.86, p.4109-4125.

Maung, T.U., K. Anscombe, and S.L. Tongilava, 1981, Assessment of petroleum potential of the southern and northern parts of the Tonga platform: CCOP/SOPAC Technical Report 18, 57 p.

Melson, W.G., E. Jarosewich, and C.A. Lundquist, 1970, Volcanic eruption of Metis Shoal, Tonga, 1967-1968: Description and petrology: Smithsonian Contributions to the Earth Sciences, v.4, p.1-18.

Missegue, F. and A. Malahoff, 1982, Etude gravimetrique de L'arc des Tonga, *in* Contributions a l'etude geodynamique du Sud-Ouest Pacific: Paris, ORSTOM, no. 147, p.293-298.

Packham, G.H., 1978, Evolution of a simple island arc: the Lau-Tonga Ridge: Bulletin of the Australian Society of Exploration Geophysicists, v.9, p.133-140.

Peddie, N.W., 1982, International Geomagnetic Reference Field: the third generation: Journal of Geomagnetism and Geoelectricity, v.34, p.309-326.

Pontoise, B., G.V. Latham, J. Daniel, J. Dupont, and A.B. Ibrahim, 1980, Seismic refraction studies in the New Hebrides and Tonga area: CCOP/SOPAC Technical Bulletin 3, p.47-58.

Pontoise, B., and G. Latham, 1982, Etude par refraction de la structure interne de l'arc des Tonga, *in* Contributions a l'etude geodynamique du Sud-Ouest Pacific: Paris, ORSTOM, no. 147, p.283-291.

Raitt, R.W., R.I. Fisher, and R.G. Mason, 1955, Tonga Trench: Geological Society of America, Special Paper 62, p.237-255.

Sangree, J.B., and J.M. Widmier, 1977, Seismic interpretation of clastic depositional facies, *in* C.E. Payton, ed., Seismic stratigraphy - applications to hydrocarbon exploration: American Association of Petroleum Geologists, Memoir 26, p.165-184.

Schofield, J.C., 1967, Notes on the geology of the Tongan Islands: New Zealand Journal of Geology and Geophysics, v.10, p.1424-1428.

Scholl, D.W., and T.L. Vallier, eds., 1985, Geology and offshore resources of Pacific island arcs - Tonga region: Circum-Pacific Council for Energy and Mineral Resources, Earth Science Series, v.2.

Scholl, D.W., T.L. Vallier, and T.U. Maung, 1985a, Introduction, *in* D.W. Scholl, and T.L. Vallier, eds., Geology and offshore resources of Pacific island arcs - Tonga region: Circum-Pacific Council for Energy and Mineral Resources, Earth Science Series, v.2, p.3-15.

Scholl, D.W., T.L. Vallier, and G.H. Packham, 1985b, Framework geology and resource potential of southern Tonga platform and adjacent terranes - a synthesis, *in* D.W. Scholl and T.L. Vallier, eds., Geology and offshore resources of Pacific island arcs - Tonga region: Circum-Pacific Council for Energy and Mineral Resources, Earth Science Series, v.2, p.457-488.

Sclater, J.G., J.W. Hawkins, J. Mammerickx, and C.G. Chase, 1972, Crustal extension behind the Tonga and Lau ridges: petrologic and geophysical evidence: Geological Society of America Bulletin, v.83, p.505-518.

Talwani, M., 1970, Gravity, *in* A.E. Maxwell, ed., The sea, Volume 4, Part 1: New York, John Wiley and Sons, p.251-298.

Tarling, D.H., 1965, The paleomagnetism of the Samoan and Tongan Islands: Geophysical Journal, v.10, p.497-513.

Tongilava, S.L., and L. Kroenke, 1975, Oil prospecting in Tonga 1968-1974: CCOP/SOPAC South Pacific Marine Geological Notes, v.1(1), 8 p.

Weissel, J.K., 1977, Evolution of the Lau Basin by the growth of small plates, *in* M. Talwani and W.C. Pitman III, eds., Island arcs, deep sea trenches, and back-arc basins: American Geophysical Union, Maurice Ewing Series 1, p.429-456.

Part 3

CRUSTS, NODULES, ROCKS, SEDIMENTS

Meylan, M.A., and G.P. Glasby 1996. Manganese nodules, manganese crusts, and rocks: distribution and description, *in:* Meylan, M.A., and G.P. Gla~by (eds) Manihiki Plateau, Machias and Capricorn Seamounts, Niue, and Tofua Trough: Results of *Tui* Cruises. SOPAC Technical Bulletin 10: 61-98.

MANGANESE NODULES, MANGANESE CRUSTS, AND ROCKS: DISTRIBUTION AND DESCRIPTION

M.A. Meylan

Department of Geology, Universiry of Southern Mississippi, USM Box 5044, Hattiesburg, MS 39406-5044, USA

G.P. Glasby

Department of Earth Sciences, Universiry of Sheffield, Sheffield 53 7 HP, England

ABSTRACT

Manganese crusts, manganese nodules, and rocks were recovered by rock and pipe dredging during two 1986 cruises of HMNZS *Tui.* Seafloor samples, usually including sediment, were collected on the submarine slopes of the coral atolls of the northern Cook Islands (Suwarrow, Manihiki, Rakahanga, Pukapuka, Tema Reef and Nassau), volcanic southern Cook Islands (Mauke, Mitiaro and Rarotonga), the crest and eastern and western margins of the Manihiki Plateau, seamounts east of the Tonga-Kermadec Trench (Machias, Capricorn), and Niue, a raised coral atoll.

About 6000 ***Mn nodules*** were recovered at 12 stations, abundant hauls of nodules being dredged from depths of3305 m to 5260 m. Our sampling confirms the presence of nodule fields in the western Penrhyn Basin and along the eastern margin of the Manihiki Plateau, and extends the distribution of Samoan Basin nodules to the western margin of the Manihiki Plateau. The nodules collected during this cruise are dominantly of small size, more than 90% having maximum diameters of less than 30 mm. Spheroidal nodule shapes are by far the most common, particularly among small nodules, while ellipsoidal and polynucleate nodules are also abundant. Virtually all of the nodules have some type of volcaniclastic nucleus, where a nucleus can be distinguished. Where the original nucleus can be discerned, accreted Mn-oxides vary in thickness up to 5 mm, but are generally 2.3 mm thick.

Mn crusts ranging in thickness from 3 mm to about 65 mm were collected at 19 stations in water depths of 1139 to 4996 m, although the volume and thickness of material collected was somewhat disappointing. All station groupings except at Machias and Capricorn Seamounts and Suwarrow yielded crusts. The substrate material consists either of a carbonate (foraminiferal or coralline limestone) or some type of volcanic rock (tuff or basalt).

The bulk of the coarse material collected consists of a variety of sedimentary (carbonate) and igneous (mostly volcaniclastic) ***rocks,*** along with the hard parts of organisms such as shell fragments and shark teeth. Coral rubble (including segments of individual shallow and deep water coral growths, coral boundstone, and encrusting algae) was the most abundant component of the dredge haul at many stations. It was recovered from steep slopes as shallow as 406 m (Stn U354, southwestern side of Niue) to as deep as 4686 m (Stn U352, southern side of Capricorn Seamount). Coral rubble, obviously emplaced by some type of mass movement, was dredged at a depth of 4816 m in the abyssal hills west of Pukapuka (Stn U328). Several percent shell fragments were found in many of the abundant coral rubble collections. Coquinoid and foraminiferal limestones were retrieved at several stations. Deep water and precious corals representing ***in situ*** samples were collected on the slopes of reef-crowned edifices on the western side of the Manihiki Plateau.

Several varieties of igneous rocks were found, all of volcanic origin: basalt (aphanitic, vesicular, and scoriaceous), pumice, and fragmental volcaniclastics (ash and tuff). The only significant hauls of basalt, in terms of quantity, apparent freshness, and variety, were dredged at Machias and Capricorn

Seamounts. At Stns U345 and U346 (Machias Seamount), coarse basalt gravel was retrieved from depths of 2069 m and 4077 m, respectively. The abundant haul at Stn U346 resembles river or beach gravel, obviously transported a considerable distance downslope. At both stations, the basalt is dark gray and dominantly aphanitic, but a sizable percentage of vesicular pebbles is also present. The collection at Stn U346 includes a few dunite inclusions, and the vesicular basalt from Stn U375 contains garnet crystals. The basaltic material from Capricorn Seamount does not resemble that from Machias Seamount. At Capricorn Seamount, the rocks may be somewhat more silica-rich, and display amygdaloidal (Stn U348) and brecciated (U349) types. Little, if any, volcanic rock appeared to have been torn from an outcrop during a dredging operation at any station.

Pumice is a common, but seldom abundant, constituent of the rock collections, usually occurring as small rounded gray pebbles. Volcaniclastics in the form of ash and tuff were found in almost one-third of the samples that contained some type of coarse solid material. Coarse-grained tuff is a common substrate for the manganese crusts, and altered fine-grained tuff is found as a nucleus material for many of the manganese nodules.

INTRODUCTION

Coarse sedimentary and igneous material was collected primarily by rock dredging and pipe dredging. The gravity corer and even the underwater camera collected additional minor amounts of material. This section describes the character and distribution of the coarse, i.e., pebble size and larger, sedimentary and igneous material. Biological components of the dredge hauls are discussed in more detail in other chapters of this volume (general occurrence by Main et al.; scleractinian corals by Grange and Veron; precious and deep-water corals by Grigg; molluscs by Beu; and forams in associated sediment sediment samples or adhering to coarse material by Hayward). Meylan et al. (1990) have reported the chemical composition, mineralogy, and physical characteristics of selected nodules and crusts collected during the *Tui* cruises. Sections of that publication were taken from an earlier version of this report.

MANGANESE NODULES

Approximately 6000 manganese nodules were recovered at 11 stations east and west of the Manihiki Plateau. An additional two nodules were collected at a station between Capricorn Seamount and Niue. Nodule hauls were either quite sizable (at five stations, more than 500 nodules were collected) or quite small (at six stations, 10 or fewer nodules were collected) (Table 1; see Appendix A for descriptive details).

Manganese nodules collected on this cruise have reinforced known nodule distribution patterns as well as

Table 1. Nodule samples.

Stn	Gear	Locality	Depth (m)	No. of Nodules	Nodule Type
U295	Pipe Dredge	Samoan Basin	5283	1	Spheroidal
U296a	Pipe Dredge	Penrhyn Basin	5130	574	Spheroidal, polynucleate
U298	Pipe dredge	Eastern margin slope, Manihiki Plateau	4996	10	Spheroidal
U299a	Rock dredge	Eastern margin slope, Manihiki Plateau	4637	4	Spheroidal
U300	Rock dredge	Eastern margin slope, Manihiki Plateau	3747-3758	ca. 1000	Polynucleate, spheroidal, ellipsoidal
U321a	Pipe dredge	Penrhyn Basin, east of Manihiki Island	5114-5047	159	Spheroidal, ellipsoidal, polynucleate, tabular
U325	Rock dredge	Pukapuka	1585-1446	1	Tabular
U327	Rock dredge	Pukapuka	3394-3217	1434	Spheroidal, ellipsoidal, tabular
U328	Pipe dredge	Pukapuka	4837-4796	1	Polynucleate
U339	Pipe dredge	Nassau	4204-4219	864	Spheroidal, ellipsoidal, polynucleate
U340	Pipe dredge	Samoan Basin near Nassau	5268-5253	1867	Polynucleate, spheroidal, ellipsoidal, tabular
U353	Short corer	Between Niue, Capricorn Seamount	5495	2	Polynucleate

Table 2. Nodule size.

Stn	Range (max. diam. in mm)	Number of nodules by template size (mm)						
		<20	20-40	40-60	60-80	>80	Total	No. of Frags
U295	8	1	0	0	0	0	1	0
U296a	10-83	185	383	6	0	0	574	ca. 50[1]
U298	16-59	5	3	2	0	0	10	0
U299a	16-46	1	2	1	0	0	4	0
U300	15-52	ca. 900	ca. 100	0	0	0	ca.1000	many
U321a	3-154	142	10	6	0	1	159	5
U325	19	1	0	0	0	0	1	0
U327	8-58	1409	25	0	0	0	1434	47
U328	21	1	0	0	0	0	1	0
U339	6-55	517	347	0	0	0	964	91[2]
U340	4-99	1716	144	5	2	0	1867	0[2]
U353	38, 46	0	2	0	0	0	2	0

[1] probably ca. 30 formed by breakage on seafloor prior to dredging
[2] >5 mm max. diam., many smaller

extended occurrence into areas not previously known to have nodules or which were even thought likely to be barren of nodules. At Stns U296a, U298, U299a, U300 and U321a, the existence of widespread nodule (and crust) deposits in the Penrhyn Basin and along the eastern margin of the Manihiki Plateau noted by Heezen et al. (1966) and several more recent investigations was confirmed. Nodules were also recovered at Stns U295, U325, U327, U328, U339 and U340, areas of the Samoan Basin and western margin of the Manihiki Plateau which were considered to be lacking nodules (cf. Piper et al., 1985). At station U353 between Capricorn Seamount and Niue, what may be a dense nodule field was found west of the "nodule western limit" of Meylan et al. (1982).

Nodules were recovered from depths of 1515 m on the western slope of Pukapuka (U325) to 5495 m between Capricorn Seamount and Niue (U353). Abundant hauls of nodules were dredged from depths of 3305 m (steep western slope of Pukapuka, Stn U327) to 5260 m (abyssal plain west of Nassau, Stn U340). Most of the nodules were found at depths of about 5000 m or slightly deeper.

The deeper nodules (> about 4800 m) lie on brown to dark brown ("abyssal red") clay. The anomalous shallow nodule at Stn U325 (1515 m) was collected with coarse carbonate sand and coral rubble. At Stn U327, abundant small nodules occur on a light brown foram/nanno ooze at a depth of 3305 m. The mixture of carbonate ooze and brown clay collected at Stn U339 (depth 4212 m) may be a product of slumping, a fluctuating Carbonate Compensation Depth, or the dredge sampling seafloor sediment at more than one depth.

Nodule finds usually retrieved other coarse material. Shark teeth or volcaniclastics (tuff, scoria or pumice) were commonly found in association with the nodules; even coral rubble was noted (Stns U325, U328), although only one nodule was collected at both of these sites.

Nodule Size

Most of the nodules collected during this cruise are small whether considered on the basis of template size (Bäcker et al., 1976), i.e., intermediate diameter, or maximum diameter (Meylan, 1974) (Table 2). Eighty one percent of the nodules fit through a 20 mm template hole, and if the fragile nodules of Stn U300 could have been sized before a large number of them broke, the <20 mm percentage would likely have been even higher. Nineteen percent of the nodules are in the 20-40 mm template range. Less than 1% are of a larger template size. Excluding hauls with few nodules, only at Stn U296a were there more 20-40 mm nodules than <20 mm ones (Figure 1).

Based on maximum diameter, 92% of the nodules are small (<3 cm), 7% are medium (3-6 cm), and less than 1%

are large (>6 cm). Almost all of the nodules from Stn U300, which have been excluded from the count, are small, as well.

We interpret these results to mean that we sampled several local nodule facies or the fringes of regional facies. Because manganese crust thicknesses are generally in the range of 2 mm, the small nodule size reflects the small size of the original nucleus. Nuclei are mostly altered glassy volcaniclastics as yet only slightly or partially replaced by Mn-oxides, or small fragments of scoria. We therefore infer that nucleus emplacement episodes have been primarily of a local nature, and that evidence of regional nucleus emplacement episodes is lacking, except in the southern Penrhyn Basin. It is interesting to note that the stations having the largest nodules (based on max. diam.) also have the smallest. Nodule size range at Stn U321a is 3-154 mm, and at Stn U340 is 4-99 mm (Figure 2). No other stations have nodules as small or as large as these.

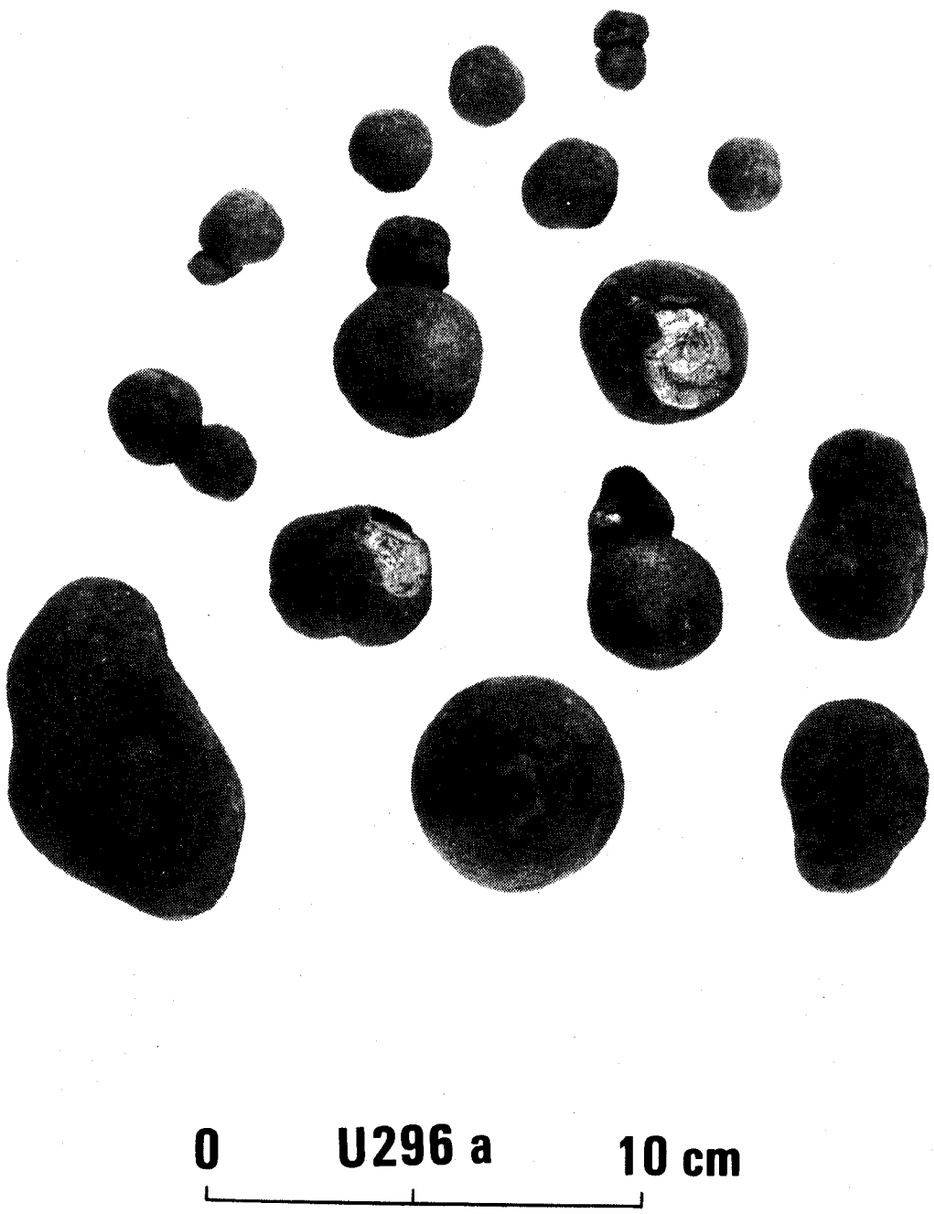

Figure 1. Selected nodules from Stn U296a (Penrhyn Basin, depth 5130 m).

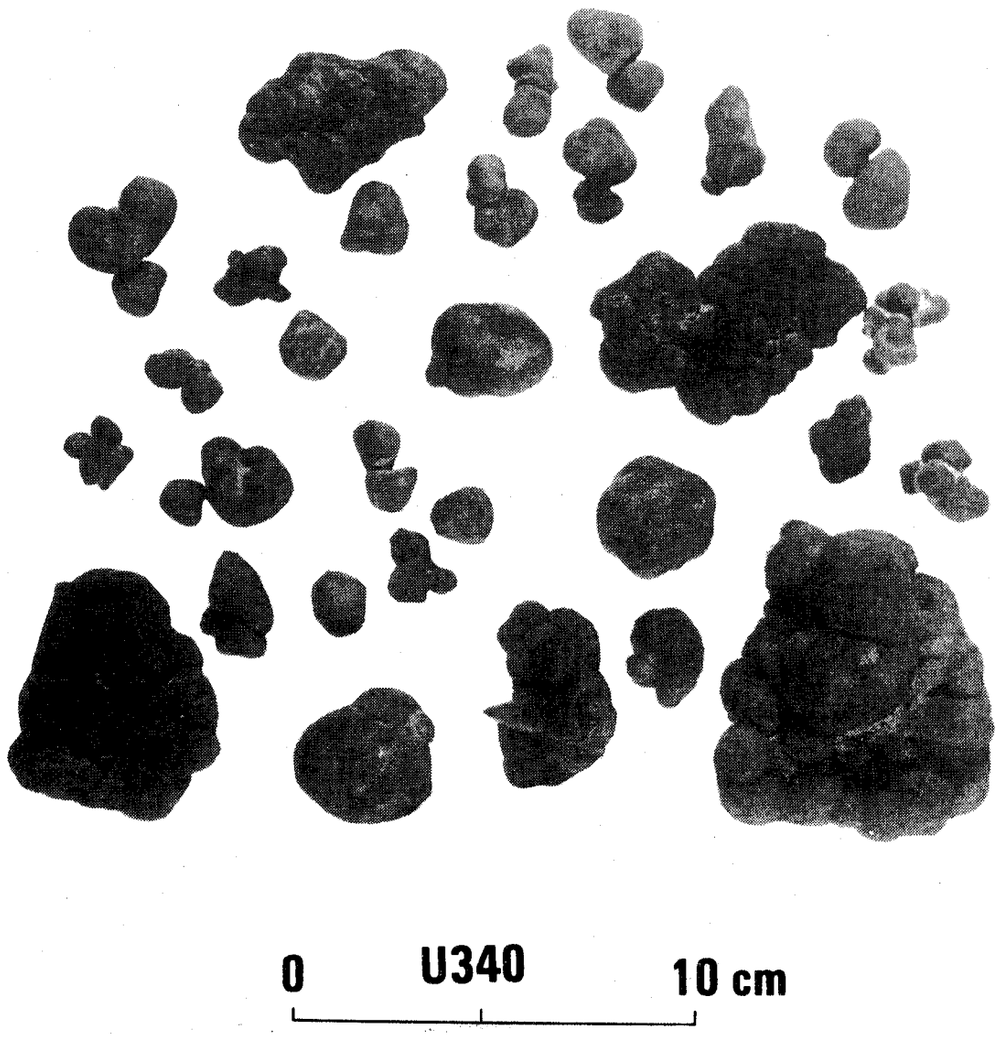

Figure 2. Selected nodules from Stn U340 (abyssal plain west of Nassau, depth 5268-5253 m). Note shark tooth incorporated into nodule, bottom row, just right of center. Note also tiny white thread-like structures on nodules in lower left- and lower right-hand corners, which are benthic foram tubes.

Nodule Shape

The nodules have been categorized in terms of general morphology using the Meylan and Craig scheme (Meylan, 1974) (Table 3; Appendix A). Spheroidal nodules are by far the most common, particularly among small nodules, while ellipsoidal and polynucleate nodules are also abundant. The regular geometric form of these nodules or nodule segments is often modified by faceting (occurrence of flat faces) or lobing (circumferential constrictions that when exaggerated produce the polynucleate morphology). Many of the medium and large nodules have tabular shapes with irregular outlines and raised margins on the sediment-water interface planes. Only a small percentage of the nodules have a shape dictated by a shark tooth, but all the large nodule hauls included at least one specimen of slightly stained to heavily encrusted tooth.

The many irregularly shaped small nodules of Stn U339 are a product of nodule fracturing and subsequent manganese encrustation on the sea floor. A large number of tiny "nodules" at Stn U321a have highly irregular shapes characteristic of scoriaceous volcanic fragments which undoubtedly serve as the nuclei for these nodules. A similar problem was presented by the small faceted basalt nuclei at Stn U327. The manganese encrustation may be so thin on many of these that they should not be considered true nodules. No discoidal nodules, other than a few with modified discoidal forms, were collected.

Table 3. Nodule types.

Stn	Large (number)	Medium (number)	Small (number)
U295			s[S]s (1)
U296a	l[E];l[P] (1) (1)	m[S]; m[P]; m[B] (159) (38) (2)	s[S]; s[P]; s[B]; s[E] (336) (15) (14) (8)
U298		m[S]r-mb; m[fS]r-mb (3) (2)	s[fS]r-mb; s[E]r; s[T-D]mb; s[I]r (2) (1) (1) (1)
U299a		m[S]mb (1)	s[fS]mb, s[B?]mb (2) (1)
U300		approx. 50% [P], 50% [S]+[E] + a few irregular shapes	
U321a	l[iT]b/mb (7)	m[iT]b/mb; m[lE]b/mb (7) (1)	s[S,fS,lS]r; s[E,fE,lE]r; s[P]r; (47) (44) (38) s[V]r; s[T]r; s[B]r; s[F]r (8) (4) (2) (1)
U325			s[T]s (1)
U327		m[X]b,mb-s (41) (where X mostly tabular or ellipsoidal)	s[Y]b,mb-s (1393) (where Y more varied than X, but mostly spheroidal)
U328			s[P]s (1)
U339		m[P]mb; m[E]mb; (82) (11) m[S]mb; m[F]mb; (1) (2) m[T]b; m[B]mb (1) (1)	s[S]mb; s[P]mb; s[E]mb; s[F]mb; (129) (64) (51) (3) s[T]mb (1) (for 20-40 mm template size only)
U340	l[T]b (5)	m[P,T,E]b or s (73)	S[P, S, E]s (1789)
U353		m[P]s (2)	

Note: Nodule type is modified from Meylan (1974) and is expressed by a three-component term as follows:

Size [Morphology] Surface Texture

where

Size —
- s = small (< 30 mm max. diam.)
- m = medium (30 - 60 mm max. diam.)
- l = large (> 60 mm max. diam.)

Morphology —
- S = Spheroidal
- fS = faceted Spheroidal
- lS = lobed Spheroidal
- E = Ellipsoidal
- fE = faceted Ellipsoidal
- lE = lobed Ellipsoidal
- F = Faceted
- P = Polynucleate
- T = Tabular
- iT = Tabular with irregular outline
- D = Discoidal
- V = Volcanic (scoriaceous)
- B = Biological, i.e., shape conforms to an organic hard part, usually a shark tooth
- I = Irregular, i.e., can not be described as conforming to any regular geometric shape

Surface Texture —
- s = smooth
- b = botryoidal
- mb = microbotryoidal (b/mb = botryoidal upper surface, microbotryoidal lower surface)
- r = rough

Nodule Surface Texture

Almost all nodules collected on this cruise have surface textures that can be considered microbotryoidal (Appendix A). The nodules are therefore covered on all sides by tiny botryoids (< 0.5 mm) which may be barely discernible to the naked eye, but which are readily distinguished with a hand lens. The relief of the microbotryoids, i.e., height above the overall nodule surface, varies somewhat. Relief is usually greatest in recesses on the nodule surface, producing more of a gritty feel, and least on protrusions, where the microbotryoids may present a smooth feel and, under the hand lens, a scaly appearance. No rough surface textures (where rubbing breaks off protruding microbotryoids) were observed. The initial assumption therefore is that nodules sampled on the *Tui* cruise are principally hydrogenous rather than diagenetic because of the lack of rough, friable surfaces.

Larger botryoids are developed on some of the medium and larger nodules. These botryoids have superimposed microbotryoids. Some large botryoids may have cores of satellite volcanic nuclei.

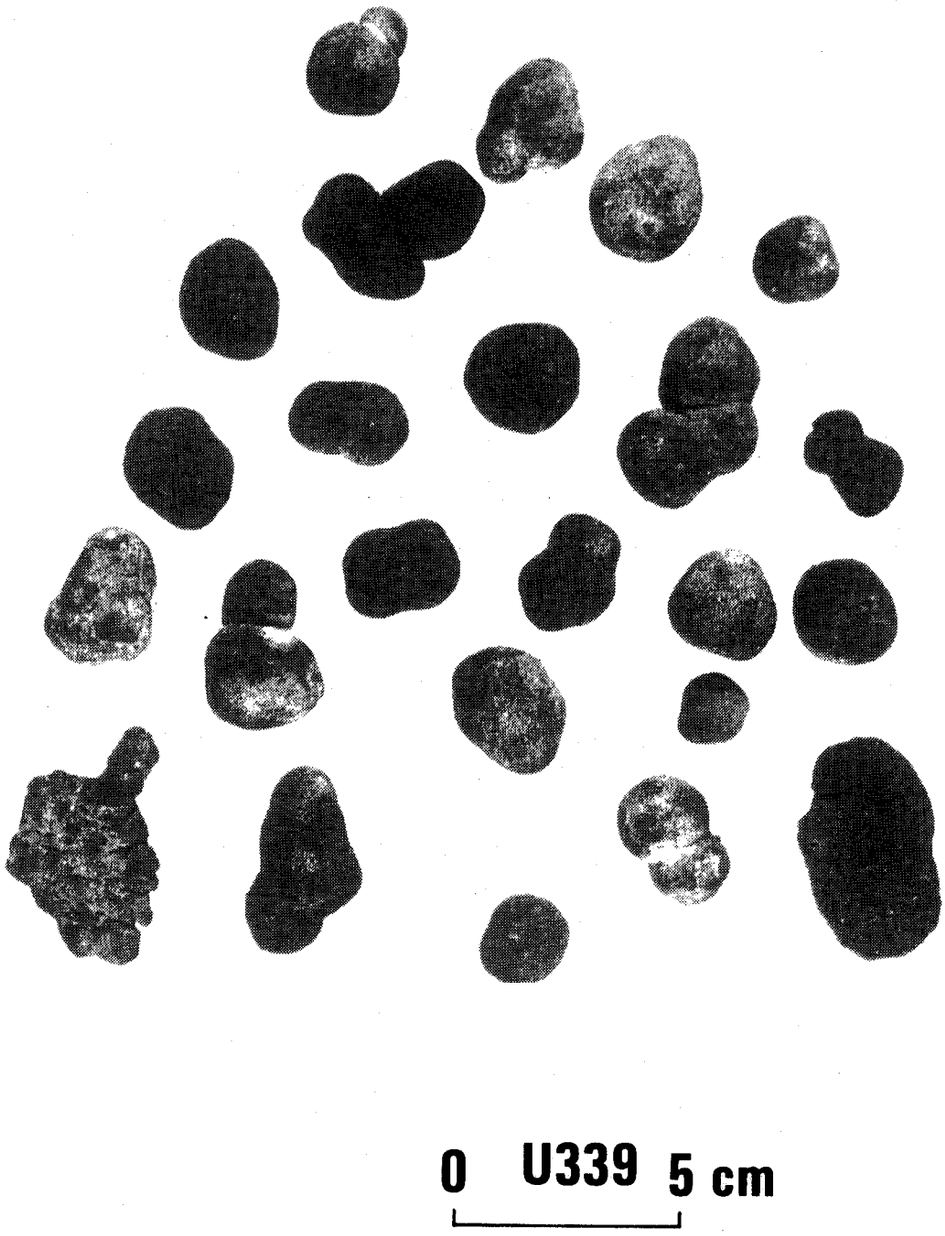

Figure 3. Selected nodules from Stn U339 (abyssal plain near base of Nassau volcanic edifice, depth 4204-4219 m).

Many smaller nodules at Stn U296a (Penrhyn Basin) show a septarian-like fracture pattern at the surface (not readily seen in Figure 1). This is usually not seen on Cook Island Facies nodules. Nodules from Stn U298 have surface cracks extending 1-2 mm inward.

Most nodules (and crusts as well) have numerous white thread-like meandering structures on their surfaces which are assumed to have been constructed by benthic foraminifera (see Dugolinsky and Meylan, this volume).

Nodule Internal Structure

A cursory inspection of the internal structure of a few nodules from stations with abundant hauls was undertaken using a hand lens. The nodules almost without exception have some type of volcaniclastic nucleus, where a nucleus can be seen (Appendix A). At Stns U296a and U321a, the original nucleus has been essentially completely replaced by Mn-oxides. At Stns 300, U327, U339 and U340, a fine-grained material assumed to be a glassy tuff, varying from

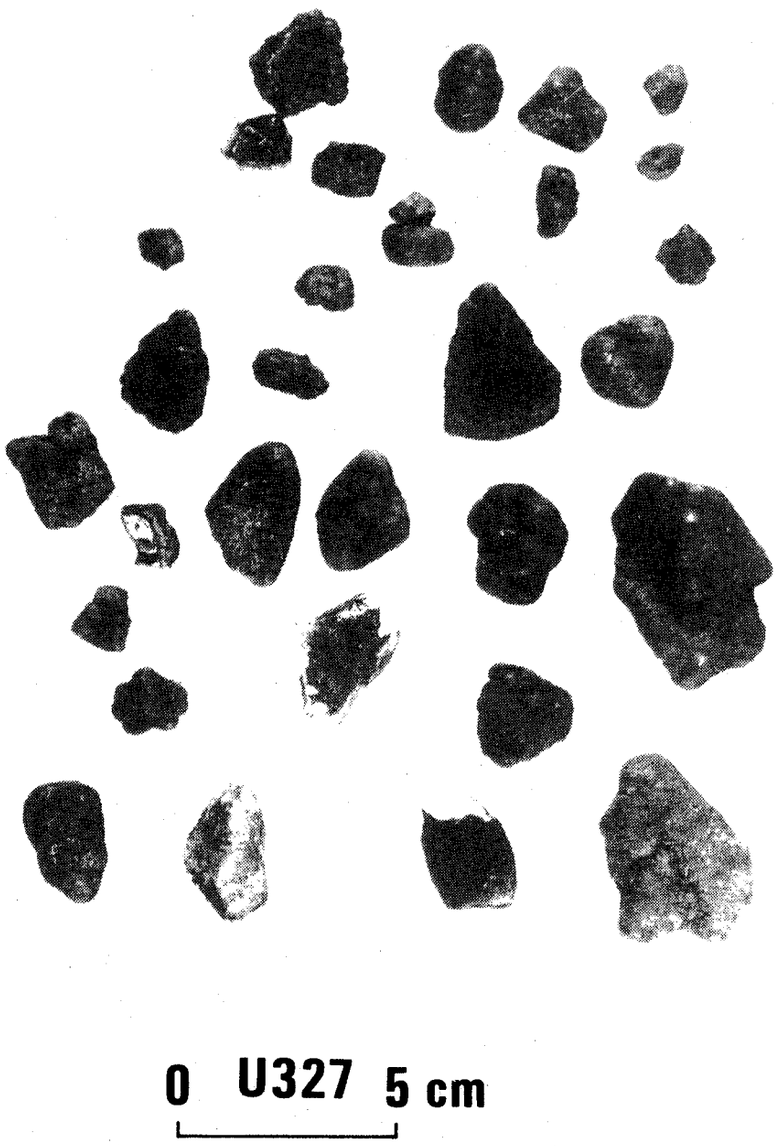

Figure 4. Selected nodules from Stn U327 (Pukapuka slope, depth 3394-3217 m).

yellow to brownish orange, is the nucleus material. Palagonite (Stn U340) and vesicular volcanic nuclei (Stns U327, U339) were also observed. The larger hauls include a small percentage of shark teeth nuclei.

Manganese crust thickness ranges up to 5 mm, although 5-mm thick outer crusts were observed only at Stns U300 and U339. Accreted manganese crusts are generally 2-3 mm thick and little structure can be seen within the crusts except for some faint parallel microlaminations.

Manihiki Plateau

Along the western margin of the Manihiki Plateau and in abyssal depths adjacent to the western margin, nodules were found at six stations. A single small spheroidal nodule was collected at Stn U295 northwest of Suwarrow in the Samoan Basin. Based on stations occupied by the R/V *Tangaroa* in 1976 north and east of the Samoan chain (Meylan et al., 1978), it was presumed that most of the northern part of the Samoan Basin was unfavorable for nodule development due to high sedimentation rates on the Samoan archipelagic apron or burial by carbonate ooze turbidites/slumps from the higher elevations of the Manihiki Plateau (see also Exon, 1982).

Subsequent dredging at the base of the western margin revealed unexpected abyssal nodule deposits. Little previous sampling has been done along this margin. Possibly slumping here has not been as widespread as previously thought (Winterer et al., 1974). Abyssal plains immediately west and east of Nassau (Stns U340 and U339) yielded exceptionally large hauls of small nodules. At Stn U339, the smaller nodules are mostly spheroidal or ellipsoidal, whereas medium nodules are polynucleate or ellipsoidal (Figure 3). Many irregularly-shaped small nodules are apparently nodule fragments, broken and further encrusted on the sea floor. At Stn U340, both small and medium nodules are polynucleate, but the very smallest nodules (< 5 mm max. diam.) are almost all spheroidal (Figure 2). The abundance of these tiny nodules is quite unusual. A few tabular "lumpy" nodules with irregular outlines were also found. At both Stns U339 and U340, the manganese oxide crusts occur on volcaniclastic material that has been altered to palagonite (or clays?), but which appears to have experienced little replacement by Mn-oxides. This aspect and the slightly thicker manganese crusts may indicate that these nodules are not part of the Cook Island Facies found south of the Manihiki Plateau, but may be a local facies.

On the upper western slope of Pukapuka, a single small tabular nodule was collected with Mn-stained and unstained gorgonian coral and coarse carbonate sand (Stn U325). This is certainly an anomalous occurrence, and difficult to explain; the nodule may have been wedged in the dredge at a previous station. Deeper on the Pukapuka edifice (Stn U327), abundant nodules were collected from what might be a break in the steep slope, on foram ooze. These nodules are mostly small spheroidal and medium tabular or ellipsoidal types (Figure 4). Many small irregular objects here counted as nodules may in fact be Mn-stained scoria. Most nodules appear to have a fine-grained tuff nucleus with a manganese crust up to about 2 mm thick. In the abyssal hills west of the base of Pukapuka, a single small polynucleate nodule was recovered with dark brown clay and abundant Mn-stained volcaniclastic scoria (Stn U328).

During traverses across the Manihiki Plateau, no evidence of nodules was found at the few stations occupied.

On the lower slope of the eastern margin of the Manihiki Plateau, nodules were recovered at Stns U298, U299a and U300. The deepest Stn (U298) provided 10 nodules, mostly spheroidal or faceted spheroidal, occurring on dark brown clay and associated with abundant weathered scoriaceous basalt and Mn-crust fragments. Differences in surface texture and shape indicate that these nodules may represent a mixture of local facies and Cook Island Facies nodules. The local facies nodules are characterized by surface cracks that extend 1-2 mm into the nodules. Slightly higher up the plateau slope (Stn U299a), a few faceted spheroidal nodules were found, while on a terrace further up the slope (Stn U300), an abundant haul of small, fragile polynucleate, spheroidal and ellipsoidal nodules lying on carbonate ooze (based on the whitish cast seen on the nodules after drying) was collected.

The southern Penrhyn Basin, an area known to contain Cook Island Facies nodules (Landmesser et al., 1976; Glasby, 1978; Exon, 1981, 1983; Skornyakova et al., 1990; Cronan et al., 1991a, b; Usui et al., 1993), was sampled at the abyssal hills of Stn U296a (Figure 1). Here, the nodules are mostly small to medium faceted-spheroidal, with a thin (1 mm) accretion crust covering a Mn-replaced volcanic(?) nucleus. Closer to the base of the plateau east of Manihiki Island (Stn U321a), mostly small spheroidal, ellipsoidal and polynucleate nodules were dredged, with dark brown clay, scoria and pumice, but the haul included a number of medium and large tabular nodules with irregular, raised margins and nearly flat bottoms. The initial impression was that these represented small spheroidal Cook Island Facies nodules partly buried by a volcaniclastic fall and then further encrusted, but this does not seem to be the case. The original nucleus appears to be tabular segments of now-replaced glassy volcanics, with the lumpy tops due to encrusted later-arriving bits of scoria.

Capricorn Seamount-Niue Transect

Two medium polynucleate nodules were trapped by the trigger core catcher along with brown clay at Stn U353, an unsuccessful piston coring attempt. Because this suggested that we had sampled a dense nodule field west of the "nodule western limit" of Meylan et al. (1982), further sampling of this site close to Capricorn Seamount was attempted during the return from Niue (Stn U360). Ambiguous results were provided by bottom photographs, and the subsequent dredging and coring attempts were unsuccessful. The site lies between Stns I168 and I169 of the 1976 *Tangaroa* cruise (Meylan et al., 1978), where gravity coring produced short cores of clayey silt unlike the

Table 4. Crust samples.

Stn	Gear	Locality	Depth (m)	No. of Frags	Size Range (mm)	Oxide Max. Thick (mm)	Substrate[1]
U298	Pipe dredge	Eastern margin slope, Manihiki Plateau	4996	2	24, 57	10	NR
U299b	Rock dredge	Eastern margin slope, Manihiki Plateau	4469-4464	5	26-75	35	NR
U308b	Rock dredge	Western margin slope, Manihiki Plateau	3991	4	19-23	12	Volc. SS
U314	Rock dredge	Rakahanga	1843-1620	1	770	10	Volc. SS
U315	Rock dredge	Rakahanga	1863-1535	46	8-68	15	Foram limestone
U316b	Rock dredge	Rakahanga	2600	27	13-47	8	Volc. SS
U319	Rock dredge	Manihiki Island	2906-2911	3	7-15	5	NR
U322b	Rock dredge	Manihiki Island	1754-1560	200+ 1	<165 78	1 4	Foram ooze Volc. SS on basalt
U326	Rock dredge	Pukapuka	2161-2121	23 2	4-28 17, 30	<1 18	Volc. SS, Basalt(?), foram(?) limestone NR
U332	Rock dredge	Tema Reef	1377-1199	8 1 1	8-62 31 ?	<1 1 6	Foram(?) limestone Basalt NR
U333b	Rock dredge	Tema Reef	1913-1575	35	6-116	20	?
U336b	Rock dredge	Nassau	1297-981	9	16-43	12	Coral(?)
U357	Rock dredge	Niue	3612-3596	12	18-45	3	Ash lumps
U358	Rock dredge	Niue	2520-2450	20	8-34	3	Coral
U361	Rock dredge	Mauke	1426-1516	8(?)	17-71	3	Volc. SS(?)
U363	Rock dredge	Mauke	2640-2780	20	11-46	8	Basalt, volc. SS(?)
U367	Rock dredge	Mitiaro	1744-1635	1	224	6	Basalt
U369	Rock dredge	Mitiaro	2141-2441	35	7-37	3	Foram limestone, volc. SS(?)
U375	Rock dredge	Rarotonga	1272	5	27-151	65	?

[1] NR = not recovered
Volc. SS = volcaniclastic sandstone

Figure 5. Stn U375 manganese crust fragments (Rarotonga slope, depth 1272 m).

silty clays that bear nodules further east. The Stn U353 nodules are therefore probably part of a local facies related to Capricorn Seamount (see Piper et al., 1985).

MANGANESE CRUSTS

About 470 manganese crust fragments were collected at 19 stations, 12 of which were along the western or eastern sides of the Manihiki Plateau (Table 4). Almost half of the total fragments were recovered at Stn U322b (southwestern slope of Manihiki Island, depth 1657 m). If any aspect of the cruise can be said to be disappointing, it is the relative lack of success in collecting Mn-crusts, especially those of appreciable thickness. Mn staining was found to be almost ubiquitous on the rocks or semi-consolidated sediment dredged, but crust development was the exception. Crusts recovered range in maximum thickness from 3 mm at the Niue stations (U357, U358) to about 65 mm at Stn U375 (Figure 5).

Crusts were found to occur at depths of 1139 m (north slope of Nassau, Stn U336b) to 4496 m (lower eastern slope of the Manihiki Plateau, Stn U298). In all but six cases (Stns U298, U299b, U319, U326, U332 and U375), the crusts were recovered with some type of attached substrate so that there is no doubt about crust thickness at most stations (Appendix B). Only at Stn U299b (lower eastern slope of the Manihiki Plateau) was neither substrate nor associated coarse material recovered (Figure 6). The substrates sampled are either limestones (foraminiferal or coralline) or some type of volcaniclastic material, both limestones or volcanics being in a rather advanced state of alteration. At six stations (U299b, U315, U336b, U358, U361 and U367), no rock material other than the substrate attached to the crust was collected. The associated coarse material found at other crust stations includes coral rubble and/or volcaniclastics, with tuff, scoria, pumice and coral rubble all occurring together at U316b (southeastern slope of Rakahanga). Substrate material is similar to the rock types collected during the cruise.

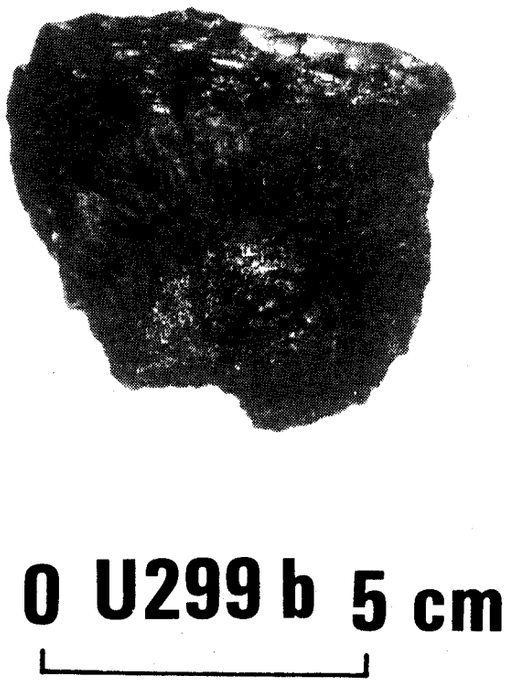

Figure 6. Stn U299b manganese crust fragment; cross-sectional view, upper crust surface at top (eastern margin of Manihiki Plateau, depth 4469-4464 m).

Both Mn-stains and thicker Mn-crusts display microbotryoidal surface textures, for the most part (Appendix B). Some crust fragments, such as the large slab recovered at Stn U314 (eastern slope of Rakahanga), have thick enough manganese oxides and cover enough surface area so that the microbotryoids are superimposed on much larger botryoids. Smooth surfaces, where the microbotryoids have a very low relief or even scaly appearance, were noted as patches on several of the crust fragments, and cover essentially the complete surfaces of samples from Stns U326 (western slope of Pukapuka) and U332 (southeastern slope of Tema Reef), where other surface types are also present. A rough surface, resembling a scoria surface, is present on crusts collected at Stn U333b (southeastern slope of Tema Reef, less than 500 m deeper than U332). Very high relief botryoids (with deep and downward-widening recesses between the individual botryoids) are displayed by crusts from several stations, particularly U315 (southwestern slope of Rakahanga) and U336b (northern slope of Nassau).

Because of the thinness of the crusts collected, little can be said about their internal structure (Appendix B). The prevalent internal structure is a massive (structureless) outer layer superimposed on a layer consisting of small botryoids as columns or branching upwards in cross-section, with what appears to be sediment trapped between the botryoidal structures. Because this botryoidal layer is underlain by another massive layer in at least one sample, the possibility exists that the massive growths have occurred during times of relatively slow sedimentation, and the botryoidal layers grew while sediment (primarily carbonate) was accumulating more rapidly.

The contact between Mn crust and its substrate is generally quite sharp, although the upper surface of the substrate is usually contorted, particularly in the case of many of the carbonates, which have been burrowed. Irregular Mn growths into the underlying tuff were observed at Stn U308b.

Manihiki Plateau

Somewhat unexpectedly, Mn crusts were found at all station groupings along the western margin of the Manihiki Plateau, i.e., near the western end of the 12°45' S traverse (Stn U308b), and at Pukapuka (Stn U326), Tema Reef (Stns U332 and U333b), and Nassau (Stn U336b). Prior to sampling, it was thought that the western margin was likely to be relatively barren of both manganese nodules and crusts in contrast to the eastern margin with its already known deposits. Western margin crusts were found at depths of 1139 to 3991 m, on both volcanic and carbonate substrates.

Figure 7. Stn U314 manganese crust slab; view of top surface (Rakahanga slope, depth 1843-1620 m).

Manganese crusts were also found at all station clusters along the eastern margin of the Manihiki Plateau, i.e., the eastern end of the 12°45' S traverse (Stns U298 and U299b), Manihiki Island (Stns U319 and U322b) and Rakahanga (Stns U314, U315 and U316b). The crusts occur at somewhat greater depths (1675 to 4996 m) than along the western margin but, as on the west, have grown on both volcanic and carbonate substrates. The single most impressive sample collected during the cruise is the 0.77 m-long, 0.13 m-thick slab of coarse tuff dredged at Stn U314 on the eastern slope of Rakahanga (Figure 7). The tuff is encrusted on all sides by a manganese crust that appears to be up to about 10 mm thick.

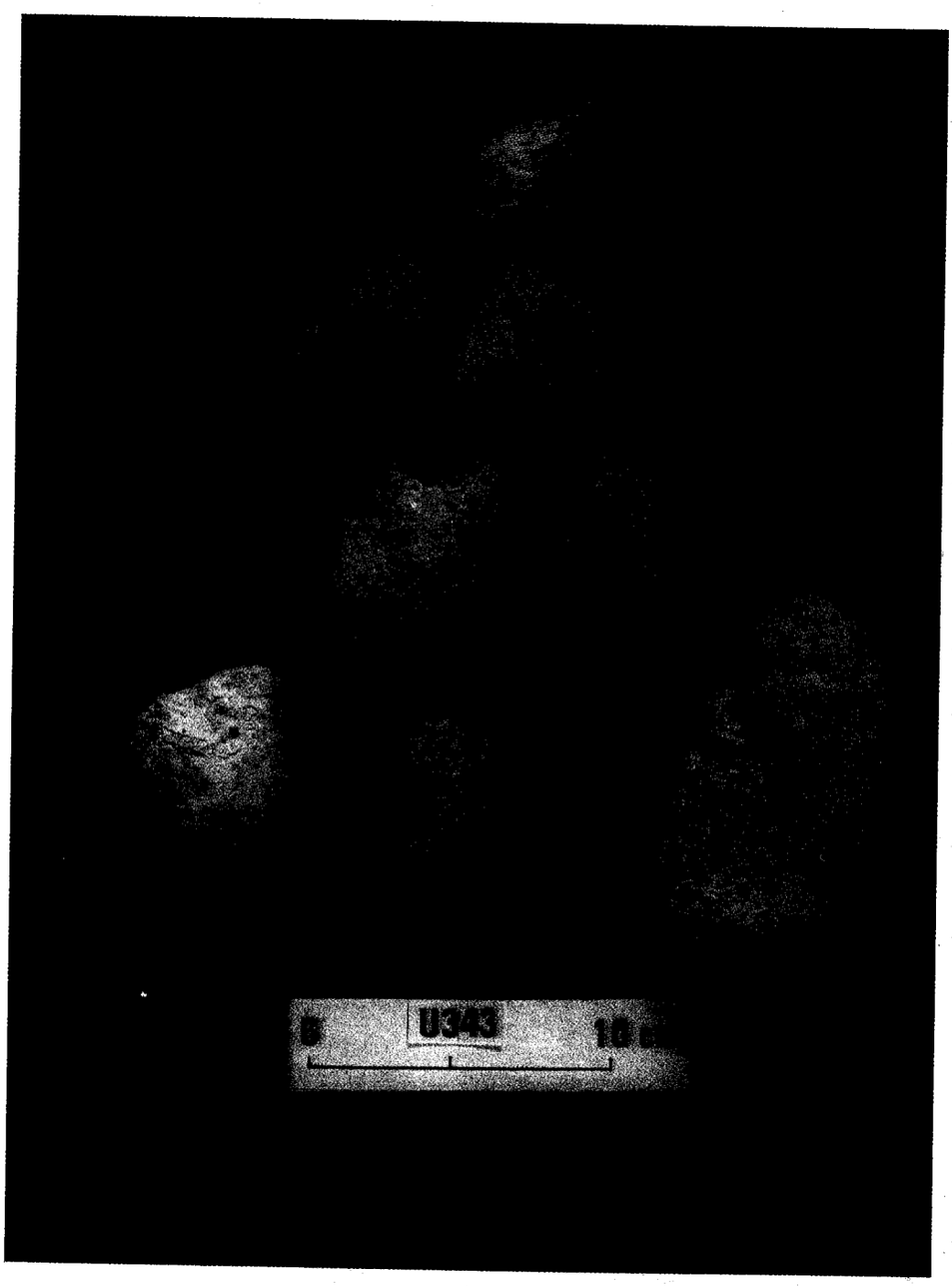

Figure 8. Stn U324 coralline cobble lacking Mn-staining; note incorporated mollusc shells (Pukapuka slope, depth 416-446 m).

Niue

Manganese crusts were found at two stations on the slopes of Niue (U357, U358), at depths of 3604 and 2485 m, respectively. Although the maximum crust thickness is only 3 mm, these crusts resemble those found along the Manihiki Plateau in surface texture, internal structure and substrate types.

ROCKS

The bulk of the coarse material collected during the cruise consists of a variety of sedimentary (carbonate) and igneous (mostly volcaniclastic) rocks, along with the hard parts of organisms such as shell fragments and shark teeth (Table 5; Appendix C). Although there is no Mn staining on the dredged rocks at a few stations, there is at least patchy staining on some of the coarse material in almost all of the dredge hauls.

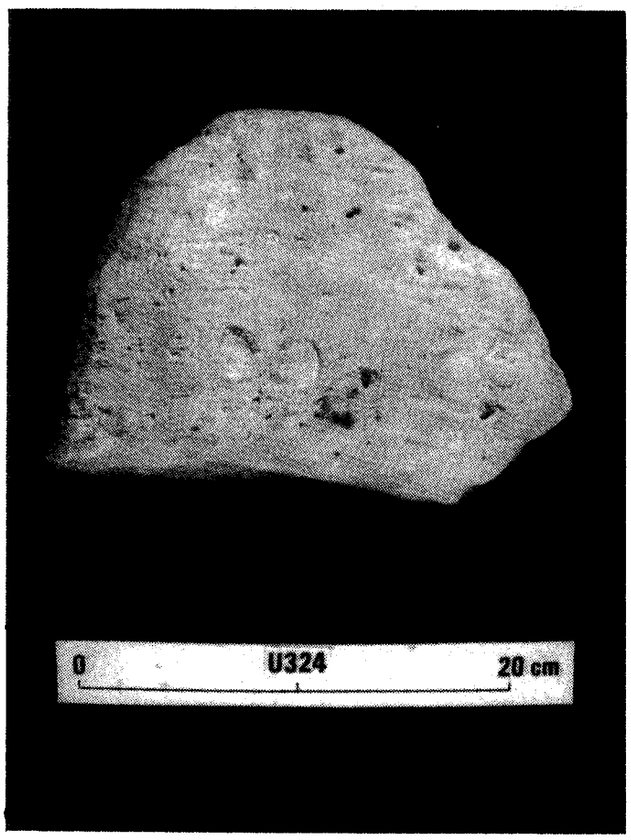

Figure 9. Stn U343 coralline rubble, the coral displaying moderate to severe recrystallization (Machias Seamount crest, depth 730-715 m).

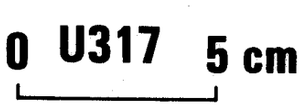

Figure 10. Stn U317 scleractinian coral fragments, some Mn-stained (Manihiki Island slope, depth 2161-2111 m).

Carbonates

Coral rubble and coralline limestone was the most voluminous component of the sample collection at many stations. In fact, at several stations so much was collected that only part of the haul could be retained for archiving and further study (Stns U317, U324, U325, U331, U337 and U342). The coral material includes segments of individual coral growths as well as coral boundstone, i.e., coralline fragments cemented by a fine-grained limy matrix and calcaeous algae. At some shallower stations, the coral is quite fresh and unstained by manganese (Figure 8). In most cases, there is brown (very thin) to black (thicker) Mn-staining. The coral usually displays some degree of chemical weathering, i.e., dissolution and reprecipitation of calcium carbonate which progressively degrades the coral structure until it is unrecognizable or makes the remaining material friable (Figure 9). Both angular and rounded coral gravel is usually present together in the larger hauls. Most of the coral is scleractinian (Figures 10, 11)(see Grange and

Table 5. Rock samples.[1]

Stn	Gear	Locality	Depth (m)	No. of Rocks	Size Range (mm)	Rock type[2]
U292	Rock dredge	North of Suwarrow on Manihiki Plateau	3036-3026	1 1	23 21	Coral Foram limestone
U294	Pipe dredge	Southern margin slope of Manihiki Plateau	3829	1	34	Pumice
U298	Pipe dredge	Eastern margin slope of Manihiki Plateau	4996	ca. 500+	34	Scoria
U307	Pipe dredge	Western margin slope of Manihiki Plateau	3586	1	72	Foram(?)limestone
U308a	Rock dredge	Western margin slope of Manihiki Plateau	3763-3707	1	30	Foram limestone
U308b	Rock dredge	Western margin slope of Manihiki Plateau	3991	35 11	10-35 15-23	Volc. SS Tuff, pumice
U316b	Rock dredge	Rakahanga	2600	ca. 45 ca. 30 1 1	6-38 7-32 38 8	Pumice, scoria, tuff, basalt Coral Foram(?) limestone Garnet crystal
U317	Rock dredge	Manihiki Island	2161-2111	ca. 1000 1 1 1(?)	102 28 pebble pebble(s)	Coral Breccia (limestone in volcaniclastic matrix) Chert(?) Volc. SS
U318	Rock dredge	Manihiki Island	1684-1555	4(?)	5-48	Foram ooze lumps
U319	Rock dredge	Manihiki Island	2906-2911	7	10-23	Coral
U321a	Pipe dredge	Penrhyn Basin, east of Manihiki Island	5114-5047	10	1-13	Scoria, pumice
U322b	Rock dredge	Manihiki Island	1754-1560	2	18, 34	Foram limestone
U323	Rock dredge	Manihiki Island	3066-2971	26 9	7-37 10-22	Coral Volc. SS, basalt
U324	Rock dredge	Pukapuka	417-446	ca. 1000 many 1	490 ca. 10 25	Coral, mostly gorgonian Encusting algae, algal plates Calcarenite
U325	Rock dredge	Pukapuka	1585-1446	400+	240	Gorgonian coral
U326	Rock dredge	Pukapuka	2161-2121	1	12	Pumice
U327	Rock dredge	Pukapuka	3394-3217	4	61	Layered coarse, fine tuff
U328	Pipe dredge	Pukapuka	4837-4796	ca. 100 4	28 21	Scoria, volc. SS, pumice Coral, foram limestone
U329	Rock dredge	Pukapuka	2825-2450	5	22-96	Coral
U331	Rock dredge	Tema Reef	1407-1100	ca. 1900	240	Coral, including gorgonian(?)
U332	Rock dredge	Tema Reef	1377-1199	101 9 1 1	7.5-40 11-27 23 17	Coral, including gorgonian(?) Basalt Volc.(?) breccia Volc. SS
U333b	Rock dredge	Tema Reef	1913-1575	35	15-570	Gorgonian coral
U334	Rock dredge	Tema Reef	2916-2851	2	20, 26	Coral
U335a	Rock dredge	Nassau	2545-2161	1 1	21 20	Coral Carbonate-encrusted basalt
U337	Rock dredge	Nassau	1001-804	ca. 1000 1	730 13	Coral, including gorgonian Chert nodule
U339	Rock dredge	Nassau	4204-4219	2	5, 13	Pumice

Stn	Gear	Locality	Depth (m)	No. of Rocks	Size Range (mm)	Rock type[2]
U340	Rock dredge	Samoan Basin near Nassau	5268-5253	4 1	7-10 6	Pumice Scoria
U341b	Rock dredge	Machias Seamount	2495-500	ca. 100 26 13 8 18	230 8-170 17-48 15-47 50	Altered tuff Coral, including gorgonian(?) Scoria Basalt Marly coquina
U342	Rock dredge	Machias Seamount	1350	ca. 200	152	Coral on algal, calcarenite substrate
U343	Rock dredge	Machias Seamount	730-715	ca. 500 7 several	186 54-99 50	Coral Calcarenite limestone Ash lumps
U344	Rock dredge	Machias Seamount	675-670	1 1	33 54	Pumice Gorgonian coral
U345	Rock dredge	Machias Seamount	1972-2166	44 1 45 1	21-285 21 15-160 51	Coral, including gorgonian(?) Coquina Basalt Ash lump
U346	Rock dredge	Machias Seamount	4077	ca. 500 1 1 6 1 1 68 1	7-145 52 42 19-28 26 28 10-108 43	Basalt Ultramafic nodule Pumice Tuff Vuggy volcaniclastic Breccia Coral Calcarenite
U348	Rock dredge	Capricorn Seamount	2825-2640	8	21-130	Amygdaloidal basalt(?)
U349	Rock dredge	Capricorn Seamount	1873-1853	1	106	Basalt breccia
U350	Rock dredge	Capricorn Seamount	1021-922	4	21-295	Coral
U351a	Rock dredge	Capricorn Seamount	996-976	22	12-24	Pumice
U351b	Rock dredge	Capricorn Seamount	942-932	?	?	Pumice
U352	Rock dredge	Capricorn Seamount	4684-4689	165+ 5 19+	<10-97 16-48 <10-126	Coral Coquina Basalt, other volcanics
U354	Rock dredge	Niue	346-467	6	16-29	Coral
U356	Rock dredge	Niue	1873-1100	ca. 250+	<10-250	Coral
U357	Rock dredge	Niue	3612-3596	1 1 1	77 27 25	Silicified(?) coral Basalt Pumice
U358	Rock dredge	Niue	2520-2450	3	24-95	Coral
U362	Rock dredge	Mauke	685-626	9 9	21-49 11-49	Branching, platy coral Encrusted coral
U366	Rock dredge	Mitiaro	1101-1179	ca. 1000	100	Coral, mostly gorgonian
U369	Rock dredge	Mitiaro	2141-2441	9	6-31	Foram limestone
U370	Rock dredge	Rarotonga	1021-1080	39 1 1	16-150 24 37	Coral Volcaniclas-tite(?) Basalt(?)
U371	Rock dredge	Rarotonga	1486-1516	30 6 28	9-162 12-158 8-60	Coral Volc./coral conglomerate Basalt

Table 5....continued

Stn	Gear	Locality	Depth (m)	No. of Rocks	Size Range (mm)	Rock type[2]
U372	Rock dredge	Rarotonga	2042-2092	1	21	Coral
U375	Rock dredge	Rarotonga	1272	231 ca. 750 5	32 86 10-29	Basalt Coral Volc. SS(?)
U376	Rock dredge	Rarotonga	1992-1968	ca. 50 7 14 1	58 21-33 15-40 20	Basalt Coral Volc. SS(?) Volc. calcarenite
U377	Rock dredge	Rarotonga	2450-2296	48 23	13-92 19-51	Basalt Coral
U378	Rock dredge	Rarotonga	3031-2961	ca. 20 1	25 27	Coral Pumice
U379	Rock dredge	Rarotonga	715-824	?	?	Basalt

[1] Including all types of corals, but not the remains of other organisms; see Main et al. (this volume) for a tabulation of the latter. Gravel fraction separated from sediment samples is also reported above.
[2] Volc. SS = volcaniclastic sandstone

Veron, this volume), but some gorgonian coral was also collected (see Grigg, this volume). At Stn U325 (Tema Reef) the gorgonian coral is unusually dense and has a chalky appearance (Figures 12, 13). At Stn U357 (south side of Niue, depth 3604 m), a large rounded coral pebble which shows partial dissolution and is extremely well indurated, apparently as a result of silicification, was found.

Coral rubble, obviously emplaced by some type of mass movement, was dredged from steep slopes as shallow as 406 m (Stn U354, southwestern side of Niue) to as deep as 4686 m (southern side of Capricorn Seamount, Stn U352). Coral rubble was even recovered at a depth of 4816 m in the abyssal hills west of Pukapuka (Stn U328).

Coral rubble was recovered from the slopes of all of the atolls sampled, as well as from Machias and Capricorn Seamounts, but not from the eastern and western margins of the Manihiki Plateau on non-atoll slopes. It seems likely that coral-capped volcanoes must have a rubble blanket that diminishes in thickness, coverage and fragment size down slope, and the existence of such a blanket probably precludes the development of extensive manganese crusts above about 3000 m.

Among the other types of carbonate found is what is tentatively identified as foraminiferal limestone. It was noted at a number of stations from both sides of the Manihiki Plateau: U292, U308a, U315, U316b, U328, U332 and possibly U326. Semi-consolidated foraminiferal sediment lumps were recovered at stations U318 and U322b on the slopes of the Manihiki Island edifice. Coquina (beachrock?) was included in the material gathered at Stns U345 (Machias Seamount) and U352 (Capricorn Seamount). A finer-grained shell hash limestone or calcarenite was found at Stns U341b and U343 (Machias Seamount). Carbonate shell fragments (mostly of pelecypods and gastropods) were collected at a number of stations, in all cases associated with more abundant coral rubble (see Beu, this volume). Conversely, most abundant coral rubble hauls included shell fragments. However, this was not the case at shallow stations U325 (1515 m, Pukapuka), U342 (1350 m, Machias Seamount) and U356 (1486 m, Niue).

Shark teeth are another type of coarse material that is common in sediments sampled during the cruise. One tooth was found with carbonates and volcaniclastics at a depth of 1278 m at Tema Reef (Stn U332), but in all other cases the teeth occurred with manganese nodules, and at depths of 3305 m or greater.

No other type of sedimentary material was noted, except for a possible chert pebble at Stn U317 (Manihiki Island) and a chert nodule at Stn U337 (Nassau).

Volcanics

Several varieties of igneous rocks were found, all of volcanic origin: basalt (aphanitic, vesicular and scoriaceous), pumice, and fragmental volcaniclastics (ash and tuff). Material of similar nature on the Manihiki Plateau has been reported by Heezen et al. (1966) and Winterer et al. (1974); see also Clague (1976).

Most of the basalt consists of small (4-8 mm) blocky, angular or scoriaceous pebbles, which may be weathered

and thinly encrusted with manganese, making them difficult to differentiate from true small nodules. This is particularly the case at Stn U321a (abyssal hills east of the Manihiki Plateau) and Stn U327 (western slope of Pukapuka). Many of the deep-water stations at which nodules were found also yielded small pebble forms of basalt.

Somewhat larger pebbles of basalt were commonly found in rock hauls, although seldom in any great number. This basalt is usually gray to dark gray, aphanitic to finely vesicular to coarsely vesicular, and occurs in the form of angular to rounded pebbles (often showing this shape range in a single haul). The degree of weathering varies, but the pebbles seldom appear fresh. Larger pebble scoria is particularly abundant at Stn U298 (lower eastern slope of

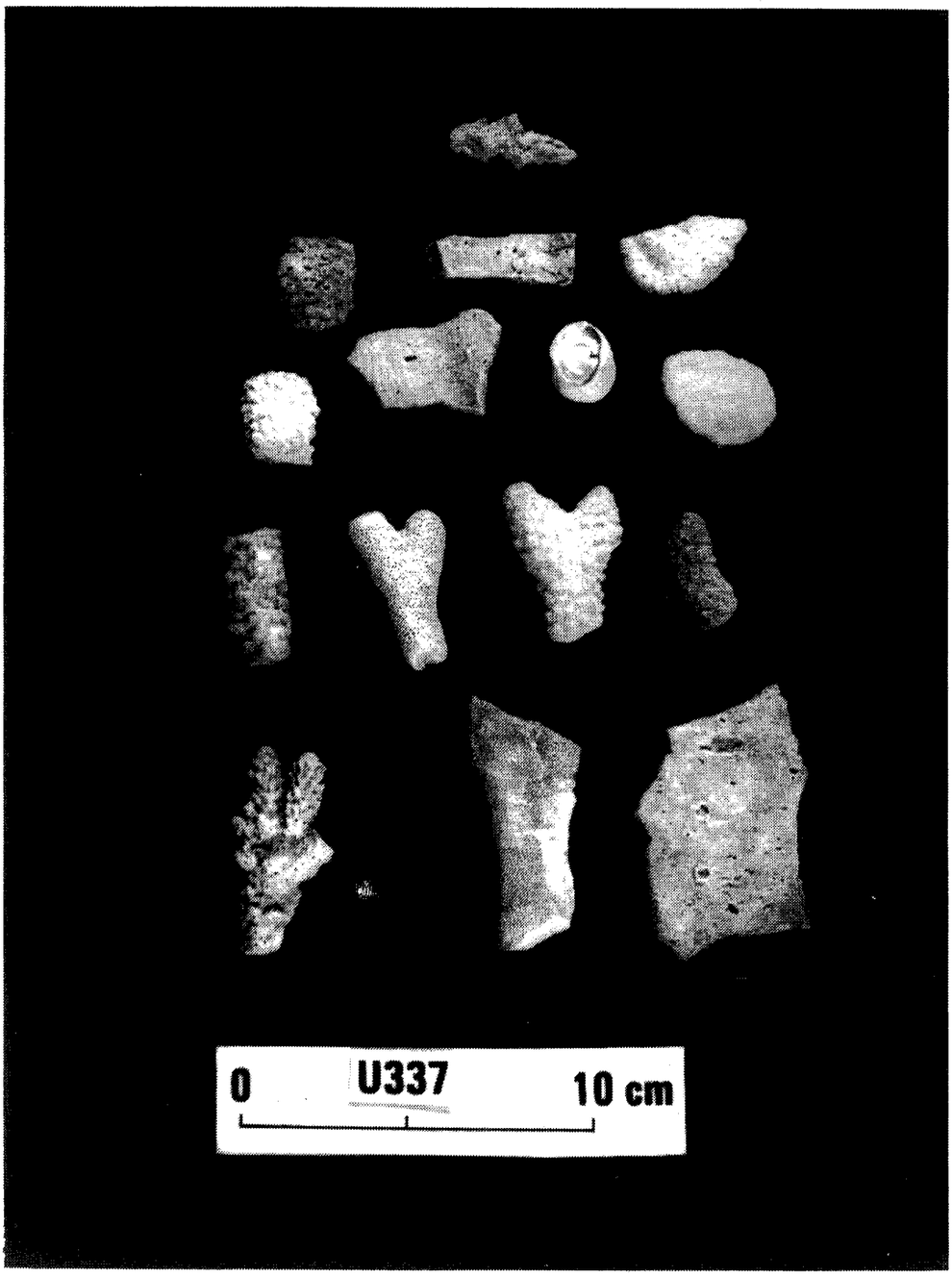

Figure 11. Stn U337 scleractinian coral fragments (Nassau slope, depth 1001-804 m).

the Manihiki Plateau), where a few nodules and crust fragments were also recovered. Basalt was found as shallow as 1278 m at Tema Reef (Stn U332).

The only significant hauls of basalt, in terms of quantity, apparent freshness, and variety, were dredged at Machias and Capricorn Seamounts. At stations U345 and U346 (Machias Seamount), coarse basalt gravel was retrieved from depths of 2069 m and 4077 m, respectively. The abundant haul at Stn U346 resembles well rounded river or beach gravel, obviously transported a considerable distance downslope. At both stations, the basalt is the typical dark gray variety, dominantly aphanitic, but a sizeable percentage of vesicular pebbles are also present. Olivine phenocrysts occur in both fresh and weathered states at the surface of the pebbles, and large dunite inclusions can be seen in some (Figure 14). The collection at Stn U346 includes an ultramafic nodule. The basalt material from Capricorn Seamount does not resemble that from Machias Seamount. At Capricorn Seamount, the rocks may be somewhat more silica-rich, and display amygdaloidal (Stn U348) and brecciated (Stn U349) types, the latter possibly having a zeolite matrix.

Pumice is a common, but seldom abundant, constitutent of the rock collections. Only at Stns U316b (Rakahanga) and U351a (Capricorn Seamount crest) were more than a few pieces of pumice recovered at any one time. Brodie (1965) also reported pumice from Capricorn Seamount. The pumice is usually in the form of gray to grayish olive green rounded pebbles, and is usually associated with other forms of volcaniclastic material. Many of the nodule hauls from abyssal depths include a few bits of pumice.

Volcaniclastics in the form of ash and tuff were found in almost one-third of the samples bearing some type of coarse solid material, and undoubtedly occur in dispersed form in most of the brown (abyssal) clay samples. Brownish gray to grayish olive green semi-consolidated fine-grained

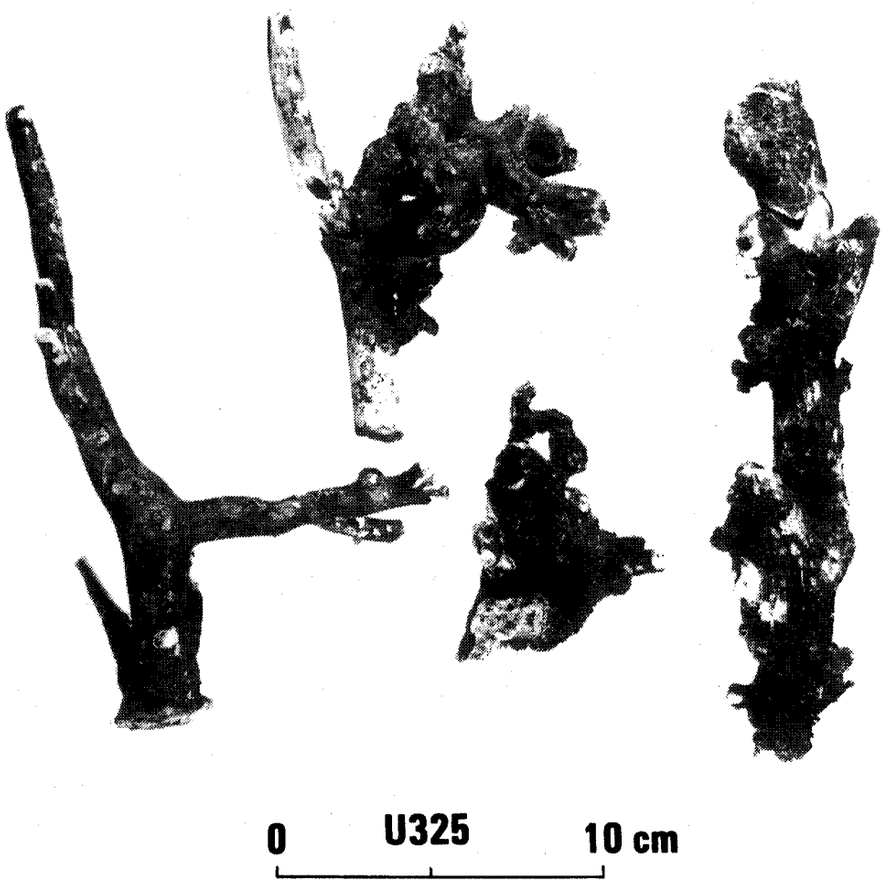

Figure 12. Stn U325 gorgonian coral with thin Mn-crust (Pukapuka slope, depth 1585-1446 m).

ash lumps were collected at Stns U343 and U345 (Machias Seamount) and U357 (Niue). The lumps include a clay fraction (smectite?) that probably is derived from weathering of volcanic glass. Clay is also an obvious component of the friable lithic/crystal/vitric tuff of Stn U341b (Machias Seamount). Ash lumps were found as shallow as 722 m (Stn U343, Machias Seamount) and as deep as 3604 m (Stn U357, Niue).

Tuff is a common substrate for the manganese crusts. Yellowish green to light yellowish olive green fine to coarse crystal/vitric tuff is found as a relatively well indurated

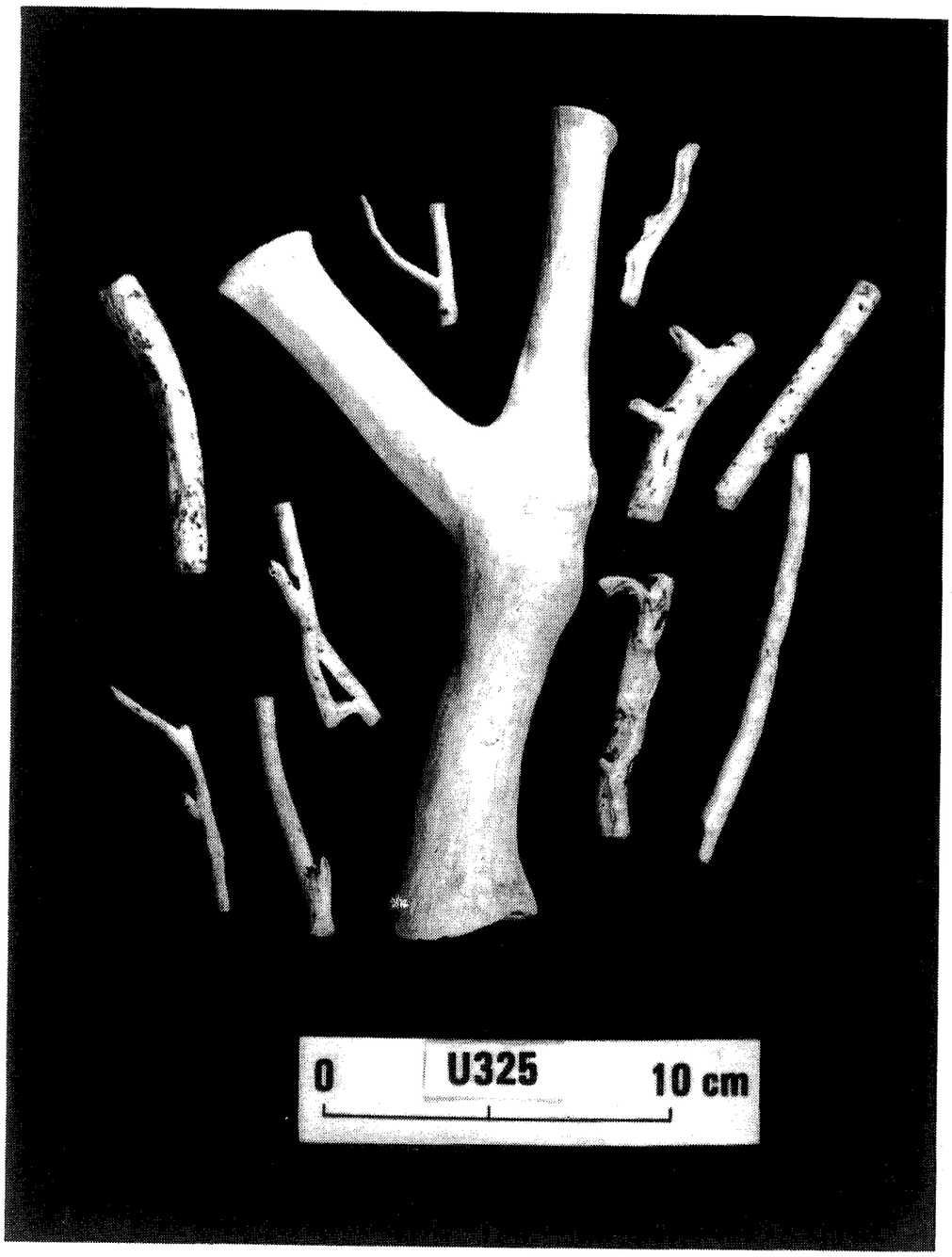

Figure 13. Stn U325 gorgonian coral; manganese encrustation absent (due to abrasion of fragments or relative freshness of samples?)(Pukapuka slope, depth 1585-1446 m).

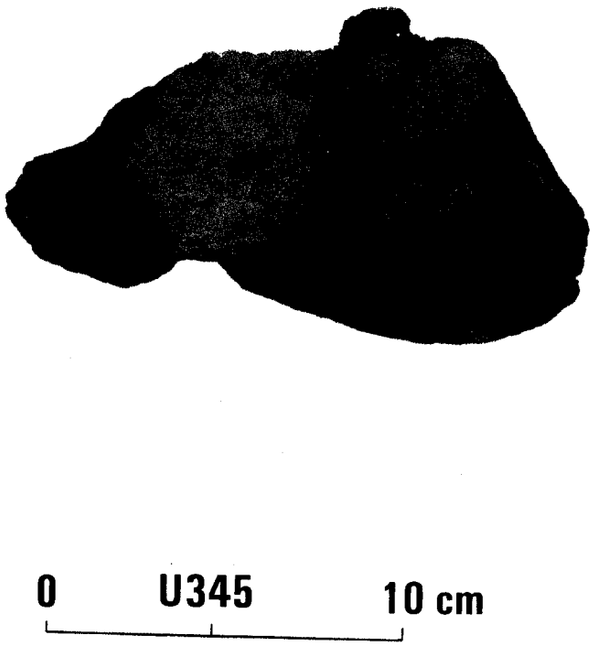

Figure 14. Stn U345 basalt cobble with dunite (light-colored) inclusion (Machias Seamount slope, depth 1972-2166 m).

substrate for crusts at Stns U314 and U316b (Rakahanga), Stn 322b (Manihiki Island) and Stn U326 (Pukapuka). Similar tuff without crusts occurs at Stn U327 (Pukapuka) in association with nodules. Tuff in the form of an orange siltstone was also found at Stn U316b (Rakahanga). Tuff occurs at depths of 1278 m (Stn U332, Tema Reef) to 4816 m (Stn U328, abyssal hills west of Pukapuka). It appears to be more common along the margins of the Manihiki Plateau than on the slopes of Machias or Carpicorn Seamounts or Niue.

REFERENCES CITED

Bäcker, H., G.P. Glasby, and M.A. Meylan, 1976, Manganese nodules from the southwestern Pacific Basin: New Zealand Oceanographic Institute, Oceanographic Field Report No. 6, 88 p.

Brodie, J.W., 1965, Capricorn Seamount, south-west Pacific Ocean: Transactions of the Royal Society of New Zealand, Geology, v.3, p.151-158.

Clague, D.A., 1976, Petrology of basaltic and gabbroic rocks dredged from the Danger Island Troughs, Manihiki Plateau, *in* S.O. Schlanger, et al., eds., Initial reports of the Deep Sea Drilling Project, v. 33: U.S. Government Printing Office, Washington, D.C., p.891-914.

Cronan, D.S., R.A. Hodkinson, and S. Miller, 1991a, Manganese nodules in the EEZ's of island countries in the southwestern equatorial Pacific: Marine.Geology, v.98, p.425-435.

Cronan, D.S., R.A. Hodkinson, S. Miller, and L. Hong, 1991b, An evaluation of manganese nodules and cobalt-rich crusts in South Pacific exclusive economic zones - nodules and crusts in and adjacent to the EEZ of the Cook Islands (the Aitutaki-Jarvis transect): Marine Mining, v.10, p.1-28.

Exon, N.F., 1981, Manganese nodules in the Cook Islands region, southwest Pacific: South Pacific Marine Geological Notes, v.2(4), p. 47-65.

Exon, N.F., 1982, Offshore sediments, phosphorite and manganese nodules in the Samoan region, southwest Pacific: South Pacific Marine Geological Notes, v.2(7), p.103-120.

Exon, N.F., 1983, Manganese nodule deposits in the central Pacific Ocean and their variation with latitude: Marine Mining, v.4, p.79-107.

Glasby, G.P., 1978, Notes on the surface texture, internal structure and mineralogy of manganese nodules from the south Penrhyn Basin: South Pacific Marine Geological Notes, v.1(7), p.71-80.

Heezen, B.C., B. Glass, and H.W. Menard, 1966, The Manihiki Plateau: Deep-Sea Research, v.13, p.445-458.

Landmesser, C., L.W. Kroenke, G.P. Glasby, G.H. Sawtell, S. Kingan, E. Utanga, A. Utanga, and G. Cowan, 1976, Manganese nodules from the South Penrhyn Basin, south-west Pacific: South Pacific Marine Geological Notes, v.1(3), p.17-39.

Meylan, M.A., 1974, Field description and classification of manganese nodules, *in* J. E. Andrews, et al., Ferromanganese deposits of the ocean floor, Cruise Report Mn-74-01, R/V *Moana Wave*: Hawaii Institute of Geophysics Report, No. HIG-74-9, p.158-168.

Meylan, M.A., G.P. Glasby, P.J. Hill, B.C. McKelvey, P. Walter, and P. Stoffers, 1990, Manganese crusts and nodules from the Manihiki Plateau and adjacent areas: Results of HMNZS *Tui* cruises: Marine Mining, v.9, p.43-72.

Meylan, M.A., G.P. Glasby, J.C. McDougall, and S.C. Kumbalek, 1982, Lithology, colour, mineralogy, and geochemistry of marine sediments from the Southwestern Pacific and Samoan Basins: New Zealand Journal of Geology and Geophysics, v.25, p.437-458.

Meylan, M.A., G.P. Glasby, J.C. McDougall, and R.J. Singleton, 1978, Manganese nodules and associated sediments from the Samoan Basin and Passage: New Zealand Oceanographic Institution, Oceanographic Field Report, No. 11, 61 p.

Piper, D.Z., T.R. Swint, and L.G. Sullivan, 1985, Manganese nodule abundance, *in* Manganese nodules, seafloor sediment, and sedimentation rates of the circum-Pacific region: American Association of Petroleum Geologists, scale 1:17,000,000.

Skornyakova, N.S., I.O. Murdmaa, S.G. Krasnov, and T.Yu. Uspenskaya, 1990, Ferromanganese nodules of the southwestern Pacific: Results of Soviet investigations: New Zealand Journal of Geology and Geophysics, v.33, p.419-437.

Usui, A., A. Nishimura, and N. Mita, 1993, Composition and growth history of surficial and buried manganese nodules in the Penrhyn Basin, southwestern Pacific: Marine Geology, v.114, p.133-153.

Winterer, E.L., P.F. Lonsdale, J.L. Mathews, and B.R. Rosendahl, 1974, Structure and acoustic stratigraphy of the Manihiki Plateau: Deep-Sea Research, v.21, p.793-814.

APPENDIX A
NODULE DESCRIPTIONS

Stn	Morphology	Surface texture	Internal structure/ nucleus	Comments
U295	Spheroidal.	Smooth appearance, but consists of very tiny rough microbotryoids.	Not examined.	—
U296a	Dominantly spheroidal, most faceted to some degree. Largest is tabular ellipsoidal. Numerous polynucleate.	Upper surface microbotryoidal; lower surface also microbotryoidal but feels more gritty due to higher relief of the microbotryoids.	Accreted layer may be only 1 mm thick. Original nucleus completely to nearly completely replaced by Mn-oxides. Many smaller nodules show septarian-like fracture pattern on surface.	14% of <20 mm nodules are polynucleate; an additional several % appear to have shark tooth nuclei. 8% of 20-40 mm nodules are polynucleate; an additional several % appear to have shark tooth nuclei.
U298	Largest basically spheroidal. Smaller ones include half-spheroidal, an ellipsoidal and more irregular shapes. Three largest spheroidal nodules have satellite protrusions.	Gritty (rough) to microbotryoidal.	Largest appear to have thin (ca. 1 mm) accreted layer. Small nodules of local facies have surface cracks that extend into nodule for 1-2 mm.	Apparently two nodule facies present — one regional (similar to that described by Meylan (1978) as belonging to the Cook Island Facies) and one local; nodules of the latter are characterized by cracks extending to the nodule surfaces.
U299a	Spheroidal; faceted, particularly the smallest nodule which may be a thickly encrusted shark tooth.	Gritty (rough) to microbotryoidal.	Accreted layer ca. 1 mm thick.	—
U300	Polynucleate, spheroidal, ellipsoidal. Most spheroidal nodules and polynucleate segments are faceted or lobed.	Smooth to slightly gritty; microbotryoidal in recesses.	Mn-oxide crust mostly 3-5 mm thick. Nucleus buff to orange fine- grained volcaniclastics.	Developed whitish cast after drying, probably indicating that the nodules rested on calcareous sediment. Nodules fragile, many broken during recovery process; accurate counting or sizing not possible.
U321a	Largest are tabular with irregular outlines, essentially flat on bottom with raised margins on top. Smaller ones are mainly	Larger ones are botryoidal on top and microbotryoidal on bottom; the tops with botryoids have superimposed microbotryoids. Smaller	Accreted layer about 2 mm thick. Nucleus appears to be replaced volcanic material.	Unusually large number of tiny nodules, most probably thinly encrusted or stained volcanic cinders.

Stn	Morphology	Surface texture	Internal structure/ nucleus	Comments
	spheroidal, ellipsoidal or polynucleate. Many are faceted, lobed or irregular in outline. Difficult to differentiate some polynucleate nodules from lobed ellipsoidal nodules.	nodules have rough microbotryoidal surfaces. All sizes are made rougher in places by recently adhered angular volcaniclastic grains.		
U325	Tabular, with elongated discoidal and "lumpy" shape modification.	Smooth (but microbotryoidal viewed with hand lens).	Accreted layer apparently ca. 2 mm thick.	Because this nodule appears so out of place in terms of setting, it may have been lodged in the dredge at an earlier station.
U327	Larger (> 30 mm max. diam.) nodules mostly tabular or ellipsoidal; one polynucleate and a few faceted spheroidal; lobes and facets common on others. Tabular nodules have irregular outlines, and one has a curled rim. Smaller (< 30 mm max. diam.) mostly spheroidal (lobed or faceted) or lobed ellipsoids. There are numerous irregular forms but surprisingly few polynucleate nodules or nodules with shark tooth nuclei.	Botryoidal or smooth with readily visible microbotryoids.	Accreted layer varies from stain on faceted small fine-grained nuclei (carbonate or volcanic?) to about 2 mm on similar nuclei or vesicular weathered volcanics or fine-grained volcaniclastic sandstone, the latter probably most common.	Stained rocks (all small, faceted) counted as nodules because of difficulty in separating them from other small nodules — may be as many as a few dozen. Must have formed later than nodules with 2 mm crusts.
U328	Polynucleate (or bilobed ellipsoidal).	Smooth (only a very slight gritty feel).	Not examined.	—
U339	Larger nodules mostly polynucleate, with some ellipsoidal. Smaller ones mostly spheroidal, many lobed or faceted; many polynucleate or ellipsoidal, latter often lobed or faceted. However, few nodules < 20 mm max. diam. are polynucleate, and none has a shark tooth nucleus; many of these smallest nodules have irregular shapes.	Small nodules smooth, but microbotryoidal viewed with hand lens. Medium nodules similar, but microbotryoids somewhat coarser, especially in recesses.	Accreted layer is microlaminated and mostly 3-5 mm thick. Nucleus volcaniclastic — yellow fine-grained ash(?) and reddish brown to orange vesicular material (palagonite?).	Nodule types listed above for 20-40 mm template size do not include one rod-shaped nodule, which has the greatest max. diam. of any of the nodules. Irregularly-shaped small nodules are apparently encrusted nodule fragments. Most medium-size nodules are only slightly over 30 mm max. diam.

Stn	Morphology	Surface texture	Internal structure/ nucleus	Comments
U340	Smaller and intermediate size nodules almost all polynucleate, with a few faceted and/or lobed spheroidals and ellipsoidals. The very smallest ones (ca. 5 mm max. diam.) are almost all spheroidal. The largest nodules are mostly lumpy and tabular with irregular outlines.	Larger nodules botryoidal (lumpy). Smaller nodules appear smooth, but have a bit of a gritty feel, and are microbotryoidal as seen with a hand lens.	Accreted layer is microlaminated and mostly 2-3 mm thick. Nucleus is volcanic — either palagonite or fine-grained tuff. Few shark tooth nuclei, but several teeth adhere to outer surface of nodules.	These are fracture-resistant nodules — almost none broken during recovery! An unusually large number of very small rounded nodules.
U353	Polynucleate (or bilobed ellipsoidal).	Smooth (only a very slight gritty feel).	Accreted layer appears to be about 1 mm thick.	—

APPENDIX B
CRUST DESCRIPTIONS

Stn	Surface texture	Internal structure	Substrate type	Substrate description
U298[1]	Microbotryoidal.	Black, vitreous, conchoidally-fractured concentric layers.	Not recovered.	—
U299b	Smooth to gritty to microbotryoidal.	Largest has three layers: Outer and inner have radial columnar structure (microbotryoids in cross-section), with yellowish brown to brown material (foram ooze? partly replaced by Mn-oxides) between the columns. Middle layer is more vitreous, with flat thin laminations, and shows conchoidal fracturing.	Not recovered.	—
U308b	Smooth to microbotryoidal; however, thickest crust appears to be cavernous botryoidal.	Massive where visible; irregular growths extend downward into substrate.	(1) Calcareous feldspar sandstone/ feldspathic calcarenite. (2) Tuff.	(1) Light grayish orange to reddish orange; grains mostly fine to very fine sand size. (2) Gray to light brownish gray; grains silt to fine sand size.
U314	Botryoids with superimposed microbotryoids. Abundant benthic foram tubes; dusting of foram ooze.	None visible.	Volcaniclastic sandstone.	Overall color light yellowish olive green with included reddish brown and dark brown to black grains. Bedded (beds 15-40 mm thick); only lowermost bed examined closely. Coarse-grained, principally volcanic glass fragments; weathered feldspar(?)-bearing.
U315	Cavernous botryoidal.	Radial columnar, with trapped reddish-brown sediment (foram tests?) between columns.	Foraminiferal limestone.	White to light reddish brown; well indurated; penetrated by burrows and Mn-dendrites.
U316b[2]	Microbotryoidal and botryoidal with superimposed microbotryoids.	Radial columnar, with trapped reddish-brown sediment (foram tests?) between columns.	Volcaniclastic sandstone.	Light yellowish olive green; fine-grained.

Stn	Surface texture	Internal structure	Substrate type	Substrate description
U319[3]	Microbotryoidal.	Radial columnar, with trapped reddish-brown sediment (foram tests?) between columns.	Not recovered.	—
U322b	(1) Irregularly developed botryoids with superimposed microbotryoids.	(1) Not visible.	(1) Foram ooze chunks.	(1) Very light gray; soft, loosely consolidated. Burrowed beneath Mn crust.
	(2) Partly smooth, partly botryoidal.	(2) Thinly laminated to microbotryoidal.	(2) Volcaniclastic sandstone and basalt	(2) Substrate core is dark gray, very fine-grained basalt; this is partly encased in a layer of volcaniclastic sandstone which includes some coarser grains up to 9 mm. Grains mostly yellow, gray, orange, brown; lighter-colored ones appear weathered. Although some grains appear to be feldspar, the grain mineralogy/ lithology is visually mostly indeterminate.
U326	(1) Microbotryoidal.	(1) Not visible.	(la) Volcaniclastic sand.	(la) yellowish olive green with reddish brown patches; coarse-grained.
			(lb) Vesicular basalt(?)	(lb) gray with reddish brown altered small phenocrysts.
			(lc) Carbonate.	(lc) foraminiferal limestone(?)
	(2) Smooth microbotryoidal (looks scaly with hand lens).	(2) Appears massive — may be thin recent encrustation on older crust fragment — but faint indication of radial columnar with trapped sediment between columns.	(2) Not recovered.	(2) —
U332	(1) Smooth microbotryoidal.	(1) Not visible.	(1) Foraminiferal limestone(?)	(1) Light gray to light yellow; burrowed so appearance is coarsely vesicular; if limestone, is partly recrystallized.
	(2) Microbotryoidal.	(2) Not visible.	(2) Porphyritic vesicular basalt.	(2) Dark gray brown matrix; phenocrysts weathered to orange-brown color; vesicles up to 1 mm diam.

Stn	Surface texture	Internal structure	Substrate type	Substrate description
	(3) Smooth.	(3) Massive outer layer; radial columnar (with trapped sediment?)	(3) Not recovered.	(3) —
U333b	Rough (scoriaceous); largest frag. has branching coral on surface.	Massive or radial columnar with sediment trapped between the columns. Largest frag. is layered, with latter structure type sandwiched between inner and outer massive layers.	Unknown.	Reddish brown; may be weathered volcaniclastite or phosphorite.
U336b	Cavernous botryoidal with gritty surface due to superimposed microbotryoids. Forams trapped between botryoids.	Outer part (which is thickest) is massive; inner section is radial columnar with sediment trapped between the columns.	Coral(?)	White to yellowish brown; weathered and burrowed. No fresh substrate recovered.
U357	Microbotryoidal.	Radial columnar.	Clayey silty sand.	Grayish olive green semi-consolidated fine-grained sand with probable major silt and clay content. Mineralogy indeterminate — probably an altered volcaniclastite. Substrate portion of frags rounded, probably during dredging. 3 crust frags lack sediment substrate; 9 sediment lumps with crust; 5 sediment lumps without crust.
U358	Microbotryoidal (but smooth on some corners).	Not visible.	Coral/coral boundstone.	White to light yellow; reddish brown to black where stained or encrusted with manganese oxides. Weathered, mostly recrystallized coralline limestone; coral structure completely obliterated in patches. Burrowed just beneath surface. Most crust frags have some adhering substrate; in addition to crust frags there are 3 substrate frags essentially lacking crusts, 24-95 mm max. diam.
U361	Botryoidal with superimposed microbotryoids.	Not readily visible; appears massive.	Volcaniclastic sand(?)	Yellowish brown to reddish brown altered volcaniclastic sand (?). One rock frag. lacking a crust (Mn-stained only) appears to be a finely laminated altered tuff, 7 mm thick.

Stn	Surface texture	Internal structure	Substrate type	Substrate description
U363	Microbotryoidal to botryoidal.	Not readily visible; appears massive.	(1) Vesicular basalt. (2) Volcaniclastic sand(?)	(1)Gray to black with reddish brown vesicle in-fillings. Apparent gradation from nearly fresh vesicular basalt to Mn-stained to Mn-replaced. Largest crust frag. has altered vesicular basalt substrate. (2)Light gray to yellowish brown to reddish brown. Thickest crust has accreted to this substrate type.
U367	Microbotryoidal clumps with deep recesses between clumps; surface feels rough.	Not readily visible; appears massive.	Basalt(?)	Appears aphanitic, glassy; gray to black. Mn-encrustation on all sides of subangular cobble. Numerous globular foram tests trapped in recesses between clumps of microbotryoidal Mn-oxide. Cluster of 0.5 mm-diam. "worm" tubes in 15 x 50 mm area along side of cobble.
U369	Clumps of microbotryoids separated by deep recesses.	Not readily visible.	(1) Calcarenite (foraminiferal limestone). (2) Volcaniclastic sand (?)	(1) White; friable. 20 frags, 8-26 mm max. diam. (2)Light yellowish brown; soft. Appears highly altered; grain size not readily apparent. 15 frags, 7-37 mm max. diam.
U375	Microbotryoidal.	Microbotryoidal (as seen by hand lens); macroscopically appears massive.	Not recovered.	Largest frag has identifiable top and bottom surfaces (based on visible organic growths). May represent volcanic rock essentially completely replaced by Mn-oxides.

[1] Smaller fragment may be a nodule rather than a crust.
[2] Thinner encrustations also occur on scoria and coral; see Rocks.
[3] May have been wedged in dredge during previous use (Stn 316b).

APPENDIX C
ROCK DESCRIPTIONS

Stn	Rock Type	Description	Mn-Encrustation
U292	(1) Coral (2) Foram limestone (biomicrite)	(1) Very pale orange. Bored, rounded. (2) Very pale orange. Rounded.	(1, 2) None.
U294	Pumice	Very light gray. Subround.	None.
U298	Scoria (basaltic)	Variously colored shades of gray, brown, yellow, and red. Irregular shapes, most with rounded corners. Frags easily broken.	A few partial thin (<1 mm) crusts.
U307	Foraminiferal(?) limestone	Very light orangish white, possibly with fine sand-size volcanic grains, and with interpenetrating Mn dendrites. Fragile.	<< 1 mm (essentially a thick stain with a smooth surface that appears microbotryoidal with hand lens); covers about 90% of substrate surface.
U308a	Limestone (lithified foram ooze)	Very light gray. Forams indistinct, giving oolitic appearance.	<< 1 mm (essentially a thick stain); appears smooth, but microbotryoidal when viewed with hand lens.
U308b	(1) Feldspathic volcaniclastic sandstone (2) Volcaniclastics (mostly tuff, but also one pumice)	(1) Light grayish orange to reddish orange. Grains mostly fine to very fine sand size. Pebbles angular to well rounded. (2) Gray to light brownish gray. Tuff particles silt to fine sand size. Most have very little Mn-encrustation. Pebbles mostly subrounded to well rounded.	(1, 2) Absent to << 1 mm; coverage up to nearly 100% of rock, but most rocks have little or no stain. Surface appears smooth, but smooth to microbotryoidal viewed with hand lens.
U316b	(1) Volcaniclastics (pumice, scoria, tuff, basalt) (2) Coral/ coral boundstone (3) Foram(?) limestone (4) Garnet crystal	(1) Pumice mostly gray brown, rounded. Scoria a variety of colors, mostly angular frags. Two largest are rounded pebbles of orange tuff siltstone. (2) Irregularly shaped frags, little rounding. All highly altered. (3) Chalky white pebble, rounded. (4) --	(1-4) Partial Mn-stain on some volcaniclastics, on a few coral, and a nearly complete stain on the foram limestone(?).
U317	(1) Coral/ coral boundstone (2) Breccia	(1) Very light gray to white. Several species of coral. Angular to rounded. Minor dissolution. A few have attached small sponges. (2) Very light gray carbonate in yellowish olive green volcaniclastic matrix.	(1-4) Two rounded coral pebbles have nearly complete staining. Many additional pebbles have patchy Mn staining, brown to black.

Stn	Rock Type	Description	Mn-Encrustation
	(3) Volcaniclastic sandstone	(3) Reddish brown to vitreous black coarse sand-sized frags in light greenish-gray matrix of finer sand-sized tuff(?).	
	(4) Chert(?)	(4) Very light brownish gray. Angular.	
U318	Foram ooze lumps	Very light gray, soft and friable, burrowed.	Stain, partial.
U319	Coral	White to very light gray, angular to rounded, well indurated.	Minor partial staining on two frags.
U321a	Scoria (basaltic), pumice	Dark reddish brown. Largest frag. is light brownish gray subrounded pumice pebble.	None.
U322b	Foram limestone	Brown to gray. Angular. Moderately to highly recrystallized.	Partial Mn-staining.
U323	(1) Coral	(1) White to very light gray, angular to rounded. Moderately to highly recrystallized.	(1) Complete stain on one coral frag., partial on others.
	(2) Volcaniclastic sandstone and basalt	(2) Gray to brownish olive green, angular to rounded.	(2) None.
U324	(1) Coral/ coral boundstone	(1) White to very light gray. Robust coral species, incl. branching, mostly rounded and showing some dissolution. Largest boundstone boulders, cobbles are 490, 300, 265, 240, 235, and 180 mm max. diam. Smaller material generally individual coral frags.	(1-3) Slight brown to black stain on a few coral rubble frags; calcarenite has appreciable Mn-stain. Reddish staining due to iron oxides?
	(2) Encrusting algae and algal plates	(2) White to very light gray. Plates thin and fragile. Encrusting material covers areas up to 10's of mm across.	
	(3) Calcarenite	(3) —	
U325	(1) Coral (Mn-stained)	(1) White to very light gray. Axial diam. up to 20 mm. Essentially only gorgonian coral. Dense, recrystallized? Includes many bases. 200+ frags, up to 225 mm max. diam.	(1) Thin to thick nearly complete stain (<< 1 mm thick) with microbotryoidal surface on many branching coral pieces.
	(2) Coral (no stain)	(2) White to very light gray. Axial diam. up to 20 mm. Essentially only gorgonian coral. Dense, recrystallized? Includes many bases. 200+ frags, up to 240 mm max. diam.	(2) None.
U326	Pumice	Light yellowish brown. Subrounded.	Slight staining in recesses.
U327	Volcaniclastic sand	Layer of light yellowish olive green coarse tuff attached to thin layer of light grayish brown finer-grained material, probably fine tuff.	Mn-stained.

Stn	Rock Type	Description	Mn-Encrustation
U328	(1) Scoria, volcaniclastic sandstone, pumice (2) Coral, foraminiferal limestone	(1) Scoria pebbles larger than volcaniclastic sandstone pebbles and granules. (2) White. Coral is weathered.	(1) Stained. (2) None.
U329	Coral	Very light gray to white. Angular. Moderate recrystallization.	Stain on surface that was probably exposed on seafloor; white surfaces may be fresh fracture surfaces.
U331	Coral/ coral boundstone	Several species of robust coral. Includes fresh frags with little dissolution or rounding as well as more weathered rubble. Numerous borings, most notably in largest piece. Most pieces in pebble-size range, esp. 10-50 mm. Many small pieces well rounded.	Brown discoloration to black stain on most frags; coverage partial on some, complete on others.
U332	(1) Branching coral (gorgonian?) (2) Carbonate (mostly coral?) (3) Carbonate (foram limestone or oolite?) (4) Vesicular basalt (5) Breccia (volcanic?) (6) Volcaniclastic sandstone	(1) Most with some borings. 32 frags, 7.5-40 mm max. diam. (2)White to light gray; yellow and orange stains in addition to black Mn-stains. Appears to be mostly weathered coral, recrystallized, burrowed and algal encrusted to give scoriaceous aspect. Includes a few fresh coral frags. 68 pieces, 9-31 mm max. diam. (3) Red and yellow. Apparently partly recrystallized. 1 frag., 16 mm max. diam. (4) Dark gray; angular to subrounded; finely vesicular. (5) Greenish gray to brownish green. Clasts mostly 2-6 mm. (6) Yellowish olive green; rounded; fine-grained. (1-3) Partial to nearly complete brown to black	stain on coral/ carbonate (<< 1 mm). Where stain is thickest on branching coral, it is smooth to finely microbotryoidal as seen with hand lens. (4-6) None.
U333b	Coral	"Soft", chalky, dense! White. Outer concentric thin shell easily broken off. Gorgonian, axial diam. mostly 20-30 mm.	Some frags with black Mn-stain (<< 1 mm; smooth) over most of surface, others with none.
U334	Coral	Very light yellow to yellow brown; weathered (partly recrystallized). Subangular.	None.
U335a	(1) Coral (2) Vesicular basalt with carbonate encrustation	(1) White to light grayish brown; rounded discoidal shape; weathered/ recrystallized. (2) Light to dark gray brown; subrounded; finely vesicular. Grayish orange encrustation (coral?), with superimposed white carbonate encrustation (algal?).	(1) Brown discoloration and 0.5 mm black Mn-stain spots, latter widely scattered, on coral. (2) None.

Stn	Rock Type	Description	Mn-Encrustation
U337	(1) Coral/ coral boundstone	(1) White to very light gray. Several robust species, commonly bored. Many frags nearly fresh with little physical wear or dissolution, but most show some weathering, and many are rounded. Common algal encrustations and growths. Largest 730 x 615 x 250 mm; several others of boulder size.	(1) Only a small percent have Mn-stain, which is mostly brown and partial, few black.
	(2) Chert nodule	(2) Very light brown; round.	(2) None.
U339	Pumice	Light brownish gray. Rounded.	None.
U340	(1) Pumice	(1) Light brownish gray; rounded.	(1, 2) None.
	(2) Scoria	(2) Light reddish brown; subround.	
U341b	(1) Altered tuff	(1) Grayish olive green. Friable, soft. Appears to be a mixture of fine sand-size ash and smectitic(?) clay alteration product of the ash. Contains small rounded pumice(?) granules, pebbles, as well as amphibole (and other femag?) crystals. One piece (70 mm long) is better indurated and has a brownish tinge. Several other pieces (20-70 mm) are also relatively well indurated. A few friable pieces are yellowish olive green. A few of the better indurated ones show sedimentary slickensides. Largest frag. 230 x 190 x 85 mm.	(1-5) Minor to nearly complete brown discoloration or black Mn-stain (<< 1 mm) on coral; partial dark brown to black Mn-stain on altered tuff frags, scoria/ basalt.
	(2) Coral	(2) White to light gray. Rounded to angular; some pieces recrystallized. Several species. Largest piece 150 x 120 x 80 mm.	
	(3) Vesicular scoria	(3) Grayish olive green to black, mostly subangular.	
	(4) Basalt	(4) Dark greenish gray to gray, mostly angular but a few pieces rounded. Patches of vesicles.	
	(5) Marly coquina (shell hash limestone/ calcarenite)	(5)Gray to greenish gray, poorly indurated. Marly appearance. Consists mostly of shell frags. < 2 mm, but some > 10 mm; includes variable proportions of volcaniclastic grains and clay.	
U342	(a) Coral/ coral boundstone	(a) White to very light gray. Moderate dissolution/ recrystallization. Some separate pieces of coral are rounded.	Patchy partial Mn-stains (<< 1 mm), especially in recesses on coral.
	on		
	(b) Encrusting algae(?)	(b) White to very light gray. Constitutes a wavy layer ca. 10 mm thick; some pieces have calcarenite interlaminae.	
	on		

Stn	Rock Type	Description	Mn-Encrustation
	(c) Calcarenite	(c) Gray. Varies from fine-grained and chalky to a coarser sand size. Burrowed near top. Some pieces lack superimposed layers and have Mn-stain instead.	
U343	(1) Coral/ coral boundstone	(1) White to very light gray to very light brown. Some light yellow to orange iron-staining. Some smaller pieces rounded; some pieces show moderate dissolution and recrystallization, while in others it is quite pronounced. Weathered frags may include algal encrustation.	(1) None.
	(2) Calcarenite limestone	(2)Light gray to gray with orange iron-staining. Some pieces friable. Some pieces may be highly weathered coral with calcarenite in-filling. About 10-15% dark (volcanic?) sand grains. Some pieces contain larger shell frags.	(2) Many partial Mn-stains (<< 1 mm); with microbotryoidal surface where thickest, on calcarenite limestone.
	(3) Volcanic ash lumps	(3)Brownish gray. Soft, friable, rounded. Fine-grained sand with silt and clay. About 10% shell frags, including turriform gastropods.	(3) None.
U344	(1) Pumice	(1) Gray with partial light yellow staining. Subangular.	(1, 2) None.
	(2) Coral (gorgonian?)	(2) Very light yellow to yellowish gray. Bored, highly weathered. Tabular/ discoidal, rounded except where freshly fractured.	
U345	(1) Coral/coral boundstone (including gorgonian?)	(1) White to very light gray to very light yellowish gray. Minor weathering/dissolution, but some pieces more weathered than others, and can be termed highly weathered. Borings, algal encrustations present. One frag. that is 54 mm max. diam. appears to be highly weathered coral on wavy algal substrate on volcanic sand-bearing calcarenite.	(1-2) Partial black Mn-stain (< 1 mm thick; microbotryoidal surface in recesses), most noticeable on coral.
	(2) Coquina	(2) White grains with light yellowish gray grains with black grains. Coarse sand/granule coquina with smaller volcanic(?) sand grains.	
	(3) Basalt	(3) Dark gray to black. Angular to very well rounded. Little apparent weathering/alteration. Dominantly aphanitic, with a few pieces vesicular or porphyritic. Largest specimen has 30 x 60 mm blocky dunite inclusion. One piece has adhering gray soft calcareous sediment, 5 mm thick.	(3) Negligible Mn-staining.
	(4) Volcanic ash lump	(4) Brown; rounded; fine grained.	(4) Partial stain.

Stn	Rock Type	Description	Mn-Encrustation
U346	(1) Basalt	(1) Gray to very dark gray. Two pebbles with reddish hue. Angular to very well rounded, with large proportion being smooth and round like river or beach gravel. Most appear relatively fresh; even some olivine grains are unweathered, although most olivine phenocrysts have been altered. Mostly aphanitic; about 35-40% vesicular; some porphyritic with amphibole phenocrysts. A few vesicles have mineral filling. Small % scoria.	(1) Minor staining, but largest piece completely stained above sediment-water interface.
	(2) Ultramafic nodule	(2) Black; rounded; weathered olivine phenocrysts.	(2) None.
	(3) Pumice	(3) Grayish brown; rounded.	(3) Nearly complete stain.
	(4) Tuff	(4) Gray. Silt- and fine sand-sized volcaniclastic grains. One with incorporated shell frags.	(4) None.
	(5) Vuggy volcaniclastic	(5) Green, red and gray volcaniclastic grains. Light-colored mineral lining irregular cavities.	(5) None.
	(6) Breccia	(6) Gray framework grains, very light gray matrix. Looks like calcite-cemented fine-grained volcaniclastic rock frags.	(6) None.
	(7) Coral/coral boundstone	(7) White to very light gray to light yellowish gray. Angular to rounded. Abundant evidence of weathering/dissolution; also encrustations, some borings.	(7) Partial brown, black Mn-staining, especially on the larger pieces.
	(8) Calcarenite	(8) Very light yellowish brown. Friable. Mostly sand-size grains; has a few % dark (volcanic?) grains.	(8) None.
U348	Amygdaloidal basalt/welded tuff(?)	Matrix gray to dark orange-brown. Quite porous due to incompletely filled amygdules — filling is dog-tooth spar (calcite). Aphanitic basaltic matrix appears transitional with granular volcaniclastic that is also porous (welded tuff?). Angular frags.	None.
U349	Basalt breccia	Gray to very dark gray. Basalt framework clasts are aphanitic with few phenocrysts. Matrix is a light-colored vitreous mineral (zeolite?) that has cubic form, and incompletely fills space between framework clasts. Surface of matrix is weathered to olive green. Angular frag.	Partial stain with microbotryoidal surface.
U350	Coral/ coral boundstone	White to very light yellow brown. Quite highly weathered, i.e., shows considerable dissolution/ recrystallization so that original coral material is nearly obscured.	Partial stain on largest frag.; surface microbotryoidal in some recesses.
U351a	Pumice	Light grayish brown to grayish brown to brownish olive gray. Rounded to well rounded, except for a few angular frags possibly broken during recovery. One smaller pebble may be tuff or basalt.	None.
U351b	Pumice	Similar to that recovered at Stn U351a; sample not retained.	None.

Stn	Rock Type	Description	Mn-Encrustation
U352	(1) Coral/coral boundstone	(1) White to very light gray to very light yellow brown. Angular to rounded. All frags weathered — recrystallization slight to complete. Most pieces have barely discernible coral structure, some have obvious structure, and a few are fine-grained (completely recrystallized?). Some algal encrustation.	(1, 2) Two recrystallized limestone pebbles are nearly completely stained. Stain surface microbotryoidal in recesses where thicker.
	(2) Coquina	(2) White to very light gray. Subrounded. Smallest and largest have ca. 5% dark rock or mineral (volcanic?) grains; little in other pieces. Consist of a variety of organic carbonate material, recrystallized and well cemented. Some may be transitional with/ counted with recrystallized coral boundstone.	
	(3) Basalt (and other igneous rocks?)	(3) Light gray to very dark gray. Angular to well rounded. Mostly aphanitic, nonvesicular basalt. Some light gray to gray rocks may be andesitic. A few smaller pebbles are vesicular, including one that is also porphyritic, with well formed phenocrysts > 1 mm long. Larger frags appear to have inclusions of coarser-grained rock. One piece may be vuggy welded tuff.	(3) Partial minor stain (<< 1 mm) on some basalt pebbles.
U354	Coral	White to light grayish brown. Angular to subround. Mostly weathered/ recrystallized, but includes one fresher piece and one living coral on weathered substrate.	None.
U356	Coral/ coral boundstone	White to very light gray, with very light yellow to red brown to black Fe, Mn oxide staining. Mostly subrounded to rounded. Highly weathered/ recrystallized; coral structure all but completely obliterated. Moderately indurated, with friable surfaces where Mn-stain not present. Burrowed near surface.	Possibly up to 1 mm thick -- essentially a thick stain with some penetration into substrate. Surface microbotryoidal where most thickly developed. Coverage partial on large frags, absent to nearly complete on smaller ones.
U357	(1) Coral	(1) Very light pink; very light yellow to yellow to brown to black where stained by Fe, Mn oxides. Subround; very well indurated (silicified?). Structure of coral nearly obliterated by dissolution.	(1) Mn-stained; stain only on part of coral that protruded above sediment-water interface.
	(2) Vesicular basalt	(2) Black with light-colored fill in some vesicles (loose sediment). Vesicles about 1 mm diam. Nearly fresh, angular frag.	(2) None.
	(3) Pumice	(3) Grayish olive green. Subround.	(3) None.
U358	Coral/ coral boundstone	Same as substrate material for Stn U358 crusts; see Appendix B.	None on these frags.
U362	(1) Branching and platy coral	(1) Light gray coralline plates ca. 1-2 mm thick. Light gray to black branching coral, 8-12 mm diam., extensively burrowed.	(1) Thin partial stain (<< 1 mm).

Stn	Rock Type	Description	Mn-Encrustation
	(2) Algal-encrusted coral	(2) White to very light gray. Platy and branching coral, encrusted by algal growths and tiny tubular coral(?); recrystallized.	(2) None.
U366	Coral	Almost all gorgonian, diameter < 10 mm. Several small solitary scleractinian corals. Minor amount of borings.	Thin (<< 1 mm) but smooth and essentially complete black stain.
U369	Foraminiferal limestone	White; subrounded to rounded friable frags.	Thin partial stain (<< 1 mm); this rock type also serves as substrate for Mn-crusts (see Appendix B).
U370	(1) Coral	(1) White to light gray; relatively fresh to rounded and dissolution- reprecipitation altered. Some frags angular or algal-encrusted. Five recognizable genera.	(1-3) None (light gray surface discoloration may be first stage of staining).
	(2) Volcaniclastite(?)	(2) Dark yellowish gray; rounded. Vesicular, with hornblende(?) crystals up to 2 mm max. diam. in finer-grained tuff matrix.	
	(3) Basalt(?)	(3) Gray angular pebble, nearly completely algal encrusted. Hard, fine-grained.	
U371	(1) Coral/ coral boundstone	(1) White to light brownish gray; angular to rounded, with only one frag. reasonably fresh. Others obviously abrasion-rounded and/or altered by dissolution/ recrystallization. Some boring and algal encrustation.	(1-3) None.
	(2) Bioclastic and tuffaceous(?) sandy coral and basalt-pebble conglomerate	(2) Light brownish gray matrix with light gray to black pebbles. Matrix appears to be a combination of small shells and shell frags with ash. Pebbles (up to 28 mm max. diam.) consist of worn and altered coral as well as more angular vesicular or fine-grained basalt. A single 29-mm pebble of coarse bioclastic sandstone is included with this rock type.	
	(3) Vesicular basalt	(3) Very dark brown to black. Glassy and highly vesicular, some resembling scoria. Frags angular to subrounded.	
U372	Coral	Light reddish gray to light yellowish gray. Irregularly shaped with rounded corners. Incorporated black coarse basalt sand grains. Coralline material highly altered by dissolution/ recrystallization.	None.

Stn	Rock Type	Description	Mn-Encrustation
U375	(1) Vesicular basalt	(1) Very dark red to black. One piece (17 mm) light gray, rounded. Fresher frags angular, more altered frags rounder. "Alteration" includes vesicle filling with sediment or Mn-oxides and smoothing of exposed vesicle margins; frags slightly friable. Vesicles mostly 1-2 mm diam. Assoc. with numerous garnet crystals, one about 18 mm across.	(1) Thin (< 1 mm) stains, vesicle fillings and replacement(?)
	(2) Coral/coral boundstone	(2) White to light grayish brown. Angular to rounded frags. Very few pieces fresh. Most show some degree of dissolution/ recrystallization in addition to abrasion of corners. Several genera of scleractinian corals. Some algal encrustation, boring.	(2) Thin (<< 1 mm) stains on a very few frags, which are either gorgonians, solitary scleractinians, or highly bored rubble.
	(3) Volcaniclastic sandstone(?)	(3) Grayish brown or black. Subrounded to rounded. Largest piece consists of coarse to very coarse sand-sized grains. Smaller pieces consist of finer sand-sized grains.	(3) Smallest and largest frags completely stained; none on other three.
U376	(1) Vesicular basalt, friable	(1) Very dark gray with intermingled white grains. Very friable; appears to be highly weathered glassy(?) vesicular basalt. Incorporated white grains probably carbonate. About 50 pieces, up to 58 mm max. diam.	(1) Apparently Mn-stained and impregnated.
	(2) Vesicular basalt, hard	(2) Light gray to light brownish gray. Angular. Includes a few small garnet(?) crystals. 1 piece, 21 mm max. diam.	(2) Very slight gray discoloration.
	(3) Coral	(3) Light gray. Tabular and rounded branching forms, mostly highly altered by dissolution/ recrystallization.	(3) Very slight gray discoloration.
	(4) Medium volcaniclastic sandstone(?)	(4) Yellowish brown with black Mn-stain. Friable; subangular. Consists of medium sand-sized altered tuff(?) grains. 1 piece, 17 mm max. diam.	(4) Thin (<< 1 mm) stain.
	(5) Fine volcaniclastic sandstone(?)	(5) Greenish gray; frags mostly rounded to subrounded and soft. Consists of fine sand-sized altered tuff(?) grains. 13 pieces, 15-40 mm max. diam.	(5) Thin (Up to 1 mm) botryoidal crust.
	(6) Volcaniclastic calcarenite(?)	(6) Light reddish gray. Subangular frag., quite well indurated. Appears to consist of subordinate black volcaniclastic sand and dominant carbonate(?) sand grains, euhedral crystals, and matrix.	(6) None.

Stn	Rock Type	Description	Mn-Encrustation
U377	(1) Coarsely vesicular basalt, fresh	(1) Dark gray to black. Angular, hard, apparently fresh frags. Vesicles mostly 2-4 mm diam. 45 pieces, 13-92 mm max. diam.	(1) Thin (<< 1 mm) stain.
	(2) Finely vesicular basalt	(2) Gray. One quadrant of rounded ellipsoidal pebble. Vesicles mostly < 1 mm diam. Most vesicles lined with fine-grained greenish-gray material. 1 piece, 21 mm max. diam.	(2) Possible thin (<< 1 mm) stain.
	(3) Vesicular basalt(?), altered (but may be phosphorite)	(3) Light gray to dark grayish brown. irregularly shaped frags with rounded corners. Alteration principally takes form of thin calcite(?) encrustation and lining of vesicles. 2 pieces, 36 and 78 mm max. diam.	(3) Possible thin (<< 1 mm) stain.
	(4) Coral/ coral boundstone	(4) White to very light yellow. Angular to rounded frags, the more rounded ones tending to show higher degree of alteration by dissolution/ recrystallization. Several genera represented.	(4) Thin (<< 1 mm) stain as partial coverage on a few frags only.
U378	(1) Coral/ coral boundstone	(1) White. Angular frags. All quite highly altered by dissolution/ recrystallization.	(1) Thin (<< 1 mm) partial stain on a few frags.
	(2) Pumice	(2) Very light gray (fresh) to gray (outer surface). Rounded.	(2) Slight partial discoloration.

)stwald, J. 1996. Mineralogical, geochemical and textural investigations on nanganese nodules from the Manihiki Plateau area, *in:* Meylan, M.A., and G.P. Jlasby (eds) Manihiki Plateau, Machias and Capricorn Seamounts, Niue, and rofua Trough: Results of TIli Cruises. SOP AC Technical Bulletin 10: 99-107.

MINERALOGICAL, GEOCHEMICAL AND TEXTURAL INVESTIGATIONS ON MANGANESE NODULES FROM THE MANIHIKI PLATEAU AREA

J. Ostwald

Broken Hill Proprietary Co. Ltd, Central Research Laboratories, PO Box 188, Wallsend, NSW, Australia

ABSTRACT

Manganese nodules from the Manihiki Plateau area are composed predominantly of ferruginous vernadite of hydrogenous origin developed on cores of feldspar, clay, phillipsite and quartz. Minor amounts of todorokite occur in some nodules. The nodules are low in Cu+ Ni +Co when compared with nodules from the Pacific 'ore zone'. Texturally, they are composed of radial columns of ferruginous vernadite with occasional interlaminations of todorokite; phillipsite commonly occurs in cavities between the columns.

INTRODUCTION

This paper describes mineralogical and petrological examinations carried out on six manganese nodules from the Manihiki Plateau. Techniques used included (1) reflected light microscopy, (2) scanning electron microscopy (SEM), (3) electron probe microanalysis (EPMA), (4) X-ray diffraction (XRD), and (5) Fourier Transform Infra-Red spectroscopy (FTIR). Specimens examined came from stations U296a, U300, U321a, U327, U339 and U340. A description of these nodules is given in Meylan and Glasby (this volume).

SPECIMEN DESCRIPTIONS

The general morphology of the specimens is indicated by Figure 1, which

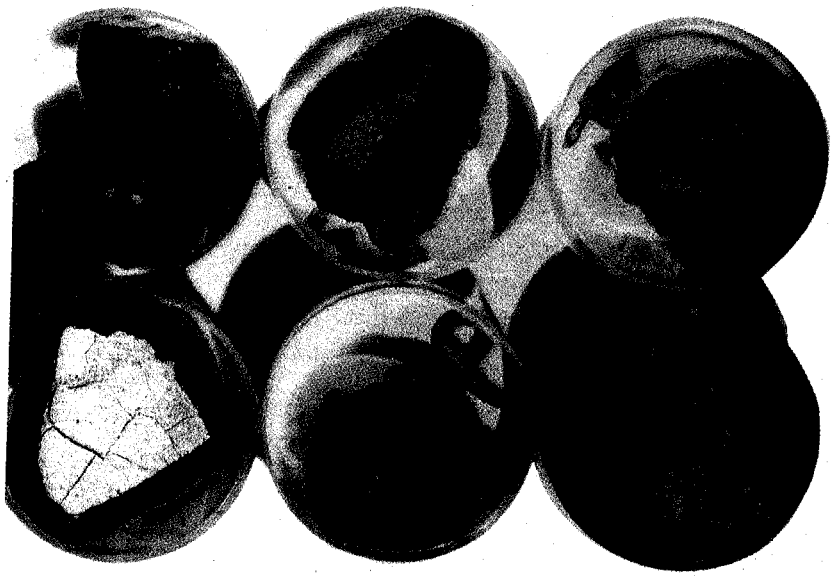

Figure 1. Photograph showing polished sections of nodules. Top row, left to right: U296a fragment, U300, U321a. Bottom row, left to right: U327, U339, U340. Diameter of individual polished blocks is 25 mm.

[1]Now at 41 Florida Avenue, New Lambton, New Castle, NSW, Australia

shows polished specimens of the nodules used for optical microscopy, SEM and EPMA.

Nodule U296a, from the Penrhyn Basin, depth 5130 m, is sub-spheroidal, diameter 25 mm. The nodule surface is finely microbotryoidal. In section, the nodule shows a dense accretionary layer approximately 1 mm thick coating a nucleus almost completely replaced by manganese oxides.

Nodule U300, from the eastern slope of Manihiki Plateau, depth 3747–3758 m, is ellipsoidal, maximum diameter 40 mm. Nodule surface is gritty. In section it consists of a manganese oxide crust 2–5 mm thick coating a pale-colored nucleus.

Nodule U321a, from abyssal hills east of Manihiki Island, depth 5114–5047 m, is sub-spheroidal, diameter 15 mm. The nodule consists of manganese oxides 5–8 mm thick, coating and partly replacing a weathered volcanic nucleus.

Nodule U327, from the western slope of the Pukapuka volcanic edifice, depth 3394–3217 m, is faceted spheroidal, maximum diameter 2 5mm. Surface texture is smooth to finely gritty. In section, the nodule consists of an accretionary crust of manganese oxide, 2–3 mm thick, surrounding a weathered volcanic nucleus.

Nodule U339, from the abyssal plain at the eastern end of the Nassau volcanic edifice, depth 4204–4219 m, is sub-spheroidal, diameter 15 mm. Surface texture is smooth to gritty. In section, the nodule consists of an accretionary crust 3–5 mm thick surrounding weathered rock material replaced by manganese oxides.

Nodule U340, from the abyssal plain west of the Nassau volcanic edifice, depth 5268–5253 m, is irregular in shape, diameter 30 mm. Surface texture is smooth to gritty. In section, the nodule shows a dense accretionary crust 2–3 mm thick, surrounding a yellowish tuffaceous rock partly replaced by manganese oxides.

MINERALOGY

The mineralogy of each sample was determined initially be optical examination and by XRD of nodule sub-samples, and confirmed by EPMA and FTIR.

Minerals identified are:

Ferruginous vernadite. This makes up the bulk of the ferromanganese oxide of the samples and occurs in all six specimens examined. This mineral (Ostwald, 1984a) is equivalent to δMnO_2 of the older nodule literature, e.g., Burns and Fuerstenau (1966). This nodule and crust mineral is recognized by its low optical reflectance, approximately 9% over the wavelength range 500-700 nm (Ostwald, 1985); the presence of broad peaks at 2.45Å, 1.4Å (and sometimes 2.2Å) in X-ray diffraction patterns and also by select area electron diffraction (Chukhrov et al., 1978); by its fibril morphology under HRTEM (Chukhrov et al., 1978) and by its chemical composition (significant amounts of Fe and Mn, analytical totals of 70-85%) (Burns and Burns, 1979). In marine nodules, vernadite is commonly closely associated with todorokite, and a transformation of vernadite to todorokite had been suggested (Burns and Burns, 1978a, b). This transformation may account for variations in analytical totals often observed in vernadite microanalyses as vernadite and todorokite contain significantly different amounts of combined water. As well as altering to todorokite, terrestrial vernadite appears to alter to a variety of manganese oxide tunnel structures, mainly cryptomelane and romanechite, and also to the dense chain structure pyrolusite (Ostwald, 1984b). However, the intimate association of layer-lattice, ferrihydrite-type iron oxides in marine vernadite (Ostwald, 1984a) suggests that pure vernadite is a layer-lattice. Extended X-Ray Absorption Fine Structure (EXAFS) analysis on the sample described in Ostwald (1984a) by A. Manceau, of the Laboratorie de Mineralogie - Cristallographie, Paris, has confirmed that vernadite consists entirely of edge - shared $[MnO_6]$ octahedra, thus making it a layer lattice (Manceau and Combes, 1987). Electron probe microanalyses on ferruginous vernadite from the six samples are given in Table 1.

Todorokite (Burns and Burns, 1979) occurs in samples U321a and U340, in small amounts, where it was determined by its relatively high reflectance, R(589nm) 10-17%, compared with ferruginous vernadite; the presence of major broad peaks in diffractograms at about 9.6Å, 4.9Å and 2.44Å (JCPDS 13-164); and EPMA analyses.

Identification based entirely on XRD may lead to incorrect results, as similar diffraction patterns may result from a variety of phyllomanganates, especially buserite, asbolane and hybrid buserite – asbolane (Chukhrov et al., 1983). The distinction between todorokite and buserite is best achieved by (1) heating the original sample for 2 hours at 100°C, and (2) intercalation of the original sample with 0.1M dodecylammonium chloride at room temperature. Buserite is determined by its collapse to a 7Å layer-lattice under heating and its expansion to 25.4Å under intercalation. The diffractogram of todorokite is unaffected by these treatments (Ostwald and Dubrawski, 1987). The identification of hybrid buserite-asbolane requires analytical electron microscopy and electron diffraction (Chukhrov et al., 1984).

Microanalyses of todorokite are given in Table 2.

Feldspars, chiefly plagioclase, with minor K-feldspar, were identified by XRD and EPMA in all nodules.

Quartz and *iron oxide* were found in minor amounts in U296a.

Phillipsite occurs in the cores of all the nodules except U296a.

The mineral composition of the nodules is summarized in Table 3 and X-ray diffractograms of the nodules are shown in Figure 2a, b.

Infra-red spectroscopy using the Fourier Transform Infra-Red (FTIR) method was carried out on all

Table 1. Electron probe microanalyses of ferruginous vernadite (wt.%).

Stn	Analysis	MnO_2	Fe_2O_3	Na_2O	K_2O	CaO	MgO	P_2O_5	TiO_2	Al_2O_3	SiO_2	NiO	CoO	H_2O+
U296a	1	21.7	38.9	1.6	0.3	2.2	2.9	1.0	1.3	2.7	4.8	ND	ND	22.6
"	2	35.7	25.6	1.6	0.3	2.5	2.5	1.3	1.5	3.2	5.9	ND	ND	19.9
"	3	48.5	21.7	3.3	0.4	3.1	2.8	1.3	2.0	3.6	4.3	ND	ND	9.0
"	4	18.0	31.3	1.1	0.2	1.4	1.1	1.0	3.7	1.6	7.1	ND	ND	33.5
"	5	23.8	24.1	1.0	0.2	2.0	1.9	1.1	2.3	3.5	7.9	0.1	ND	32.1
"	6	28.3	39.5	1.9	0.4	2.1	1.9	1.3	3.8	2.9	9.9	0.1	ND	7.9
U300	7	25.9	27.5	1.2	0.3	2.0	1.7	1.1	3.0	5.6	8.3	ND	ND	23.5
"	8	39.3	26.8	2.3	0.4	2.6	2.3	1.4	2.0	3.5	6.8	0.1	ND	12.5
"	9	27.2	24.9	1.2	0.4	1.9	1.3	1.1	1.9	3.0	6.3	0.2	ND	30.6
"	10	39.8	28.1	1.3	0.3	3.3	1.8	1.3	2.0	2.7	6.3	0.1	ND	12.4
"	11	20.1	24.2	1.1	0.3	2.5	1.7	1.1	2.1	2.5	7.7	0.1	ND	28.6
"	12	38.9	25.9	2.1	0.4	3.2	2.1	1.3	1.8	2.6	6.9	0.2	ND	14.6
"	13	40.3	26.9	1.5	0.3	3.3	2.0	1.3	1.7	2.3	6.7	0.3	ND	13.4
"	14	41.6	27.5	2.8	0.4	2.8	2.7	1.4	1.6	3.0	6.9	0.2	ND	19.1
"	15	35.2	28.2	1.9	0.3	2.7	2.2	1.5	2.5	3.2	8.4	0.1	ND	13.8
U321a	16	31.3	24.4	1.0	0.3	2.4	1.6	1.2	1.4	4.9	6.4	0.1	ND	25.2
"	17	27.1	19.8	1.8	0.3	3.3	1.5	1.0	1.3	7.9	12.6	ND	ND	23.4
"	18	42.6	18.9	2.0	0.4	2.1	3.5	0.9	1.0	4.1	4.1	0.8	ND	19.0
"	19	33.6	23.0	1.5	0.3	2.4	2.0	1.1	1.4	3.8	6.2	0.1	ND	23.9
"	20	28.2	22.0	1.4	0.3	1.7	2.2	1.1	2.0	4.2	6.5	ND	ND	30.5
"	21	36.1	25.5	2.2	0.3	2.1	4.1	1.4	2.4	5.8	8.4	0.4	ND	11.8
"	22	31.5	31.5	1.5	0.3	2.1	2.4	1.4	2.9	4.8	8.5	0.2	ND	12.9
"	23	30.1	23.3	1.1	0.3	2.1	1.8	1.2	1.8	4.1	6.6	0.3	0.9	26.4
U327	24	39.0	22.1	2.2	0.3	2.7	1.8	ND	1.4	1.8	9.3	0.4	ND	19.0
"	25	40.7	22.8	2.0	0.3	3.1	1.8	ND	1.6	2.0	8.6	0.9	ND	16.4
"	26	46.6	21.9	2.2	0.3	3.4	2.4	ND	1.6	2.7	4.7	0.5	ND	13.7
"	27	40.9	23.8	2.6	0.3	3.1	2.6	ND	2.0	3.4	6.4	0.3	1.3	13.3
U339	28	45.5	22.1	2.4	0.3	3.1	2.5	ND	1.7	2.8	5.8	0.4	ND	13.4
"	29	41.0	19.1	2.9	0.3	3.2	2.9	ND	2.3	3.0	6.2	0.3	0.7	18.1
"	30	46.6	18.5	2.6	0.4	3.5	2.5	ND	2.3	2.5	5.7	0.7	1.2	13.5
"	31	39.7	22.4	1.8	0.3	3.2	1.8	ND	2.6	3.0	6.0	0.1	0.8	18.3
U340	32	35.7	26.3	3.0	0.5	2.2	2.7	ND	2.9	4.0	9.1	0.5	0.7	12.4
"	33	31.7	23.6	1.2	0.3	2.0	1.7	ND	2.2	3.8	8.3	0.2	0.3	24.7
"	34	46.7	19.3	2.6	0.5	2.9	1.9	1.0	1.4	3.4	5.9	0.7	0.3.	13.4
"	35	37.9	26.0	2.8	0.4	2.9	2.3	1.3	1.8	3.8	7.6	0.1	0.5	12.6

Note: H_2O+ (structural water) by difference from 100%. ND = not detected.

Table 2. Electron probe microanalyses of todorokite (wt.%).

Stn	Analysis	MnO_2	Fe_2O_3	Na_2O	K_2O	CaO	MgO	P_2O_5	TiO_2	Al_2O_3	SiO_2	NiO	CuO	CoO	H_2O+
U321a	1	67.7	2.7	3.0	0.6	1.4	5.6	0.7	ND	3.0	2.1	ND	ND	ND	13.2
"	2	55.7	4.1	2.3	0.5	1.3	6.7	0.6	0.6	5.8	1.7	2.0	ND	ND	18.7
"	3	54.4	8.3	2.9	0.4	1.5	7.9	0.6	0.9	6.2	2.9	2.2	1.2	0.4	10.2
"	4	54.9	5.5	1.6	0.6	1.8	5.8	0.5	0.8	5.5	3.2	2.6	1.1	0.6	15.5
U340	5	60.4	3.2	2.6	0.4	1.3	8.1	0.5	0.2	5.8	1.4	2.9	1.7	0.3	11.2
"	6	62.0	1.9	3.2	1.1	0.9	7.7	0.4	0.1	5.7	3.0	3.5	ND	ND	10.5

Note: H_2O+ (structural water) by difference from 100%. ND = not detected.

*Table 3. Mineralogy of nodules from Manihiki Plateau area.**

Stn	Vernadite	Todorokite	Feldspar	Phillipsite	Quartz	Iron Oxide
U296a	M	-	L	-	L	T
U300	M	-	L	L	-	-
U321a	M	L	L	L	-	-
U327	M	-	L	L	-	-
U339	M	-	L	L	-	-
U340	M	L	L	L	-	-

*M = major, L = minor, T = trace

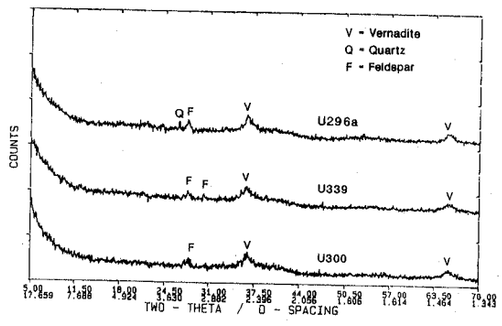

Figure 2(a). X-ray diffractograms of ferromanganese crusts of nodules from Stns U296a, U339 and U300.

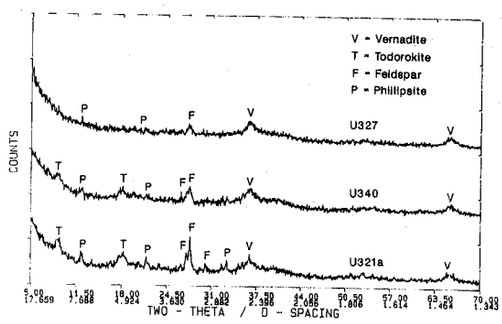

Figure 2(b). X-ray diffractograms of ferromanganese crusts of nodules from Stns U327, U340 and U321a.

ferromanganese coatings of the nodules (no core material included). All spectra (absorbance against wave number) are essentially similar with peaks at about 480, 680, 1018, 1625 and 3420 cm^{-1}. The spectrum of nodule U296a is shown in Figure 3.

This type of spectrum appears characteristic of nodules composed chiefly of ferruginous vernadite as it is essentially similar to that recorded by Ostwald (1984a) for an Indian Ocean ferruginous vernadite nodule and also for ferruginous vernadite from a Vanuatu marine nodule (Ostwald, unpublished data) (Figure 4). Non-iron-containing vernadite in terrestrial deposits has quite a different spectrum, with

peaks at 530, 1620 and 3400 cm^{-1} (Ostwald 1984b, 1985). IR peaks for the todorokite component are almost certainly covered by the broad absorbance centered on 480 cm^{-1}. The peak at about 1020 cm^{-1} in the spectrum is possibly due to the iron oxide component of the ferruginous vernadite (Ostwald, 1984a).

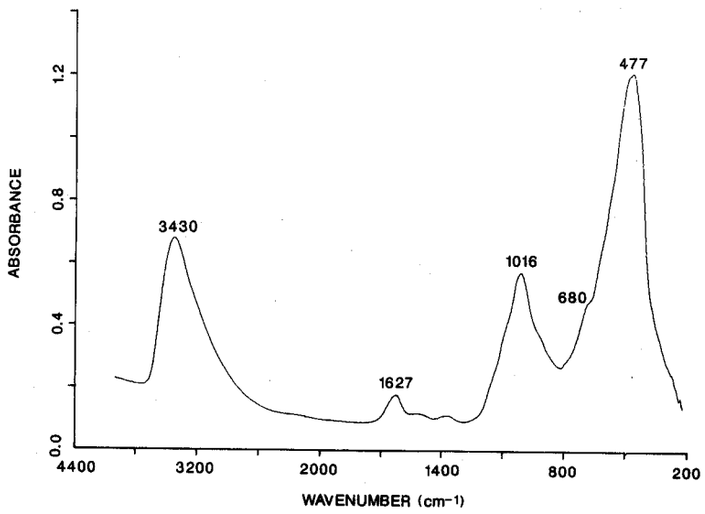

Figure 3. Fourier-Transform Infra-Red spectrum of Fe-Mn crust from Stn U296a nodule.

INTERNAL STRUCTURE

The *microtexture* of polished sections of the nodules was examined both in reflected light and by back-scattered electron (BSE) techniques. The latter technique correlates well with optical methods of identification, e.g., optically more reflective (brighter) phases such as todorokite are also brighter in BSE mode owing to lesser amounts of combined water (higher average atomic number). Microtextural descriptive terminology in this section is based on that of Sorem and Fewkes (1977).

Nodule U296a is composed chiefly of radially-directed columnar material composed of ferruginous vernadite. Such columnar texture is commonly highly convoluted. The columns tend to be initiated by detrital grains of feldspar which occur within the layers (Figure 5). Sections transverse to the columns show this texture to best advantage (Figure 6).

Nodule U300 also has an outer layer composed of finely-layered columns of ferruginous vernadite which often show branching. The cavities between the branches are commonly filled with granular phillipsite (Figure 7).

Nodule U321A has an outer layer composed of radially-directed, finely laminated ferruginous vernadite, which at various growth intervals is coated by thin (typically 10–20 ìm) laminae of todorokite (Figure 8). Although the todorokite coats the vernadite, it does not occur in the form of the thick "massive" layers noted by Sorem and Fewkes (1977) but more as their mottled zone material. Such an alternating layering of vernadite and todorokite has been explained by Giovanoli (1980) as due to fluctuations in silica and ferric hydroxide in the growth solution.

Nodule U327 consists of an outer layer of columnar ferruginous vernadite coating a core of clay and zeolite (Figure 9). Phillipsite occurs also

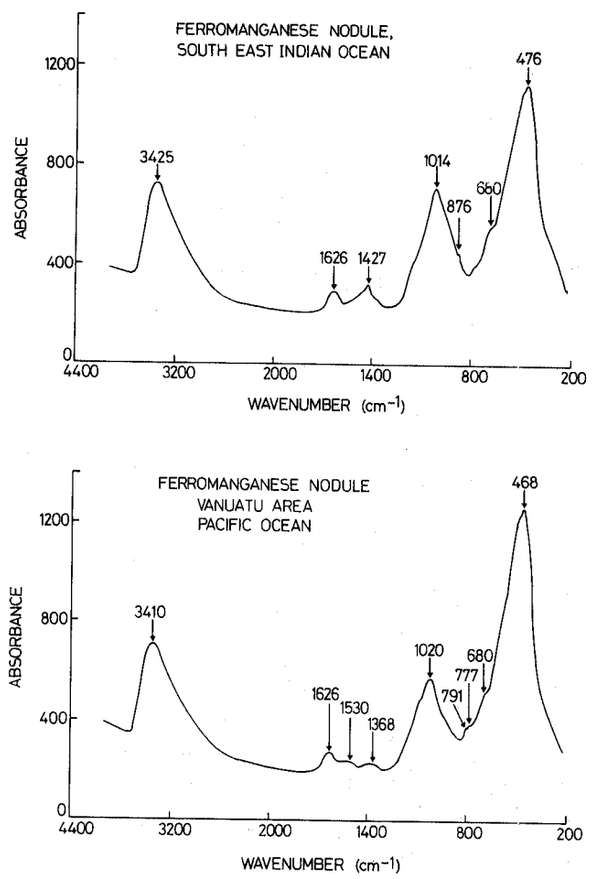

Figure 4. Fourier-Transform Infra-Red spectra of ferruginous vernadite from SE Indian Ocean nodule (top) and Vanuatu Basin, Pacific Ocean (bottom).

in finely-granular material in the cavities between the columns (Figure 10).

Nodule U339 consists essentially of radiating columnar branches of finely-laminated ferruginous vernadite.

Nodule U340 is also composed of finely laminated columnar material. Figure 11 shows a section through a series of columns in which there is a definite break in deposition. The older material (top left) is composed of ferruginous vernadite with few todorokite layers. Following a break in deposition (indicated in the photomicrograph), laminated, columnar material dominated by todorokite (with lesser amounts of vernadite) developed.

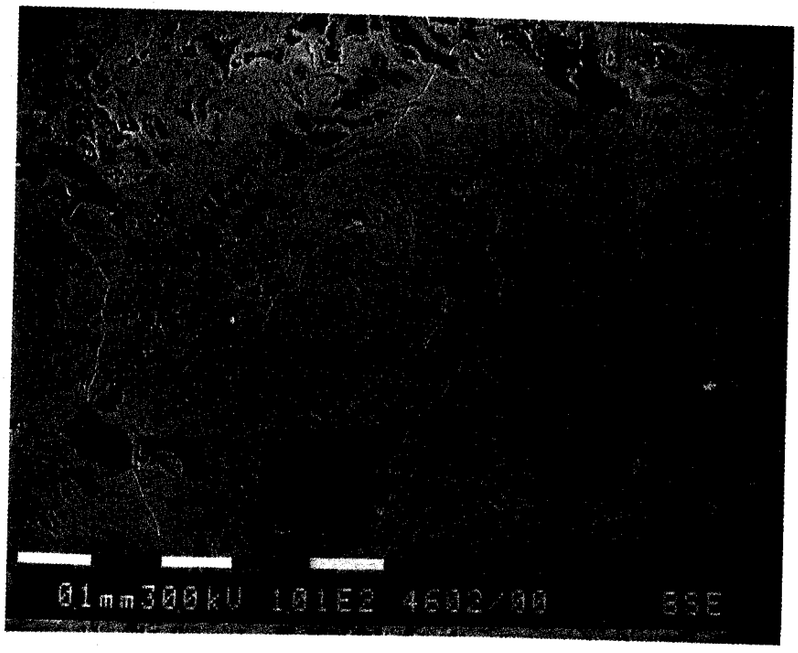

Figure 5. SEM micrograph of polished section of U296a nodule showing columnar ferruginous vernadite. Large dark grains at bottom left are detrital feldspars. Length of each white section of the scale bar is 0.1 mm.

DISCUSSION

The abundance of ferruginous vernadite and low amounts of todorokite in the Manihiki Plateau area nodules indicate a hydrogenous origin in an oxidizing environment of deposition (Cronan, 1980). There is no mineralogical evidence for the occurrence of phases such as crystalline birnessite or buserite which may indicate a hydrothermal origin (Corliss et al., 1978; Toth, 1980; Chukhrov et al., 1984). The origin of thin layers of todorokite generally parallel to the more common ferruginous vernadite layers is not, in the writer's opinion, fully resolved. Where todorokite occurs as a 'thick' layer, apparently cross-cutting ferruginous vernadite columns ('massive' zones of Sorem and Fewkes, 1972), an origin by diagenetic reaction between vernadite and decaying organic material(often containing Cu and Ni) to produce the todorokite layers, as suggested by Burns and Burns (1978a, b), seems reasonable. While it is not impossible that the fine laminae of todorokite in nodules from the Manihiki Plateau developed by such a mechanism, the ideas put forward by Giovanoli (1980), that such fine alternations of vernadite (Z-disordered birnessite) and todorokite (equivalent to some forms of 10Å manganate) in nodules is due to hydrogenous precipitation under oscillating concentrations of silica and ferric hydroxide in the growth solution, also deserve further study.

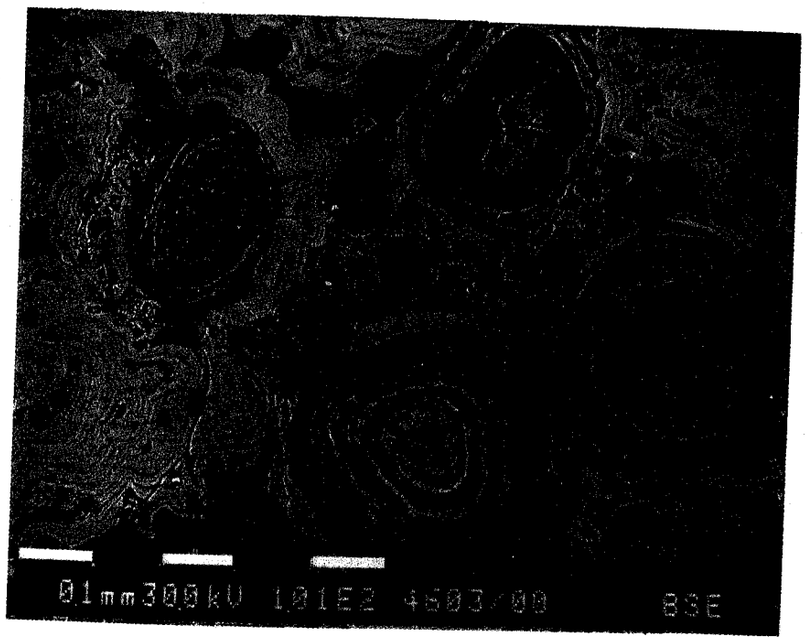

Figure 6. SEM micrograph of polished section of U296a nodule, transverse to four columns of ferruginous vernadite. Length of each white section of the scale bar is 0.1 mm.

The concept that the nodules of the southwest Pacific

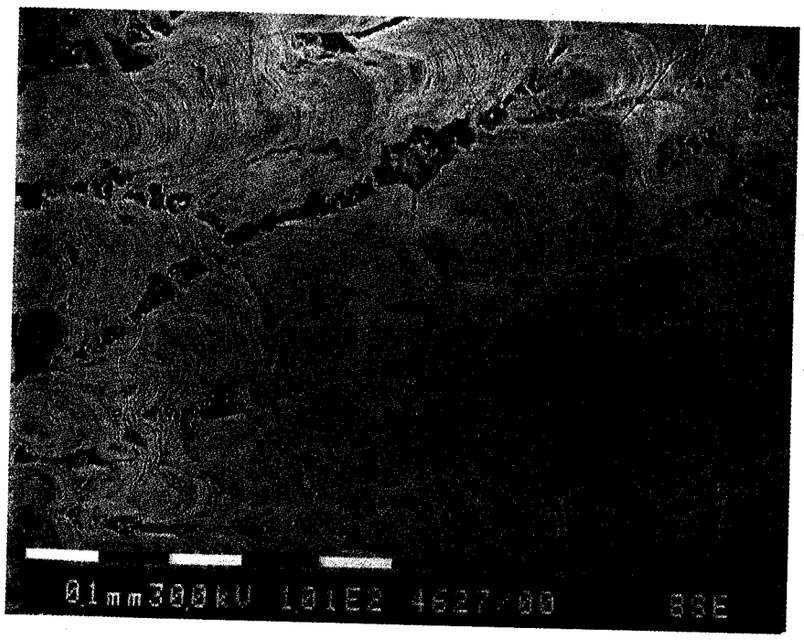

Figure 7. SEM micrograph of polished section of U300 nodule showing branching columns of ferruginous vernadite. Dark granular material between columns is largely phillipsite. Length of each white section of the scale bar is 0.1 mm.

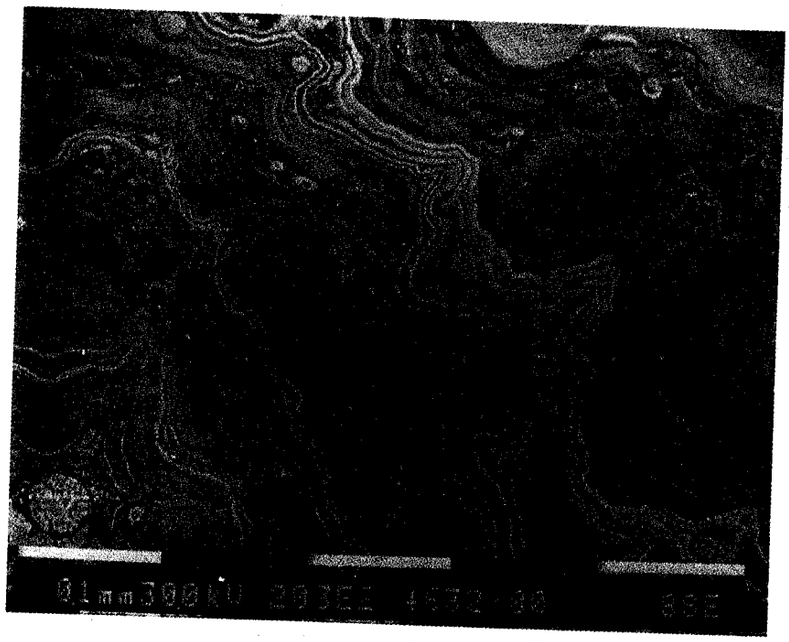

Figure 8. SEM micrograph of polished section of U321a nodule showing finely laminated todorokite (white) and ferruginous vernadite layers (shades of gray).

Ocean occupy definite sedimentary facies was developed by Meylan (1978), who defined two basic categories.

1. Cook Island Facies, composed of generally spheroidal nodules; internal structure consisting of a ferruginous vernadite crust coating a decomposed volcanic glass nucleus; Mn/Fe near or below 1 and low Cu and Ni.
2. Southwestern Pacific Basin Facies, composed of polynucleate nodules, with an internal structure of layered ferruginous vernadite and todorokite, without a definite nucleus; Mn/Fe above 1 and significant Cu and Ni.

In addition, SW Pacific nodules appear to be composed typically of three structural zones which are significantly different from those of North Equatorial Pacific zone nodules (Goodell et al., 1971; Glasby et al., 1986). These layers are:

1. an outer ferromanganese oxide accretionary crust layer 0.5–2.0 mm thick.
2. a thicker, inner ferromanganese oxide layer showing evidence of replacement of core material.
3. a core of volcanic glass, palagonite or clay commonly veined by replacement manganese oxides.

In terms of mineralogy, geochemistry and internal structures, the suite of nodules from the Manihiki Plateau area reported in this paper clearly approximates to the Cook Island Facies material, which it geographically borders.

The low Cu + Ni + Co of these nodules (when compared to those of the Pacific "ore zone") (Cronan, 1980) is directly related to manganese oxide mineralogy and ultimately to the depositional environment. For reasons not fully understood, ferruginous vernadite may contain Co but no, or limited, Ni and Cu (Burns and Burns, 1979). Nodules developed in relatively shallow, well-oxygenated waters tend to be vernadite-rich, (Glasby, 1977; Cronan, 1980). As the Cook Island Facies occurs in an area characterized by low biological productivity of the surface waters, low organic content in bottom sediments and red clay rather than siliceous ooze as the principal sediment type (Glasby et al., 1986), it follows that

ferruginous vernadite will dominate in this area. On the basis of the theory of Burns and Burns (1978a, b), todorokite development will be minimized by lack of decaying organic remains. Furthermore, if the elements Cu and Ni are derived from the remains of marine microorganisms, then the low biological productivity of the area will limit availability of Cu and Ni as well as limit todorokite formation.

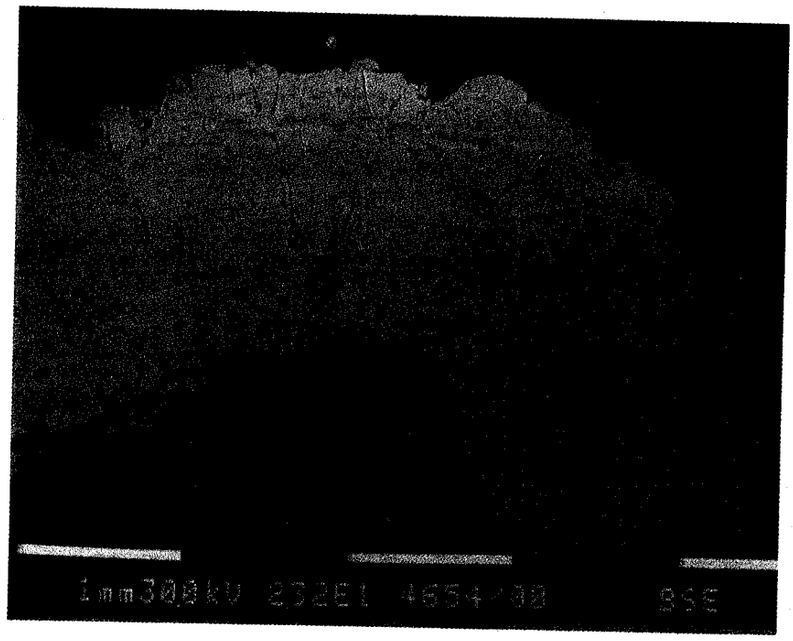

Figure 9. SEM micrograph of polished section of U327 nodule showing an outer layer of columns of ferruginous vernadite coating an angular core composed of clay minerals and phillipsite. Length of each white section of the scale bar is 1 mm.

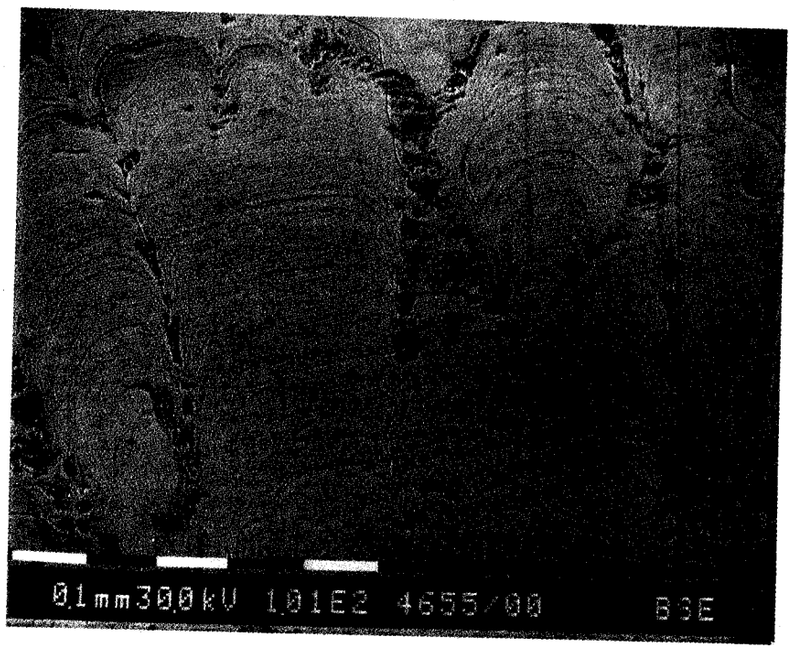

Figure 10. SEM micrograph of polished section of U327 nodule showing columnar ferruginous vernadite with granular phillipsite between the columns. Length of each white section of the scale bar is 0.1 mm.

REFERENCES

Burns, R.G., and V.M. Burns, 1979, Manganese oxides, *in* R.G. Burns, ed., Marine minerals: Mineralogical Society of America, Short Course Notes, v.6, p. 1-40.

Burns, R.G., and D.W. Fuerstenau, 1966, Electron probe determination of inter-element relationships in manganese nodules: American Mineralogist, v.51, p.895-902.

Burns, V.M., and R.G. Burns, 1978a, Diagenetic features observed inside deep-sea manganese nodules from the north equatorial Pacific: Scanning Electron Microscopy, v.1, p.245-252.

Burns, V.M., and R.G. Burns, 1978b, Authigenic todorokite and phillipsite inside deep-sea manganese nodules: American Mineralogist, v.63, p.827-831.

Chukrov, F.V., A.I. Gorshkov, E.J. Rudnitskaya, V.V. Berezovskaya, and A.V. Sivtsov, 1978, Vernadite: Izvestiya Akademii Nauk SSR, Seriya Geologicheskaya, v.6, p.5-19.

Chukrov, F.V., A.A. Gorshkov, V.A. Drits, V.I. Finko, A.V. Sivtsov, Y.P. Dikov, and A. Sakharov, 1983, Structurally disordered asbolanes with tetrahedrally coordinated manganese: Izvestiya Akademii Nauk SSR, Seriya Geologicheskaya, v.12, p.85-95.

Chukrov, F.V., A. A. Gorshkov, V.A. Drits, A.V. Sivtsov, T.Y. Uspenskoya, and A. Sakharov, 1984, Structural models and methods of study of buserite: Izvestiya Akademii Nauk SSR, Seriya Geologicheskaya, v.10, p.65-74.

Corliss, J.D., M. Lyle, J. Dymond, and K. Crane, 1978, The chemistry of hydrothermal mounds near the Galapagos Rift: Earth and Planetary Science Letters, v.40, p.12-24.

Cronan, D.S., 1980, Underwater minerals: London, Academic Press, 362 p.

Glasby, G.P., ed., 1977, Marine manganese deposits: Amsterdam, Elsevier, 523 p.

Glasby, G.P., N.F. Exon, and M.A. Meylan, 1986, Manganese nodules in the SW Pacific, *in* D.S. Cronan, ed., Sedimentation and mineral deposits in the southwestern Pacific Ocean: London, Academic Press, p.237-262.

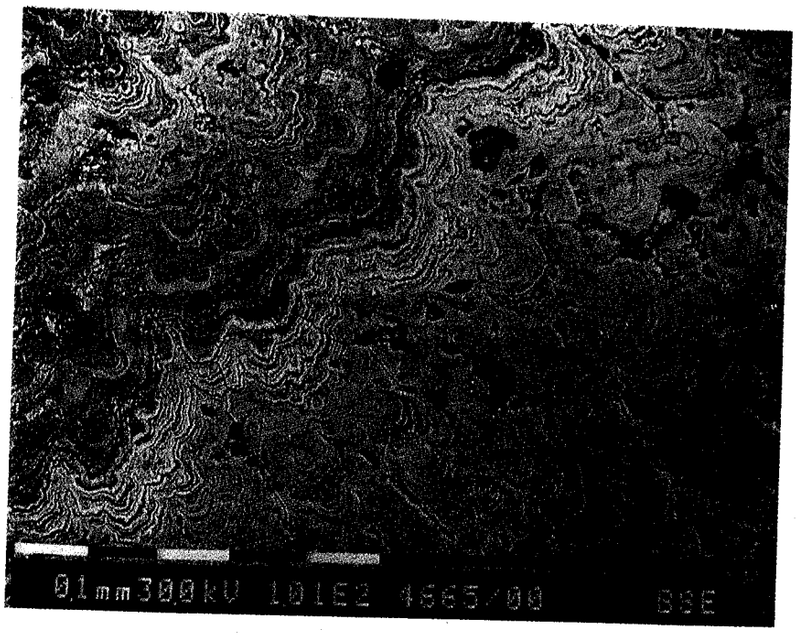

Figure 11. SEM micrograph of polished section of U340 nodule showing dark ferruginous vernadite-rich layers (top left) and lighter, more todorokite-rich layers (center to bottom right). Length of each white section of the scale bar is 0.1 mm.

Giovanoli, R., 1980, Layer-structured manganese oxide hydroxides VI: Recrystallisation of synthetic buserite and the influence of amorphous silica and ferric hydroxide as its nucleation: Chimia, v.34, p.308-310.

Goodell, H.G., M.A. Meylan, and B. Grant, 1971, Ferromanganese deposits of the South Pacific Ocean, Drake Passage and Scotia Sea: American Geophysical Union, Antarctic Research Series, v.15, p.27-92.

Manceau, A., and I.M. Combes, 1987, Structure of Mn and Fe oxides and oxyhydroxides: a topological approach by EXAFS: Chemistry and Physics of Minerals, v.10, p.68-79.

Meylan, M.A., 1978, Marine sedimentation and manganese nodule formation in the southwestern Pacific Ocean [unpubl. Ph.D. diss.]: Department of Oceanography, University of Hawaii, Honolulu, 312 p.

Ostwald, J., 1984a, Ferruginous vernadite in an Indian Ocean ferromanganese nodule: Geological Magazine, v.121, p.483-488.

Ostwald, J., 1984b, Vernadite - a possible hybrid-structured mineral: Australian Mineralogist, July, p.269-271.

Ostwald, J., 1985, Mineralogy of battery-active manganese ore from Groote Eylandt, *in* W.C. Park, ed., Applied mineralogy: American Institute of Metallurgical Engineers, p.1095-1108.

Ostwald, J., and J.V. Dubrawski, 1987, Buserite in a ferromanganese crust from the southwest Pacific Ocean: Neues Jahrbuch für Mineralogie Abhandlungen, v.157, p.19-34.

Sorem, R.K., and R.H. Fewkes, 1977, Internal characteristics, *in* G.P. Glasby ed., Amsterdam, Elsevier, p.147-184.

Toth, J.R., 1980, Deposition of submarine crusts rich in manganese and iron: Geological Society of America Bulletin, v.91, p.44-54.

Cullen, D.]. 1996. Ferromanganese crusts on seamounts in the Notth Fiji Plateau - Samoa Basin region, *in:* Meylan, M.A., and Glasby (eds) Manihiki Plateau, Machias and Capricorn Seamounts, Niue, and Tofua Trough: Results of *Tlli* Cruises. SOPAC Technical Bulletin 10: *109-117.*

FERROMANGANESE CRUSTS ON SEAMOUNTS IN THE NORTH FIJI PLATEAU - SAMOA BASIN REGION

D.J. Cullen!

National Institute of Water and Atmosphere Research Ltd, PO Box 14901, Kilbimie, Wellington, New Zealand

ABSTRACT

During a survey of phosphatic sediments on seamounts in the tropical SW Pacific between 1980 and 1983, ferromanganese crusts up to about 40 mm thick were collected by dredging in water depths of 620 to 1800 m. Crusts are thinnest on recent scleractinian coralla, thicker on semi-consolidated to consolidated calcarenites and coarse coral limestone, and thickest on ancient phosphatized limestone substrates. X-ray diffraction analyses indicate that the crusts are amorphous to very poorly crystalline, likely a mixture of a-MnO_2 and goethitic iron oxyhydroxide. The Mn:Pe ratio varies from about 0.5 to 2; a linear relationship exists between increasing Mn:Pe values and total Co+Ni+Cu content. Highest trace metal values were encountered in samples from Albert Henry, Kalolo, and Perez Seamounts in the northern part of the region surveyed (up to 2.7% for combined Co+Ni+Cu, and up to 1.8% for Co alone).

INTRODUCTION

A number of samples, thickly encrusted by iron and manganese oxides, were collected between August 1980 and November 1983 on New Zealand Oceanographic Institute (NZOI) cruises 1113, 1135 and 1152 aboard R/V *Tangaroa,* in the course of a survey of phosphatic sediments on seamounts in the tropical SW Pacific Ocean. An earlier report (Cullen and Burnett, 1986) concentrated on the geology and distribution of the phosphorite substrates; this account describes the relative thicknesses, structural and textural variations, and geochemistry of the ferromanganese crusts.

The area covered by the survey extends from the vicinity of Rotuma on the North Fiji Plateau eastward to seamounts near Pukapuka and Aitutaki (in the northern and southern Cook Islands, respectively), and northward to include seamounts northwest of the Tokelau Islands (Figure 1). It spans part of the North Fiji Plateau and the entire Samoa Basin between longitudes 177°E and 159°W, and latitudes 6°-19°S, but lies to the south of the Kiribati-Tuvalu region described by De Carlo et al. (1987).

The majority of samples described here were recovered from depths between 1300-1800 m (Table 1), on the upper slopes of peaked volcanic seamounts that rise from abyssal plain depths in excess of 4000 m. Unlike the lower slopes of the seamounts, which tend to be smoothly curved, their crests and upper slopes are normally precipitous and rugged. The two exceptions encountered in the course of this investigation are the practically flat-topped MacLeod and Solomoni Guyots, which have been interpreted by Cullen and Burnett (1986) as deeply submerged coral atolls, down-faulted by late Cenozoic tectonism.

THICKNESS, STRUCTURE AND SURFACE TEXTURE OF THE CRUSTS

The thicknesses and structural and textural characteristics of the accretionary ferromanganese oxides vary widely throughout the region (Figures 2-5). Crustal thicknesses range from 0.1-0.2 mm on recent scleractinian

[1]Now at 74 West Street, Greytown, Wairarapa, New Zealand

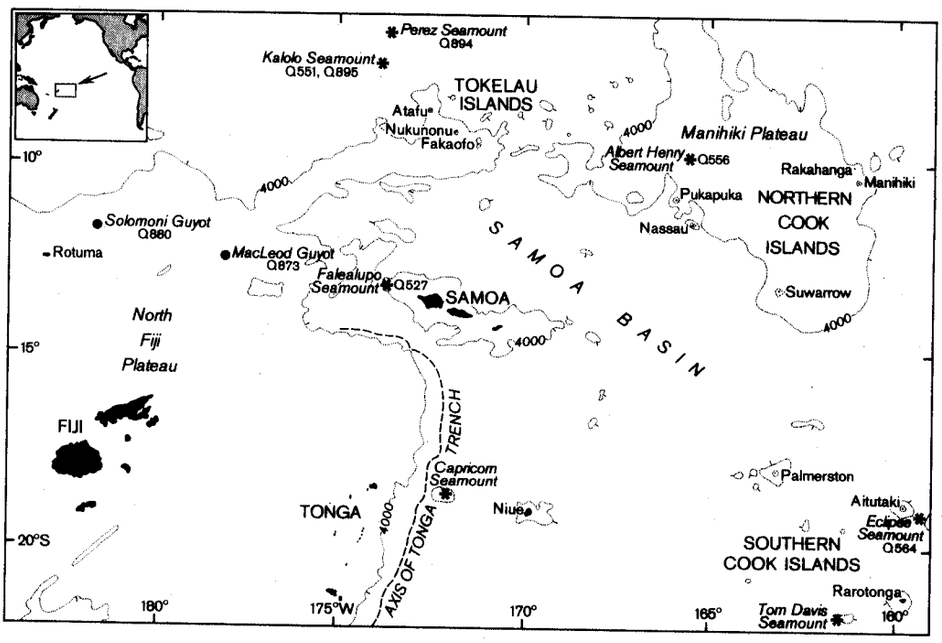

Figure 1. Locality map showing the distribution of sampling stations around the Samoa Basin and on the northern margin of North Fiji Plateau. Asterisks denote peaked seamounts; solid dots represent guyots.

Table 1. Sample/station data.

NZOI Station No.	Location	Latitude	Longitude	Depth (m)	Sampling Gear
Q527	Falealupo Seamount	13° 15.3'S	173° 39.2'W	1300-1350	Pipe dredge
Q551	Kalolo Seamount	7° 17.1'S	173° 50.4'W	1325-1380	Pipe dredge
Q556	Albert Henry Seamount	9° 46.8'S	165° 31.1'W	1780	Rock dredge
Q564	Eclipse Seamount	19° 09.6'S	159° 19.1'W	1655-1800	Pipe dredge
Q870	MacLeod Guyot	12° 30.1'S	178° 04.0'W	1210-1230	Rock dredge
Q873	MacLeod Guyot	12° 24.2'S	178° 32.5'W	1520	Rock dredge
Q880	Solomoni Guyot	11° 39.7'S	178° 26.4'E	920-1060	Rock dredge
Q889	Solomoni Guyot	11° 12.3'S	178° 15.8'E	620	Rock dredge
Q890	Solomoni Guyot	11° 26.0'S	178° 06.3'E	770	Rock dredge
Q894	Perez Seamount	6° 28.6'S	173° 34.4'W	1450	Pipe dredge
Q895	Kalolo Seamount	7° 15.9'S	173° 52.0'W	1300-1325	Pipe dredge

coralla (e.g., Stns Q564 and Q890) to between 1.0-10.0 mm on consolidated and semi-consolidated calcarenites (Q870, Q873) and coarse coral limestone (Q880, Q889), and up to a maximum of about 40 mm on ancient phosphatized pelagic limestone substrates (Q551, Q556, Q894, Q895).

Coatings on Corals

While the ultra-thin coatings on coral skeleta tend to have matt surfaces in protected, unworn areas, with microbotryoidal surface structures plainly visible under the microscope, elsewhere the coatings often appear smooth and glossy, and are characterized by wavy patterns of fine parallel striae (Figure 2). These patterns are almost certainly molded upon and partly replace remnants of a superimposed octoradiate (probably a gorgonid) coral. Although a subdued form of microbotryoidal structure persists over, and helps to impart a gloss to, the striated surfaces, some of the surficial glazing may reflect the presence of the keratinous skeletal material that characterizes the gorgonid corals. In places, where the striated ferromanganese crust has flaked

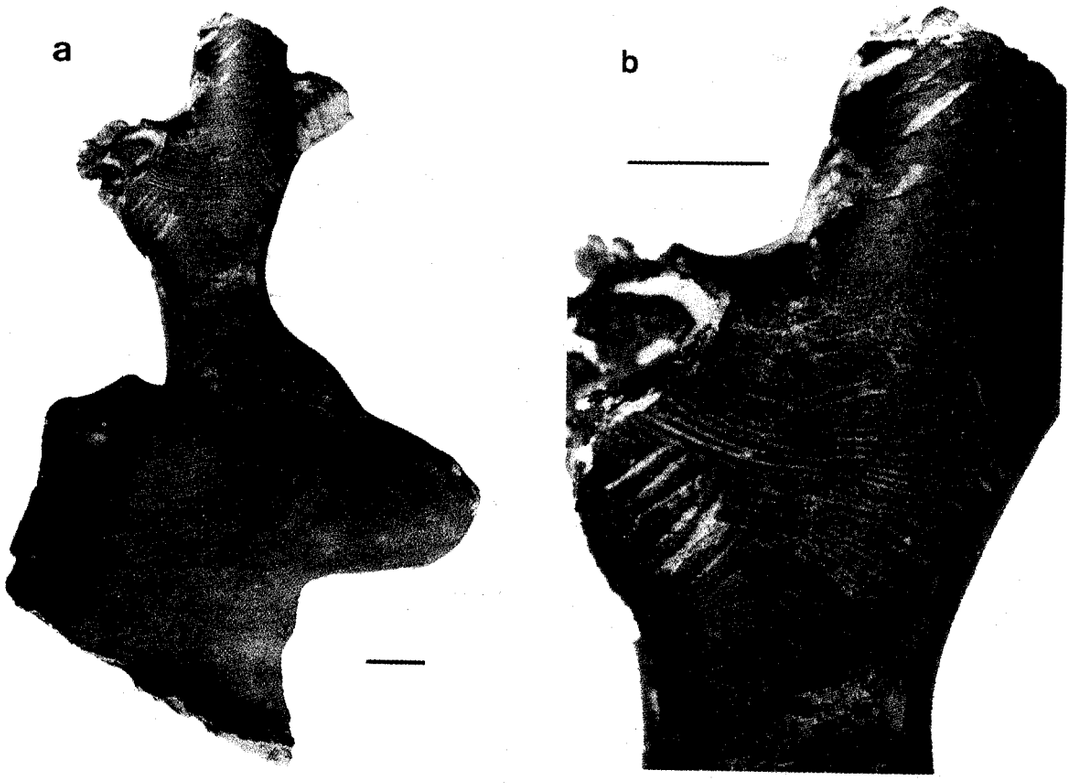

Figure 2. (a) Thin, striated, ferromanganese oxide coating on scleractinian coral skeleton (Station Q564). (b) Note the thinness of the coating where broken and gouged on the left side, and also the gloss on the microbotryoidal surface. Scale bars represent 5 mm in both photographs.

away, the underlying scleractinian coral surface is seen to be perfectly smooth and is therefore not itself contributing to the striated structure. Small-scale fluting, indicative of gentle, erosional current action, locally gouges through the crust to expose the underlying scleractinian coral.

Radiocarbon dating, by accelerator mass spectrometry, provides an age of 39,635 + 3116 years (Late Pleistocene) for the outer layers of the coated corallum illustrated in Figure 2. This indicates an accumulation rate of ferromanganese oxides in the order of 2.5-5.0 mm/10^6 yrs.

Crusts on Calcarenite and Limestone Breccia Substrates

Thicker ferromanganese crusts, those that have formed on calcarenites and coarser coral limestone breccias, display a variety of botryoidal surface structures. On finer-grained substrates, the botryoidal lobes tend to be widely spaced and to project prominently above the general crustal surface, providing distinct elevations and depressions upon which microbotryoidal microstructures are plainly visible under the microscope. Fractured crustal surfaces have a hackly, earthy and sometimes cellular texture, with fine mottling in black (N1; color designations from Rock-Color Chart Committee, 1948) and light brown (5YR 5/6) providing an overall dark yellowish brown (approximately 10YR 3/2) color. For some 5 mm below the actual crust, the calcarenite is irregularly iron-stained, the color rapidly decreasing in intensity inward, from dark yellowish orange (10YR 6/6) to very pale orange (10YR 8/2). Submarine erosion of this type of crust tends to remove the heads of the projecting lobes, producing a slightly polished, compact, knobbly grayish-black (N2) surface. Traces of the underlying calcarenite are often discernible on the more deeply eroded and more highly-glazed surfaces of major protuberances (e.g., Q889).

Ferromanganese crusts on the coarser, cavernous coral limestone breccias present a rather more spectacular appearance. The external structure of close-packed botryoidal surfaces provides a morphology resembling, except for its dull grayish-black (N2) to brownish-black (5YR 2/1) color, a young, inflorescent cauliflower head (Figure 3a). The cavernous nature of the subjacent coral limestone is usually almost totally masked. At about 10-20 mm beneath the surface of the crust, however, cavities and burrows in the limestone breccia are seen to be lined by a thin, but distinct, layer of a ferruginous mineral that ranges in color from moderate reddish brown (10R 4/6) to dark reddish brown (10R 3/4) in proximity to internal growths of microbotryoidal manganese oxides. Where the manganiferous and ferruginous layers merge, the former

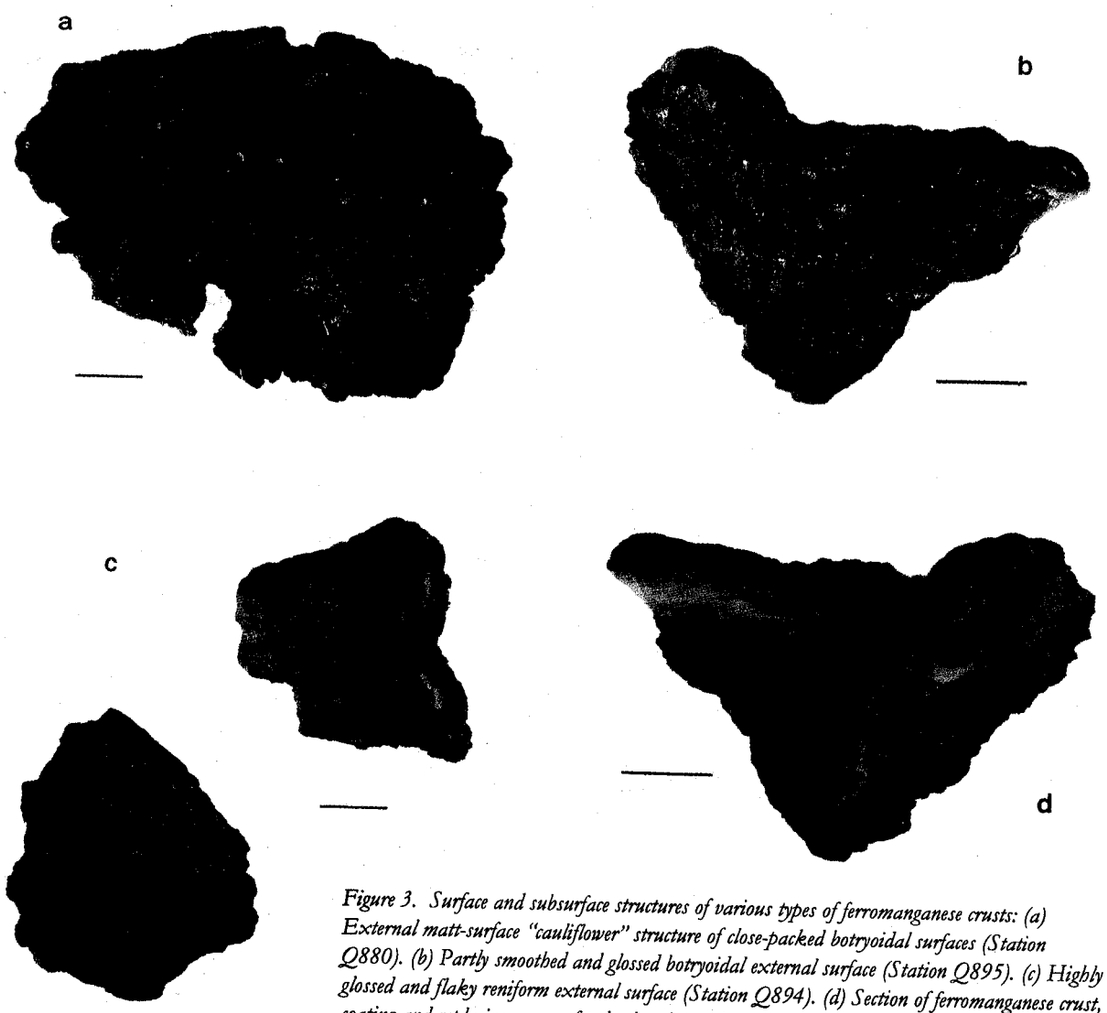

Figure 3. Surface and subsurface structures of various types of ferromanganese crusts: (a) External matt-surface "cauliflower" structure of close-packed botryoidal surfaces (Station Q880). (b) Partly smoothed and glossed botryoidal external surface (Station Q895). (c) Highly glossed and flaky reniform external surface (Station Q894). (d) Section of ferromanganese crust, coating and replacing a core of pale phosphatized pelagic limestone. Note the rounded and embayed margins of the limestone, and the impregnation of the latter by dendritic and massive dark oxides (Station Q895; cf. Figure 3b, above). Scale bars represent 25 mm in each photograph.

clearly overlie the latter. Sometimes, the ferruginous coating material forms hollow, blister-like structures with smooth, semi-glossy surfaces and a vaguely scoriaceous or slag-like appearance (Figure 4). In the absence of independent evidence of hydrothermal activity associated with such occurrences, however, these structures are presumed to be entirely hydrogenous in origin. Porous limestone fragments are stained pale to dark yellowish orange (10YR 8/6-6/6), but the more consolidated or partly recrystallized coral clasts retain their original very light gray (N8) color.

Crusts on Pelagic Limestone Substrates

Ferromanganese accumulations upon ancient phosphatized pelagic limestone substrates are usually massive and much thicker, reaching a known maximum for the region surveyed of about 40 mm on Kalolo Seamount, northwest of the Tokelau Islands (Q551). Micropaleontological dating of the limestone on Kalolo Seamount is ambiguous. Although the youngest microfossils present are of Late Pliocene age (i.e., 2.8-3.0 x 10^6 yrs old), there is some suggestion that the limestone is of earlier Tertiary age but contaminated by younger microfossils (Burnett et al., 1987). A Late Pliocene age, if correct, would indicate a relatively rapid accretionary rate, in excess of 13 mm/10^6 yrs, for the ferromanganese crust at this location.

Externally, the crusts on the indurated pelagic limestones display a close-spaced, botryoidal ("cauliflower-type") surface morphology, similar to that found on calcarenites and coral breccias. Not infrequently, however, submarine erosion has modified the surfaces by first flattening the crests of the botryoidal lobes, and, at a more advanced stage, producing large patches with a glazed, but flaky, reniform morphology (Figures 3b,c). The reniform shapes and the flakiness presumably reflect a cryptic or latent layering of at least part of the lower levels of the crusts.

Macroscopically, the crusts appear mostly structureless, with resinous to subvitreous lusters and hackly to subconchoidal fractures that give them a coal- or pitch-like appearance. Under the microscope, however, crude micro-banding can often be discerned as an alternation of either bright and dull layers or layers enriched and impoverished in light-brown ferruginous inclusions. Rarely, the banding is concentrically arranged, with associated traces of radial growth structures, around cavities within the crust. A zone of microbotryoidal columnar growths, aligned perpendicular to the limestone rim, occasionally supervenes at the crust-limestone interface. The phosphatized limestone itself is fine-grained and compact, and ranges in color from white (N9) to yellowish gray (5Y 7/2) with irregular moderate yellowish brown (10YR 5/4) blotches.

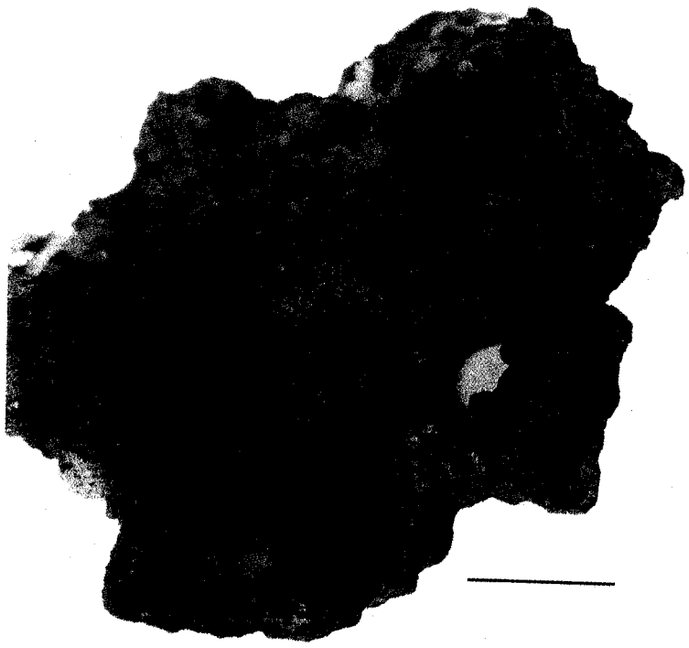

Figure 4. Merging of manganiferous (bottom) and ferruginous (top) zones on the inner surface of a ferromanganese crust (Station Q880). Note the glossy, blister-like structures at top right (arrow). Scale bar represents 50 mm.

The distribution of iron oxides within the limestones is not extensive; they are mostly restricted to a thin, but discrete, ochreous seam at the junction of the limestone and crust. The limestone interface with the crust is almost invariably curved and embayed, with finely divided manganese oxide impregnating the marginal, and sometimes the inner, limestone as dendritic growths and dense grayish black (N2) patches (Figure 3d). The latter features are a clear indication that the ferromanganese oxides comprise more than a mere encrusting layer: they provide evidence of widespread and substantial metasomatic replacement of the limestone by the oxides.

The origin of the ochreous layer that frequently occurs beneath the black crusts on phosphatized limestone, calcarenite and coral breccia is uncertain and open to at least two interpretations. One postulates a greater mobility of dissolved iron in penetrating pore spaces in limestone, calarenite and breccia substrates, ahead of the manganese oxides. The "scoriaceous" iron oxide structures that appear in some cavernous breccias, as described above, evidently precipitated directly from solution and would seem to favor such an interpretation. On the other hand, some iron oxides, especially those rimming the metasomatically replaced limestones, could be regarded as residual concentrations of a minor, but primary, component of the limestones.

MINERALOGY AND GEOCHEMISTRY

Apart from traces of crystalline calcite, dolomite and (possibly) goethite, the mineral components of the ferromanganese crusts on the seamounts under consideration are shown by X-ray diffraction analysis to be entirely amorphous or very poorly crystalline. The colloidal nature of these deposits is indeed evident from the isotropic, cuspate micro-banding that characterizes thin-sections of the crusts (Figure 5). By analogy with comparable crusts and manganese nodules in adjacent areas of the Pacific Ocean (Meylan et al., 1978; Koski et al., 1985), the main mineral phases present are assumed to be δ-MnO_2 and an X-ray amorphous, goethitic, iron oxyhydroxide (possibly mixed α- and γ-FeOOH). The small amounts of carbonate minerals detected in the crusts probably represent incompletely replaced substrate material.

Major and trace element concentrations in bulk crust samples were determined by X-ray fluorescence analyses (Tables 2, 3). It is readily apparent from the analytical results that samples Q527 and Q880 contain abnormally high proportions of calcium and magnesium, and have correspondingly diminished contents of most other elements. The high CaO and MgO values in these samples, which differ from the others in possessing unusually thin ferromanganese crusts, clearly reflect heavy contamination by the carbonate substrates. Except in the two samples specified, the combined manganese and iron (MnO + Fe_2O_3) content maintains relatively high values (between 40-46%), although the proportions of manganese and iron vary considerably. Sample Q556 from Albert Henry Seamount is unusual in having a combined MnO + Fe_2O_3

content of nearly 60%. The amount of material lost during analysis through ignition to 1000°C (LOI) is also consistently high, ranging mostly between about 39-45% by weight. This includes surface and intergranular moisture, water of hydration, and the carbon dioxide embodied in accessory calcite and dolomite.

The carbonate-rich sample Q527 shows a marked depletion (relative to the other samples) in practically all trace elements, implying that the latter are associated mainly with the thin ferromanganese crust. The one obvious exception is strontium, which, at roughly three times the average value for other samples, evidently has a closer affinity with the primary coralline carbonate. The relationship between iron and manganese and their fellow transition metals, nickel, cobalt and copper, is a very positive one. Plotting the proportions of Fe and Mn in the crusts against the combined totals for Co+Ni+Cu indicates a very clear linear increase in the latter with increasing Mn (Figure 6). In effect, this trend is governed by the Co and Ni values, as Cu values remain fairly constant throughout (mostly between 350-550 ppm) and are apparently unaffected by variations in the proportions of Fe and Mn in the crusts.

These results differ significantly from those obtained, for instance, for manganese nodules from the central Indian Ocean (Jauhari, 1987), where it has been found that the cobalt content, unlike the nickel, decreases as the Mn:Fe ratio increases. The depth regime and sedimentary

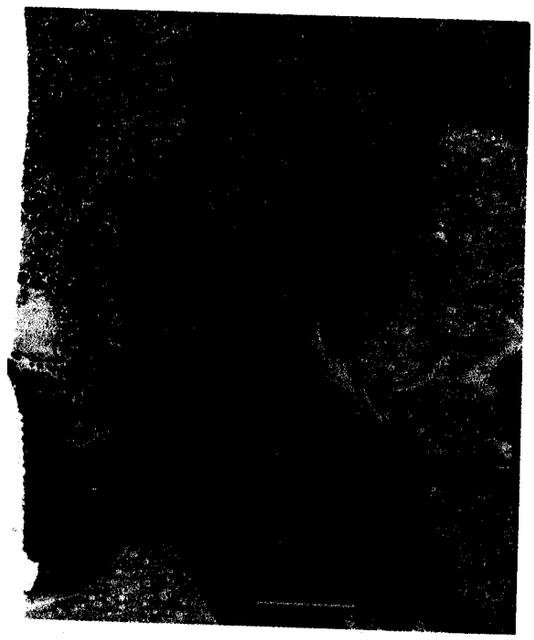

Figure 5. Photomicrograph showing opaque ferromanganese oxides encrusting and impregnating pale foraminiferal limestone. Totally opaque layers are separated by mottled zones of microbotryoidal growth. Note also the dendritic oxide growths within the limestone fragment (right). (Station Q551). Scale bar represents 5 mm.

Table 2. XRF analysis of major elelments in SW Pacific bulk ferromanganese encrustations.

Wt%	Q527 Falealupo Smt	Q551 Kalolo Smt	Q556 Alb. Henry Smt	Q564 Eclipse Smt	Q873 MacLeod Guyot	Q880 Solomoni Guyot	Q894 Perez Smt	Q895 Kalolo Smt
SiO_2	1.93	2.08	3.39	6.67	6.85	0.74	2.41	1.39
TiO_2	0.18	1.20	1.86	1.46	1.07	0.90	1.20	1.13
Al_2O_3	0.66	0.59	1.26	1.55	2.05	0.92	0.71	0.47
Fe_2O_3 *	2.33	20.01	20.22	20.40	26.54	15.89	18.79	16.51
MnO	11.01	25.69	38.99	21.23	14.82	9.74	23.55	29.50
MgO	2.92	1.67	2.78	1.53	1.43	8.33	1.49	1.92
CaO	44.60	2.83	4.43	4.20	4.13	19.51	4.90	2.75
Na_2O	0.52	2.14	3.07	1.95	1.81	1.23	1.72	1.94
K_2O	0.06	0.39	0.06	0.40	0.38	0.16	0.37	0.47
P_2O_5	0.08	0.71	1.39	0.83	0.91	0.61	1.61	0.57
LOI **	45.20	40.77	19.00	38.19	39.09	39.74	41.19	42.27
Total	99.49	98.08	97.54	98.41	99.08	97.77	97.94	98.91

* total iron

** loss on ignition to 1000°C

*Table 3. XRF analyses of trace elements in SW Pacific bulk ferromanganese encrustations.**

	Q527 Falealupo Smt	Q551 Kalolo Smt	Q556 Alb. Henry Smt	Q564 Eclipse Smt	Q873 MacLeod Guyot	Q880 Solomoni Guyot	Q894 Perez Smt	Q895 Kalolo Smt
Sr	3687	1356	-	1362	1309	805	1328	1231
Rb	3	3	-	3	3	2	3	5
Th	6	26	-	26	14	16	35	32
U	<1	9.3	-	10.0	8.4	6.1	10.0	9.7
Y	186	-	201	202	123	244	151	Zr
Zr	30	391	-	473	474	227	386	310
Nb	5	59	-	49	83	67	68	58
Ga	<1	2	-	3	3	3	3	4
Pb	68	1463	-	1178	930	784	1396	1649
Cu	60	374	521	459	531	241	470	538
Ni	126	5068	7786	2776	2002	1484	5351	7570
Co	148	11469	18369	6307	3172	3928	9508	13530
Zn	51	540	-	496	496	300	575	700
As	29	565	-	495	472	328	523	573
W	14	86	-	64	62	35	87	106
Ba	187	1661	-	1614	1381	1058	2101	1743
Cr	23	42	-	29	22	26	39	66
V	63	701	-	705	651	585	756	658
Sc	3	4	-	9	11	10	8	3
Ce	14	332	-	406	135	184	462	389
La	19	243	-	385	314	188	252	169
Sb	8	47	-	37	46	46	47	42
Ag	5	7	-	7	7	2	5	7

* ppm, vacuum-dried basis, i.e., minus free water, but including combined water

associations in the Indian Ocean are, of course, quite different from those on the SW Pacific seamounts.

The highest value for combined Co+Ni+Cu encountered in the SW Pacific crusts considered here is 2.67% in the thick crust at station Q556 on Albert Henry Seamount. The Mn:Fe ratio for this crust is about 2:1. Projection of the linear trend to the commercially critical 3% value for total Co+Ni+Cu suggests that such a value is likely to be attained only when Mn:Fe ratios exceed 2.5:1 (Figure 6). Nevertheless, the commercially critical value of 1.0% for cobalt alone (cf. De Carlo et al., 1987) is exceeded on both Albert Henry Seamount and on Kalolo Seamount northwest of the Tokelau Islands, and it would appear that the thick ferromanganese crusts on these seamounts, and perhaps on Perez Seamount also, are potentially of economic grade.

The explanation for the linear relationship between the combined trace metal values on the one hand, and the relative proportions of Mn and Fe on the other, remains obscure. Latitude is not obviously a critical factor. The highest Co+Ni+Cu values (1.5-2.6%) do occur in the lowest latitudes (between 6°30'- 10°00'S), on Albert Henry, Kalolo and Perez Seamounts, but the next highest value (0.95%) is found in the southeastern extremity of the area investigated, on Eclipse Seamount (Q564, 19°09'S) in the southern Cook Islands. A third category of ferromanganese

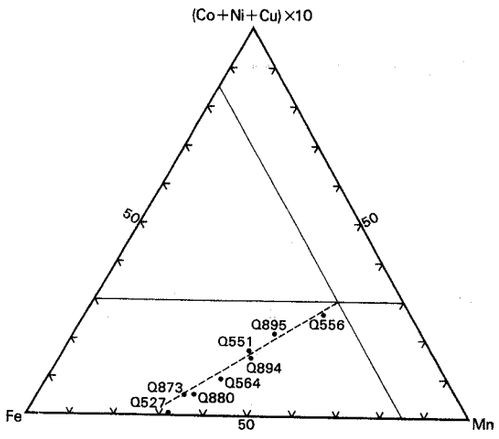

Figure 6. Ternary diagram comparing the Fe, Mn, and combined Co + Ni + Cu contents of ferromanganese crusts in the region of the SW Pacific covered by this survey.

crusts, with appreciably lower Co+Ni+Cu values (0.56-0.57%), characterizes Solomoni and MacLeod Guyots which are situated in intermediate latitudes (11°-13°S).

Similarly, the existence of a relationship between trace metal content and water depth remains uncertain. The highest Co+Ni+Cu values at Albert Henry, Kalolo and Perez Seamounts occur at depths between 1300-1800 m, and mainly in the same depth range as the extremely low values on Falealupo Seamount. The moderately high trace metal values on Eclipse Seamount are found at depths between 1650-1800 m, whereas the low values on Solomoni and MacLeod Guyots relate to depths of about 1000 m and 1500 m, respectively.

There may be some significance in the fact that the highest Co values encountered in this part of the SW Pacific occur in crusts that have accumulated on phosphatized limestone substrates. This parallels the situation in the equatorial Atlantic Ocean, where Goddard et al. (1987) have also found highest Co values in ferromanganese encrustations on phosphatized limestones. These authors attributed the high Co values to scavenging of transition metals by incipient Mn-rich colloids, in persisting zones of vigorous upwelling with elevated oxygen-minimum layers, conditions that would also favor phosphogenesis.

Bearing in mind the appreciable age of the limestone substrates in the SW Pacific, and the great thickness of some of the ferromanganese accumulations upon them, it is possible that the generation of high Co values may be episodic. Pichocki and Hoffert (1987), for instance, reported a layered sequence in nodules and crusts from the eastern Pacific, with low (0.5%) Co values in a 20 mm-thick, well crystallized, old *inner* layer, rising to over 2% Co in the relatively thin (5 mm), poorly crystallized, botryoidal, young *outer* layer. Such a clear-cut sequence has not, as yet, been observed megascopically in the sector of the SW Pacific covered here, and it is not certain that the layering described by Pichocki and Hoffert (1987) has occurred in this region.

No equivalent of the well crystallized inner layer of Pichocki and Hoffert has been recognized, while the smooth, reniform surfaces of the high-Co crusts in the SW Pacific suggest that any local representatives of the outer cobalt-rich botryoidal layer, if they ever existed in this region, have either been removed by erosion or had their growth inhibited by current action. In their amorphous or very poorly crystalline nature, and also in their proportions of the critical elements Mn (18-23%), Co (0.9-1.3%), Ni (0.5-0.7%) and Fe (11-14%), the SW Pacific cobalt-rich crusts most closely resemble the outer layer of crusts in the eastern Pacific.

CONCLUSIONS

Ferromanganese crusts are present on Kalolo and Perez Seamounts in the Central Pacific Basin north of the Tokelau Islands, on Albert Henry Seamount west of the Manihiki Plateau, on Eclipse Seamount southeast of Aitutaki in the southern Cook Islands, on Falealupo Seamount northwest of Western Samoa, and on Solomoni and MacLeod Guyots of the North Fiji Plateau. The crusts vary in thickness from 0.1-0.2 mm on Late Pleistocene scleractinian coralla to about 40 mm on much older pelagic limestone substrates which have been phosphatized. Other types of substrates (semi-consolidated to consolidated calcarenites and limestone breccias) display intermediate Fe-Mn crust thicknesses. The surface texture of the crusts is principally a function of crust thickness, modified (flattened or grooved) in some samples by what appears to be post-accumulation submarine erosion. Internal structure is reflected externally in the surface texture of the crusts. Thin crusts on the youngest substrates show microbotryoidal surfaces, while thicker crusts show a cauliflower-like surface of botryoids which have superimposed microbotryoids.

The substrate surfaces on which the crusts have precipitated are typically uneven, and substrates with the thickest crusts have been replaced to a variable extent by Fe-Mn oxides. As determined by X-ray diffraction analysis, the crusts are composed of very poorly crystalline to amorphous δ-MnO_2 and presumably some form of iron oxyhydroxide. Values of total Co+Ni+Cu are a function of both the Mn:Fe ratio and the amount of incompletely replaced carbonate included in crust samples, the latter factor reducing the total value. Higher Mn:Fe ratios are accompanied by increases in total Co+Ni+Cu. The highest value for total Co+Ni+Cu found in this study (2.67%) occurs in the thickest (40 mm) crust collected (Albert Henry Seamount). Cobalt values in excess of 1.0% characterize the crusts of Albert Henry Seamount (northern Cook Islands) and Kalolo Seamount (northwest of the Tokelau Islands), indicating that they may be of economic interest at some time in the future.

REFERENCES CITED

Burnett, W.C., D.J. Cullen, and G.M. McMurtry, 1987, Open-ocean phosphorites - in a class by themselves?, *in* P.G. Teleki,

M.R. Dobson, J.R. Moore, and U. von Stackelberg, eds., Marine minerals: resource assessment strategies: NATO Conference Series, Dordrecht, D. Reidel Publishing Co., p.119-134.

Cullen, D.J., and W.C. Burnett, 1986, Phosphorite associations on seamounts in the tropical southwest Pacific: Marine Geology, v.71, p.219-236.

De Carlo, E.H., P.A. Pennywell, and C.M. Fraley, 1987, Geochemistry of ferromanganese deposits from the Kiribati and Tuvalu region of the west central Pacific Ocean: Marine Mining, v.6, p.301-321.

Goddard, D.A., G. Thompson, E.J.W. Jones, and H. Okada, 1987, The chemistry and mineralogy of ferromanganese encrustations on rocks from the Sierra Leone Rise, equatorial Mid-Atlantic Ridge and New England Seamount Chain: Marine Geology, v.77, p.87-98.

Jauhari, P., 1987, Classification and inter-element relationships of ferromanganese nodules from the Central Indian Ocean Basin: Marine Mining, v.6, p.419-429.

Koski, R.A., J.R. Hein, R.M. Bouse, and R.E. Sliney, 1985, Composition and origin of ferromanganese crusts from Tonga Platform, southwest Pacific, *in* D.W. Scholl and T.L. Vallier, eds., Geology and offshore resources of Pacific island arcs - Tonga region: Circum-Pacific Council for Energy and Mineral Resources, Earth Science Series 2, p.179-186.

Meylan, M.A., G.P. Glasby, J.C. McDougall, and R.J. Singleton, 1978, Manganese nodules and associated sediments from the Samoan Basin and Passage: New Zealand Oceanographic Institute Oceanographic Field Report, v.11, 61 p.

Pichocki, C., and M. Hoffert, 1987, Characteristics of Co-rich ferromanganese nodules and crusts sampled in French Polynesia: Marine Geology, v.77, p.109-119.

Rock-Color Chart Committee, 1948, Rock-color chart: Geological Society of America, Boulder, Colorado (reprinted 1979).

McKelvey, B.C. 1996. Sediment description and distribution, *in:* Meylap, M.A., and G.P. Glasby (eds) Manihiki Plateau, Machias and Capricorn Seamounts, Niue, and Tofua Trough: Results of *Tui* Cruises. SOPAC Technical Bulletin 10: 119123.

SEDIMENT DESCRIPTION AND DISTRIBUTION

B.C. McKelvey

Department of Geology and Geophysics, University of New England, Armidale, NSW 2351, Australia

ABSTRACT

Sediment samples were collected at 79 stations, mostly by pipe dredges or in a plastic tube strapped into rock dredges; gravity coring produced four short sediment cores. Nanno-foram oozes were found at depths shallower than 4000 m on the flanks and top of the Manihiki Plateau and associated atolls. Coarser foram oozes or carbonate sands occur on the flanks of Rarotonga in the southern Cook Islands. Abyssal clays were found at depths greater than 4800 m adjacent to the Manihiki Plateau in the Penrhyn and Samoan Basins, and in the Southwestern Pacific Basin east of the Tonga-Kermadec Trench. Much of the pelagic sediment in the Manihiki Plateau and southern Cook Islands areas contains a resedimented component along with coral rubble, but little volcaniclastic or other non-carbonate material. Volcaniclastics make up to 5% of the pelagic sediments from Machias and Capricorn Seamounts, Niue, and adjacent deep-sea areas. Pteropod ooze occurs on the crest of Capricorn, and both pteropod-bearing foram ooze and volcaniclastic sand were dredged from the crest of Machias. Based on non-resedimented carbonate contents, the CCD appears to be deeper in the Manihiki Plateau area than in the Machias-Capricorn area.

INTRODUCTION

Varied sedimentary detritus was recovered from 79 stations (Table 1). The samples range from pelagic carbonate oozes and clays; to (solitary) pebbles and gravel composed of lava, hyaloclastite and volcaniclastic clasts; and abraded debris of coral, algal and limestone origin. The pelagic clays and oozes predominate by far. The gravels and pebbles were recovered from the slopes of seamounts and islands, and from scarps. Almost all of this coarse detritus is considered to be redeposited by downslope movement or slumping, and is described in more detail by Meylan and Glasby (this volume; see also Glasby and Meylan, this volume). Some coarse material may be from actual outcrop. With the exception of four gravity cores, all the samples were recovered by either pipe-dredge or rock-dredge. This is in part responsible for the admixing of some sediment types. None of the dredged oozes or clays show any sign of lithification. From U315 onwards, plastic core liner tubes were affixed inside the rock dredges in order to retain any fine fractions (i.e., pelagic sediment) present. In the following descriptions, the sedimentary materials recovered from the Manihiki Plateau, from Machias Seamount–Capricorn Seamount–Niue, and from the southern Cook Islands are discussed separately.

MANIHIKI PLATEAU (U291–340)

Sediment was recovered from 36 of the 49 stations occupied. Pelagic carbonate oozes (predominantly nanno-foram) and abyssal red clays (5 YR 3/4) predominate by far, being recovered from 33 stations. The oozes were recovered from 4000 m and above, whereas the abyssal clay samples ranged from 4796-4837 m (U328) down to 5283 m (U295). However, from two stations (U311 at 4412 m and U339 at 4204–4219 m) mixtures (due to dredging) of clay and ooze were recovered. These latter data suggest the Carbonate Compensation Depth in the Manihiki Plateau region to be in the vicinity of 4200–4000 m. Areal petrographic variations of the pelagic sediments are few and minor. Many do contain trace amounts of volcanic glass, but there is no evidence for major proximal contemporaneous volcanism. A few authigenic minerals (e.g., ?celestobarite) are present

Table 1. Sediment sample data.

Stn	Depth (m)	Sediment type	Color
12°45'S transect			
U293	2916-2921	Nanno-foram ooze	5Y7/2
U294	3829	Nanno-foram ooze	5Y7/2
U295	5283	Abyssal clay	5YR3/4
U296a	5130	Abyssal clay	5YR3/2
U297a	5227	Abyssal clay	5Y3/2
U298	4996	Abyssal clay	5YR3/2
U301	2720	Nanno-foram ooze	5Y7/2
U302	2630	Nanno-foram ooze	5Y7/2
U303	2530	Nanno-foram ooze	5Y7/2
U304a	2366	Nanno-foram ooze	5Y7/2
U305	2385	Nanno-foram ooze	5Y7/2
U306a	2460	Nanno-foram ooze	5Y7/2
U307	2586	Nanno-foram ooze	5Y7/2
U309	4000	Nanno-foram ooze	5Y7/2
U310	5154	Abyssal clay	5YR3/2
Manihiki-Rakahanga			
U311	4412	Abyssal clay, foram-rich nanno ooze	10YR4/2, 5Y7/2
U312	3971	Nanno-foram ooze	5Y7/2
U316b	2600	Foram ooze	5Y7/2
U317	2111-2161	Nanno-bearing foram ooze	5Y7/2
U318	1208-1231	Nanno-bearing detrital clay-foram ooze	5Y7/2
U320	2788-3813	Foram ooze	5Y7/2
U321a	5047-5114	Volcanic-rich abyssal clay	5YR3/2
U322b	1560-1754	Foram ooze	5Y7/2
U323	2971-3066	Foram ooze	5Y7/2
Pukapuka, Tema Reef, Nassau			
U324	417-446	Algal gravel	5Y7/2
U326	2121-2161	Foram ooze	5Y7/2
U327	3394-3217	Detrital clay-foram ooze	5Y7/2
U328	4796-4837	Abyssal clay	5YR3/4
U332	1199-1377	Detrital clay-rich foram ooze	5Y7/2
U333b	1913-1575	Foram ooze	5Y7/2
U336b	981-1297	Detrital clay-rich foram ooze	5Y7/2
U337	1001-804	Algal gravel	5Y7/2
U339	4219-4204	Nanno-bearing detrital clay-foram ooze	10YR5/4, 5Y7/2
U340	5253-5268	Abyssal clay	5YR3/4
Machias and Capricorn Seamounts, Niue			
U343	725-730	Volcaniclastic sand	10YR4/2

Stn	Depth (m)	Sediment type	Color
U344	670-675	Pteropod-bearing foram ooze	5Y7/2
U347	3684-3905	Nanno-bearing abyssal clay	-
U351	996-976	Pteropod ooze	5Y5/2
U352	4684-4689	Calcareous abyssal clay	10YR4/2
U353	5495	Abyssal clay	10YR4/2
U357	3596-3612	Detrital clay-foram ooze	5Y7/2
U359	5299	Abyssal clay	10YR4/2
Rarotonga			
U371	1486-1516	Foram-bearing carbonate sand	5Y7/2
U372	2042-2092	Foram ooze	5Y7/2
U373	2450-2490	Nanno-bearing foram ooze	5Y7/2
U374	1472-2012	Foram-bearing carbonate sand	5Y7/2
U375	1272	Foram-bearing carbonate sand	5Y7/2
U376	1992-1968	Nanno-bearing foram carbonate sand	5Y7/2
U377	2450-2296	Nanno-bearing-foram carbonate sand	5Y7/2
U378	3031-2961	Nanno-bearing foram carbonate sand	5Y7/2

in some of the abyssal clays. Coarse detritus, either sparse gravel admixtures in pelagic sediment or else discrete samples and even single pebbles were recovered at 24 stations, from depths down to 5150 m at U310. Prior to the fitting of tubes at U315, the rock dredges retained only such coarse fractions. Most of this detritus is limestone fragments, or else abraded coral and shell debris. The remainder recovered are of basalt or else basaltic volcaniclastic provenance. All this coarse material is interpreted as being of downslope mass movement (resedimentation) origin. Similarly, volcanic sand admixtures in pelagic sediment (e.g., U310, U316b) are interpreted as resedimented.

12 °45' S Transect (U292-310)

The pelagic sediments recovered from 15 stations occupied on an east-west transect across the Manihiki Plateau (see Table 1) are yellowish gray carbonate oozes (5 YR 7/2) and grayish-brown to moderate brown abyssal red clays (5 YR 3/2 to 5 YR 3/4). The carbonate oozes were recovered from depths of 4000 m (U309) and above. The red clays occur at depths of nearly 5000 m (U296 at 4996 m) and deeper, on either flank of the plateau. Volcaniclastic pebbles were recovered by rock dredge from U292, north of Suwarrow, and from U308a and U308b low on the western margin of the Manihiki Plateau. Because the rock dredge was not at that time fitted with collecting tubes, the nature of any pelagic sediment present at these two sites is not known.

Carbonate Oozes

Of the 10 carbonate samples, all are nanno-foram oozes except for U309, the deepest recovered, which is a foram-nanno ooze from 4000 m. The deepest nannofossil-bearing foram ooze (U294) is from 3829 m. These carbonate oozes nearly all contain less than 1% non-carbonate fraction.

Nanno-Foram Oozes

These consist simply of a framework of broken and complete forams and a variable matrix (20-50%) of nannofossils. Some of this matrix is presumably composed also of microcrystalline carbonate. A very few siliceous spines (radiolarian, sponge) are also present. The non-biogenic component (<1%) includes brown or colorless volcanic glass, opaque oxides and fish debris (collophanite). Textural diversity is brought about by variation in the nannofossil component, and more especially by the size distribution of the foram types present. These latter are remarkably bimodal with two size classes averaging around 0.1 mm and 0.35 mm respectively. Forams in the latter size class are often broken fragments, and are much more abundant in samples U293, U294 and U305.

Foram-Bearing Nannofossil Ooze

The one sample recovered (U309) consists simply of small forams (ca 0.09 mm) dispersed in an abundant matrix

(ca 90%) of nannofossils (and microcrystalline carbonate). Accessory components (<1 %) include trace amounts of volcanic glass, opaque oxides, ?sponge spicules, fish debris and an authigenic relatively coarse (ca 0.03 mm) carbonate, probably siderite or dolomite.

Abyssal Red Clays

In addition to the non-resolvable reddish brown (in smear slide) clay minerals (frequently diagenetically or organically pelleted), the other components are present only in trace amounts (cumulatively usually less than 1%). These include opaque oxides, a ?zeolite (U295), volcanic glasses, forams (U310), fish debris, microcrystalline carbonate granules, small (0.07 mm) siderite or dolomite rhombs (U310) and ?celestobarite (U309, 310). The latter site sample also contains appreciable (<5%) resedimented volcanic detritus.

Manihiki/Rakahanga (U311-323)

Samples of pelagic sediment were recovered from 9 of the 13 stations in the vicinity of these two islands (Table 1). Six samples are yellowish-gray carbonate oozes recovered from between 1555 m and 3971 m. Another sample (U311) of mixed (due to dredging) carbonate ooze and pelagic clay was obtained from 4412 m. The remaining sample (U321a) is a grayish brown (5 YR 3/2) abyssal red clay from 5114-5047 m.

Carbonate Oozes

The six carbonate ooze samples show considerable textural variation, ranging from nanno-foram ooze (U312) and nanno-bearing foram ooze (U317) to coarse foram oozes (U320, U322b, U323) apparently devoid of nannofossils. Only U311, 312 and 320 are devoid of any coarse resedimented admixture. Coarse carbonate debris (limestone and coral rubble) dredged from U322 and U323 strongly suggests that these coarse oozes and probably also U317 are resedimented from shallower depths. U316 is a similar coarse foram ooze with a small (<2%) component of altered volcanic glass and sparse volcanic pebbles. All the oozes contain trace amounts of fish debris, siliceous spicules, opaque iron oxide granules and authigenic microcrystalline carbonate. U323 also contains volcaniclastic (hyaloclastite) pebbles similar to the solitary pebble dredged at U314.

Volcanic (Sand)–Rich Abyssal Red Clay (U321a)

A sand fraction (<0.45 mm) of up to 30%, and composed of varieties of usually altered (to clay minerals) volcanic glass and subordinate plagioclase is present. Interpenetration twins of ?phillipsite were noted. The bulk of the sample consists of non-resolvable clay minerals studded with reddish opaque oxide granules. A small (<1%) biogenic contribution includes siliceous (radiolarian and/or sponge spicules or spines), small foraminifera and fish debris.

Pukapuka/Tema Reef/Nassau (U324–340)

Fine-grained sediments were recovered from 7 of the 17 stations occupied (Table 1). Two samples are moderate brown (5 YR 3/4) abyssal red clays (U328, U340) recovered from 4837 m and 5268 m, respectively. The other five are essentially foram oozes, but with considerable textural variation, and some (e.g., U326) may be resedimented. These oozes were dredged from depths ranging between 981–1297 m and 4204–4219 m. Abraded (i.e., resedimented) coral and shell debris admixtures are not uncommon in the carbonate oozes. Two coarse (i.e., non-pelagic) carbonate sediment samples (U324, U327) dredged from between 417-446 m, and from between 804–1001 m, respectively, are resedimented algal gravels (4–10 mm). Volcaniclastic or basaltic pebbles were recovered with carbonate oozes at U332 and U333, and with red clay at U328.

Carbonate Oozes

Of definite pelagic origin are foram oozes U327, U336b and U339. U327 and U336b contain an appreciable (10–25%) optically non-resolvable clay mineral component (which may also obscure some nannofossils), although the bulk of the samples are forams. The clays are colorless in marked contrast to those in the abyssal red clays. The distinctly mottled appearance of U339 (i.e., 10 YR 5/4 and 5 YR 7/2) suggests that it is a mixed sample (due to dredging) of nanno-foram ooze and pelagic clay. Of presumed resedimented origin is U327, a relatively coarse foram ooze (0.6 mm–1.5 mm) devoid of both nannofossils and clays, and displaying remarkably delicate preservation of the foram tests.

Abyssal Red Clays

The two abyssal red clays sampled (U328, U340) contain few accessories. Both contain very fine-grained granules of authigenic carbonate and trace amounts of siliceous spicules and fish debris. A coarse volcaniclastic sand fraction was recovered from U328, suggesting either mixing during resedimentation or else mixing during sampling.

MACHIAS AND CAPRICORN SEAMOUNTS AND NIUE (U341–359)

Relatively few samples of pelagic sediment were recovered from the stations in this region. Collecting-tubes

fitted into the rock dredges did recover carbonate oozes from the crests of both Machias and Capricorn seamounts. In contrast to the Manihiki Plateau, the pelagic sediments do contain an appreciable (up to 5 %) volcanic component. However, dredging the flanks of these two seamounts and also those of Niue, whilst producing an abundance of carbonate rubble and pebbles of basalt and basaltic volcaniclastics, recovered little truly pelagic sediment. Piston cores taken between Capricorn and Niue (e.g., U353, U359) recovered abyssal red clay.

The recovery of abyssal red clay at Site 347 (3905–3864 m) suggests the Carbonate Compensation Depth to be less deep in the Machias–Capricorn region than on the flanks of the Manihiki Plateau.

Machias Seamount (U341–346)

Two smear slides were examined, U344 (670–675 m) from near the top of the seamount, and U343 taken from a slightly lithified pebble dredged from 725–730 m. U344 is a relatively coarse (up to 1.5 mm) yellowish gray pteropod-bearing foram ooze or sand, devoid of any fine fraction and also containing relatively abundant (ca 5 %) ?fish debris or collophanite. Apart from a few grains of volcanic glass there is no non-biogenic component. The lack of a fine fraction and the presence of coralline pebbles and shell debris in the sample suggests resedimentation or else current winnowing.

U343 is a volcaniclastic dark yellowish-brown fine sandstone (10 YR 4/2) with a crystal vitric tuff admixture of feldspars, pyroxenes and glass. The (originally glassy) sand grains are either coated with opaques and/or altered to clay minerals. Forams are present in trace amounts only. It is assumed this sample is a resedimented sand slightly lithified *in situ*.

Capricorn Seamount (U347–352)

U347 (3864–3905 m) is a nanno-bearing pelagic clay, studded with ferruginous granules and containing only a very few forams. U352 (4684-4689 m) is a remarkably calcareous pelagic clay or marl, occurring as a fine admixture within a sample of resedimented fine gravel and coarse sand. It is not known whether most of the carbonate is highly corroded biogenic material, or else of diagenetic origin. Several grains of rhomboidal siderite are present. Volcanic detritus (glass, feldspars, ferromagnesian minerals) composes approximately 5 % of the slide. Forams and radiolarians are present only in trace amounts.

Capricorn—Niue Transect (U353–360)

U357 (3596–3612 m) is a detrital clay foram ooze with a small (ca 2 %) volcanic component of feldspars, ferromagnesian minerals and several varieties of glass and pumice. Nannofossils, radiolarians and sponge spicules are present only in trace amounts.

U353 (5495 m) and U359 (5299 m) are both abyssal red clays (10 YR 3–4/2) with appreciable volcanic components of fresh glass and pumice, feldspars, and ferromagnesian minerals. U353, in particular, shows a diversity of delicately preserved pumiceous and vesicular glass. In both cases, radiolarians and forams are present in trace amounts only. U359, taken from the core-catcher of a 5 m core, shows incipient lithification.

SOUTHERN COOK ISLANDS (U371–378)

Eight samples of unconsolidated fine-grained sediments (U371–U378) were dredged from the southeast and northeast slopes of Rarotonga. All proved to be essentially detrital carbonate sands and silts with subordinate foram and very minor nannofossil components. U375 contains an appreciable coarse component (>4 mm) of abraded shell and algal debris. In contrast to the Manihiki Plateau sediments, none of those recovered from Rarotonga are truly pelagic carbonate oozes. No bathyal or abyssal clays were recovered. The detrital carbonate sand and silt grains (angular to subrounded) are mainly composed of micro-crystalline carbonate (micrite), although some abraded sand grains are almost certainly fine ?shell debris. All samples contain a small (<3%) admixture of translucent brown volcanic glass.

Part 4

BIOLOGY AND BOTTOM PHOTOGRAPHY

Main, W.deL., D.G. McKnight, and G.P. Glasby 1996. Pelagic and benthic megafauna and bOllom photography, *in:* Meylan, M.A., and G.P. Glas~y (eds) Manihiki Plateau, Machias and Capricorn Seamounts, Niue, and Tofua Trough:
Results of *Tui* Cruises. SOP AC Technical Bulletin 10: 125-131.

PELAGIC AND BENTHIC MEGAFAUNA AND BOTTOM PHOTOGRAPHY

W.deL. Main, D.G. McKnight

National Institute of Water and Atmosphere Research Ltd, PO Box *14901,* KiJbirnie, Wellington, New Zealand

G.P. Glasby

Department of Earth Sciences, University of Sheffield, Sheffield S3 7HP, England

ABSTRACT

Scleractinian coral rubble was the dominant biological material recovered during the *Tui* cruise, but at 29 stations some other type of organic hard part was collected. These are mostly gorgonian corals or mollusc shells on atoll slopes, while in the abyssal depths of the Penrhyn and Samoan Basins, only shark teeth were dredged. Sample abundance and diversity decrease with increasing depth around atolls. Bottom photography in the Penrhyn Basin showed an abundance of Mn nodules at the surface in a location where an abundant haul of nodules was dredged; photographs at another site in the basin where abundant nodules were also collected showed that the nodule field had been at least partially buried by volcanic-rich abyssal clay. An extensively bioturbated carbonate ooze sediment surface was photographed on the Manihiki Plateau.

INTRODUCTION

It was envisioned that biological samples collected by rock and pipe dredge would be preserved for detailed study. Unfortunately, only limited samples other than coral were obtained because of the nature of the samplers used and specimens of fragile organisms were not well preserved. In this paper, the specimens have been identified only to major group, but some groups have been studied in detail by other investigators (see below). In addition, underwater photographs were taken at five stations. These gave an indication of manganese nodule distribution, particularly in deep-water stations adjacent to the Manihiki Plateau, as well as of biological activity on the seafloor.

MEGAFAUNA SAMPLES

Except for the scleractinian corals discussed by Grange and Veron (this volume) and the gorgonian corals included in the study of Grigg (also this volume), the dredged faunal remains are small. They include numerous whole or fragmented pelecypod and gastropod shells (see Beu, this volume), but only a limited number of other organisms. Excluding scleractinian corals, which were recovered in most of the dredge hauls, biological hard parts were recorded at 29 stations (Table 1). At 14 of these stations, scleractinian corals in varying states of preservation were also collected (cf. Appendix C, Meylan and Glasby, this volume). Phyla other than Coelenterata (Cnidaria) which are represented include Porifera (Parazoa) (calcareous and siliceous sponges), Annelida (polychaetes), Echinodermata (ophiuroids, crinoids, and echinoids), Arthropoda (crustaceans – barnacles and a crab), and some small Mollusca (scaphopods and pteropods) in addition to the pelecypods and gastropods.

At deep-water stations (depths >5000 m) in the Penrhyn and Samoan Basins, the only megafaunal remains collected were shark teeth associated with Mn nodules (Stns U296a, U321a, and U340); some of the teeth display partial

Table 1. Megafauna samples (excluding scleractinian corals).

Stn	Gear	Locality	Depth (m)	Sample description
U296a	Pipe dredge	Penrhyn Basin	5130	5 shark teeth, 14-30 mm long; some with thick Mn-stain.
U300	Rock dredge	Eastern margin slope, Manihiki Plateau	3747-3758	1 shark tooth, 31 mm long.; vitreous crown, but Mn-encrustation with microbotryoidal surface up to 2 mm thick on root.
U301	Pipe dredge	Eastern side of crest of Manihiki Plateau	2720	2 delicate scaphopods.
U307	Pipe dredge	Western margin slope, Manihiki Plateau	3586	1 polychaete tube.
U316b	Rock dredge	Rakahanga	2600	1 siliceous sponge; mollusc shell frags.
U317	Rock dredge	Manihiki Island	2161-2111	Mollusc shell frags.
U321a	Pipe dredge	Penrhyn Basin, east of Manihiki Island	5114-5047	8 shark teeth, 19-34 mm long; Mn-stained to partly encrusted.
U322b	Rock dredge	Manihiki Island	1754-1560	1 shell frag., 43 mm max. diam., with purple patches on surface.
U323	Rock dredge	Manihiki Island	3066-2971	3 gastropod frags, 20-33 mm max. diam.
U324	Rock dredge	Pukapuka	417-446	Gorgonian corals[1]; 1 calcareous sponge; shallow water molluscs; some small damaged crustaceans; crinoids; and 1 ophiuroid.
U325	Rock dredge	Pukapuka	1585-1446	Gorgonian corals[1]; 1 calcareous sponge; cirripede plates; polychaetes; 2 species of crinoids; 1 ophiuroid; and worn echinoid spines.
U326	Rock dredge	Pukapuka	2161-2121	1 calcareous sponge; 1 ophiuroid.
U327	Rock dredge	Pukapuka	3394-3217	1 shark tooth, 29 mm long, Mn-stained.
U331	Rock dredge	Tema Reef	1407-1100	Gorgonian(?) corals; ca. 100 shells/ shell frags, mostly 5-15 mm max. diam., including numerous shallow water mollusc species, echinoid spines[2]; 1 siliceous sponge.
U332	Rock dredge	Tema Reef	1377-1199	Gorgonian(?) corals; 4 shells/ shell frags, 12-37 mm max. diam.; 1 shark tooth, 31 mm long.
U333b	Rock dredge	Tema Reef	1913-1575	Gorgonian corals[1], including 1 grown on Mn-crust; 1 stalked barnacle; 1 ophiuroid.
U337	Rock dredge	Nassau	1001-884	Gorgonian corals[1]; ca. 50 shells/ shell frags (shallow water molluscs[2]) up to 20 mm max. diam.; worn echinoid spines.
U339	Pipe dredge	Nassau	4204-4219	6 siliceous sponge frags, 9-34 mm long, with brown to black Mn-stain.; 3 shark teeth (2 Mn-stained), 7-16 mm long.
U340	Pipe dredge	Samoan Basin near Nassau	5268-5253	8 shark teeth, 12-25 mm long, incompletely Mn-encrusted.
U341b	Rock dredge	Machias Seamount	2495-2500	Gorgonian(?) corals.
U342	Rock dredge	Machias Seamount	1350	ca. 20 shell frags, up to 45 mm max. diam.

Stn	Gear	Locality	Depth (m)	Sample description
U343	Rock dredge	Machias Seamount	730-715	ca. 40 shells/ shell frags, up to 30 mm max. diam. (molluscs); turriform gastropods and other mollusc remains within volcanic ash lumps.
U344	Rock dredge	Machias Seamount	675-670	1 gorgonian coral[1]; 1 ophiuroid.
U345	Rock dredge	Machias Seamount	1972-2166	Gorgonian(?) coral; 4 mollusc shell frags, 22-41 mm max. diam.[2]
U351a	Rock dredge	Capricorn Seamount	996-976	Solitary corals; 1 calcareous sponge; alcyonaceans; 1 polychaete; and 1 mollusc.
U356	Rock dredge	Niue	1873-1100	1 siliceous sponge.
U366	Rock dredge	Mitiaro	1101-1179	Gorgonian corals.
U375	Rock dredge	Rarotonga	1272	At least 10 shells/ shell frags and teeth, mostly molluscs[2]; includes barnacle plates[2], a 15-mm tooth and a few larger possible shark teeth. Thin Mn-stains on very few shell frags, teeth.
U377	Rock dredge	Rarotonga	2450-2296	Mollusc frags[2].

[1] (see Grigg, this volume) [2] (see Beu, this volume)

manganese encrustations. The shark teeth are most likely from pelagic rather than benthic sharks. At several other deep-water stations, nearly completely to completely encrusted shark teeth were found as the nuclei for Mn nodules (see Meylan and Glasby, this volume).

Deep-slope samples (depths about 3000–4200 m) contained only limited amounts of biological remains. At Stn U300 on the eastern slope of the Manihiki Plateau and U327 at Pukapuka, only shark teeth were collected, associated with Mn nodules as was commonly the case in deep-water basin samples. At U339 near the base of the Nassau volcanic edifice, shark teeth were dredged along with Mn-stained siliceous sponge remains. Scleractinian corals collected in deep basin and slope areas are obviously not *in situ* samples, and it is likely that most, if not all, of the other benthic biological remains have also been delivered by mass gravity transport. Gorgonian corals were found in both mid-slope and upper slope samples, the larger specimens probably long-dead and/or transported to their collection depth (see Grigg, this volume).

Limited abundance and diversity at any particular station characterizes mid-slope samples (depths about 1500–3000 m) as it does deeper stations. However, in upper slope hauls (depths about 400–1500 m), abundance and diversity typically are greater. Although much of this material has been transported downslope from depths less than 100 m, some samples apparently include the remains of organisms living in the dredged depths (see Grange and Veron, this volume; and Beu (this volume).

UNDERWATER PHOTOGRAPHS

Stn U296b (Penrhyn Basin, 5119 m, abyssal clay)

The frames, only one of which is here included indicate almost complete coverage of the sediment surface by small to medium spheroidal to ellipsoidal manganese nodules, some of which are faceted. Some of the nodules show evidence of *in situ* fracturing on the seafloor. Many nodules have flecks of sediment on the upper surfaces and a few may have small encrusting organisms, though these cannot be identified as to type. Fecal casts, probably from holothurians (e.g., frame #93, original negatives), are present in 70% of the frames, up to three on each frame. On some frames, the casts have broken down into piles of sediment (e.g., #18; Figure 1). A shark's tooth is visible in frame #4. At the associated pipe dredge station (U296a), an abundant haul of manganese nodules was collected along with several shark teeth.

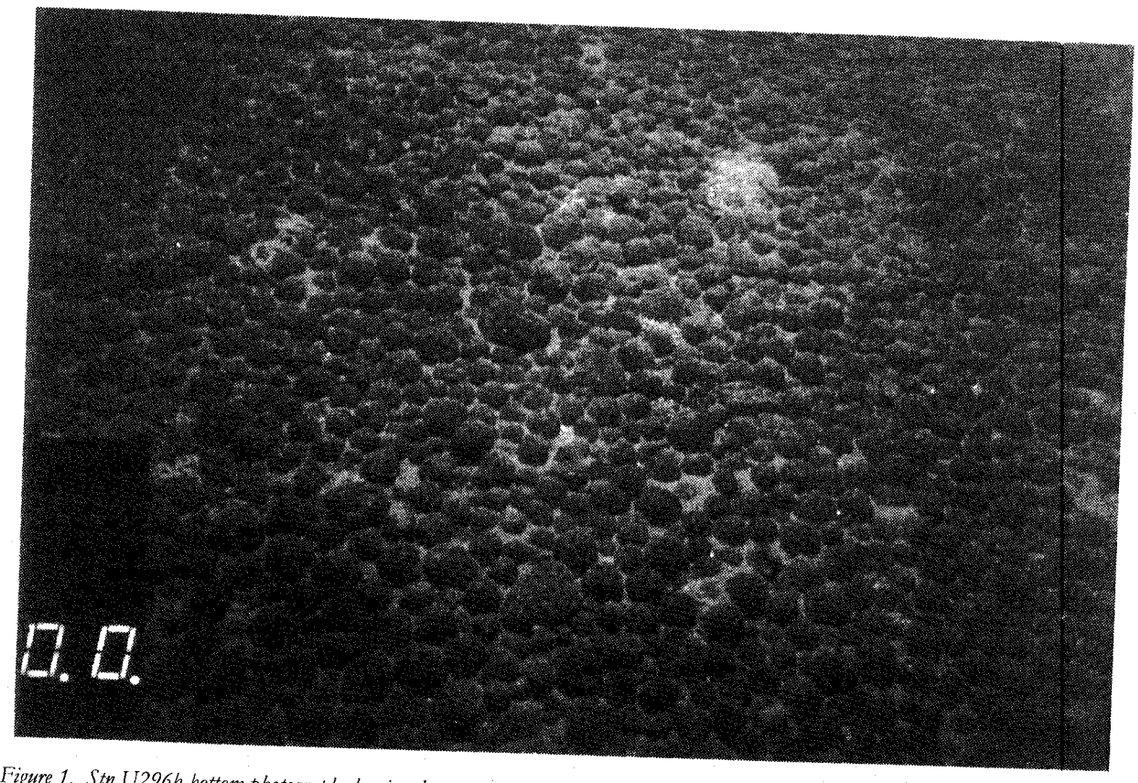

Figure 1. Stn U296b bottom photograph showing dense coverage of spheroidal and ellipsoidal manganese nodules, along with several fecal casts.

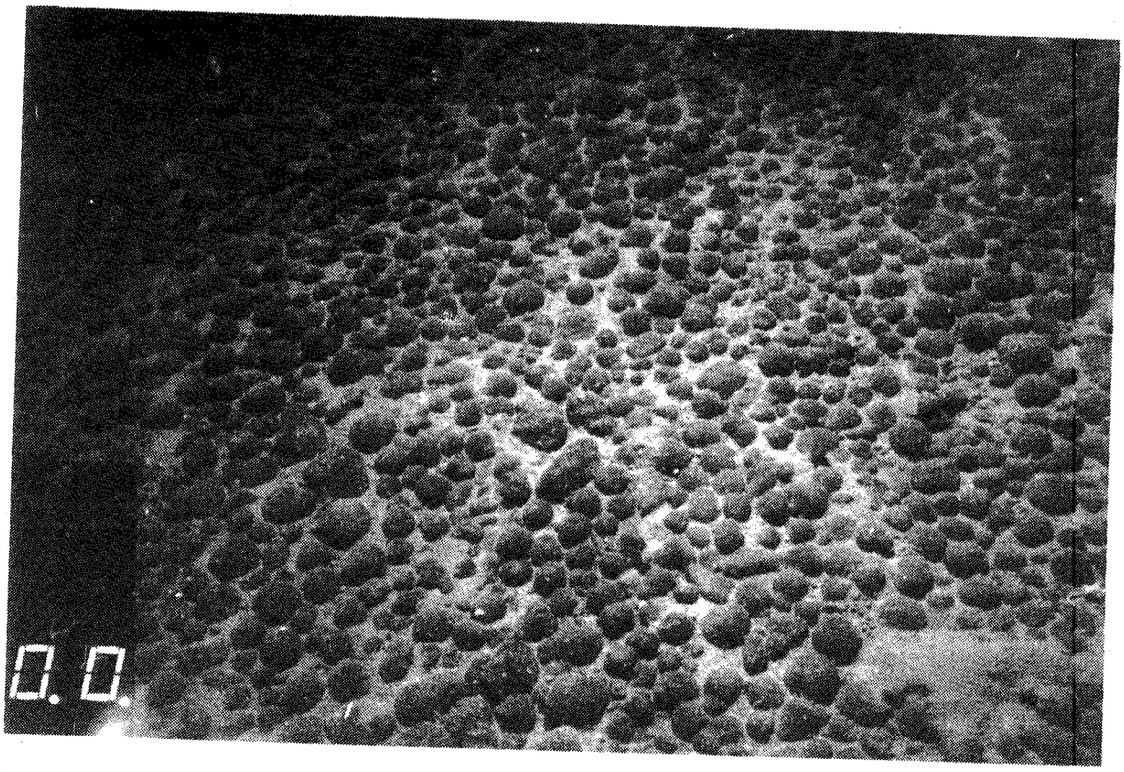

Figure 2. Stn U297b bottom photograph showing abundant spheroidal and ellipsoidal manganese nodules, as well as possible tabular ones.

Figure 3. Stn 304b bottom photograph showing a fecal cast (center) and bioturbated sediment.

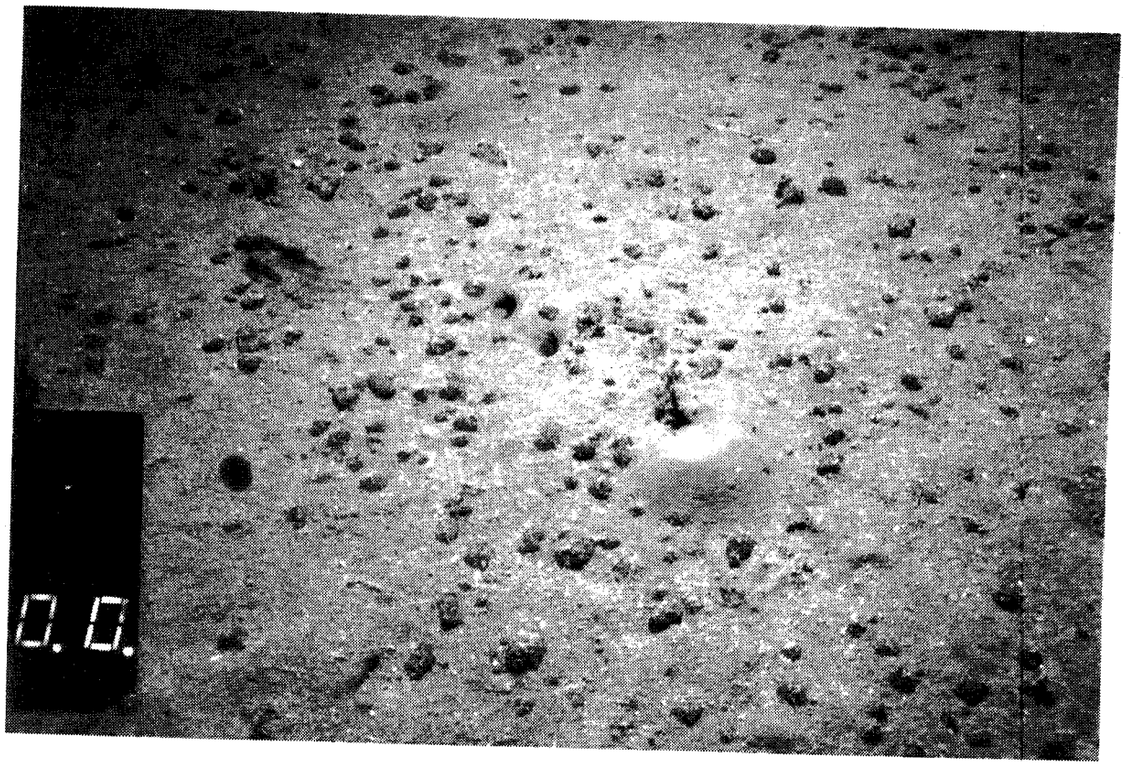

Figure 4. Stn U321b bottom photograph showing scattered, partially buried manganese nodules and evidence of sediment reworking by organisms.

U297b (Penrhyn Basin, 5330-5320 m, abyssal clay)

The nodules are somewhat less abundant than at U296b and include a number of larger, flatter nodules. Fecal casts are present in 40% of the frames and appear smaller and less frequent than those at the previous station. One frame (#86; Figure 2) shows possible sediment reworking. No dredging was done in the immediate vicinity of the camera station, but a short corer recovered 0.5 m of surface sediment.

U304b (crest of Manihiki Plateau, 2435 m, nanno-foram ooze)

These frames show bioturbated carbonate ooze. Visible animals are rare but there are fairly common tracks, burrows and impressions, as well as fecal casts of varying shapes and sizes. Some, though not all, burrows show signs of sediment reworking. Distinct impressions indicative of a five-armed asteroid are present on two frames (#89, #44). Frame #89 also has a small erect organism, possibly a sponge, in the foreground, and frame #80 shows a possible holothurian (upper left margin). Frame #57 (Figure 3) has a very conspicuous fecal cast (center). A worm tube or scaphopod is visible in frame #44. At the associated pipe dredge station (U304a), the recovered sediment did not include any coarse material (nodules, rocks, or other biological remains other than microfossils).

U321b (Penrhyn Basin east of Manihiki, 5258 m, volcanic-rich abyssal clay)

The frames show bioturbated abyssal sediment with scattered, partially buried manganese nodules present in some frames. Tracks and paths are present, although not on all frames, and are broad in comparison with those present

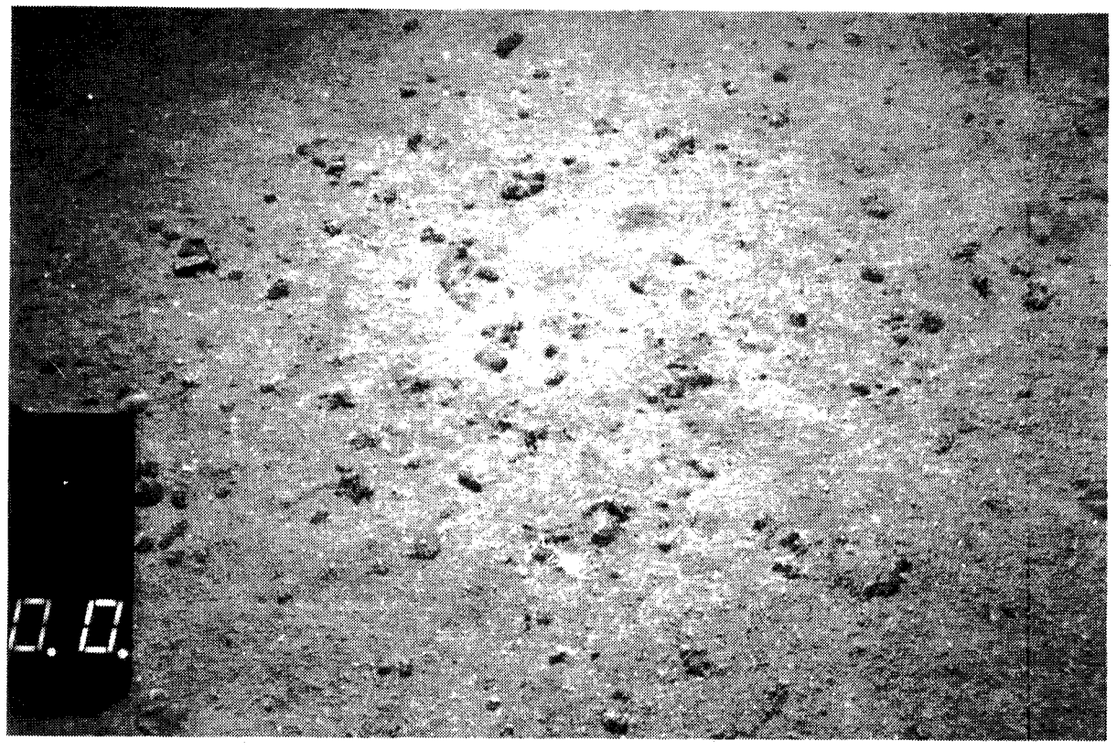

Figure 5. Stn U321b bottom photograph showing what might be a nearly buried part of a manganese nodule field.

at U304b. Frame #79 (Figure 4) shows a burrow with a distinct mound of finer reworked sediment. A dark indistinct object (left foreground) may be an animal, while frame #77 has a holothurian(?) (upper left). Frame #69 has a broad track and a partially erect animal (center front). Frame #95 (Figure 5) shows an animal with conspicuous spines (center front). At the associated pipe dredge station (U321a), an abundant haul of Mn nodules was collected along with several shark teeth. Apparently a geologically recent increase in the rate of delivery of volcaniclastic sediment has effectively terminated nodule growth.

U360a (Niue - Tofua transect, 5495 m, abyssal clay)

The frames show bioturbated abyssal sediment. The sediment is fine-grained with burrows quite common, as well as indistinct tracks. Fecal casts are present and sometimes conspicuous (frames #82, #61, #54; latter is Figure 6). Frames #50 and #49 each have a small "armed" organism standing erect (center-rear margin). Coring and dredging attempts in the immediate vicinity were unsuccessful.

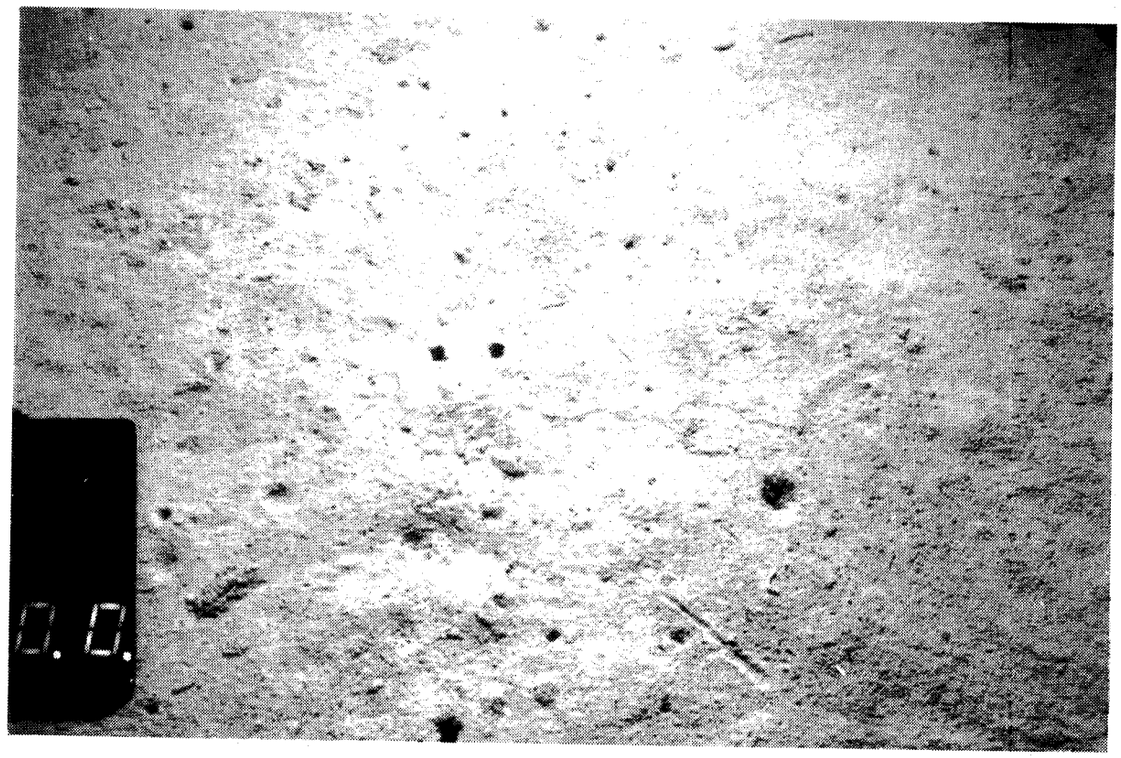

Figure 6. Stn U360a bottom photograph showing a bioturbated and tracked sediment surface.

Glasby, G.P., and M.A. Meylan, 1996. The distribution of corals, molluscs and foraminifera around islands and seamounts in the southwestern Pacific c~lIected during the 1986 HMNZS *TIli* Cruises: Introduction, *in:* Meylan, M.A., and G.P. Glasby (eds) Manihiki Plateau, Machias and Capricorn Seamounts, Niue,and Tofua Trough: Results of *TIli* Cruises. SOPAC Technical Bulletin 10: 133-135.

THE DISTRIBUTION OF CORALS, MOLLUSCS AND FORAMINIFERA AROUND ISLANDS AND SEAMOUNTS IN THE SOUTHWESTERN PACIFIC COLLECTED DURING THE 1986 HMNZS *TUI* CRUISES: INTRODUCTION

G.P. Glasby

Deparunem of Earth Sciences, University of Sheffield, Sheffield S3 ?HP, England

M.A. Meylan

University of Southern Mississippi, USM Box 5044, Hattiesburg, USA

ABSTRACT

Two cruises of *HMNZS Tui* were undertaken in 1986 to search for Co-rich manganese crusts on the slopes of islands and seamounts in the SW Pacific. At many of the dredge sites, only thin manganese crusts were recovered, but corals, molluscs and forams were collected. Many of these organisms had lived at much shallower depths than those sampled and were transported to their present positions by mass wasting. The frequency of mass wasting in this coral-reef type of environment explains the poor recovery of crusts. The following papers report on the biological material collected, including attempts to date some coral and shell samples.

INTRODUCTION

A 1986 *HMNZS Tui* cruise to the Manihiki Plateau and adjacent areas of the SW Pacific was undertaken by the governments of New Zealand, Australia and the United States in cooperation with the Committee for the Co-ordination of Joint Prospecting for Mineral Resources in South Pacific Offshore Areas (CCOP/SOPAC) as part of the Tripartite II Programme. The principal aim of the cruise was to assess the distribution, abundance, and metal contents of marine mineral deposits, particularly Co-rich manganese crusts, in selected areas which had not yet been systematically sampled and surveyed. A later cruise of *HMNZS Tui* in 1986 sampled around the islands of Mauke, Mitiaro and Rarotonga in the southern Cook Islands.

COBALT-RICH MANGANESE CRUSTS

Co-rich manganese crusts are manganese crusts enriched in cobalt (with values in excess of 1%) which at the time of the cruises had only recently been discovered and were attracting interest as a potential economic source of cobalt (Halbach et al., 1982). These crusts are generally found in water depths of 1000–2500 m and it was thought that the high cobalt content of these crusts is related to the position of the oxygen minimum zone in the water column. They are considered to be of hydrogenous origin, that is, precipitated from ambient bottom water, in contrast to other types of crusts which may be of hydrothermal origin and enriched in metals other than cobalt.

Cronan (1984) had reviewed the criteria for the occurrence of economic Co-rich Mn crusts in the CCOP/SOPAC region of the SW Pacific and listed the following requirements as being necessary:

a) depth between 300–2000 m

b) latitude not more than about 15°S

c) exposed non-sedimented slopes

The latitudinal requirement stems from the observation that O_2 minimum zones with dissolved O_2 contents in the water column <2.2 ml/l do not occur south of about 20°S.

On this basis, Cronan (1984) had delineated a number of areas within the CCOP/SOPAC region as potential sites of Co-rich Mn crust occurrence. These included the islands of Suwarrow, Rakahanga, Manihiki, Pukapuka, Tema Reef and Nassau on the Manihiki Plateau and Machias Seamount. These are, in fact, the only areas in the appropriate depth range in this region for Co-rich Mn crusts to form.

TUI SURVEY

The cruise plan for the 1986 *HMNZS Tui* cruise to the Manihiki Plateau and adjacent areas of the SW Pacific was based in part on this assessment of Cronan (1984) of the likely occurrence of Co-rich Mn crusts. For this reason, a series of dredges was undertaken up the slopes of each of these islands as well as around Machias and Capricorn Seamounts and Niue Island in order to assess the extent of Co-rich Mn crust occurrence. Note that sampling in adjacent abyssal areas was directed at assessing manganese nodule abundance and metal content.

The results of this survey of Mn crusts and nodules have been presented by Meylan et al. (1990). Although Mn crusts were found around all the islands surveyed (although not on Machias or Capricorn Seamounts), these crusts are in general thin (average maximum thickness at the 15 stations at which hydrogenous Mn crusts were recovered was 8 mm) and have an average Co content of 0.65%. The resource potential of these crusts was considered minimal.

MASS WASTING

Murray and Lee (1909) reported coral mud and sand encircling many coral islands in the tropical and subtropical regions of the Pacific. These deposits covered an area of 4.5 million km^2 and extended to depths of almost 6000 m. Emery et al. (1954) showed that debris moved down the outer slopes of atolls and Fairbridge (1950) and Moore (1964) deduced the nature of landslide patterns around oceanic volcanoes and atolls. Wood and Hay (1970) have described the geology of the northern Cook Islands and, in particular, noted the role of hurricanes and seaslides on erosion of the coral reefs. They suggested that extensive erosion may have occurred on these islands during the last glacial eustatic lowering of sea level. Helsley et al. (1985) concluded that mass wasting and downslope transport of rock debris on the slopes of Hawaiian seamounts is common. This debris is, however, concentrated in channels such that less than half the submarine slope is covered by debris. On Cross Seamount, Hawaii, for example, there has been continuous mass wasting of the edifice with talus chutes located between submarine ridges (Malahoff et al., 1985). Hein et al. (1985) documented mass movement of material, particularly on S.P. Lee Guyot. As a result, thin manganese crusts were recovered there in contrast to much thicker crusts on an adjacent small seamount (cf. Manheim, 1986).

In the Pacific, archipelagic aprons make up about 8% of the seafloor (Menard, 1956). The extent of these aprons can be judged by the fact that the Samoan Apron contains about 5 x 10^{13} m^3 of sediment deposited over the last 5 m.yrs. These aprons have a number of factors contributing to their formation, of which gravitational sliding of material down steep volcanic slopes is one. According to Lonsdale (1975), such slopes are vulnerable to sliding because of their steep gradients, high seismicity, rapid sediment accumulation and unstable sediment structure.

Coral rubble and associated remains of shelled organisms were recovered on the slopes of all the atolls surveyed as well as from Machias and Capricorn Seamounts (Figure 1). As suggested by previous workers for analogous findings, we believe that this material must have been moved downslope by some type of mass gravity process. In particular, the recovery of significant amounts of coral debris on the flanks of the reef-fringed islands studied here points to the importance of such processes around these islands. Islands are probably more susceptible than

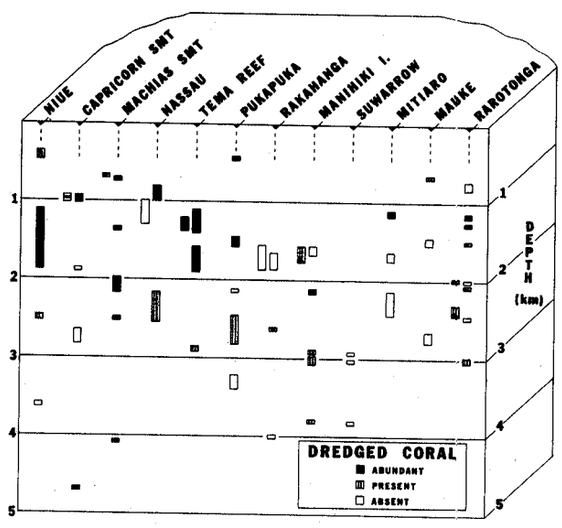

Figure 1. Distribution of dredged coral (all types) from the slopes of SW Pacific islands and seamounts as determined by the Tui *cruises.*

seamounts to such erosion because of the effects of storm and wave action and the relative ease of detachment of coraline reef material (Emery et al. 1954; Stoddart and Steers, 1977). In addition, it should be noted that Co-rich crusts have an optimum depth range of 1000 - 2500 m. The greater elevation of an island compared to a 1000 m-deep seamount would likely lead to a much greater throughput of debris in this depth range. Although we are in no position to calculate downslope transport of debris around these islands, Lonsdale (1975) did estimate a sedimentation rate of at least 200 m/10^6 yrs for the proximal part of the Samoan Achipelagic Apron.

Manganese crusts accrete very slowly (a few mm/10^6 yrs) and require long-term exposure at the seafloor to acquire a substantial thickness of precipitated metal oxides. The sudden arrival of mass-wasted material could bury crusts, halting their further growth. Hein et al. (1988) have, subsequent to the *Tui* and other surveys, listed 11 criteria for the occurrence of economic Co-rich Mn crusts. These include volcanic structures not capped by large modern atolls or reefs. Our findings confirm the importance of this criterion and the need for long-term slope stability for the development of these slow growing crusts. Mass wasting of material down the slopes of these coral-capped islands and seamounts is therefore seen as the major reason for the limited occurrence of thick Co-rich Mn crusts in this region of the subtropical Pacific.

The object of the following set of papers is to describe the occurrence of corals, molluscs and forams around each of the islands and seamounts surveyed, to establish whether they occur at their *in situ* depth or have slumped to their present position, and to date selected coral and shell samples radiometrically to establish whether this material is modern or relict.

REFERENCES CITED

Cronan, D.S., 1984, Criteria for the recognition of areas of potentially economic manganese nodules and encrustations in the CCOP/SOPAC region of the central and southwestern tropical Pacific: South Pacific Marine Geology Notes, v.3, p.1-17.

Emery, K.O., J.I. Tracey, and H.S. Ladd, 1954, Geology of Bikini and nearby atolls: U.S. Geological Survey Professional Paper 260-A, 265 p. + 64 plates.

Fairbridge, R.W., 1950, Landslide patterns on oceanic volcanoes and atolls: Geographical Journal, v.115, p.84-88.

Halbach, P., F.T. Manheim, and P. Otten, 1982, Co-rich ferromanganese deposits in the marginal seamount region of the Central Pacific Basin - results of the Midpac '81 cruise: Erzmetall, v.35, p.447-453.

Hein, J.R., F.T. Manheim, W.C. Schwab, and A.S. Davis, 1985, Ferromanganese crusts from Necker Ridge, Horizon Guyot and S.P. Lee Guyot: Geological considerations: Marine Geology, v.69, p. 25-54.

Hein, J.R., W.S. Schwab, and A.S. Davies, 1988, Cobalt- and platinum-rich ferromanganese crusts and associated substrate rocks from the Marshall Islands: Marine Geology, v.78, p.255-283.

Helsley, C.E., B. Keating, E. DeCarlo, G. McMurtry, M. Pringle, F. Campbell, L. Kroenke, and P. Jarvis, 1985, Resource assessment of cobalt-rich ferromanganese crusts within the Hawaiian Exclusive Economic Zone: Hawaii Institute of Geophysics Final Report (In six sections).

Londsale, P., 1985, Sedimentation and tectonic modification of Samoan Archipelagic Apron: AAPG Bulletin, v.59, p.780-798.

Malahoff, A., R. Grigg, D. Vonderhaar, K. Kelly, and A. Arquit, 1985, Mass wasting and manganese crust growth on Cross Seamount, Hawaii: E0S Transactions of the American Geophysical Union, v. 66, p.1083-1084 (Abstract).

Manheim, F.T., 1986, Marine cobalt resources: Science, v.232, p. 600-608.

Menard, H.W., 1956, Archipelagic aprons: AAPG Bulletin, v.40, p. 2195-2210.

Meylan, M.A., G.P. Glasby, P.J. Hill, B.C. McKelvey, P. Walter, and P. Stoffers, 1990, Manganese crusts and nodules from the Manihiki Plateau and adjacent areas: Results of HMNZS *Tui* cruises, Marine Mining, v.9, p.43-72.

Moore, J.G., 1964, Giant submarine landslides on the Hawaiian Ridge: U.S. Geological Survey Professional Paper, v. 501-D, p. 95-98.

Murray, J., and G.V. Lee, 1909, The depth and marine deposits of the Pacific: Memoirs of the Museum of Comparative Zoology at Harvard College, v.38, 169 p. + 11 figs and 3 maps.

Stoddart, D.R., and J.A. Steers, 1977, The nature and origin of coral reef islands, *in* O.A. Jones, and R. Endeau, eds., Biology and geology of coral reefs, Volume IV, Geology 2: Academic Press, New York, p.59-105.

Grange, K.R., and J.E.N. Veron, 1996. Scleractinian corals collected from the *T* iii cruises to the Southwest Pacific, *in:* Meylan, M.A., and G.P. Glasby (eds) Manihiki Plateau, Machias and Capricorn Seamounts, Niue, and Tofua Trough: Results of *TlliCruises.* SOPAC Technical Bulletin 10: 137-140.

SCLERACTINIAN CORALS COLLECTED FROM THE *TUI* CRUISES TO THE SOUTHWEST PACIFIC

K.R. Grange

National Institute of Water and Aunosphete Research Ltd, PO Box 893, Ndson, New Zealand

J.E.N. Veron

Australian Institute of Marine Science, Townsville, Queensland, Austtalia

ABSTRACT

Scleractinian corals were collected during the *Tui* cruises in 1986 at dredge stations in water deeper than 350 m in the Cook Islands region, adjacent to Niue, and over Machias and Capricorn Seamounts. Almost all are fragments of hermatypic corals presumed to have been transported from shallower water reefal environments.

INTRODUCTION

The area sampled by the *Tui* expedition (between 10° S and 20° S) is within the zone of extensive coral reef development surrounding islands and atolls. Coral reefs in the area have been studied by various workers, e.g., Hoffmeister (1925) (American Samoa and Fiji); Crossland (1928) (Tahiti, Moorea, and Rarotonga); Wells (1954) (Samoa and Tonga); Gibbs et al. (1971) (Cook Islands); Stoddart and Pillai (1973) (Cook Islands); McCann (1974) (Manihiki); Gibbs et al. (1975) (Cook Islands); and Ditlev (1980) (Indo-Pacific), so the general fauna is well known. In general, coral Genera decrease in diversity from west to east across the South Pacific (Wells, 1954; Stoddart and Pillai, 1973), but all reefs that do occur can be considered "typical", i.e., they occur in shallow (< 70 m) water around islets or form reefs and lagoon structures around atolls.

Hermatypic (reef-building) corals require sunlight for growth due to the symbiotic unicellular zooxanthellae algae present in tissues that assist in nutrition. Consequently, the collecting of hermatypic coral fragments in dredge samples below 350 m requires some explanation as to their origins.

RESULTS

Scleractinian corals were identified by one of us (JENV) from 19 stations around Suwarrow, Manihiki, Pukapuka, Tema Reef, Nassau, Machias Seamount, Niue, and Rarotonga. Other stations where shipboard notes referred to "coral" turned out to be limestone boulders, pieces of *Tridacna* clam shells, or deep-water gorgonians, rather than scleractinians. Table 1 shows the general locality, depth, and coral Genera identified from these stations. Only five stations are shallower than 1,000 m, and the deepest is 4,689 m (U352). All Genera identified other than *Caryophyllia* (Stns U366 and U375) are hermatypic, reef-building scleractinia. The depths sampled are well beyond the range in which hermatypic corals can grow in the Indo-Pacific (Ditlev, 1980). *Caryophyllia* is an ahermatypic, solitary coral which does not contain zooxanthellae and is therefore widely distributed in deep water, not necessarily restricted to the tropics.

Although most specimens collected were worn fragments, all Genera listed in Table 1 have been previously recorded from the Cook Islands area (Stoddart and Pillai,

Table 1. Scleractinian corals identified from Tui *samples.*

Stn	Locality	Depth (m)	Coral
U292	North of Suwarrow	3036-3026	*Porites*
U317	West slope of Manihiki Island volcanic edifice	2161-2111	*Fungia granulosa* *Fungia* *Pocillopora* *Pachyseris* *Pavona* *Acropora* *Porites* *Turbinaria peltata* *Turbinaria* *Goniopora* *Leptoseris mycetoseroides* *Galaxea fascicularis*
U319	East slope of Manihiki Island volcanic edifice	2906-2911	*Porites* *Pocillopora*
U324	West of Pukapuka	417-446	*Leptoserisfoliosa* *Pavona minuta* *Porites*
U329	East slope of Pukapuka volcanic edifice	2825-2450	*?Goniopora*
U331	NW slope of Tema Reef volcanic edifice	1407-1100	*Pocillpora ?verrucosa* *Pocillopora* *Goniopora* *Pavona ?maldivensis* *Porites* *Montipora* *Acropora* *Lobophyllia* *Pachyseris* ?Faviidae
U337	East slope of Nassau volcanic edifice	1001-804	*Pachyseris* *Acropora ?valida* *Fungia* *Pocillopora* *Porites*
U341b	SE slope of Machias Smt	2495-2500	*Acropora palifera* *Porites* Faviidae
U342	South slope of Machias Smt	1350	*Acropora* *Fungia (Pleuractis)* *Pachyseris speciosa*
U343	NW crest of Machias Smt	730-715	*Goniopora* *Acropora* *Pachyseris*

Stn	Locality	Depth (m)	Coral
U345	NW slope of Machias Smt	1972-2166	*Goniopora* *Cycloseris* *Acropora* *Pavona*
U346	Lower NW slope of Machias Smt	4077	*Acropora* *Pavona* *Pachyseris* *Goniopora*
U352	SE flank of Capricorn Smt	4684-4689	*Galaxea ?fascicularis* Faviidae
U354	SW point Niue	346-467	*?Madrepora*
U362	SE slope of Mauke	685-626	*Favia* *Acropora* Pocilloporidae
U366	SE slope of Mitiaro	1101-1179	*Caryophyllia* *Madrepora* undetermined Genus
U370	NE slope of Rarotonga	1021-1086	*Galaxea* *Pavona* *?Cyphastrea*
U375	SE slope of Rarotonga	1272	*Caryophyllia* *Leptoseris* *Cycloseris* *Pavona* *Pachyseris* *Acropora* *Galaxea* *Goniopora* undetermined Genus
U377		2450-2296	*Cycloseris* *Leptoseris* cf. *incrustans* *Montipora*

1973; Gibbs et al., 1975; JEN Veron, pers. obs.). The most widespread Genera in the samples are *Acropora* (42% of stations), and *Porites, Pachyseris, Pavona,* and *Goniopora*, all of which occurred at 37% of the stations (Table 1).

DISCUSSION

The Genera collected in the *Tui* samples are dominated by hermatypic scleractinia, common in shallow reefal environments in the localities sampled, despite the samples being collected from well below the depths at which such corals can grow.

The bathymetry of the stations indicate that steep drop-offs seaward of lagoons and reefs predominate. Although it has been impossible to identify many of the worn fragments to species level, the samples are likely to be of extant species. These indicate that the samples have been transported to the depths at which they were collected

from reefal environments, rather than reflecting some past geological history when the stations were in shallow water.

REFERENCES CITED

Crossland, C., 1928, Coral reefs of Tahiti, Moorea and Rarotonga: Journal, Linnean Society of London, v.36, p.577-620.

Ditlev, H., 1980, A field-guide to the reef-building corals of the Indo-Pacific: Rotterdam, Dr. W. Backhuys, Publisher, 291 p.

Gibbs, P. E., D. R. Stoddart, and H. G. Vevers, 1971, Coral reefs and associated communities in the Cook Islands: Bulletin of the Royal Society of New Zealand, v.8, p.91-105.

Gibbs, P. E., H. G. Vevers, and D. R. Stoddart, 1975, Marine fauna of the Cook Islands: Checklist of species collected during the Cook Bicentenary Expedition in 1969: Atoll Research Bulletin, v.190, p.133-148.

Hoffmeister, J. E., 1925, Some corals from American Samoa and the Fiji Islands: Papers of the Department of Marine Biology, Carnegie Institute, Washington, D.C., v.22, p.1-89.

McCann, C., 1974, Scleractinian corals from Manihiki Atoll: New Zealand Oceanographic Institute, Memoir 31, p.35-40.

Stoddart, D. R., and C. S. G. Pillai, 1973, Coral reefs and reef corals in the Cook Islands, South Pacific, *in* R. Fraser, comp., Oceanography of the South Pacific 1972: New Zealand National Commission for UNESCO, Wellington, p.475-483.

Wells, J. W., 1954, Recent corals of the Marshall Islands: United States Geological Survey, Professional Paper 260-I, p. 385-479.

Grigg, R.W. 1996. Precious and deep-water corals in dredge samples collected during the 1986 HMNZS *Tui* cruises, *in:* Meylan, M.A., and G.P. Glasby' (eds) Manihiki Plateau, Machias and Capricorn Seamounts, Niue, and Tofua Trough:
Results of *Tui* Cruises. SOPAC Technical Bulletin 10: 141-143.

PRECIOUS AND DEEP-WATER CORALS

IN DREDGE SAMPLES COLLECTED DURING THE 1986 HMNZS *TUI* CRUISES

R. W. Grigg

Department of Oceanography, SOEST, University of Hawaii, Honolulu, Hawaii 96822, USA

ABSTRACT

Samples of commercial grade pink coral *Corallium* spp. and other deep-water gorgonians including gold corals *(primnoa* and *Narella* spp.) and bamboo corals *(LePidisis* sp.) collected on the flanks of atolls on the margins of the Manihiki Plateau indicate that the commercial potential for precious coral in the region is reasonably good. Further exploration in the area is recommended. The optimum depth of exploration appears to be about 400 m. At greater depths, most samples of precious corals consist of dead fragments, suggesting that their occurrence there is a result of slumping processes.

INTRODUCTION

Precious corals are known to exist in the North Pacific Ocean within two rather well defined depth zones, one between 100 and 400 m and the other between 1000 and 1500 m (Kishinouye, 1904; Grigg, 1984). In the first depth zone, about six species of *Corallium* exist at depths between 100 and 300 in the far western Pacific. In the Hawaiian Archipelago, the pink coral *Corallium secundum,* the gold coral *Gerardia* sp., and the bamboo coral *Lepidisis olapa* exist in this depth zone on rocky bottoms in areas of strong bottom currents. The second depth zone, between 1000 and 1500 m, is found in the Emperor Seamounts in the north Pacific also in areas of rocky bottoms with strong currents. An undescribed species of pink coral *(Corallium)* known as Midway coral is very abundant there. This species has not been found elsewhere in the Pacific so that the 1000-1500 depth habitat may be restricted to the north Pacific.

Deep-Water Corals

Because the primary objective of the *Tui* cruises was to explore for manganese crusts, most of the stations (>2000 m) were beyond the known depths of living precious coral. Only two dredge samples from the *Tui* cruises were located in the shallow water zone and only ten were within the deeper water zone. However, since the deeper zone may not exist in the region of the Manihiki Plateau, only two stations may be relevant in terms of assessing precious coral potential. An exception to this may be occurrences of shallow water specimens that are transported as fragments down-slope by debris avalanches, slumping or other erosional processes.

Two of the stations located in the shallow zone (Stns U324 and U354) contained specimens of precious corals. Stations U324 and U354 were located between 417–446 m and 346–467 m, respectively. Station U324 contained seven

species of deep-water corals: two black corals, one primnoid gold coral, one bamboo coral and three gorgonians of no commercial value. The primnoid gold coral measures 65 mm in diameter at the base which makes it large enough to be of commercial value. This specimen alone would warrant further exploration of the area, especially considering that only two dredge stations in the entire expedition were probably located at the proper depth for sampling live specimens of precious coral. Station U354 contained six small pieces of coral but these were not available for examination by the author.

The diversity and species composition of the corals collected at Stn U324 is a good indication of favorable environmental conditions for the growth of precious corals in the area of the Manihiki Plateau (see Tables 1 and 2). Species of *Narella, Lepidisis* and *Primnoa,* all found at Stn U324, commonly co-occur in beds rich in several species of pink coral *(Corallium)* in the Hawaiian Archipelago (Grigg and Bayer, 1976). Species of pink, red and white coral belonging to the genus *Corallium* make up 95% of the world's landings of precious coral (Grigg, 1984). Although no large living colonies of *Corallium* were collected during the *Tui* cruises, several dead but very large specimens were dredged from deeper water. At Stn U333b, one fragment of *Corallium* 35 mm in diameter and of commercial grade color (pink or momoiro) was recovered. This specimen was covered by a layer of manganese oxide about 1 mm thick. Manganese oxide crust normally accumulates at a very slow rate, on the order of 1-40 mm/10^6 years (Cronan, 1980). Even if the rate of manganese oxide formation on coral fragments at Station U333b (depth 1575-1913 m) is much greater than normal, a very old age for this fragment would be indicated. It may be that this region lacks the boring organisms (sponges and bivalves) that commonly cause the bioerosion of *Corallium* skeletons in the shallow zone of the far western Pacific (Kishinouye, 1904). The large fragment of *Corallium* probably originated in the shallow zone near

Table 1. Precious coral samples collected during the 1986 HMNZS Tui *cruises.*

Station	Depth (m)	Bottom Topography	Sample Contents
U324	417-446	steep slope west of Pukapuka (westernmost reef)	1) large primnoid gorgonian coral, maximum diameter of basal section 10 mm above holdfast is 65 mm, skeleton heavily calcified, cf. *Primnoa resedaeformis* in Alaska 2) *Lepidisis* sp. abundant, live material finely branched 3) *Antipathes* sp. 1, 10 mm length, alive, finely branched 4) *Antipathes* sp. 2, pinnules of equal length, alternately branched in four planes, alive, 40 mm length S) *Acanthogorgia* sp., alive, sclerites large, spindles arranged *en cheveron*, some projecting beyond tentacle crown 6) *Versluysia* sp., alive, 20 mm length 7) *Narella* cf. *dichotoma*, colony 150 mm in height
U325	1446-1585	steep slope west of Pukapuka	1) Manganese-coated fragments of *Corallium* sp., largest stem diameter 10 mm, color pink 2) dead fragments of *Lepidisis* sp., maximum stem diameter 16 mm, stained with manganese oxide
U333b	1575-1913	steep SE slope of Tema reef, volcanic substrate	1) fragments of large *Corallium* sp., basal diameter 10 mm above holdfast is 35 mm, color pink, coated with Mn oxide, dead 2) fragments of large dead gold coral (*Primnoa* sp.), maximum diameter of branches 20 mm, coated with oxidized calcite
U337	804-1001	steep east slope of Nassau seamount	1) fragments of *Lepidisis* sp. maximum diameter 11 mm 2) solitary coral 50 in length
U344	650-670	crest of Machias Seamount	1) *Corallium* sp., small white colony, 30 mm high, maximum stem diameter 4 mm

Table 2. Ecological and economic significance of coral samples collected during HMNZS Tui *cruises.*

Station	Comments
U324	*Primnoa* sp. (65 mm maximum diameter), commercially important
U325	*Corallium* sp. of commercial size and color, displaced from shallow water, all material dead, stained with Mn oxide, large colonies of bamboo coral 16 mm in diameter, both specimens indicate favorable conditions exist at shallow depths
U333b	Material is of commercial grade and color, no evidence of boring organisms (sponges, bivalves and polychaetes), specimens coated with Mn oxide suggest material has been dead for many years, specimens of pink coral are similar to *C. secundum* in Hawaii, depth range of *C. secundum* is 375-450 m in Hawaii suggesting *Tui* material originated at depths much shallower than the depth of collection; this interpretation is consistent with steep bathymetry in area
U337	Samples of no commercial value but presence of moderate sized bamboo corals is an indication of favorable environmental conditions
U344	*Corallium* sp., colonies miniature, white, of no commercial importance, stunted size suggests poor ecological conditions

400 m depth. Large fragments of other species common in the shallow zone such as primnoid gold corals were also recovered in the dredge haul taken at Station U333b. This is a very good indication that commercial grade precious coral exists in the region of the Manihiki Plateau. Species found at Stn U324 at 417-446 m suggest that this depth range would be a good target for further exploration.

CONCLUSIONS

This paper is the first report of precious coral in the area of the Manihiki Plateau. Species collected during the 1986 HMNZS *Tui* cruise include specimens of commercial grade material in terms of both size and color. Important environmental parameters to consider for locating future beds of precious coral include, 1) depths between 100 to 500 m, 2) areas with rocky bottoms, 3) areas with strong bottom currents, 4) areas free of sediment or removed from sources of sediment, such as steep slopes or submarine canyons, and 5) areas in close proximity to sources of larvae of species of precious coral.

REFERENCES CITED

Cronan, D.S., 1980, Underwater minerals: London, Academic Press, 362 p.

Grigg, R.W., 1984, Resource management of precious corals: a review and application to shallow water reef building corals: Marine Ecology, v.5, p.57-74.

Grigg, R.W., and F.M. Bayer, 1976, Present knowledge of the systematics and zoogeography of the Order Gorgonacea in Hawaii: Pacific Science, v.30, p.167-175.

Kishinouye, K., 1904, Notes on the natural history of corals: Imperial Fisheries Bureau, Tokyo, Journal, v.14, p.1-32.

Beu, A.G. 1996. The distribution of mollusca in dredge samples collected during the 1986 HMNZS *Tui* cruises, *in:* Meylan, M.A., and G.P. Glasby (eds) Manihiki Plateau, Machias and Capricorn Seamounts, Niue, and Tofua Trough: Results of *Tui* Cruises. SOPAC Technical Bulletin 10: 145-149.

THE DISTRIBUTION OF MOLLUSCA IN DREDGE SAMPLES COLLECTED DURING THE 1986 HMNZS *TUI* CRUISES

A.G. Beu

Institute of Geological and Nuclear Sciences Ltd, PO Box 30368, Lower Hurt, New Zealand

ABSTRACT

Mollusca were recovered in four samples dredged from around Nassau and Rarotonga in the Cook Islands and in one sample from Machias Seamount, in water depths of804-2450 m. The four Cook Islands samples are dominated by fresh, brighdy colored fragments and whole specimens of Mollusca that now live in depths of only about 0-50 m around coral reefs, although one large sample contains stained specimens of three taxa from the *in situ* deep-water fauna. Sample U337 (from around Nassau, in 1001- 804 m) contains two specimens of *ypraea bernardi* (Richard), a rare species previously recorded only from Tahiti and Pitcairn Island in 1.5-130 m, and a large fragment o*f Bursa lamarckii(Deshayes),* a coral-reef species whose nomenclature was previously obscure. The Machias Seamount sample contains only three taxa that represent the *in situ* deep-water fauna.

The common shells of shallow-water coral-reef mollusc species in most samples indicate that large volumes of sediment have slumped into the sampled depths from much shallower water.

INTRODUCTION

A significant molluscan fauna (and a few other non-coral invertebrates) was recovered in five dredge samples during the 1986 cruises of HMNZS *Tui.* At least one of the molluscs is a significant new locality record. The samples containing molluscs were taken around Nassau (U331, 1407–1100 m; U337, 1001–804 m), Rarotonga (U375, 1272 m; U377, 2450–2296 m) and on Machias Seamount (U345, 1972–2166 m). The faunas are listed in Table 1.

FAUNAL COMPOSITION

The molluscan fauna of U331 consists almost entirely of fragments of shallow-water species. Two whole but abraded small oyster valves and a small, abraded valve of the venerid bivalve *Timoclea* are the only complete specimens. The other taxa present are the scallop *Gloripallium pallium* (Linné), brightly colored fragments of the cemented "thorny oyster" *Spondylus*, the large cockle *Trachycardium* cf. *elongatum* (Bruguière), the very heavy-shelled venerid *Periglypta*, the intertidal turban shell *Turbo (Argyrostoma)*, a fragment of a cowry *(Cypraea)*, a fragment of the common intertidal frog shell *Bursa* cf. *granularis* (Röding), and small unidentified fragments of gastropods belonging to the Buccinidae, Mitridae, *Oliva, Conus,* and Volutidae or Naticidae. Also present are several large, thick spines of echinoids, probably referable to Cidaroida. The sample was collected in 1407–1100 m, but the fauna consists entirely of taxa that now live in less than about 50 m of water around coral reefs.

The fauna of U337 is diverse and interesting. It consists of several valves and fragments of large, thick-shelled oysters referred to *Lopha cristagalli* (Linné) and *Dendrostrea folium* (Linné), a single fresh, brightly colored valve of the coral-reef scallop *Gloripallium pallium* (Linne), a brightly colored *Spondylus* fragment, several brightly colored specimens of two species of the cemented bivalve *Chama,* a single valve of a small *Trachycardium* cockle, two specimens of the rare cowry *Cypraea bernardi* (Richard) (discussed

Table 1. Mollusca and other invertebrates (other than corals) in five dredge samples from the 1986 HMNZS Tui *cruises: Numerals indicate the numbers of specimens or fragments in each sample; M indicates several to many specimens or fragments.*

TAXA PRESENT / SAMPLE NUMBER	U331	U337	U345	U375	U377
BIVALVIA					
Lopha cristagalli (Linné), fragments	.	2	.	.	.
? *Dendrostrea folium* (Linné)	.	3	.	.	.
? *Hyotissa hyotis* (Linné), fragments	.	.	.	M	.
Ostreidae, indet.	2	.	.	.	.
Gloripallium pallium (Linné), fragments	M	1	.	.	.
? *Comptopallium* sp., fragments	.	.	.	2	.
Spondylus sp., fragments	M	1	.	M	1
Lima cf. *lima* (Linné)	.	.	.	1	1
Pteriidae?, indet., fragment	.	.	1	.	.
Lucinidae?, indet. (aff. *Anodontia* ?), fragment	.	.	1	.	.
Chama spp. (2 taxa), fragments	.	M	.	4	.
Trachycardium (Trachycardium) cf. *elongatum* (Bruguiere), fragments	M	.	.	.	.
Trachycardium (Regozara) ? sp., small	.	1	.	.	.
Periglypta cf. *reticulata* (Linné), fragments	M	.	.	.	.
Timoclea cf. *costellifera* (A Adams & Reeve)	1	.	.	.	.
Veneridae, indet., fragment	.	.	.	.	1
Verticordiidae, ? *Euciroa* sp., fragments	.	.	.	2	.
GASTROPODA					
Cellana sp.	.	.	.	5	.
Scutellastra ? or *Patelloida* ? sp., 2 taxa	.	.	.	3	.
Turbo (Argyrostoma) sp., fragments	1	.	.	1	.
Vermetidae?, indet.	.	.	.	1	.
Cypraea bernardi (Richard)	.	2	.	.	.
Cypraea cf. *carneola* Linné, fragments	.	2	.	.	.
Cypraea sp., fragment	1	.	.	.	.
Bursa (Bursa) lamarckii (Deshayes), fragment	.	1	.	.	.
Bursa (Colubrellina) granularis (Röding), fragment	1	.	.	.	.
? *Oocorys* sp., fragment	.	.	1	.	.
Chicoreus brunneus (Link)	.	1	.	.	.
Buccinidae, ?aff. *Belomitra* sp, fragments	.	.	.	2	.
Buccinidae?, indet., fragment	1	.	.	.	.
Peristernia nassatula (Lamarck), fragment	.	1	.	.	.
Mitridae?, indet., fragment	1	.	.	.	.
Oliva sp., fragment	1	.	.	.	.
Conus sulcatus Hwass in Bruguière	.	.	.	1	.
Conus sp., fragments	2	.	.	.	.
Morum (Oniscidia) aff. *cancellatum* (Sowerby)	.	1	.	.	.
Volutidae? or Naticidae?, smooth, fragment	1	.	.	.	.
CIRRIPEDIA					
Barnacle plates	.	.	.	2	.
ECHINOIDEA					
Cidaroida, spines	M	.	.	.	.

below), two fragments of a cylindrical cowry referred to *Cypraea carneola* (Linné), a brightly colored aperture from a specimen of *Bursa lamarckii* (Deshayes) (also discussed below), a small abraded murex shell, *Chicoreus brunneus* (Link), a fragment of *Peristernia* close to *P. nassatula* (Lamarck) with a bright purple aperture, and a large, well preserved, brightly colored fragment of the gastropod *Morum (Oniscidia)* aff. *cancellatum* (Sowerby). *Cypraea bernardi* and the species of *Morum* are recorded from depths of up to about 130 m, but all other taxa present in U337 are restricted to water less than about 50 m deep around coral reefs. The sample was dredged in 1001-804 m.

Sample U375 consists of more than 90% shallow-water taxa; more than half the sample consists of large, brightly colored, thick fragments of the cemented bivalve *Spondylus,* apparently representing several species. Other shallow-water taxa are oysters referred to *Hyotissa hyotis,* an elaborately sculptured scallop referred to *Comptopallium,* a fragment of the swimming bivalve *Lima,* four brightly colored valves of *Chama,* eight shells of three taxa of intertidal limpets, the intertidal turban shell *Turbo (Argyrostoma),* a fragment of an irregularly coiled shell referred to the gastropod family Vermetidae, and a single complete specimen of the cone shell *Conus sulcatus* Hwass in Bruguière. However, three other taxa in U375 are stained dark brown to black, and have a very different appearance from those listed above. Two fragments of a large, thin, inflated, finely cancellate, nacreous bivalve belong in the family Verticordiidae, and probably in the bathyal and abyssal genus *Eucirva.* Two broken gastropods closely resemble the buccinid *Belomitra* (Bouchet and Warén, 1986, pl. 11, 12), a genus recorded widely in bathyal and abyssal depths in the Atlantic. Finally, two large, almost smooth barnacle plates are also stained dark brown. The stained taxa appear to represent the *in situ* fauna at the sampling depth of 1272 m, whereas all other taxa in U375 live in less than about 50 m around coral reefs.

The three specimens in sample U377 are less diagnostic of depth than the faunas in the above three samples. A single brightly colored fragment of the cemented bivalve *Spondylus* presumably represents a shallow-water species, but the single valve of a white *Lima* species close to *L. lima* (Linné) and the unidentified fragment of a venerid bivalve could have lived at greater depths.

Sample U345 (Machias Seamount) contrasts strongly with the other four. It consists of a single thick fragment of an unidentified white calcitic bivalve tentatively referred to the Pteriidae; a large fragment of an almost smooth, inflated, white, thin-shelled bivalve, apparently a member of the Lucinidae related to *Anodontia*; and a single broken white specimen of the cassid gastropod *Oocorys*, with fine spiral sculpture and an only narrowly reflected outer lip. *Oocorys* is a well known bathyal and abyssal genus in the Atlantic Ocean (Turner, 1948; Quinn, 1980) and has been trawled commonly around New Zealand in the lower bathyal zone (unrecorded specimens observed at the New Zealand Oceanographic Institute). There seem to be no records of *Oocorys* living in depths shallower than about 400 m anywhere in the world, and the two bivalves are of uncertain depth significance.

There is therefore no evidence that the fauna of U345 is anything other than the *in situ* bathyal fauna at the sampling depth of 1972-2166 m.

TAXONOMIC NOTES

Two of the Mollusca in sample U337 call for comment on their nomenclature or on their recorded geographic range.

CLASS GASTROPODA

Family Cypraeidae

Cypraea bernardi (Richard, 1974). Fig. 1-4.
Adusta (Cribraria) bernardi Richard, 1974, p. 377, pl. 1.
Adusta bernardi; Salvat and Rives, 1975, p. 292, fig. 134.
Cypraea kingae Rehder and Wilson, 1975, p. 2, frontispiece fig. 1, 4, 5, 7, 8; text-fig. 1-3; Burgess, 1985, p. 259.
Cypraea bernardi; Burgess, 1985, p. 251.

Two specimens of *Cypraea* in sample U337 belong in one of the rarest of cowry species. Distinctive characters of *Cypraea bernardi* are its small size (to about 20 mm long); its extremely fine teeth (among the narrowest of modern *Cypraea* species) on both inner and outer lips; the presence of three or more low denticles on the anterior end of the fossular ridge, well inside the aperture, in most specimens not connected to the corresponding teeth on the inner lip; the elevation and, in many specimens, partial fusion of two or three of the anterior-most teeth on the inner lip, and their separation from the terminal ridge by a particularly marked groove; and, in well calcified mature specimens, the prominent angled ridges along the sides of the base, producing a low, wide shape of lenticular cross-section and a wide, flattened base.

The holotype and the single paratype of *Cypraea bernardi* were collected under coral blocks by diving in shallow water (1.5 m) in the lagoon at Hitiaa, Tahiti, Society Islands. They are both relatively weakly calcified specimens lacking the prominent lateral ridges of the type material of *Cypraea kingae* Rehder and Wilson (1975). The type material of *C. kingae* consists of 23 specimens from Pitcairn Island dredged by M/V *Pele* in 45-130 m; all specimens have prominent lateral ridges, a wide base, and a lenticular cross-section. These are apparently the only previous records of this species. Rehder and Wilson (1975, p. 5) considered but discounted the possibility that their Pitcairn Island specimens belong in *C. bernardi*, but subsequent comparison has demonstrated that they are conspecific (Prof. E. Alison Kay, Univ. Hawaii, letter 18 June 1987). One of the Cook Islands specimens (Figures 1, 2) in U337 is a relatively heavily calcified shell with prominent lateral ridges,

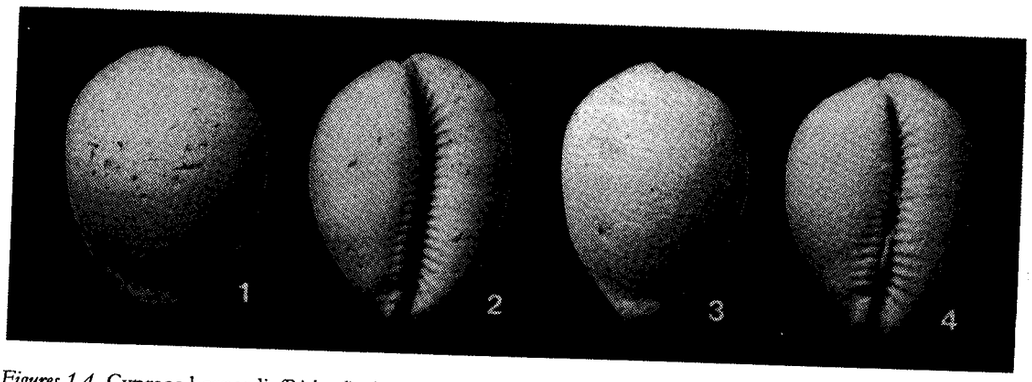

Figures 1-4. Cypraea bernardi *(Richard), the two specimens from Stn U337, enlarged 2x.*

resembling the type material of *C. kingae*. The other specimen in U337 (Figures 3, 4) is narrower and has the lateral ridges much less well developed than the other, and resembles the type material of *C. bernardi*. These specimens therefore help confirm the synonymy of *C. kingae* and *C. bernardi*. The two long-dead, bleached specimens in U337 therefore represent a very marked range extension for *C. bernardi* to the west of previous records. The previous depth records of 1.5 to 130 m for C. *bernardi* contrast strongly with the depth of 1001-804 m for station U337.

Dimensions: 19.9 x 15.1 mm (Fig. 1, 2); 18.9 x 13.7 mm (Fig. 3, 4).

Family Bursidae

Bursa (Bursa) lamarckii (Deshayes, 1853)
Ranella lamarkii [sic] Deshayes, 1853, "Explications des planches", p. 67; pl. 112, fig. 1, 2.
Bursa bufonia; Shikama, 1963, p. 64, pl. 49, fig. 1 (not *Murex bufonius* Gmelin, 1791).
Bursa species: Cernohorsky, 1967, p. 316, pl. 42, fig. 2.
Bursa lamarckii: Beu, 1985, p. 63, fig. 40.

The opportunity is taken to point out the very obscurely published valid name for the common coral reef "black-mouthed *Bursa", Bursa lamarckii* (Deshayes, 1853, p. 67, pl. 112, fig. 1, 2), as until recently this species has either been confused with the almost uniform white *Bursa bufonia* (Gmelin), or regarded as unnamed. Excellent colored drawings of this species, in both dorsal and ventral views, were provided by Deshayes (1853, pl. 112, fig. 1, 2) and the name *Ranella lamarkii* appears in the "Explications des planches", p. 67. Cox (1942) discussed the dates of publication of this book; this portion of the "Explications" was published in 1853. The name is therefore validly published in Deshayes's (1839-1858) unfinished textbook on conchology; complete copies of this work are very rare. Although Deshayes spelled the name *"lamarkii",* there can be no doubt that the name was intended to honor his predecessor in the Paris Museum, J.B.P.A. de M. de Lamarck, and the correct spelling should be used (ICZN Article 32d). Several other generic and specific names are incorrectly spelled in Deshayes's "Explications des planches" (e.g., *Aphysia* for *Aplysia*, p. 59; *Nerita pelerouta* for *peloronta*, p. x) and *lamarkii* is evidently one of several typographical errors.

Bursa lamarckii is moderately common on coral reefs and in shallow water (down to about 20 m) near reefs from East Africa to Hawaii, and from the southern Great Barrier Reef, eastern Australia, north to the Amami Islands in southern Japan. The single large aperture in U337 shows the diagnostic dark brown coloration and prominent paler ridges of the aperture of *B. Lamarckii.*

CONCLUSIONS

1. More than 90% of the Mollusca in the four Cook Islands samples are brightly colored, freshly preserved specimens or (in most cases) fragments of taxa now restricted to shallow water around coral reefs, in depths down to about 50 m. The fauna of station U345 (Machias Seamount) and three specimens in the large Cook Islands sample U375 seem to represent the *in situ* faunas at their sampling depths. The occurrence of large numbers of shallow-water molluscs in depths of 804 to 2450 m presumably results from the slumping of large volumes of coral reef sediment into these depths from much shallower water.
2. Two specimens of *Cypraea bernardi* (Richard) from the northern Cook Islands constitute a marked range extension to the west of the two previous records, from Tahiti and Pitcairn Island.
3. The valid name for the common coral reef "black-mouthed *Bursa"* is *Bursa lamarckii* (Deshayes, 1853).

ACKNOWLEDGMENTS

I thank Dr G.P. Glasby for the opportunity to work the present samples, Professor E. A. Kay (University of Hawaii) for the identification of *Cypraea bernardi,* Dr P.A. Maxwell (formerly of New Zealand Geological Survey) for comments on the manuscript, and Wendy St George (Institute of

Geological and Nuclear Sciences) for photography. The text was typed by Alison Lee (formerly of New Zeàland Geological Survey) and Irene Galuszka.

REFERENCES CITED

Beu, A.G., 1985, A classification and catalogue of living world Ranellidae (= Cymatiidae) and Bursidae: Conchologists of America Bulletin, v.13, p.55-66.

Bouchet, P., and A. Warén, 1986, Mollusca Gastropoda: taxonomical notes on tropical deep water Buccinidae with descriptions of new taxa: Mémoires de la Muséum National d'Histoire Naturelle, ser. A, Zoologie, v.133, p.457-499.

Burgess, C.M., 1985, Cowries of the world: Cape Town, Seacomber Publications, 289 p.

Cernohorsky, W.O., 1967, The Bursidae, Cymatiidae and Colubrariidae of Fiji (Mollusca: Gastropoda): The Veliger, v.9, p.310-329.

Cox, L.R., 1942, Publication dates of Traité élémentaire de conchyliologie, by G.P. Deshayes: Proceedings of the Malacological Society of London, v.25, p.94-95.

Deshayes, G.P., 1839-1858, Traité élémentaire de conchyliologie, avec les applications de cette science à la géologie. Paris, Victor Masson, Librairie. Tome premier. Première partie. - Introduction (1839-1853), xii + 368 p. Seconde partie. - conchifères dimyaires (1839-1858), 824 + 384 p. Explication des planches (1839-1853), ii + 80 + xi p.; pl. 1-58, 60-79, 81-85, 88-93, 100-128, 131, 132; 8 bis, 12 bis, 14 bis, 32 bis, 41 bis, 44 bis, 59 bis, 59 ter, 60 bis, 73 bis, 73 ter (= 131 pl.).

Quinn, J.F., 1980, A new genus, species and subspecies of Oocorythidae (Gastropoda: Tonnacea) from the western Atlantic: The Nautilus, v.94, p.149-158.

Rehder, H.A., and B.R. Wilson, 1975, New species of marine mollusks from Pitcairn Island and the Marquesas: Smithsonian Contributions to Zoology, no. 203, iv + 16 p.

Richard, G., 1974, *Adusta (Cribraria) bernardi*, sp. n. (Mesogastropoda, Cypraeaidae) des Iles de la Société et les porcelaines de Polynésie: Bulletin de la Sociétée des Etudes Océaniennes, v.16, p.377-383.

Salvat, B., and C. Rives, 1975, Coquillages de Polynésie: Papeété, Les Editions du Pacifique, 391 p.

Shikama, T., 1963, Selected shells of the world illustrated in colours [vol. 1]: Tokyo, Hokuryu-kan Publishing Co., 154 p.

Turner, R.D., 1948, The family Tonnidae in the western Atlantic: Johnsonia, v.2, p.165-192.

Hayward, B. W. 1996. Foraminiferal age and paleoenvironmental assessments of dredge samples collected during the 1986 HMNZS *Tui* cruises, *in:* Meylan, M.A., and G.P. Glasby (eds) Manihiki Plateau, Machias and Capricorn Seamounts, Niue, and Tofua Trough: Results of Tui Cruises. SOPAC Technical Bulletin 10: 151-155.

FORAMINIFERAL AGE AND PALEOENVIRONMENTAL ASSESSMENTS OF DREDGE SAMPLES COLLECTED DURING THE 1986 HMNZS *TUI* CRUISES

B.W. Hayward

Auckland Institute and Museum, Private Bag 92018, Auckland, New Zealand

ABSTRACT

Sediments dredged at 600-1700 m depth on the flanks of atoll-capped or coral reef-fringed volcanic seamounts in the Cook Islands contain Late Pliocene to Holocene foraminifera of mixed deep-water and shallow reef or fore-reef origin. Marine erosion and mass wasting have therefore provided significant quantities of shallow water bioclastic sediment to the seamount flanks.

Sediment dredged from the submerged crest (ca 650 m) of Machias Seamount and the lower flanks of submerged Capricorn Seamount (crest ca 900 m) contain similar mixed deep and shallow reef- and fore-reef-derived foraminifera. These indicate that prior to the beginning of subduction into the Tonga Trench, sometime during the Late Miocene to Early Pleistocene, the crests of these seamounts were capped by coral reefs or atolls.

INTRODUCTION

Eight sediment samples from seven dredge hauls made during the 1986 HMNZS *Tui* cruises (Table 1) were processed to examine their foraminiferal faunas (Table 2). These faunas provide clues to the age, paleoenvironment, and provenance of the sediments. Age assessments are based on the planktic foraminiferal time ranges given by Kennett and Srinivasan (1983). Full station data are given by Glasby et al. (this volume).

PALEOENVIRONMENTS

Planktic foraminiferal faunas

In general, the planktic percentage of a foraminiferal fauna reflects the oceanic or neritic character of the overlying water mass. Here, in the subtropical SW Pacific, where there is little true neritic water, planktic percentage in depths above the lysocline presumably reflects the depth stratification of the live planktic foraminifera (in the upper few hundred meters), the higher benthic productivity in shallow water and the fragility of planktic tests in high-wave-energy environments.

Chaproniere (1985) quoted planktic percentages for the Solomon and Tongan areas of 0-30 % for 0-100 m depth, increasing to ca 75% at 300 m and 99 % at 1600 m.

In addition to planktic percentages, the taxonomic composition of the planktic fauna may also be an indication of paleobathymetry. Most spinose genera (e.g., *Globigerina*, *Globigerinoides*, *Orbulina*) are phytoplankton feeders and live predominantly in the photic zone (Bé, 1977) at 0-ca 100 m and are the dominants in shallow planktic faunas. Non-spinose genera (e.g. *Globorotalia, Sphaeroidinella)* are omnivorous and live mostly below the photic zone (Bé, 1977) at ca 100-500 m. Deeper planktic faunas are therefore usually more diverse.

In the *Tui* samples, the lowest diversity planktic faunas (U343, U362, U371 (I and II)) are dominated by shallow-living spinose forms, have few *Globorotalia* specimens and have lower planktic percentages (2-90 %). Like the benthics, the planktics in these samples are therefore dominantly of shallow-water origin.

Table 1. Foraminiferal sample data.

Foram Sample	Stn No.	Fossil Record No.	Depth (m)	Locality
1	U322b	SW10163/fl	1754–1560	Manihiki I.
2	U343	SW14172/fl	730–715	Machias Smt
3	U344	SW14172/f2	675–670	Machias Smt
4	U351a	SW18172/fl	996–976	Capricorn Smt
5	U352	SW18172/f2	4684–4689	Capricorn Smt
6	U362	SW20157/fl	685–626	Mauke
7	U371 (I)	SW21159/fl	1516–1486	Rarotonga
8	U371 (II)	SW21159/flA	1516–1486	Rarotonga

Planktic faunas in the other four samples (Table 2) comprise 90-99% of the foraminifera, are more diverse and have greater numbers of deeper-living non-spinose forms. Like the benthics, many or most of the planktics in these samples accumulated in a deep-water setting.

Benthic foraminiferal faunas

A quiet, deep-water association and a higher energy, shallow-water association of benthic foraminifera are easily distinguished in these faunas, often with elements of both associations mixed together in one sample.

Deep-water association: This association is characterized by a diverse fauna with no dominants. Extensive studies (e.g., Cushman et al., 1954; Todd, 1966) have shown that the following taxa that occur here generally do not live at shallow depths (less than 100-200 m) around tropical islands and atolls in the Pacific: *Cassidulina delicatula, Globocassidulina gemma, Ehrenbergina, Hoeglundina, Pyrgo lucernula, P. murrhyna, Lenticulina, Bolivina, Bolivinita, Pullenia, Discanomalina, Nonion, Ophthalmidium, Spirophthalmidium, Oridorsalis, Sphaeroidina, Stilostomella, Trifarina bradyi, Karreriella, Uvigerina* and *Planulina wuellerstorfi.* Taxa often restricted to even deeper water in tropical oceans (mid bathyal-abyssal) and only recorded here in the sample from 4600 m (U352) include *Ammodiscus, Cyclammina, Eggerella, Epistominella exigua* and *E. umbonifera.*

All samples except U371(I) contain elements of this deep water association. Pteropod sand (U351a) from the crest of Capricorn Seamount has an exclusively deep-water benthic association. U322b, U344 and U352 have a subequal mix of shallow and deep associations, whereas U343, U362 and U371(II) have only a minor proportion of deep association forms.

Shallow-water association: In these samples, the shallow-water assemblage is dominated by large, robust foraminifera, especially *Amphistegina* spp. but also *Heterostegina, Marginopora, Operculina, Baculogypsina, Calcarina, Tinoporus, Spirolina, Peneroplis* and *Sorites.* Smaller forms, yet significant elements in this shallow-water association, include *Eponides repandus, Cymbaloporetta, Gaudryina siphonifera, Hauerina, Quinqueloculina, Miliolinella, Spiroloculina angulata, Triloculina, Textularia conica, Reussella, Elphidium, Bolivinella, Buliminella, Pileolina, Neoconorbina* and *Rosalina.*

This association occurs today on the shallow (0-100 m) fore-reef slopes of tropical coral atolls or reef-fringed islands (Cushman et al., 1954; Todd, 1966). Most of the robust forms live predominantly at shallow depths (0-40 m) and dominate modern reef faunas. They are easily swept off the reefs and carried down into quieter, deeper (30-100 m) environments where many of the smaller forms live most abundantly. Many of the taxa in this association can also be found together today in quiet lagoon sediments protected by coral reefs, but the total assemblage and its preservation in the *Tui* samples is more suggestive of fore-reef slopes.

All samples, except U351a, contain elements of this shallow-water association. Pebbly sandstone from 1500 m on the flanks of Rarotonga has an exclusively shallow-water benthic association. The sand matrix from interstices in a lump of coral on Machias Seamount (U343) and calcareous sand from the flanks of Mauke and Rarotonga (U362, U371(II)) contain a dominantly shallow-water association. U322b, U344 and U352 contain a subequal mix of shallow and deep associations.

SAMPLE ASSESSMENTS AND AGES

Manihiki Island, Northern Cook Islands

Manganese-coated pebbles of foraminiferal ooze (U322b) from the middle flanks (1750-1560 m) of Manihiki Plateau contain a rich and diverse planktic foraminiferal fauna. The presence of *Pulleniatina praecursor* (plankic foraminiferal zones N19-N21), *Neogloboquadrina humerosa* (N18-early N22), *Globorotalia pertenuis* (N21-early N22), *Globigerinoides fistulosa* (N21-early N22),*Globorotalia tumida flexuosa* (N18-N21) and *Globorotalia ronda* (N20-N21) give a Late Pliocene (N21) age. The sediment appears to have accumulated at similar depths to the present (as shown by its abundant, diverse planktics and sparse deep-water benthics), with downslope addition of transported material (sparse shallow-water benthics) from the shallow-water environment around a tropical atoll.

Machias Seamount

Sand (U343) from the interstices of a lump of worn, manganese-coated reef coral, from near the crest of Machias Seamount, accumulated on a shallow fore-reef slope (sparse, low diversity planktics and shallow water benthics). Like the coral, the sediment therefore dates from the time when the crest of Machias Seamount was at sea-level and capped by an atoll. The sparse planktic fauna indicates that this was no earlier than Late Miocene (N16).

Carbonate sand (U344) dredged from the very crest of Machias Seamount is a mixed sample of modern, deep-water sediment and brown-stained, shallow-water (0-100 m) sediment of Pliocene or Early Pleistocene (N19-N22) age (based on several specimens of *Globorotalia* cf. *crassaformis).*

Capricorn Seamount

Pteropod sand (U351a) from the crest of Capricorn Seamount is of Late Pleistocene to Holocene age and accumulated at similar upper bathyal depths to the present. However, sandy mud (U352) dredged from the lower flanks of the seamount is a mixture of Late Pleistocene to Holocene deep-water sediment and brown-stained sediment that had been transported downslope from coral reef depths when the seamount crest was at sea-level. The presence of stained specimens of *Globorotalia ronda* (N20-N21) and *Globorotalia tosaensis* (N20-early N22) date this as Late Pliocene (N20-N21).

Table 2. Species lists for foram samples listed in Table 1.

PLANKTIC FORAMINIFERA	1	2	3	4	5	6	7	8
planktic percentage	99%	2%	90%	99%	90%	65%	90%	70%
Candeina nitida			*	*	*			
Globigerina digitata		*		*				
Globigerina falconensis					*			
Globigerinella adamsi					*			
Globigerinella aequilateralis	*	*	*	*	*	*	*	*
Globigerinita glutinata				*				*
Globigerinoides conglobatus	*	*	*	*	*	*	*	*
Globigerinoides fistulosa	*							
Globigerinoides ruber	*	*	*	*	*	*		*
Globigerinoides sacculifer	*	*	*		*	*	*	*
Globigerinoides tennellus			*					
Globorotalia crassaformis	*		*					
Globorotalia crassula			*	*		*		*
Globorotalia inflata					*			
Globorotalia menardii			*					
Globorotalia pertenuis	*				*			
Globorotalia ronda	*				*			
Globorotalia scitula	*		*	*				
Globorotalia tosaensis					*			
Globorotalia truncatulinoides			*	*	*	*		*
Globorotalia tumida	*		*	*	*		*	
Globorotalia tumida flexuosa	*							
Hastigerina pelagica			*	*				
Hastigerinopsis riedeli				*				
Neogloboquadrina dutertrei			*					
Neogloboquadrina humerosa	*							
Orbulina universa	*		*	*	*	*	*	*
Pulleniatina praecursor	*							
Pulleniatina cf. praecursor		*						
Pulleniatina obliquiloculata	*		*					
Sphaeroidinella dehiscens	*		*		*			*

BENTHIC FORAMINIFERA	1	2	3	4	5	6	7	8
Ammodiscus spp.					*			
Ammolagena clavata			*					
Amphistegina bicirculata	*	*			*	*		
Amphistegina lessonii	*	*				*	*	*
Amphistegina papillosa		*	*		*	*		
Amphistegina radiata	*							*
Amphistegina sp.			*				*	
Anomalinella rostrata		*						
Anomalinoides sp.			*					
Astacolus crepidulus			*			*		
Astrononion stelligerum					*			
Baculogypsina sphaerulata		*				*		
Bolivina spathulata						*		
Bolivina subreticulata						*		
Bolivina sp.						*		
Bolivinella elegans		*				*		
Bolivinita quadrilatera								*
Buliminella elegantissima		*						
Calcarina calcar					*			
Cassidulina crassa		*						
Cassidulina delicatula			*	*		*		
Ceratobulimina pacifica			*	*	*			
Cibicides lobatulus		*						
Cibicides refulgens			*					
Cibicides spp.					*	*		*
Cyclammina sp.					*			
Cymbaloporetta tabellaeformis		*				*		*
Dentalina sp.					*			
Discanomalina semipunctata			*	*				
Eggerella bradyi					*			
Ehrenbergina perumbonata								*
Ehrenbergina reticulata				*				
Ehrenbergina trigona			*	*				
Elphidium sp.		*						
Elphidium crispum					*			
Epistominella exigua					*			
Epistominella umbonifera					*			

Mauke, Southern Cook Islands

Calcareous sand (U362) from the upper submarine flanks (650 m) of Mauke is of Late Pleistocene to Holocene age. Foraminifera indicate that the sediment is dominantly derived from the shallow fore-reef area (0-100 m) upslope, with a minor deep-water, *in situ* component.

Rarotonga, Southern Cook Islands

Calcareous sand (U371(I)) from the middle submarine flanks (1500 m) of Rarotonga is similar in origin to that from Mauke. It is of Late Pleistocene to Holocene age, derived mostly from the shallow, fore-reef area with a minor deep-water, *in situ* component.

Pebbly sandstone (U371/II) from the same dredge haul has a sparse planktic fauna of indeterminate age but no older than latest Miocene (N18). The sediment contains no definite deep-water foraminifera and probably accumulated entirely at shallow, fore-reef depths (0-100 m). It may have been transported downslope at a later time in a semi-lithified state.

CONCLUSIONS

1. All four samples from the bathyal flanks of Manihiki Island, Mauke and Rarotonga contain significant quantities of shallow reef- or fore-reef-derived bioclastic sediment. This suggests that marine erosion and mass wasting processes play a major role in providing sediment to the flanks of tropical seamounts that rise to sea-level. The many eustatic sea level oscillations of the last few million years have possibly greatly enhanced these processes.

2. The present crests of the Machias and Capricorn Seamounts are ca 650 m and 900 m below sea-level. The presence of shallow fore-reef and reef-derived foraminifera on the crest of Machias and on the lower flanks of Capricorn indicate that both crests previously reached to sea-level and were capped by coral reefs. The timing of the subsequent submergence is difficult to date accurately. Planktics associated with shallow-water benthics on the crest of Machias are no older than Late Miocene in U343 and of Pliocene or Early Pleistocene age in U344. Deep-water planktics associated with shallow benthics on the lower flanks of Capricorn are Late Pliocene.

	1	2	3	4	5	6	7	8
Eponides repandus	*				*	*	*	*
Fissurina aperta		*						
Frondicularia robusta						*		
Gaudryina convexa								*
Gaudryina siphonifera		*	*					
Globocassidulina gemma		*	*	*	*	*		*
Globocassidulina subglobosa	*							
Hauerina involuta		*	*					
Hauerina orientalis							*	*
Hauerina speciosa		*						
Heterostegina depressa			*		*	*		*
Hoeglundina elegans		*	*					
Karreriella bradyi	*							
Lagena spp.			*	*				
Lenticulina calcar						*		*
Lenticulina peregrina			*					
Lenticulina spp.			*					
Liebusella bradyi						*		
Loxostomum limbatum		*		*				
Marginopora vertebralis		*				*		
Miliolinella subrotundata		*				*		
Mychostomina sp.						*		
Neoconorbina sp.					*			
Nonion sp.				*				
Nonionella sp.					*			
Nummoloculina irregularis				*				
Operculina ammonoides		*	*			*	*	
Ophthalmidium acutimargo			*	*				
Oridorsalis umbonatus	*							
Patellina corrugata		*		*				
Peneroplis pertusus		*						*
Pileolina patelliformis		*				*	*	
Planulina wuellerstorfi			*		*			
Pullenia bulloides					*			
Pyrgo anomala			*					
Pyrgo denticulata		*						
Pyrgo depressa	*		*					
Pyrgo lucernula								*
Pyrgo murrhyna	*		*	*				
Pyrgo spp.						*		*
Quinqueloculina spp.			*			*	*	*
Ramulina globulifera			*					
Rectobolivina columellaris						*		
Reussella aculeata		*						
Reussella simplex	*						*	*
Rosalina bradyi		*						
Rotalia sp.					*			
Rugidia corticata						*		
Saracenaria sp.			*					
Siphogenerina raphanus		*				*		*
Sorites marginalis		*				*	*	*
Sphaerogypsina globulus						*		*
Sphaeroidina bulloides								*
Spirillina tuberculata-limbata		*						
Spirillina spp.		*		*		*	*	*
Spirolina arietina	*							
Spiroloculina angulata						*		
Spiroloculina foveolata		*						
Spiroloculina mayori		*						
Spirophthalmidium pusillum				*				
Stilostomella lepidula	*				*			
Svratkina sp.		*						
Textularia conica		*					*	
Textularia indenta		*						
Textularia pseudogramen						*		
Textularia spp.				*				*
Tinoporus spengleri			*		*			
Trifarina bradyi						*		
Triloculina tricarinata	*	*						
Triloculina trigonula					*			
Uvigerina peregrina		*						
Wiesnerella auriculata		*						

Both Machias and Capricorn Seamounts are on the western limit of the Pacific Plate. Their fairly recent submergence reflects this location as they begin to be subducted down into the Tonga Trench.

ACKNOWLEDGMENTS

G.H. Scott and C.P. Strong are thanked for their critical comments on the manuscript.

REFERENCES CITED

Bé, A.W.H., 1977, An ecological, zoogeographic and taxonomic review of Recent planktonic foraminifera, *in* A.T.S. Ramsay, ed., Oceanic micropaleontology: London, Academic Press, p.1-100.

Chaproniere, G.C.H., 1985, Late Neogene and Quaternary planktonic foraminiferal biostratigraphy and paleobathymetry of dredge samples from the southern Tonga Platform (Cruise L5-82-SP), *in* D.W. Scholl and T.L. Vallier, eds., Geology and offshore resources of Pacific island arcs - Tonga region: Circum-Pacific Council for Energy and Mineral Resources, Earth Science Series, v. 2, p.131-139.

Cushman, J.A., R. Todd, and R.J. Post, 1954, Recent foraminifera of the Marshall Islands: United States Geological Survey, Professional Paper 260-H, p.319-384.

Kennett, J.P. and M.S. Srinivasan, 1983, Neogene planktonic foraminifera. A phylogenetic atlas: Stroudsburg, Pennsylvania, Hutchinson Ross Publishing Company, 265 p.

Todd, R., 1966, Smaller foraminifera from Guam: United States Geological Survey Professional Paper 403-I, p.1-41.

Dugolinsky, BK, and M.A. Meylan 1996. Microorganisms occurring on deep-sea manganese nodules and crusts collected during the 1986 HMNZS *Tui* cruis~s, *in:*
Meylan, M.A., and Glasby (eds) Manihiki Plateau, Machias and Capricorn Seamounts, Niue, and Tofua Trough: Results of *Tui* Cruises. SOPAC Technical Bulletin 10: 157-165.

MICROORGANISMS OCCURRING ON DEEP-SEA MANGANESE NODULES AND CRUSTS COLLECTED DURING THE 1986 HMNZS *TUI* CRUISES

B.K. Dugolinsky

Department of Earrh Sciences, State University of New York, Oneonta, New York 13820, USA

M.A. Meylan

Department of Geology, University of Southern Mississippi, USM Box 5044, Hattiesburg, Mississippi 39406-5044, USA

ABSTRACT

The surfaces of manganese nodules and crusts collected during the 1986 HMNZS *Tui* cruises display a variety of micro- and meiofaunal remains, particularly tubular benthic agglutinated foraminifera. The remains occur on all nodules examined, representing eight stations in water depths from 3305 to 5260 m. They were also observed on thinly Mn-encrusted rocks and thicker Mn crusts from an additional eight stations (water depths 1288 to 3991 m). Most meiofaunal morphotypes preferentially occupy recesses between nodule or crust surface microbotryoids rather than more exposed positions. A few of the crust samples examined apparently lack attached microorganism remains. Many of the epifauna have not been identified, and some may represent species not yet described.

INTRODUCTION

Cursory visual inspection of the nodules collected during the 1986 HMNZS *Tui* cruises revealed the presence of tiny, white, thread-like structures that were assumed to be the remains of benthic Foraminifera.

Organisms attached to the surfaces of manganese nodules were noted as long ago as the HMS *Challenger* Expedition (Murray and Renard, 1891). Subsequent work has indicated that nodules (as well as manganese crusts) provide a solid substrate for the growth of a variety of attached organisms such as bacteria (Ehrlich, 1963; LaRock and Ehrlich, 1975; Burnett and Nealson, 1981), benthic agglutinated Foraminifera (Graham and Cooper 1959; Greenslate, 1974; Dudley, 1976; Dugolinsky et al., 1977; Mullineaux, 1987), sponges, scyphozoan polyps, actinians, octocorals and other hydrozoans, and polychaetes (Greenslate et al., 1975; Mullineaux, 1987), as well as molluscs, crustaceans, bryozoans, brachiopods, crinoids, and tunicates (Mullineaux, 1987). The broader subject of the influence of organisms (bacteria, protozoa, metazoa) on nodules has been reviewed by Thiel and Schneider (1988).

The purpose of this paper is to document the occurrence and nature of the meiofauna (and larger microfauna) attached to nodule and crust surfaces. Because of the rough treatment the nodules and crusts experienced during dredging and with no attempt being made to ensure preservation of organic remains, ecological, biogeographic and taxonomic interpretations can not be made. Emphasis here will be on organisms that are a few microns to about a millimeter in diameter, rather than smaller microflora such as bacteria or the rare larger macrofauna.

Although SW Pacific manganese nodules were included in an earlier study by Dugolinsky et al. (1977), the present study represents the first survey of organisms attached to solid substrate samples from the submarine slopes of the

Manihiki Plateau and some of its associated atolls, as well as from Capricorn Seamount, around the island of Niue and from the floor of the adjacent Penrhyn and Samoan Basins. A list of the station locations is given in Table 1.

SAMPLING PROCEDURES

Nodule and crust samples were recovered with rock and pipe dredges. No special handling to preserve very delicate or soft-bodied organisms was attempted. This study therefore involves only those organisms that constructed some type of durable habitat on the nodule and crust surfaces. Samples were chosen from dredge hauls by examining a number of nodules and/or crusts from each haul with a hand lens. Those nodules with the apparent greatest abundance and diversity of life forms were selected. Because abundance varied so much from nodule to nodule within a single dredge haul, no attempt was made to quantify abundance. This would require detailed examination of a large number of nodules from each haul.

After viewing each sample with a binocular microscope to locate the meiofauna, selected sections of nodules and crusts were cut and/or broken off, and the sections glued to aluminium scanning electron microscope (SEM) plugs. Samples were sputter-coated with gold using a Polaron E5100 SEM Coating Unit. SEM examination was performed

Table 1. Manganese nodules and crusts examined by scanning electron microscopy.

Stn	Location	Depth (m)*	Sample Type	Max.Diam.(mm)
U296a	Penrhyn Basin	5130	Nodule (polynucleate) Nodule (spheroidal) Nodule (shape?)	33 24 (est.) ?
U298	Manihiki Plateau, eastern slope	4996	Nodule (spheroidal)	32
U300	Manihiki Plateau, eastern slope	3752	Nodule (polynucleate)	31
U315	Rakahanga	1731	Nodule (ellipsoidal) Crust	17 ?
U316b	Rakahanga	2600	Crust	?
U321a	Penrhyn Basin	5080	Nodule (ellipsoidal)	20
U326	Pukapuka	2141	Crust	25
U327	Pukapuka	3305	Nodule (ellipsoidal)	21
U332	Tema Reef	1288	Crust	?
U333b	Tema Reef	1744	Crust	?
U339	Samoan Basin	4212	Crust	148
U340	Samoan Basin	5260	Nodule (spheroidal)	?
U348	Capricorn Seamount	2732	Nodule (spheroidal) Rock	? ?
U358	Niue	2485	Crust	22

* Mid-range of sampling traverse; corrected.

initially at low magnifications (about 20-40x) to survey the complete sample surface, using AMR Models 1000, 1200, and 9000. The larger meiofauna visible at this magnification were then examined more closely, and selected specimens photographed. Random traverses were made at higher magnifications in an attempt to locate and photograph specimens of smaller microfossils. It should be noted that because of the virtual absence of diagnostic structures such as a foraminiferal proloculus, the specimen identifications reported here must beconsidered tentative.

RESULTS

The most obvious and most common microorganisms observed were *Saccorhiza* sp. These are white tubular remains that look like tiny threads to the naked eye. *Saccorhiza* tubes are constructed of foreign particles which include fine silt-sized coccoliths and detrital silicate particles. The tubes have been broken open (Figure 1) in most cases, presumably by dredging and handling, often for considerable distances along their length. They occur preferentially in recesses between botryoids and botryoidal clumps (Figure 2), and may extend along nodule surfaces for distances of 10 mm or more, occasionally bifurcating. The observed preference for recesses may have been somewhat enhanced by the breaking off of more exposed sections.

Whereas *Saccorhiza* tests are constructed of discrete scavenged particles, some tubular protozoans apparently construct tests of clay and secreted organic matter, producing smoother interiors and patterned exteriors (Figures 3, 4).

Most occurrences of tubes on nodules are solitary, but networks of tubes were observed on some Mn-encrustations (Figures 5-9). These may belong to the genus *Tolypammina*. Included are rough-appearing tubes (Figures 5-7) constructed of particles of a range of shapes and sizes, as well as smoother tubes (Figures 8, 9) which also appear to

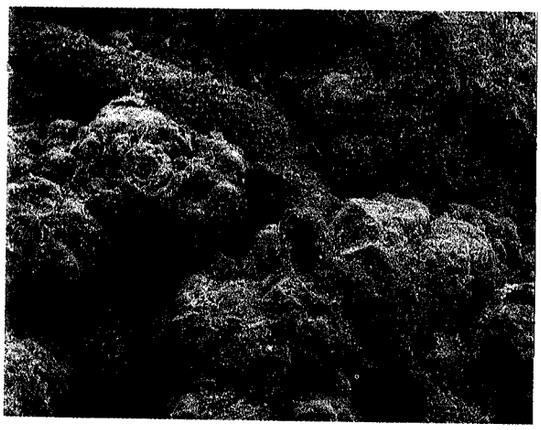

Figure 1. Stn U296a. Tubular agglutinated benthic foraminifer, probably Saccorhiza. *Note that part of the test has been broken off, as have parts of adjacent nodule botryoids. Field of view 1.49 mm across.*

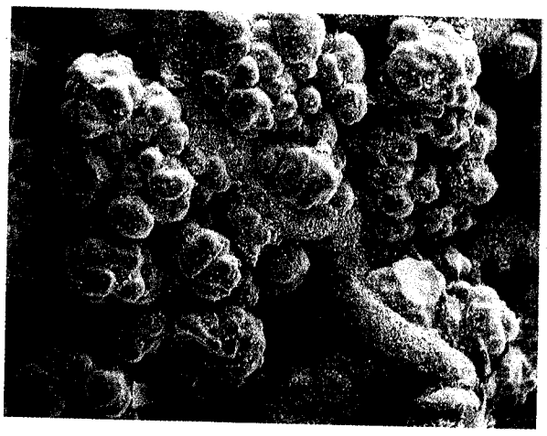

Figure 2. Stn U300. Tubular agglutinated benthic foraminifer, probably Saccorhiza. *Cross-section of broken tube visible in lower right. Field of view 1.79 mm across.*

Figure 3. Stn U315. Tubular agglutinated benthic foraminifer(?). Note thin fractured Mn-encrustation on part of tube aligned vertically in center of photo. Field of view 3.27 mm across.

Figure 4. Stn U315. Close-up view of broken end of tube shown in Figure 3. Note smooth internal surface, ringed exterior. Field of view 0.70 mm across.

Figure 5. Stn U348. Network of branching tubular agglutinated benthic foraminifers. Possibly Tolypammina. *Tubes broken in several places. Field of view 0.84 mm across.*

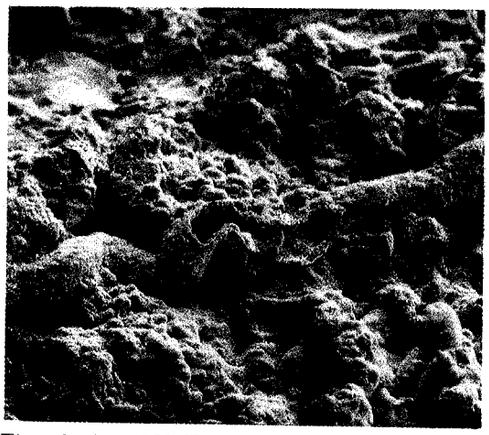

Figure 8. Stn U358. Tubular agglutinated benthic foram. Note broken sections of tube. Foreign particles apparently mostly coccoliths. Field of view 1.00 mm across.

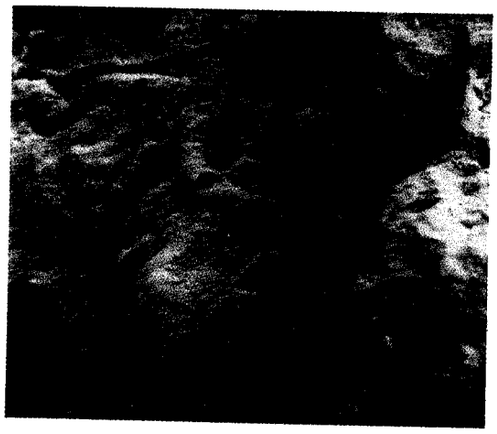

Figure 6. Stn U332. Cluster of tubular agglutinated benthic forams, possibly Tolypammina. *Note numerous broken sections of tubes; possible aperture lower left. Field of view 0.84 mm across.*

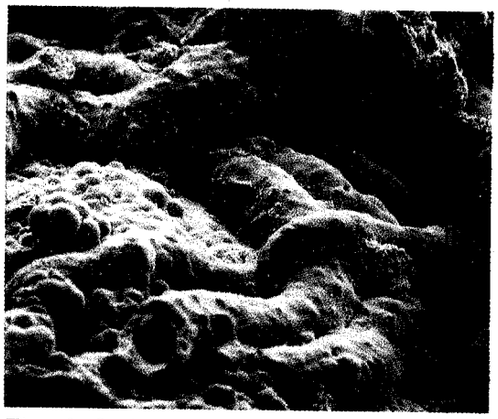

Figure 9. Stn U358. Intertwined cluster of tubular agglutinated benthic forams similar to the one displayed in Figure 6. Smoothness of test due to Mn-oxide coating over coccoliths? Field of view 1.71 mm across.

Figure 7. Stn U332. Close-up view of section of tube shown in Figure 6. Foreign particles mostly fragments of pelagic foram tests; some coccoliths. Field of view 0.087 mm across.

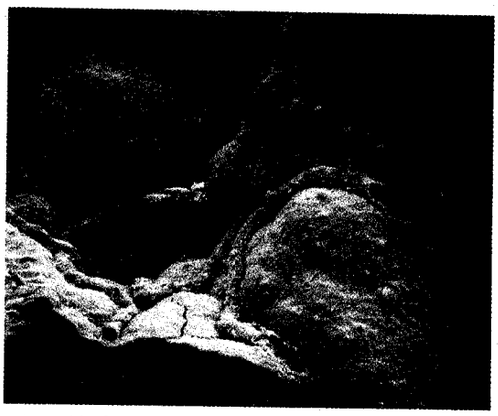

Figure 10. Stn U332. Tubular agglutinated benthic foraminifers, possibly Tolypammina. *Note that tube terminations are the result of breakage. Tubes closely follow recesses between botryoids. Field of view 1.49 mm across.*

consist mostly of individual grains. As with the larger *Saccorhiza*, the *Tolypammina* tubes are commonly located in low areas between botryoids (Figure 10). Tubes within tubes (Figure 11) are probably the result of smaller tubes being incorporated into or grown over by the tubes of somewhat larger tube-forms. Although most tubes appear to lack chambers, a test from Capricorn Seamount has been broken open to reveal chamber walls (Figure 12).

Tunnels (Figures 13-16) and hemispherical chambers (Figures 17-19) with or without irregular tunnel-like extensions are relatively common on nodules. Tunnels differ from tubes in that the organism does not cover the underlying substrate with test material, and the test simply represents a hard covering. Tunnels and chambers, like tubes, preferentially occur between botryoids, although some larger chambers may cover small botryoids (Figure 17). Tunnels and chambers are built with individual particles, mostly in the silt-sized range (see especially Figures 15, 16).

Irregular mat-like tests (tunnels?) are restricted to nooks and crannies at the bases of botryoids (Figures 20-22). The irregular appearance of a specimen from the flanks of Rakahanga is partly due to the nature of the foreign particles, which are needlelike masses that may be authigenic crystals (Figures 21, 22).

A cluster of orange thin-walled spheroidal tests was observed on a Mn-crust from the flanks of Tema Reef (Figures 23, 24). These fragile structures with multiple cone-like apertures are also constructed of silt-sized sediment particles, both carbonate (coccoliths) and silicate.

In addition to the structures that have probably been fabricated by benthic protozoans are more enigmatic features that may or may not represent the work of nodule- or crust-dwelling organisms (Figures 25, 26). Some nodule surfaces as well as the thinly Mn-encrusted gorgonian coral from the flanks of Tema Reef (Figure 27) apparently lack any evidence of attached organisms. While the agglutinating forams scavenge particles such as the tests and test fragments of pelagic organisms or silicate mineral grains, ferromanganese oxide precipitates may incorporate such material directly into nodules or crusts by binding grains to the surface and eventually covering them.

The distribution of benthic agglutinated foraminifers on nodules appears to follow a pattern. They are most abundant on those parts of the nodules that offer the most "hiding" space, i.e., recesses between botryoids or at the constriction between lobes of polylobate nodules. For larger nodules which have botryoids developed on all surfaces, abundance appears to be greatest just above the sediment line indicating the position of the sediment-water interface relative to the nodule. For many of the smaller spheroidal nodules, it is difficult to ascertain a top or bottom, and attached organisms are found scattered on the entire surface.

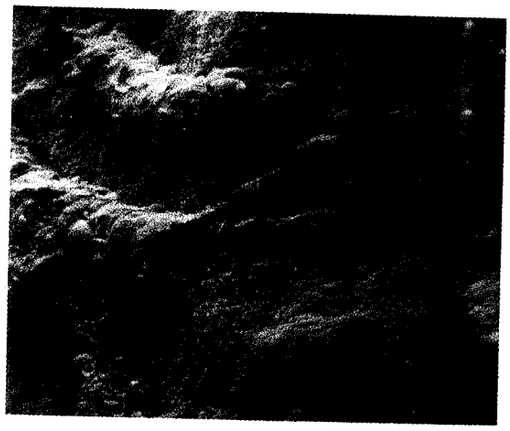

Figure 11. Stn U332. Tubular agglutinated benthic forams, possibly Tolypammina. *Smaller tube exposed by fracture removal of larger tube which crossed over it. Foreign particles are pelagic foram fragments, small whole globular pelagic forams, and coccoliths. Field of view 0.35 mm across.*

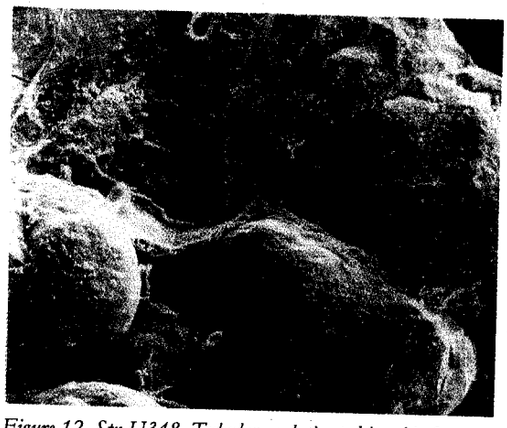

Figure 12. Stn U348. Tubular agglutinated benthic foram, with numerous chamber walls visible due to fracture removal of upper part of tube. Field of view 0.84 mm across.

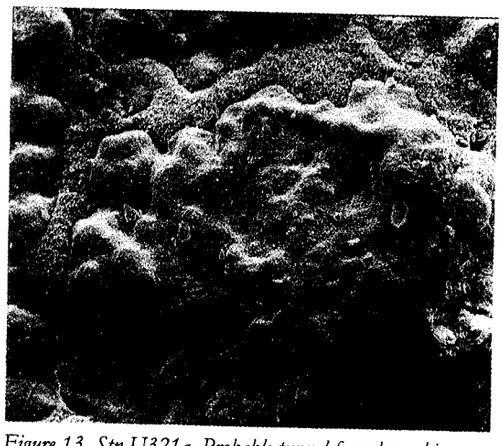

Figure 13. Stn U321a. Probable tunnel-form branching agglutinated benthic foram. Field of view 0.66 mm across.

Figure 14. Stn U321a. Close-up view of section of tunnel shown in Figure 13. Note that tunnel boundary is well defined, and tunnel follows recesses between botryoids. Foreign particles probably mostly silicate mineral grains. Field of view 0.35 mm across.

Figure 17. Stn U340. Elongated hemispherical chamber of agglutinated benthic foram. Note that chamber appears broken open. Field of view 1.74 mm across.

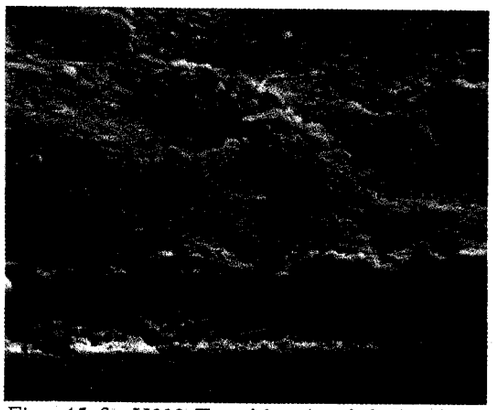

Figure 15. Stn U332. Tunnel-form (or tubular?) agglutinated benthic foram, branching. If apertures are natural rather than the result of breakage, entire test may be seen in this view. Field of view 0.17 mm across.

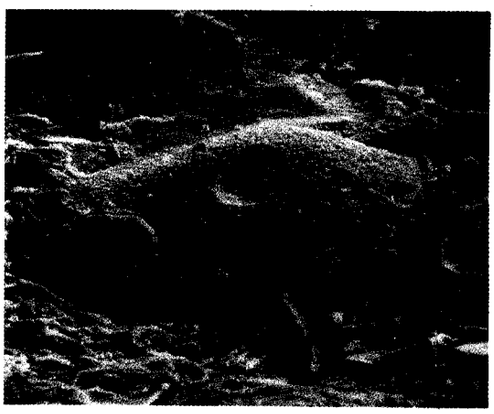

Figure 18. Stn U332. Dimpled hemispherical mass, possibly a benthic agglutinated foram. Central dimple may be partial collapse rather than constructional feature. Field of view 0.35 mm across.

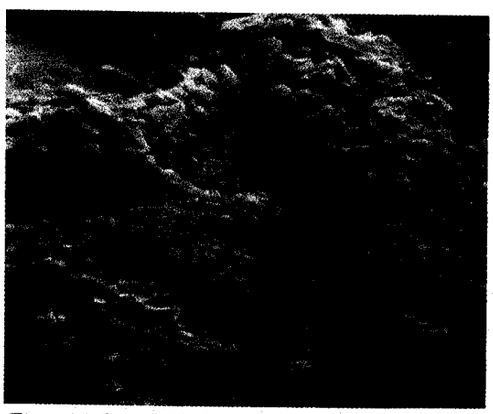

Figure 16. Stn U332. Close-up view of section of structure shown in Figure 15. Foreign particles mostly angular (silicate?) grains. Field of view 0.087 mm across.

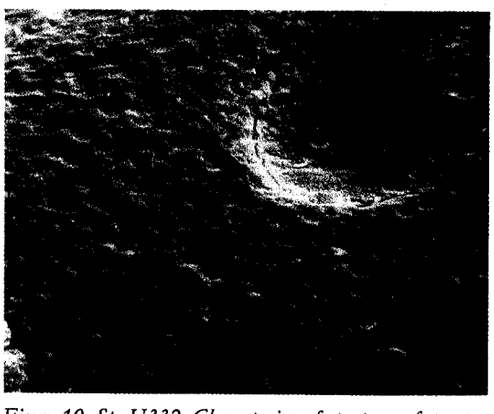

Figure 19. Stn U332. Close-up view of apertures of structure shown in Figure 18. Loose sediment grains litter surface. Character of foreign particles not discernible. Field of view 0.087 mm across.

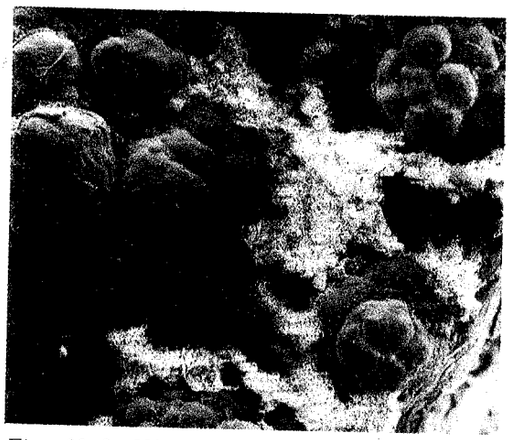

Figure 20. Stn U327. Chambered tunnel-form(?) agglutinated benthic foraminifer. Note how "tunnel mat" anastomoses around adjacent nodule botryoids. Field of view 0.92 mm across.

Figure 21. Stn U316b. Tunnel-form (?) mat-like agglutinated benthic foram. Large square aperture and smaller round aperture. Field of view 1.67 mm across.

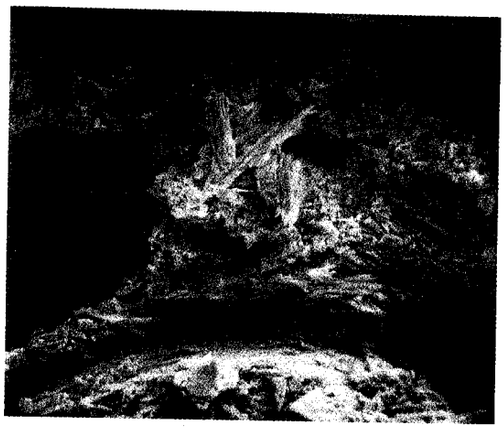

and adjacent test of structure shown in Figure 21. Foreign particles may be variable clumps of an authigenic mineral with a needlelike habit. Field of view 0.35 mm across.

Figure 23. Stn U333b. Thin-walled spheroidal agglutinated benthic forams. About one-half of lower one has been broken away. Field of view 1.76 mm across.

Figure 24. Stn U333b. Close-up view of aperture cone of foraminifer shown in Figure 23. Note that test is constructed of detrital silicate(?) grains and coccoliths. Field of view 0.082 mm across.

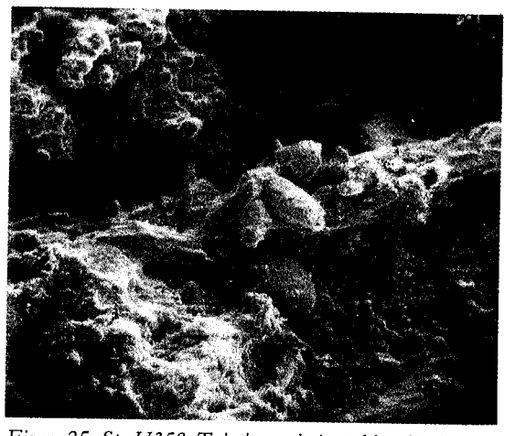

Figure 25. Stn U358. Tubular agglutinated benthic foraminifer (?). Foreign particles appear to be ichthyoliths. Field of view 1.67 mm across.

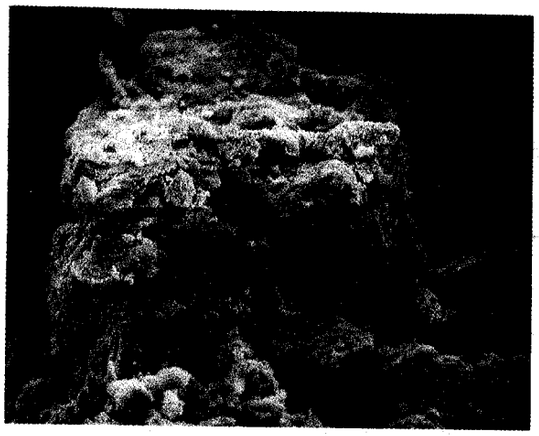

Figure 26. Stn U296a. Agglutinated benthic foraminifer(?). May be constructed in part of plates with central perforations. Field of view 0.25 mm across.

Figure 27. Stn U333b. Organic and inorganic sediment particles on surface of Mn-encrusted gorgonian coral. Field of view 0.090 mm across.

DISCUSSION AND CONCLUSIONS

Microscopic examination of the surfaces of manganese nodules and crusts collected during the 1986 HMNZS *Tui* cruises has revealed the presence of a diverse epifauna. While the existence of microorganisms on such surfaces has previously been noted (e.g., most recently by Mullineaux, 1987), the epifauna of samples from the present study area has not been reported. This study is a tantalizing first look at the remains of some of the test-making protozoans that are part of the meiofauna and larger microfauna.

Essentially all Mn-encrusted substrates display some type of epifaunal organism. Our non-systematic examination indicates that smoother surfaces are relatively devoid of epifauna, whereas the organisms seem to occur in greatest abundance on ferromanganese oxide surfaces with well developed botryoids and microbotryoids regardless of the nature or depth of the substrate on which the oxides precipitated. An observation which also lacks statistical support at this time is that the faunal composition on nodules and crusts may differ. *Saccorhiza* and similar tubular agglutinated benthic foraminifers appear to be the dominant members of the epifauna on nodules, and are less common on crusts. Although this specific observation does not agree with the findings of Mullineaux (1987), she did note differences in nodule and crust faunal composition.

Members of the epifauna probably feed on microorganisms such as bacteria. Lipps (1983) has stated that benthic agglutinated forams are passive herbivores, and the existence of bacteria on nodule surfaces has been documented (LaRock and Ehrlich, 1975; Burnett and Nealson, 1981). At a more primordial level, the latter authors note that a "variety of fragile filamentous and coccoid bacterial morphotypes" are associated with an organic-rich layer 1-10 μm thick on nodules collected by box corer in the central North Pacific. The thickness and distribution of this layer may influence not only the abundance and diversity of benthic organisms, but ultimately the morphology and chemical composition of manganese nodules and crusts which form in an environment subtly but pervasively overprinted with life.

ACKNOWLEDGEMENTS

Access to the AMR Model 1000 SEM was provided by Dr R.W. Scheetz (Department of Biological Sciences, University of Southern Mississippi). Technical assistance was provided by W. Blackburn (Department of Geological Sciences, SUNY-Binghamton) and K. Hamlin (Department of Geology, University of Southern Mississippi).

REFERENCES CITED

Burnett, B.R., and K.H. Nealson, 1981, Organic films and microorganisms associated with manganese nodules: Deep-Sea Research, v.28A, p.637-645.

Dudley, W.C., 1976, Cementation and iron concentration in Foraminifera on manganese nodules: Journal of Foraminiferal Research, v.6, p.202-207.

Dugolinsky, B.K., S.V. Margolis, and W.C. Dudley, 1977, Biogenic influence on growth of manganese nodules: Journal of Sedimentary Petrology, v.47, p.428-445.

Ehrlich, H.L., 1963, Bacteriology of manganese nodules I. Bacterial action on manganese in nodule enrichments: Applied Microbiology, v.11, p.15-19.

Graham, J.W. and S.C. Cooper, 1959, Biological origin of manganese-rich deposits of the sea floor: Nature, v.183, p.1050-1051.

Greenslate, J., 1974, Microorganisms participate in the construction of manganese nodules: Nature, v.249, p.181-183.

Greenslate, J., R.R. Hessler, and H. Thiel, 1975, Manganese nodules are alive and well on the seafloor: Proceedings of the

Marine Technology Society, Tenth Annual Conference, p.171-181.

LaRock, P.A., and H.L. Ehrlich, 1975, Observations of bacterial microcolonies on the surface of ferromanganese nodules from Blake Plateau by scanning electron microscopy: Microbial Ecology, v.2, p.84-96.

Lipps, J.H., 1983, Biotic interactions in benthic Foraminifera, *in* M.J.S. Tevesz and P.L. McCall, eds., Biotic interactions in recent and fossil communities: New York, Plenum Press, p. 321-376.

Mullineaux, L.S., 1987, Organisms living on manganese nodules and crusts: Distribution and abundance at three North Pacific sites: Deep-Sea Research, v.34, p.165-184.

Murray, J., and A. Renard, 1891, Manganese nodules, *in* Report of the scientific results of the voyage of HMS *Challenger*, v. 5, Deep-sea deposits: London, Eyre and Spottiswoode, p.341-378.

Thiel, H., and J. Schneider, 1988, Manganese nodule - organism interactions, *in* P. Halbach, G. Friedrich, and U. von Stackelberg, eds., The manganese nodule belt of the Pacific Ocean: Stuttgart, Ferdinand Enke Verlag, p.102-110.

McCabe, W.]., R.G. Ditchburn, and G.P. Glasby, 1996. Uranium, series disequilibrium dating of coral and shell fragments dredged around islands and seamounts during the 1986 HMNZS *Tui* cruises, *in:* Meylan, M.A., and G.P. Glasby (eds) Manihiki Plateau, Machias and Capricorn Seamounts, Niue, and Tofua Trough: Results of *Tui* Cruises. SOPAC Technical Bulletin 10: 167-174.

URANIUM SERIES DISEQUILIBRIUM DATING OF CORAL AND SHELL FRAGMENTS DREDGED AROUND ISLANDS AND SEAMOUNTS DURING THE 1986 HMNZS *TUI* CRUISES

W.J. McCabe, RG. Ditchburn

Instirute of Geological and Nuclear Sciences Ltd, PO Box 31312, Lower Hutt, New Zealand

G.P. Glasby

Department of Earth Sciences, University of Sheffield, Sheftield S3 7HP, England

ABSTRACT

Nine coral and two shell samples dredged from the flanks of various islands and seamounts in the subtropical SW Pacific were processed through the uranium series analysis system and ages calculated. Although there is a tendency for sample ages to increase with water depth, the presence of corals less than 1000 years old at water depths of 400 to almost 1000 m indicates the influence of recent slumping rather than crustal warping or eustatic changes as reasons for their present position. This phenomenon is related to mass wasting of material down slope. It is possible that samples collected systematically down the slopes of these islands would enable the frequency and times of slumping to be determined.

INTRODUCTION

During the 1986 cruises of HMNZS *Tui*, coral and shell samples were collected in a number of dredge hauls at depths well below which they would be normally expected to occur. For this reason, it was thought desirable to determine the ages of these samples in order to ascertain whether these were modern corals and shells living at their *in situ* depth of occurrence or rather fossil material which had slumped to its present position. For this reason, selected samples were chosen for uranium series disequilibrium dating. Sample locations and depths are given in Table 1. The "C" and "S" coding to the station numbers indicate coral and shell samples collected at those stations and /1 and /2 indicate duplicate analyses of those samples.

METHODS

Crystallographic Examination

The coral samples were examined by X-ray diffraction to determine the extent of recrystallization. The results are give in Table 2.

Sample Pretreatment

Most samples showed some visible external alteration with the interior being sound. This related visually to the note book sketches made by A.J. Tulloch and B.M. Fry (pers. comm.) and the XRD results. The outer material of all samples was removed by grinding with an abrasive wheel

Table 1. Coral and shell sample station data.

Station, Sample	Sample description	Location	Lat. (°S)	Long. (°W)	Depth (m)
U317 C/1 U317 C/2	Coral pieces Coral pieces	Manihiki Island	10°23.7'- 10°24.2'	161°05.6'- 161°05.4	2161- 2111
U324 C/1 U324 C/2	Coral crushed Coral crushed	Pukapuka	10°53.0' 10°52.7'	165°55.2'- 165°55.4'	417- 466
U331 C/1 U331 C/2 U331 S	Coral crushed Coral crushed Shell	Tema Reef	11°06.0'- 11°06.2'	165°37.0'- 165°36.6'	1407- 1100
U337 C/1 U337 C/2 U337 S	Coral pieces Coral pieces Shell	Nassau	11°32.2'- 11°33.4'	165°23.5'- 165°23.8'	1001- 804
U342 C/1 U342 C/2	Coral crushed Coral crushed	Machias Seamount	15°00.9'- 15°00.5'	172°08.3'- 172°12.2'	1350
U345 C/1 U345 C/2	Coral crushed Coral crushed	Machias Seamount	14°56.1'- 14°56.8'	172°15.3'- 172°14.6	1972- 2166
U350 C/1 U350 C/2	Coral crushed Coral crushed	Capricorn Seamount	18°34.1'- 18°45.5'	172°09.8'- 172°08.8'	1021- 922
U356 C/1 U356 C/2	Coral crushed Coral crushed	Niue	19°10.2' 19°10.0'	169°55.0'- 169°54.7'	1873- 1100
U370 C/1 U370 C/2	Coral crushed Coral crushed	Rarotonga	21°10.5'	159°46.5'	1021- 1086

and the center parts cleaned by washing in an ultrasonic bath. Samples U324, U331, U342, U345, U350, U356 and U370 were crushed for sampling while pieces of samples U317 and U337 were selected for duplicate analysis (see Table 1).

Analytical Procedures

Dried samples weighing between 8 and 56 grams were combusted overnight at 550°C. They were then dissolved in dilute HNO_3 and the Harwell ^{232}U-^{228}Th spike added except for those samples run unspiked to allow the natural ^{228}Th level to be determined. The spiked runs are indicated in Table 3 under the ^{228}Th heading by a dash which means that the natural ^{228}Th could not be determined because of the presence of ^{228}Th spike.

The sample solutions were filtered through a 0.47 μm membrane filter, any residue washed with 20 ml of 6M HCl to remove polonium and the washings added to the main filtrate. The residues were then washed with 10 ml of 6M HCl/0.05 M HF to remove any remaining protactinium and the washings set to evaporate after adding a few millilitres of HNO_3 and $HClO_4$. Meanwhile, the main filtrate was scavenged with about 30 mg of Fe^{3+} and

ammonium hydroxide to recover the uranium, thorium, protactinium and polonium, free from elements which form insoluble fluorides. The hydroxide precipitate was centrifuged and washed, and the supernatant and washings again scavenged and the precipitates combined. They were then dissolved in a small amount of concentrated HNO_3 and HF, added to the evaporated residue washings, to which had already been added 10 mg of Al^{3+}, and evaporated to fumes. The Al^{3+} was added to maintain a source of fluoride ions during the evaporation.

The activities of the radionuclides are given in disintegrations per minute per gram and the associated one standard deviation error relates to uncertainties arising from counting statistics, spike calibration, counter efficiencies and pipette volumes.

Details of the development of the method and the protactinium procedure are given in McCabe et al. (1979) and Ditchburn and McCabe (1987a, b). An outline of the present procedure appears in Burnett et al. (1988).

Table 2. X-ray diffraction analyses of coral samples.

Station	% Calcite in Aragonite
U317	2 ± 1.5
U324	0 ± 1.5
U331	2 ± 1.5
U337	0 ± 1.5
U342	58 ± 3
U345	0 ± 1.5
U350	100 ± 4
U356	100 ± 4
U370	1 ± 1.5

Table 3. Disintegrations/minute/gram of isotopes measured in coral and shell samples.

Station	^{238}U	^{235}U	^{234}U	^{232}Th	^{230}Th	^{228}Th	^{231}Pa	^{210}Po
Corals								
U317 C/1	1.96±.05	0.094±.002	2.02±.05	<0.001	2.10±.03	-	0.102±.004	2.10±.03
U317 C/2	2.67±.06	0.123±.003	2.83±.06	<0.001	2.69±.04	-	0.135±.004	2.73±.05
U324 C/1	2.41±.06	0.111±.003	2.75±.06	<0.001	0.006±.001	-	0.0014±.0002	0.063±.002
U324 C/2	2.31±.05	0.106±.002	2.63±.05	<0.001	0.006±.001	0.001±.001	0.0009±.0002	0.075±.003
U331 C/1	1.84±.04	0.085±.002	1.99±.05	<0.001	1.94±.03	-	0.097±.003	2.17±.04
U331 C/2	1.88±.04	0.086±.002	2.00±.04	<0.001	1.99±.04	-	0.106±.003	2.46±.05
U337 C/1	2.18±.05	0.101±.002	2.56±.06	<0.001	0.615±.013	-	0.051±.002	0.50±.01
U337 C/2	2.35±.06	0.108±.003	2.66±.07	0.02±.001	0.785±.019	-	0.59±.003	0.61±.01
U342 C/1	1.58±.04	0.073±.002	1.74±.04	0.100±.003	1.42±.03	-	0.070±.002	1.12±.02
U342 C/2	1.57±.03	0.072±.002	1.70±.04	0.096±.003	1.43±.03	0.096±.003	0.072±.002	1.14±.02
U345 C/1	1.76±.04	0.081±.002	1.91±.04	0.001±.001	1.67±.03	-	0.087±.002	1.52±.03
U345 C/2	1.76±.04	0.081±.002	1.88±.04	0.001±.001	1.70±.03	0.001±.001	0.086±.002	1.59±.03
U350 C/1	2.73±.04	0.126±.002	2.75±.04	<0.001	2.72±.04	-	0.129±.003	2.72±.04
U350 C/2	2.94±.06	0.136±.003	3.00±.06	<0.001	2.87±.06	-	0.127±.003	2.69±.05
U356 C/1	0.220±.007	0.0101±.0003	0.236±.007	0.010±.001	0.282±.005	-	0.0128±.0007	0.71±.01
U356 C/2	0.210±.006	0.0097±.0003	0.226±.007	0.012±.001	0.294±.006	0.013±.001	0.0124±.0007	0.76±.02
U370 C/1	1.90±.04	0.087±.002	2.17±.05	<0.001	0.014±.002	-	0.0015±.0003	0.156±.006
U370 C/2	1.97±.04	0.091±.002	2.23±.05	<0.001	0.014±.001	0.002±.001	0.0011±.0002	0.139±.005
Shells								
U331 S	0.769±.016	0.035±.001	0.927±.019	<0.001	0.598±.010	-	0.036±.001	1.29±.03
U337 S	0.420±.010	0.0193±.0005	0.525±.012	<0.001	0.261±.005	-	0.0148±.0007	0.295±.008

RESULTS

Most of the coral samples are in the form of the original aragonite but three of the coral samples (U342, U350 and U356) have converted extensively to calcite (Table 2). This conversion of calcite to aragonite is, in general, slow (Reeckmann 1988), although there is no clear relationship between sample age and degree of mineral conversion in these samples.

The uranium series disequilibrium data are listed in Tables 3–6. These show good agreement between duplicates for specimens which were homogenized prior to weighing out. However, significant differences are evident for the coral pieces of samples U317 and U337 which were not homogenized. Since these samples were collected by dredging on a steep slope, some variation in sample composition is not surprising. Those samples which were run without the ^{232}U–^{228}Th spike had their concentrations calculated on the assumption of a 98% recovery which is routine for the system. All show that ^{228}Th and ^{232}Th are in equilibrium and this condition was assumed for all the other samples when thorium recoveries were being calculated. These results illustrate the advantages of the NSG system of determination which gives consistently high and near quantitative results over methods which give variable, qualitative results and which rely on ^{228}Th to determine the yields.

Table 4. Uranium and thorium contents of corals and shells calculated from ^{238}U and ^{232}Th activities.

Station	Uranium (ppm)	Thorium (ppm)
Corals		
U317 C/1	2.65 ± .06	<0.001
U317 C/2	3.70 ± .06	<0.001
U324 C/1	3.24 ± .08	<0.001
U324 C/2	3.11 ± .06	<0.001
U331 C/1	2.49 ± .06	<0.001
U331 C/2	2.53 ± .06	<0.001
U337 C/1	2.94 ± .07	<0.001
U337 C/2	3.17 ± .08	0.001 ± .001
U342 C/1	2.13 ± .05	0.41 ± .01
U342 C/2	2.11 ± .04	0.39 ± .01
U345 C/1	2.38 ± .06	0.003 ± .003
U345 C/2	2.37 ± .05	<0.01
U350 C/1	3.68 ± .05	NC
U350 C/2	3.97 ± .08	NC
U356 C/1	0.296 ± .009	0.042 ± .002
U356 C/2	0.284 ± .008	0.048 ± .002
U370 C/1	2.56 ± .06	<0.001
U370 C/2	2.65 ± .06	0.003 ± .001
Shells		
U331 S	1.04 ± .02	<0.001
U337 S	0.57 ± .01	<0.001
NC = Not Calculable		

The natural thorium concentration is very low in all samples, except U342 which consequently has a low $^{230}Th/^{232}Th$ ratio of around 14. Correction of the ^{230}Th activity, assuming an initial $^{230}Th/^{232}Th$ ratio of 1.0 for the contaminating thorium, gives a Th/U age which is concordant with that obtained from the other isotopic ratios.

Uranium is present at the usual 2–3 ppm concentration levels in all corals except that from Niue Island where a value typical of the coral mass of that island of less than 0.3 ppm was found (cf. Whitehead et al., 1991).

The $^{234}U/^{238}U$ ratio of all the corals seems to be a reasonably reliable, although not very sensitive, indicator of age. However, the ratios in the shells with values of 1.21 ± .01 and 1.25 ± .02 show evidence of their containing uranium of other than seawater origin. Seawater has a ratio of 1.1436 ± 0.0017.

Similar $^{234}U/^{238}U$ values have been found by us in shells from a shallow New Zealand marine core and in fossil *Tridacna* samples taken from Niue Island in raised coral terraces. In the first case, sediment pore water is presumed responsible and, in the second, groundwater percolating through the porous structure. It is not clear which of these two possibilities is correct for the present samples.

A recent paper by Bard et al. (1991) argues that old corals show evidence of being partially open systems for dating. They cite $^{234}U/^{238}U$ values of >1.14 in some samples. However, even if this is so, the slight changes envisaged would not alter the conclusions of this paper since we are not discussing small time differences.

Figure 1 shows a concordia line for $^{230}Th/^{234}U$ and $^{231}Pa/^{235}U$ and where the results obtained lie in relation to it. The concordia line is the line obtained when ^{230}Th and ^{231}Pa are not present initially but grow into equilibrium with their parents ^{234}U and ^{235}U. It is apparent that a number of values lie to the right of the curve and some well above the equilibrium limit for the $^{230}Th/^{234}U$ ratio. As there is almost no natural thorium in these samples, it is argued that there has been no addition of other isotopes of thorium or protactinium. This leaves the alternative explanation for the position of these points that uranium has been lost.

The effect of removing uranium from the system is to move points off the curve towards higher ratio values, along a line which passes through the original position of the point on the curve and the origin. If the loss of uranium is recent, then moving the points back along the line to the curve may give a better indication of the true age or at least a minimum age. Table 7 gives the calculated ages for these

Table 5. Calculated isotopic ratios in coral and shell samples.

Station	$^{234}U/^{238}U$	$^{230}Th/^{232}Th$	$^{230}Th/^{234}U$	$^{231}Pa/^{235}U$	$^{231}Pa/^{230}Th$	$^{210}Po/^{230}Th$
Corals						
U317 C/1	1.030±.013	-	1.04±.03	1.13±.05	0.049±.002	1.09±.03
U317 C/2	1.062±.010	-	0.95±.02	1.10±.04	0.050±.002	1.02±.02
U324 C/1	1.142±.008	-	0.0020±.0002	0.013±.002	0.26±.05	11±1
U324 C/2	1.140±.008	-	0.0022±.0002	0.008±.002	0.15±.03	12±1
U331 C/1	1.082±.016	-	0.97±.03	1.15±.05	0.050±.002	1.11±.03
U331 C/2	1.064±.015	-	1.00±.03	1.22±.05	0.053±.002	1.24±.03
U337 c/1	1.171±.015	>1000	0.241±.008	0.51±.03	0.083±.004	0.81±.03
U337 C/2	1.129±.021	330±150	0.295±.010	0.54±.03	0.075±.004	0.79±.03
U342 C/1	1.100±.001	14.1±.4	0.81±.02	0.96±.03	0.050±.002	0.79±.02
U342 C/2	1.083±.011	14.9±.4	0.83±.02	0.98±.03	0.050±.002	0.80±.02
U345 C/1	1.086±.013	>1000	0.87±.03	1.07±.04	0.052±.002	0.91±.02
U345 C/2	1.067±.013	>1000	0.91±.03	1.07±.04	0.051±.002	0.93±.02
U350 C/1	1.008±.004	-	0.99±.02	1.03±.03	0.047±.001	0.98±.02
U350 C/2	1.019±.007	>2000	0.96±.03	0.94±.03	0.044±.001	0.94±.03
U356 C/1	1.07±.03	27±2	1.19±.04	1.27±.07	0.045±.002	2.53±.06
U356 C/2	1.07±.03	25±1	1.30±.05	1.28±.087	0.042±.002	2.58±.07
U370 C/1	1.146±.014	>100	0.007±.001	0.018±.003	0.11±.02	10.8±1.3
U370 C/2	1.134±.015	22±6	0.006±.001	0.012±.003	0.08±.02	10.0±.7
Shells						
U331 S	1.205±.014	1000	0.645±.017	1.02±.04	0.061±.002	2.16±.06
U337 S	1.25±.02	>1000	0.498±.015	0.77±.04	0.057±.003	1.12±.04

samples using the corrected $^{230}Th/^{234}U$ ratios read off the graph. Otherwise, for those samples lying off the line, the best estimate of their age is calculated from the $^{231}Pa/^{230}Th$ ratio. The agreement between the ages calculated from the $^{230}Th/^{234}U$ ratios after correcting for loss of uranium and the measured $^{231}Pa/^{230}Th$ ratios is very close. The preferred ages for each of the samples are given in bold type in Table 6.

Figure 2 shows the ages of samples plotted against the depth or range of depths from which the samples were dredged. The data show that the ages of coral samples from the two seamounts (Machias Seamount and Capricorn Seamount) (samples U342, U345 and U350) are in the range 170– > 400 ka. This is consistent with the corals being older material found on submerged, former coral-capped islands. Of the remaining samples from around islands, there is a tendency for older samples to be from greater depths, although there is no clear relationship between age and water depth. Nonetheless, it seems likely that these materials have been moved to their present positions as a result of slumping and that the determined ages do not represent *in situ* ages of coral at that location. The mineralogical data show that the coral samples with the highest degree of conversion to calcite (U342, U350 and U356) are taken from seamounts (Capricorn and Machias Seamounts) or from around the island of Niue. The reef corals from around the other islands, on the other hand, have all remained essentially as the original aragonite.

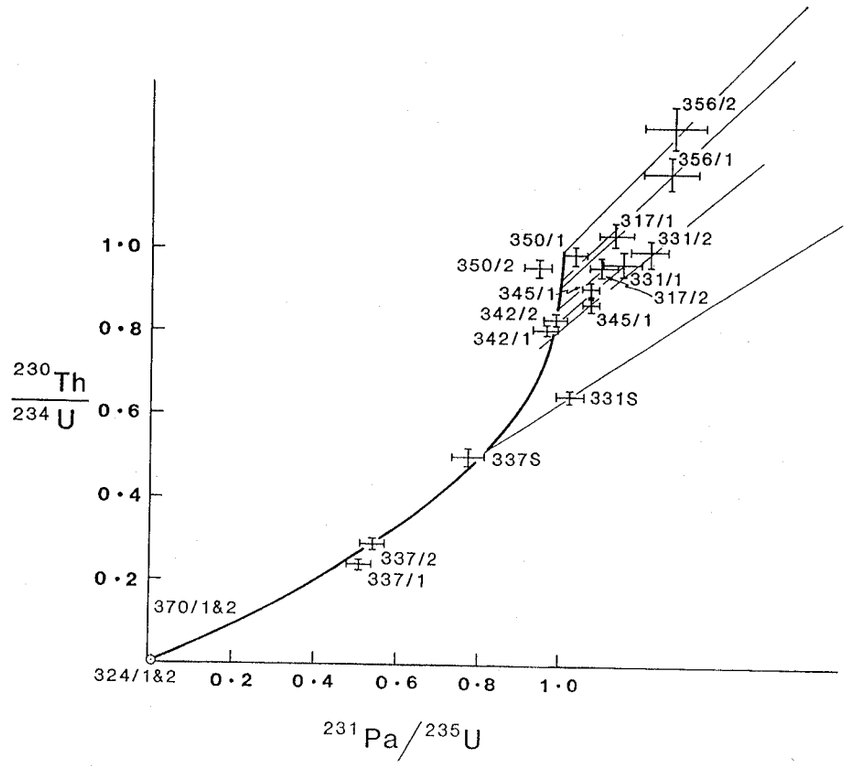

Figure 1. Concordia diagram (heavy curve) also showing discordia lines (light lines to right of main curve) due to loss of uranium in coral and shell samples. For explanation see text.

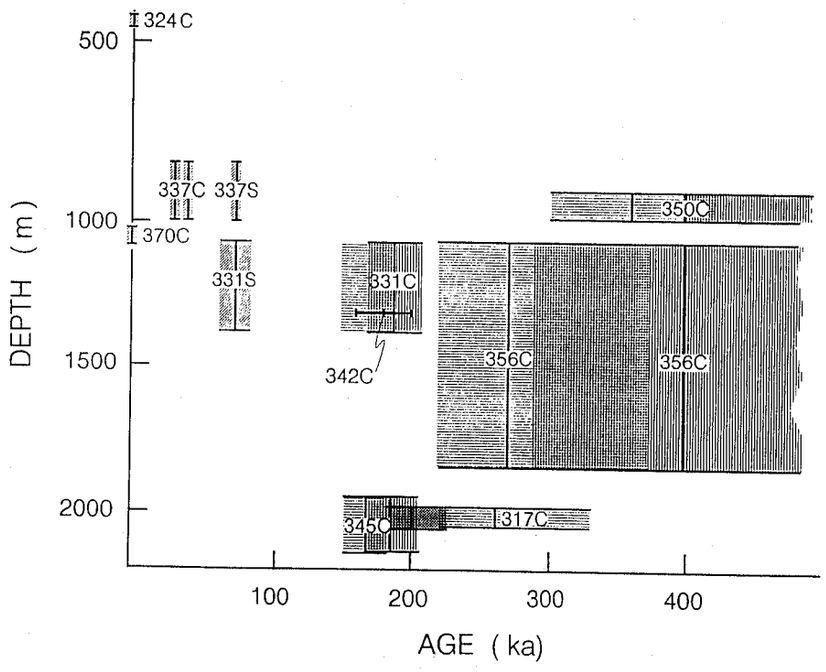

Figure 2. The relationship between the measured age of the coral and shell samples and water depth.

*Table 6. Age (in kilo years) of coral and shell samples calculated from isotopic ratios.**

Station	$^{234}U/^{238}U$	$^{230}Th/^{234}U$	$^{231}Pa/^{235}U$	$^{231}Pa/^{230}Th$
Corals				
U317 C/1	540	NC	NC	**260 +70/-40**
U317 C/2	285 ± 55	290 ± +43/-31	NC	**200 +25/-20**
U324 C/1	<0.3	**0.25 ± .05**	0.6 ± .1	NC
U324 C/2	<0.3	**0.25 ± .05**	0.4 ± .1	NC
U331 C/1	190+/-60	324 +67/-42	NC	**185 +25/-20**
U331 C/2	280 +95/-75	400 ± 80	NC	**165 +20/-15**
U337 C/1	NC	**30 ± 1**	34 ± 3	14 ± 9
U337 C/2	29 +90/-29	**38 ± 1**	37 ± 3	41 ± 10
U342 C/1	120 ± 40	**170 ± 12**	155 +100/-30	175 +20/-15
U342 C/2	185 +50/-45	**186 ± 14**	190 +200/-50	185 +20/-15
U345 C/1	175 ± 60	212 ± 20	>200	**165 ± 15**
U345 C/2	260 +80/-60	240 ± 25	>200	**185 ± 20**
U350 C/1	1050 +200/-150	**>400**	>200	360 ± 60
U350 C/2	720 +180/-120	330 +75/-50	130 +30/-20	**>400**
U356 C/1	210 +180/-120	NC	NC	**270 +100/-50**
U356 C/2	220 + 200/-130	NC	NC	**400 +NC/-100**
U370 C/1	<20	**0.8 ± .1**	0.8 ± .1	0.1 +13/-.1
U370 C/2	15 ± 15	**0.7 ± .1**	0.6 ± .1	20 ± 20
Shells				
U331 S	NC	108 ± 5	>180	**73 ± 10**
U337 S	NC	**73 ± 3**	70 ± 9	79 ± 14

* Preferred values are shown in bold type; errors are one standard deviation.
NC = Not Calculable

There is some grouping of ages apparent in Table 6 with three corals having values around 175 ka and both shells being close to 73 ka. However, there are too few samples to determine a frequency distribution with time. Further, these samples were dredged from a number of islands and seamounts. It is therefore not possible to estimate the timing of major slumping events. Nevertheless, the data do suggest that some measure of the time scale of the slumping processes might be obtained by systematically collecting samples down the slopes of islands away from and normal to the coastline.

CONCLUSIONS

Ages have been determined for six coral and two shell samples taken at various depths around several islands in the subtropical Pacific and for three coral samples from the slopes of Machias and Capricorn Seamounts. The results show that only coral samples dredged around Pukapuka and Rarotonga can be described as reasonably modern (0.25–0.8 ka). Other coral and shell samples from around the islands have ages in the range 30–400 ka. This indicates that the samples are fossil material introduced to their present depths by slumping. The data on the seamount corals show that they are old (in the range 170–>400 ka). This is consistent with their being reef material formed on islands which have subsequently submerged.

ACKNOWLEDGMENTS

X-ray diffraction analyses of coral samples were ably performed by A.J. Tulloch and B.M. Fry of the New Zealand Geological Survey.

REFERENCES CITED

Bard, E., R.G. Fairbanks, B. Hamelin, A. Zindler, and C.T. Hoang, 1991, Uranium-234 anomalies in corals older than 150,000 years: Geochimica et Cosmochimica Acta, v.55, p.2385-2390.

Burnett, W.C., K.B. Baker, P.A. Chin, W.J. McCabe, and R.G. Ditchburn, 1988, Uranium series and AMS ^{14}C studies of modern phosphatic pellets in Peru shelf muds: Marine Geology, v.80, p.215-230.

Ditchburn, R.G., and W.J. McCabe, 1987a, An improved method for the purification and electrodeposition of protactinium for application to the INS uranium series dating project: Institute of Nuclear Sciences (New Zealand), Report INS-R—372, 13 p.

Ditchburn, R.G., and W.J. McCabe, 1987b, Provisional manual for processing carbonate samples for uranium series dating: Institute of Nuclear Sciences (New Zealand), Report INS-M–95, 19 p.

McCabe, W.J., R.G. Ditchburn, and N.E. Whitehead, 1979, The quantitative separation, electrodeposition and alpha spectrometry of uranium, thorium, and protactinium in silicates and carbonates: Institute of Nuclear Sciences (New Zealand), Report INS-R—262, 30 p.

Reeckman, S. A., 1988, Diagenetic alterations in temperate shelf carbonates from southeastern Australia: Sedimentary Geology, v.60, p.209-219.

Table 7. Ages of coral and shell examples calculated from the $^{230}Th/^{234}U$ ratios corrected for uranium loss by means of the Concordia Diagram (Figure 1), and the corresponding $^{231}Pa/^{230}Th$ ratio ages.

Station	$^{230}Th/^{234}U$ ratio	$^{230}Th/^{234}U$ age (ka)	$^{231}Pa/^{230}Th$ age (ka)
Corals			
U317 C/1	0.915	260	260
U317 C/2	0.86	205	200
U331 C/1	0.83	185	185
U331 C/2	0.80	170	165
U345 C/1	0.80	170	165
U345 C/2	0.83	185	185
U356 C/1	0.935	270	270
U356 C/2	1.0	>400	400
Shells			
U331 S	0.51	76	73

Whitehead, N.E., R.G. Ditchburn, W.J. McCabe, and P. Rankin, 1992, A new model for the origin of the anomalous radioactivity in Niue Island (South Pacific) soils: Chemical Geology (Isotope Geoscience Section), v.94, p.247-260.